

TH 0741

PETRO-CHEMISTRY OF THE BACHELOR LAKE VOLCANIC COMPLEX AND ASSOCIATED ORE DEPOSITS ABITIBI
EAST N.W. QUEBEC

Documents complémentaires

Additional Files



Licence



License

Cette première page a été ajoutée
au document et ne fait pas partie du
rapport tel que soumis par les auteurs.

Énergie et Ressources
naturelles

Québec 

PETRO-CHEMISTRY
OF THE
BACHELOR LAKE VOLCANIC COMPLEX
AND ASSOCIATED ORE DEPOSITS
ABITIBI EAST
N.W. QUEBEC

By

BERNARD NORMAN MCQUADE

A thesis
Submitted to the School of Graduate Studies
In partial fulfillment of the
Requirements for the degree of
Doctor of Philosophy
In Geology

University of Ottawa
Ottawa, Canada

1981

TH0741

PETRO-CHEMISTRY
OF THE
BACHELOR LAKE VOLCANIC COMPLEX
AND ASSOCIATED ORE DEPOSITS
ABITIBI EAST
N.W. QUEBEC

by

Bernard Norman McQuade

A Thesis
submitted to the School of Graduate Studies
in partial fulfillment of the
requirements for the degree of
Doctor of Philosophy
in Geology

University of Ottawa
Ottawa, Canada

© Bernard Norman McQuade, Ottawa, Canada, 1981.

UNIVERSITÉ D'OTTAWA / UNIVERSITY OF OTTAWA
Ecole des études supérieures/School of Graduate Studies

Title of thesis PETRO-CHEMISTRY OF THE BACHELOR LAKE VOLCANIC COMPLEX AND
ASSOCIATED ORE DEPOSITS ABITIBI EAST N.W. QUEBEC

Name of candidate McQUADE, Bernard Norman

Degree Ph.D. (Geology) Department GEOLOGY

Date of defence September 22, 1981.

This thesis prepared under the supervision of Dr. G.A. Armbrust has been approved by a jury
composed of the following examiners:

F.T. AGTERBERG
A. BAER
R. KRETZ
W. JOLLY

Paul Hagen
(Dean of Graduate Studies)

The University of Ottawa requires the signatures of all persons using or photocopying this publication. Please sign below, and give address and date.

FOR THE EXAMINING COMMITTEE

W. J. [unclear]

External Examiner

J. H. [unclear]

Supervisor

[unclear]

Examiner

D. [unclear]

Examiner

[unclear]

Examiner

ABSTRACT

The Bachelof Lake complex is a roughly linear, Archean volcano - sedimentary sequence, located midway between Senneterre and Chibougamau, in northwestern Quebec. Trending northeast, supracrustals extend through and beyond the six township (600 sq.mi.) study area as part of the Pusticamica - Opawica - Obatagamau zone of the Abitibi greenstone belt.

Samples were collected using a 150m. sampling interval, across strike and along three widely spaced traverses, in an effort to obtain a representative collection of rock types in the pile. Classification of the rocks proved difficult due to the pervasive effects of regional greenschist facies metamorphism. No commonly used classification scheme is acceptable for the broad range in composition and alteration of Archean volcanic rocks. Modification of an existing scheme provides a workable system for this project.

Overall, the area appears to be a synclinal trough of downwarped volcanics and minor sediments, with high angle dips. The lower platform sequence consists primarily of primitive, mafic flows. Upwards, a thick sequence of mainly mafic to intermediate rocks is encountered, followed by a sedimentary horizon, marking a period of erosional, non-volcanic deposition and the upper limit of the platform sequence. The upper, domal unit, containing a variety of ore deposits and prospects, is formed of less frequent mafic volcanics, alternating with intermediate to felsic differentiates and pyroclastics.

A proposed model of greenstone belt formation envisages graben-like rifting of a sialic crust and quiescent effusion of ultramafic-mafic flows into deep water. Further accumulations of mafic lavas into shallower water completes the platform sequence, which sags deep into the crust, due to gravitational instability. Depression of the pile into a region of high heat flow results in doming via partial melting and diapiric rise of calc-alkaline magmas, thus forming the upper, domal sequence. The calc-alkaline sequence is seen as a recycling of previous crustal material, as distinct from a lower crustal or mantle source for the platform rocks.

The change in volcanic style is intricately tied to a corresponding progression of ore metals. Geothermal

systems, capable of concentrating base metals, develop mainly in the calc-alkaline stage of volcanism (high volatiles and localized heat source near surface). These features are absent in platform sequences, where segregation deposits (Ni-Cu, Cr) are tied directly to the magma.

SOMMAIRE

Le complexe du Lac Bachelor, situé à mi-chemin entre Senneterre et Chibougamau au nord-ouest du Québec, consiste en une série volcanosédimentaire archéenne, à peu près linéaire. Les roches supracrustales s'étendent au delà de la région étudiée (6 cantons - 600 mi.2), comprenant en partie la zone Pusticamica - Opawica - Obatagama de la zone de roches vertes de l'Abitibi.

Afin d'obtenir une collection représentative de roches dans la pile, les coulées ont été échantillonnées à un intervalle de 150 m. au long de trois traverses très espacées, perpendiculairement à la direction. La classification des roches est difficile à cause des effets du métamorphisme régional aux faciès schiste-vert et amphibolite. Plusieurs versions modifiées des classifications récentes, appliquées à la géochimie et à la pétrographie détaillée, fournissent un plan pétrochimique pratique.

En général, la région ressemble à une auge synclinale, à pendage fortement incliné, contenant des roches volcaniques et des sédiments mineurs. La succession plate-formale inférieure se compose, pour la plupart, de coulées mafiques primitives. Vers le haut, on rencontre une épaisse série, principalement faite de coulées mafiques et intermédiaires qui est suivie par un horizon sédimentaire, marquant une période d'érosion et de non-dépôt volcanique. Cet horizon indique la limite supérieure de la série plate-formale. Le group supérieur, en dôme, renfermant une variété de gîtes minéraux, consiste en coulées mafiques alternant avec des roches volcaniques abondantes de composition intermédiaires et felsiques, et des roches pyroclastiques.

Un modèle proposé pour la formation des zones de roches-vertes, envisage la formation d'une fente, comme un graben dans une croûte sialique, et l'épanchement tranquille des coulées ultramafiques en eau profonde. L'accumulation supplémentaire des coulées mafiques en eau peu profonde, termine la série plate-formale qui s'affaisse profondément dans la croûte, à cause de son instabilité gravitationnelle. Le bas de la pile entre dans une région de haut flux thermique, avec formation d'un dôme par fusion partielle, et ascension diapirique d'un magma calco-alcalin, formant la série supérieure en dôme. Cette série calco-alcaline représente un remaniement de la croûte, alors que les roches

de la plate-forme dérivent du manteau ou de la croûte inférieure.

Le changement du style volcanique est lié à une progression correspondante des métaux. Des systèmes géothermaux capables de concentrer des métaux de base se sont développés, pour la plupart, au stage du volcanisme calco-alcalin (volatiles abondants et une source de chaleur près de la surface). Ces traits sont absents des séries de la plate-forme où les dépôts (Ni-Cu, Cr) sont liés directement au magma.

ACKNOWLEDGEMENTS

The author is deeply grateful to Dr. G.A. Armbrust who suggested the study area and acted as thesis supervisor throughout the project. Especially helpful was his assistance in the editing stage of this text. Research support was provided by NRC grant A8840.

Quebec Sturgeon River Mines Limited personnel allowed information to be gathered for the underground workings of both the Coniagas and Quebec Sturgeon ore deposits. Their cooperation with sample collection from the first level crosscut of the Quebec Sturgeon gold mine was sincerely appreciated.

Rock crushing facilities were provided by Bondar-Clegg labs in Ottawa. The advice of Mr. G. Lachance, of the Geologic Survey of Canada, in development of x-ray fluorescence computer analysis was also greatly appreciated.

Assistance of Mr. J.M. Aprix (Computer Applications Department) in processing the original Laser printing of this text, the first at the University of Ottawa, is acknowledged.

I am also indebted to my wife, Wendy, who provided much enthusiasm and encouragement for the completion of this project.

TABLE OF CONTENTS

FOR THE EXAMINING COMMITTEE	iii
FRONTISPIECE	iv
ABSTRACT	v
SOMMAIRE	vii
ACKNOWLEDGEMENTS	ix

Chapter	page
1. INTRODUCTION	1
1.1 Purpose of Study	1
1.2 Location, Access and Topography	2
1.3 Previous Work	4
2. FIELD AND ANALYTICAL METHODS	6
2.1 Field Methods	6
2.2 Sample Preparation	7
2.2.1 Crushing, Grinding and Sieving	7
2.2.2 Preparation of Pellets	9
2.3 Analytical Techniques	10
2.3.1 X-ray Spectrometry	10
2.3.2 Ferrous Oxide Determination	11
2.3.3 X-ray Diffraction Analysis (XRD)	13
2.3.4 Evaluation of Analytical Methods	15
2.4 Statistical Evaluation of Data	19
2.4.1 Correlation Analysis	19
2.4.2 Factor Analysis	23
2.4.3 Discriminant Analysis	26
3. CLASSIFICATION OF VOLCANIC ROCKS	29
3.1 Introduction	29
3.2 Mineralogical Classifications	30
3.3 Chemical Calculations and Graphical Plots	32
3.3.1 Peacock's Classification	33
3.3.2 Niggli's Classification	34
3.3.3 CIPW Norms	36
3.3.4 Harker Diagram	38
3.3.5 Larsen Diagram	40
3.3.6 Alkalies vs Silica Diagram	44

3.3.7 Al ₂ O ₃ vs Normative Plagioclase Diagram	45
3.3.8 Color Index vs Normative Plagioclase Diagram	45
3.3.9 Al ₂ O ₃ vs FeO/(FeO + MgO) Diagram	46
3.3.10 AFM Diagram	51
3.3.11 Pearce Diagram	52
3.4 Chemical Rock Classification Methods	55
3.4.1 Church-Murata Diagram	55
3.4.2 Jensen Diagram	57
3.5 Classification of Bachelor Lake Rocks	63
3.6 Summary of Classification	69
4. REGIONAL GEOLOGY	73
5. GEOLOGY OF THE BACHELOR LAKE REGION	79
5.1 Introduction	79
5.2 Area 1	82
5.2.1 Ultramafic Intrusive-Cumulate Bodies	83
5.2.2 Mafic - Intermediate Volcanic Rocks	83
5.2.3 Felsic Volcanic Rocks	84
5.3 Area 2	85
5.3.1 Mafic - Intermediate Volcanic Rocks	86
5.3.2 Felsic Volcanic Rocks	89
5.3.3 Sedimentary Rocks	91
Clastic Sedimentary Rocks	92
Chemical Sedimentary Rocks	94
5.4 Area 3	96
5.4.1 Mafic - Intermediate Volcanic Rocks	97
5.4.2 Felsic Volcanic Rocks	100
5.5 Area 4	101
5.5.1 Mafic-Intermediate Volcanic Rocks	102
5.5.2 Felsic Volcanic Rocks	104
5.6 Area 5	105
5.6.1 Mafic - Intermediate Volcanic Rocks	108
5.6.2 Felsic Volcanic Rocks	110
5.7 SUMMARY	110
6. GEOCHEMISTRY	114
6.1 Introduction	114
6.2 Whole Bachelor Lake Region	117
6.2.1 Area 1	127
6.2.2 Area 2	132
6.2.3 Area 3	140
6.2.4 Area 4	143
6.2.5 Area 5	145
6.3 Geochemical Summary	152
7. MINERAL DEPOSITS	155
7.1 Coniagas Mines Ltd. - Base Metal Deposit	155
7.1.1 Introduction	155
7.1.2 General Geology	156

Date

September 22, 1981.

Signature

Fernand N. G. Zuehlke

NL-91 (4/77)

Host Rocks	156
Structure	158
7.1.3 Orebodies	159
7.1.4 Petrography	159
7.1.5 Geochemistry	162
7.2 Quebec Sturgeon River Mines Ltd. - Gold Deposit	168
7.2.1 Introduction	168
7.2.2 General Geology	170
7.2.3 Orebodies	172
7.2.4 Petrography	172
7.2.5 Geochemistry	175
7.3 Soquem Lté. - Base Metal Prospect	181
7.3.1 Introduction	181
7.3.2 General Geology	182
7.3.3 Orebodies	183
7.3.4 Petrography	185
7.3.5 Geochemistry	188
8. DISCUSSION	193
8.1 Introduction	193
8.2 Stratigraphy	195
8.3 Petrology	201
8.3.1 Platform Sequence	202
8.3.2 Domal Sequence	206
8.4 Geochemistry	207
8.4.1 Platform Sequence	208
8.4.2 Domal Sequence	216
8.5 A Model for the Evolution of the Bachelor Lake Region	219
8.5.1 The Crust in the Early Archean	219
8.5.2 Greenstone Belts	220
8.5.3 The Model	221
Creation of a Platform Sequence	221
Creation of a Domal Sequence	224
Evolution of Greenstone Belt Magmatism	225
8.5.4 Structural Features of Greenstone Belt Orogenesis	230
8.6 Relationship of Orebodies to Archean Volcanic Belts	235
8.6.1 Ore Deposits of the Lower Platform Sequence	235
8.6.2 Ore Deposits of the Upper Platform Sequence	240
8.6.3 Ore Deposits of the Domal Sequence	243
Introduction	243
Coniagas Massive Sulphide Deposit	243
Speculations on the Genesis of Massive Sulphide Ores	247
Guides to Base Metal Exploration	249
8.6.4 Ores of Uncertain Stratigraphic Location	253
QSRML Gold Property	253

Soquem Base Metal Property	254
9. SUMMARY AND CONCLUSIONS	257
9.1 Conclusions	257
9.2 Suggestions for Further Work	265
Appendix	page
A. PREPARATION AND ASSESSMENT OF PELLETS	266
9.1 Preparation of Pressed Powder Pellets	266
9.2 Fusion as an Alternative to Pressed Powders	268
B. CORRECTION OF ANALYTICAL DATA	271
9.1 Correction for Background Effect	271
9.2 Correction for Interelement Interferences	272
9.3 Correction for Mass Absorption	274
9.4 Construction of Calibration Curves	279
C. PETROGRAPHIC DATA FOR THE BACHELOR LAKE AREA	284
D. HARKER VARIATION DIAGRAMS - BACHELOR LAKE GEOCHEMISTRY	295
E. GEOCHEMICAL DATA FOR THE BACHELOR LAKE AREA	315
REFERENCES	324

LIST OF FIGURES

Figure	page
1.1 Location of the Bachelor Lake Volcanic Complex	3
2.1 Calibration Curve for Determination of Ferrous Iron	14
3.1 Peacock (1931) Rock Series Classification	35
3.2 Harker-type Variation Diagram (after Barth, 1962)	41
3.3 Larsen Variation Diagram, San Juan Mts. Colo. (after Barth, 1962)	42

3.4	Nockold & Allen Diagram, Thingmuli Series (after Carmichael, Turner & Verhoogen, 1974)	43
3.5	Al ₂ O ₃ vs FeO/(FeO + MgO) Diagram	48
3.6	World Archean Mafic-Ultramafic Rock Suites on the Al ₂ O ₃ vs FeO/(FeO + MgO) Diagram	50
3.7	Calc-alkaline & Tholeiitic (Gabbroic) Trends a) Comparison of Features b) Location on an AFM Diagram (after Meuller, 1977)	53
3.8	Pearce (1975) Tectonic Environment Diagram	54
3.9	Church (1975) Volcanic Rock Classification Diagram	58
3.10	Jensen (1976) Volcanic Rock Classification Diagram	61
3.11	Distribution of Bachelor Lake Samples on the Jensen Diagram	62
3.12	Modified Irvine-Baragar (1971) Classification Flow-Chart for the Bachelor Lake Suite	67
3.13	Silica Screen for Common Volcanic Rocks	68
4.1	Volcanic Complexes - Abitibi Belt (after Goodwin & Ridler, 1971)	77
5.1	Simplified Geology of the Bachelor Lake Region . .	80
6.1	Whole Bachelor Lake Region - Alkali-Silica Variation For Fresh Rocks	118
6.2	Whole Bachelor Lake Region - AFM Diagram a) All Samples b) Area Means	119
6.3	Whole Bachelor Lake Region - Church-Murata Diagram	121
6.4	Whole Bachelor Lake Region - Pearce Diagram . .	122
6.5	Whole Bachelor Lake Region - Naldrett Plot a) All Basalts b) Means for Geographic Areas	123
6.6	Whole Bachelor Lake Region - Harker Variation Diagram	125
6.7	Harker Variation Diagram for Daly's (1933) & Nockold's (1954) Average Composition for Phanerozoic Rocks	126
6.8	AFM Diagrams for a) Area 1 and b) Area 2	128

6.9	Church-Murata Diagram - Area 1	129
6.10	Pearce Diagram - Area 1	130
6.11	Naldrett Diagram a) Area 1 b) Area 2	131
6.12	AFM Diagram - Subareas a) 2a b) 2b	133
6.13	AFM Diagram - Subareas a) 2c b) 2d	134
6.14	Church-Murata Diagram - Area 2	136
6.15	Pearce Diagram a) Area 2 b) Area 3	137
6.16	Naldrett Diagram - Subareas a) 2a b) 2b	138
6.17	Naldrett Diagram - Subareas a) 2c b) 2d	139
6.18	AFM Diagram a) Area 3 b) Area 4	141
6.19	Church-Murata Diagram - Area 3	142
6.20	Naldrett Diagram a) Area 3 b) Area 4	144
6.21	Church-Murata Diagram - Area 4	146
6.22	Pearce Diagram a) Area 4 b) Area 5	147
6.23	AFM Diagram - Area 5	149
6.24	Church-Murata Diagram - Area 5	150
6.25	Naldrett Diagram - Area 5	151
7.1	Coniagas Mine Cross- Section (after Coniagas Ann. Rept., 1967)	157
7.2	Coniagas Minesite - Sketch Plan & Sample Locations	161
7.3	Coniagas Minesite Geochemistry a) Alkali-Silica b) AFM Variation	164
7.4	QSRML Gold Deposit - 1st Level Plan	171
7.5	Alkali-Silica Diagrams a) QSRML b) Soquem Properties	176
7.6	AFM Diagrams a) QSRML b) Soquem Properties	178
7.7	Soquem Property Map	184
8.1	Relationship of Volcanosedimentary Belts to the Kapuskaing Feature (after Kalliokoski, 1968)	194

8.2	Major Chemical Trends in the Noranda Complex . .	215
8.3	SiO ₂ Frequency Distribution for Selected Volcanic Sequences	217
8.4	Schematic Illustration of Greenstone Belt Evolution (mod. after Gorman et al., 1978)	223
8.5	Structural Features formed by Greenstone Belt Orogenesis (after Gorman et al., 1978)	233
8.6	Major Fault Systems in the Abitibi Belt a) Jolly, 1976 b) Kalliokoski, 1968)	234
8.7	Geology of Ore Deposits - Noranda Region (after Spence & deRosen Spence, 1975)	246
8.8	Wallrock Alteration in Massive Sulphide Deposits a),b) (after Gannicott et al., 1979) c) (after Sangster, 1976)	251
B.1	Calibration Curves Used in This Study	281

LIST OF TABLES

Table	page
2.1	XRF Operating Parameters for Bachelor Lake Analyses 12
2.2	Repeatability on the Analytical Normalizer 17
2.3	Comparison of Three Rotation Methods in Factor Analysis 27
3.1	Corren's (1969) Mineral/SiO ₂ Classification of Igneous Rocks 31
3.2	Niggli Values for the Wurmberg Granite, Germany (after Correns, 1969) 37
3.3	Mineral Composition and CIPW Norm - Wurmberg Granite 39
5.1	Number of Samples of each Rock Type Collected in the Bachelor Lake Region 81
6.1	Geochemical Statistics for Bachelor Lake Data . . . 116

6.2	Summary of Geochemical Variation Diagrams	153
7.1	Significant Geochemical Differences Between Rock and Alteration Types a) Coniagas Minesite b) QSRML	165
7.2	Coniagas Geochemistry - Summary Statistics	166
7.3	Quebec Sturgeon Geochemistry - Summary Statistics	179
7.4	Significant Geochemical Differences Between Rock and Alteration Types in the Soquem Deposit	190
7.5	Soquem Property Geochemistry - Summary Statistics	191
8.1	Quartz-Olivine Normative Ratios For Bachelor Lake Areas	203
8.2	Factor Analysis Summary - Mineralogy & Chemistry	209
8.3	Factor Analysis Summary - Chemistry	210
8.4	Selected Metal Ratios for Potential Host Rocks of Ni- sulphide Deposits	239
A.1	Comparison of XRF Data using Fused Discs and Pressed Powder Pellets	270
B.2	Suggested Operating Parameters (after Allman & Lawrence, 1972)	273
B.3	Variation of Count Rate with Wavelength & Matrix (after Salmon, 1964)	276
B.4	Oxide Coefficients Used for Mass Absorption Correction	278
B.5	International Rock Standards	280

The change in volcanic style is intricately tied to a corresponding progression of ore metals. Geothermal

- v -

Chapter 1

INTRODUCTION

1.1 PURPOSE OF STUDY

The purpose of this study is to examine the anatomy of a typical Archean greenstone belt and to illustrate the relationships between its petrography, geochemistry and structure. Many petrochemical studies, prior to instigation of this project, were made either on a limited area, such as several hundred meters around minesites (i.e. Sakrison, 1966; Adams, 1971; Davenport, 1972; Spitz, 1973) or on an extensive area covering several thousands of square km. (i.e. Eade et al., 1971; Descarreaux, 1973). Thus, either sample density or area covered have approached extremes. Also, many large and small scale geochemical investigations have described trends relating to surficial material but not to the petrologic characteristics of the bedrock (i.e. Pollock et al., 1960; Dreimanis, 1960; Donovan et al., 1967; Hawkes, 1970; Garrett, 1971). This study attempts to interpret regional trends of a moderate-sized region (1500 sq.km.) through sufficiently concentrated sample density to monitor sequential variations in petrographic and chemical parameters. The intention was not to perform detailed mapping, but to obtain samples of major units, along several

sections across the volcanic belt, with a sample spacing of approximately 150 m.

It is difficult to classify Archean volcanic rocks because most classification schemes were devised for unmetamorphosed rocks. The writer therefore reviews various classification methods to determine the most appropriate one(s) for metamorphosed greenstone belts.

The area chosen was selected because little geologic work had previously been done, outcrops are relatively abundant, and two ore deposits are associated with the volcanic complex: the Coniagas zinc-lead-silver deposit and the Quebec Sturgeon River gold deposit. Drill core was also available (Soquem Lté) from a sub-economic zinc-copper prospect. Results of the study could then be related to these deposits and possibly form new ideas to aid in mineral exploration.

1.2 LOCATION, ACCESS AND TOPOGRAPHY

The area of study is located in the Abitibi-East electoral district of northwestern Quebec, at longitude 75°40'-76°40'W and latitude 49°10'-49°50'. It is situated approximately halfway between Senneterre and Chibougamau and is centered on the village of Desmaraisville (Fig. 1.1).

A paved road, Quebec Highway 113, bisects the area and provides the main access. A branch of the CNR from the main

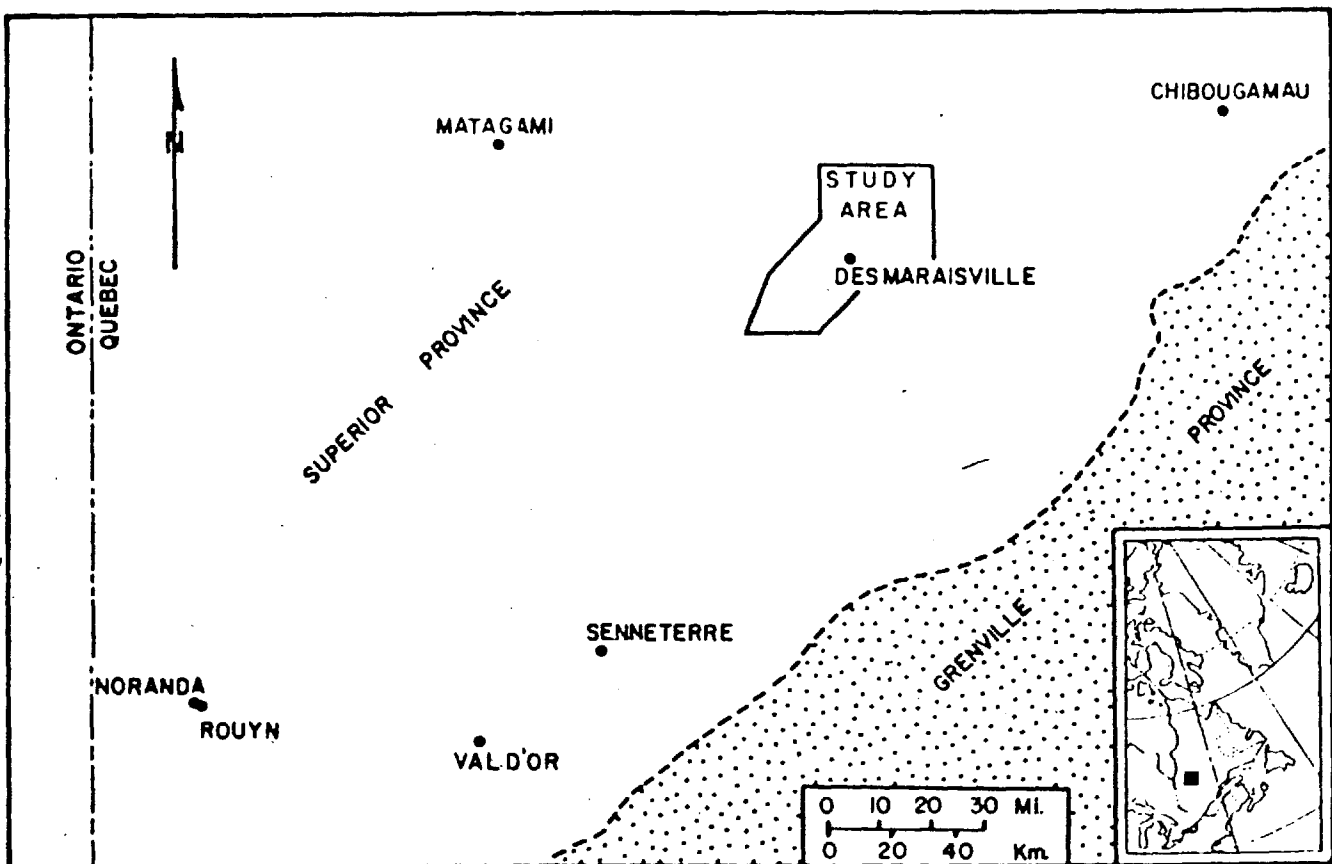


Figure 1.1: Location of the Bachelors Lake Volcanic Complex

line near Senneterre also cuts the region. Numerous small lakes can accommodate float-equipped bushplanes but are not generally required as reasonable land routes extend to most areas.

The region is generally flat, with scattered low, rolling hills. Relief is greatest in localized areas of intrusive rock masses. Most streams become intermittent as the summer season progresses, at which time the larger rivers become unnavigable due to rapids and debris.

Timber is thick and consists mainly of spruce, poplar and birch. It is mostly second growth, due to forest fires and logging. This results in heavy brush in certain areas but also provides good access along abundant feeder trails. These paths have not been maintained for several years and a rugged bush vehicle is required for deep penetration.

Outcrop is reasonably abundant in the south but is scarce north of the Bachelor River. Best exposures occur along major lakes and rivers. Pleistocene sand plains are common to the east, but, in general, glaciofluvial deposits are not thick.

1.3 PREVIOUS WORK

Much of the mapping in this part of Quebec was done before the road or railway were built. The significance of some geologic features, such as pillow structure, were not

recognized by these early workers, but valuable information is provided by outlined outcrop areas and general structure.

G.Shaw (1939) filed a preliminary report on the Opawica and Lewis Lakes area that furnishes the only published data for the extreme eastern part of the area. The western townships have been mapped by G.S.MacKenzie (1934) and J.C.Sproule (1940). Central areas have been mapped by W.W.Longley (1951), R.B.Graham (1957), J.A.MacIntosh (1967), M.Van de Walle (1970), and J.Dugas, (1950, 1975). Unpublished company reports (R.Doucet, 1973; Dumont, 1959) have provided other valuable information. Discovery of the O'Brien gold deposit (later Quebec Sturgeon River Mines Ltd.) in 1946 resulted in a staking rush to the district. The next year, Dome Exploration discovered a zinc-lead deposit (later Coniagas Mines Ltd.) one kilometer to the west. Through these discoveries, the region became a focal point of exploration in the ensuing years, but other commercial deposits were not found.

Chapter 2

FIELD AND ANALYTICAL METHODS

2.1 FIELD METHODS

Mapping was done along all roads and trails in the area, and along three 8 to 25 km. long cross-sections that are located 10 to 15 km. apart. Access along the cross-sections was by road, canoe and pace and compass traverses. Field data was plotted on air photographs and transferred to 4 mile to the inch base maps. The photographs used were National Air Photo Library 1946 (1"=4166') series from 1:250,000 Federal Topographic Map NTS 32F (Waswanipi) and 32G (Chibougamau). The 1946 series was too old to show new roads, trails and vagrant geography, such as beaver marshes, but this low altitude survey does show clearer topographic features than the higher 1970 survey. Unavailable at the time of mapping, in the summer of 1974, were a 1974 NAPL series (1"=4466') which covers a large portion of the central area, and an extensive Quebec Department of Lands and Forests survey of 1965 (1"=1320').

Outcrop locations from published reports and maps proved invaluable in choosing sampling locations. Duplicate specimens were collected from 305 sample locations. One sample from each location was kept in case anomalous results

3.3.4 Harker Diagram	38
3.3.5 Larsen Diagram	40
3.3.6 Alkalies vs Silica Diagram	44

needed to be checked. In all cases, an attempt was made to obtain samples representative of the outcrop. Fresh samples were collected whenever possible, and separate samples taken where weathering accentuated textural or structural features. A relatively large sample size (5kg) was used to provide sufficient material for thin section slabs, analytical powder and a retained specimen.

An additional 140 samples were collected from underground workings, drill cores and outcrops near mineralized areas. Sample intervals of 20 meters or less were used to allow better definition of the effects of the ore-bearing solutions upon wallrocks.

2.2 SAMPLE PREPARATION

2.2.1 Crushing, Grinding and Sieving

Field specimens were examined and weathered material removed with a hammer or diamond saw. A slab was then cut for thin section preparation, and one half of each rock was retained for reference, while the other half was set aside for pulverization. Wherever possible, veined or altered material was removed.

The sample was first passed through a jaw crusher containing hardened steel jaws. Contamination at this stage would not seem to be a problem, for, as Volborth (1969, p.17) states, "pounding on a rock with a hammer, similar

7.1 Coniagas Mines Ltd. ~ Base Metal Deposit . . .	155
7.1.1 Introduction	155
7.1.2 General Geology	156

action with a steel mortar and pestle, or even a jaw crusher does not constitute a major source of contamination as long as twisting or turning motions are avoided". Material less than one millimeter diameter was sieved and discarded during this initial crushing to remove any fine bits of jaw plate that spalled off on impact. Oversize particles were then recrushed to obtain a maximum size of ten millimeters.

No magnetic separation was attempted at this or other stages of pulverization, since insignificant metal contamination was expected to remain in the plus one millimeter fraction, and magnetic separation would also remove magnetite, pyrrhotite, and ilmenite grains.

The crushed sample was then passed through a disc mill equipped with hardened steel plates. Steel, rather than ceramic plates were used because the latter introduce considerable alumina and trace amounts of silica, calcium, barium, magnesium, rubidium and zinc (Volborth, 1969). Steel plates do not contribute any elements that were determined as traces but could be a source of some iron and possibly titanium. However, it appears to be the best overall approach, and the small amount of addition should be roughly the same for all samples.

All powders were reduced to -200 mesh (74 μ). Particles of this size are acceptable for X-ray fluorescence studies, and further grinding could cause lattice problems

in x-ray diffractometry patterns. As Easton (1972, p.62) suggests, "as a rule, the analysis sample should be crushed and ground to the coarsest powder required -- for the attack used -- needless fine grinding is not only a waste of time but may also lead to chemical changes in the sample -- expelling water of crystallization, or air-oxidation of the ferrous iron or sulphide material".

2.2.2 Preparation of Pellets

Approximately 1.5 gms. of sample powder (-200mesh) was manually mixed with 0.25 gms. of Somar cellulose binding powder. Allman & Lawrence (1972, p.243) report that the binding agent has little effect on count rates, even for elements lighter than potassium, as long as the sample-binder ratio is constant.

The mixture was placed in a steel die with highly polished, chrome-plated surfaces, lightly packed, and surrounded with boric acid backing material. This was then compacted in a hydraulic press at 12 tons/sq.in. (2000 kg/cm²) for one minute and gradually decompressed. Final thickness of the pellet powder was at least 1-2 mm. As the depth of penetration of x-rays is only a few thousandths of a centimeter (Shalgosky, 1960, p.134), these discs can be considered "infinitely thick", and are capable of generating maximum secondary radiation for counting. All samples were compacted to the same degree since variation would cause

- xiv -

fluctuation in count rates. A pressure of 12 tons/sq.in. should achieve 99.5% of the count rate available.

Further discussion of pressed pellets is found in Appendix A.

2.3 ANALYTICAL TECHNIQUES

A total of 318 samples were analysed for Si, Al, Fe, Mg, Ca, Na, K, Ti, Mn, P, S, Ba, Rb, Sr, Cu, Zn, Co, and Ni, using x-ray fluorescence spectrometry (XRF). Ferrous oxide was determined by titration. Semi-quantitative x-ray diffraction analysis (XRD) was done on all samples.

2.3.1 X-ray Spectrometry

Chemical analysis was done using a Philips PW1450 automatic sequential XRF spectrometer. This technique has become the most efficient method for rapid and precise determination of large amounts of geochemical data. Corrections for background effects, interelement interference and mass absorption are described in Appendix B.

Parameters used for analysis of the Bachelor Lake samples are shown in Table 2.1 . Analysis of major elements was performed separate from the trace elements, and standard samples run before the unknown samples, to obtain calibration curve intensity data. Two standard samples were

run a number of times between batches of unknowns in order to check on reproducibility of the analyses.

For detailed discussion of the principles of XRF spectrometry, the reader is referred to Shalgosky (1960), Norish and Chappell (1967), Jenkins and DeVries (1967), Leake et al. (1970), Wanerdi (1971), Allman & Lawrence (1972), and the bibliographical review in Analytical Chemistry (X-ray Absorption and Emission), published in biennial issues.

2.3.2 Ferrous Oxide Determination

Iron analysis by XRF spectroscopy is given as Fe2O3t. The ferrous iron content is needed for certain geochemical applications such as normative calculations and some variation diagrams.

Determination of ferrous iron was done by decomposing powdered samples in a 5ml. 50% H2SO4, 5ml saturated boric acid solution, 5ml 85% phosphoric acid and 4 drops diphenylamine sulphonate. Titration was then immediately performed with dichromate solution until the pure green colour changed to grey-green. Then dichromate solution was added drop by drop until a purple hue appeared.

Results of 24 samples from a wide compositional range of Fe2O3t are shown in Fig. 2.1 The relatively high linearity of the curve suggests that little post-

XRF Operating Parameters for Bachelor Lake Analyses

TABLE 2.1

A) Major Elements								
El. ^a	At. Wt.	Goniom. 2θ Position	Crystal Order	Det.-Coll. ^{**}	KV	MA	Preset Counts	Preset Time (sec.)
Si	28.09	09.18	Pet	F-C	50	45	1,000,000	out
Ti	47.90	77.33	LiP	F-F	50	45	100,000	out
Al	26.98	45.15	Pet	F-C	50	45	100,000	out
Fe(t)	55.85	51.68	LiP	F-C	50	45	100,000	out
Mn	54.94	62.92	LiP	F-C	50	45	100,000	out
Mg	24.31	36.73	ADP	F-C	50	45	20,000	out
Mg(b)		35.73	ADP	F-C	50	45	20,000	out
Ca	40.08	61.87	QE	F-C	50	45	100,000	out
Na	22.99	54.95	Rap	F-C	50	45	10,000	out
Na(b)		53.45	Rap	F-C	50	45	10,000	out
K	39.10	50.65	Pet	F-C	50	45	100,000	out
P	30.97	40.98	QE	F-C	50	45	10,000	out
P(b)		38.98	QE	F-C	50	45	10,000	out
B) Minor Elements								
S	32.06	75.84	Pet	F-C	50	45	out	40
S(b)		73.84	Pet	F-C	50	45	out	40
Co(b)		52.27	LiP	S-C	50	30	out	40
Co	58.93	52.80	LiP	S-C	50	30	out	40
Co(b)		53.25	LiP	S-C	50	30	out	40
Ba(b)		84.22	LiP	F-F	60	45	out	40
Ba	137.34	87.22	LiP	F-F	60	45	out	40
Ba(b)		90.22	LiP	F-F	60	45	out	40
Sr(b)		24.55	LiP	S-F	90	30	out	40
Sr	87.62	25.20	LiP	S-F	90	30	out	40
Sr-Rb(b)		25.65	LiP	S-F	90	30	out	40
Rb	85.47	26.65	LiP	S-F	90	30	out	40
Rb(b)		27.15	LiP	S-F	90	30	out	40
Zn(b)		41.45	LiP	S-C	90	30	out	40
Zn	65.37	41.82	LiP	S-C	90	30	out	40
Zn(b)		42.55	LiP	S-C	90	30	out	40
Cu	63.55	45.03	LiP	S-C	90	30	out	40
Cu(b)		47.05	LiP	S-C	90	30	out	40
Ni	58.71	48.67	LiP	S-C	90	30	out	40

^a (b) - Background position

^{**} F - Flow Counter S - Scintillation Counter C - Coarse F - Fine

depositional oxidation has occurred in the volcanic rocks and thus the curve is used to interpolate ferrous values for all other samples.

2.3.3 X-ray Diffraction Analysis (XRD)

Extensive use of XRD analysis was made in the present study as an aid in determining mineralogical constituents, especially in fine-grained, altered rocks.

Diffractograms of whole-rock powders were run for all samples through diffraction angles of 2-70° and relative peak intensities were measured. Although it was realized that the more abundant phases in such complex mineral assemblages tend to decrease the intensity of minor phases, the four or five most abundant minerals in each sample were detected, and their relative peak intensities used to indicate high, moderate and low mineral abundances. These values were checked by examining thin sections. Results of the XRD analyses of each sample are included in Appendix C.

Determination of An content of plagioclase was done using the method outlined by Smith (1956) and Smith and Yoder (1956). This technique is based on measurements of 2θ angle differences between any one of the following three pairs of diffraction peaks: (111)-(1 $\bar{1}$ 1), (131)-(1 $\bar{3}$ 1), or (1 $\bar{3}$ 2)-(131). The method works well for low temperature plagioclase in the An 0 to 40 range. However, the (1 $\bar{1}$ 1) and

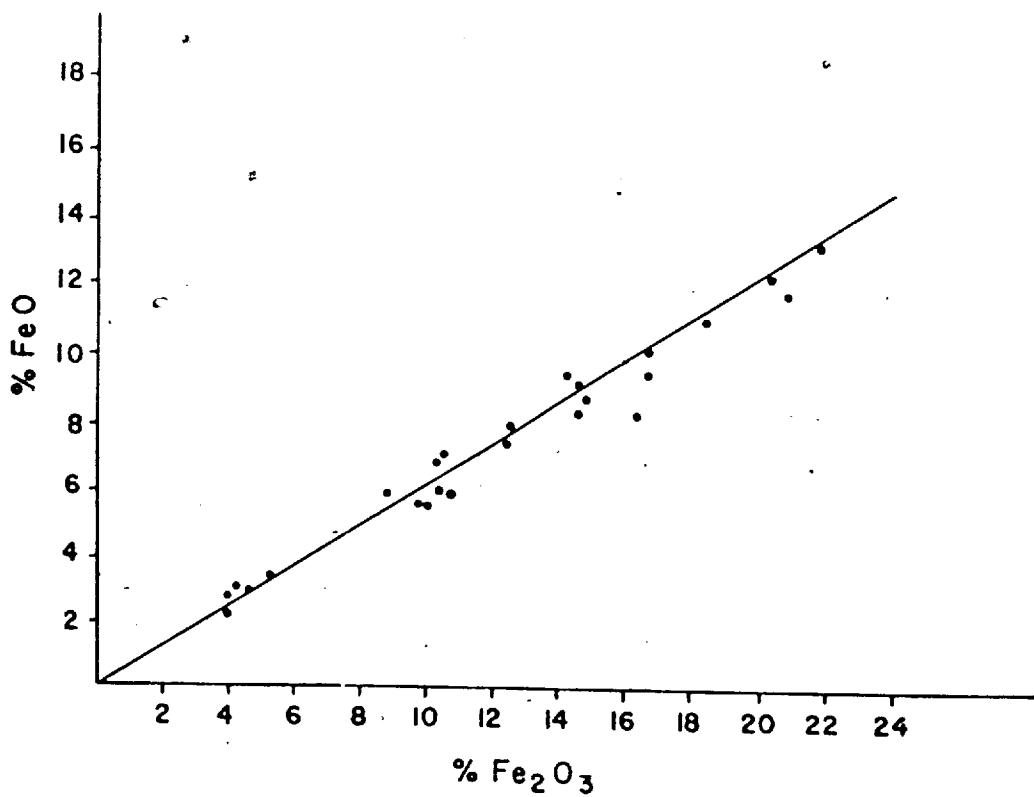


Figure 2.1: Calibration Curve for Determination of Ferrous Iron

(131) peaks are usually very weak, and can therefore only be identified when plagioclase is very abundant in the rock. The advantage over the Michel-Levy method, which uses extinction angles, is that An contents can be obtained for very fine grained, untwinned plagioclase.

An additional XRD technique in this study was the use of Debye-Scherrer powder cameras for identification of single mineral grains. It was found that, using a diamond-tipped scribe, very small grains could be powdered on the surface of a thin section and picked up on a glass spindle mount dipped in a non-diffracting medium. This technique was particularly useful for fine-grained and skeletal opaque minerals and for fine-grained translucent minerals on which optical properties were difficult to measure.

2.3.4 Evaluation of Analytical Methods

Most components of analytical evaluation can be dealt with under the terms: precision, the extent to which results scatter about the mean value; accuracy, the extent to which an analysis can give a true value; and sensitivity, or, lower limit of detection.

Precision can be separated into repeatability, where the sample is reanalysed in the same position, and, reproducibility, where the whole analysis is repeated using the same or subsequent preparation of a particular sample.

The former can be measured as a standard deviation of a series of results made at approximately the same time. It is used mainly to assess stability of the instrumental technique and is not reported by most investigators. Some variability involved in repeatability is negated by use of a counting standard (normalizer) against which all unknowns are ratioed. A normalizer was used for the present study and an evaluation of its repeatability is provided in Table 2.2. It should be noted that calculations in this table are based upon counts ratioed against a normalizer, as opposed to mean counts per second in some repeatability estimates.

Reproducibility varies for both the chemical element under consideration and for the level of concentration of the element. In general, major elements were found to vary a maximum of +2% (>10% conc.) and +15% (0.1 - 10% conc.), and trace elements varied a maximum of +10% (>50ppm), +50% (20-40ppm), and +100% (<20ppm), all taken at the 99% confidence level. It can be seen that reproducibility deteriorates rapidly at low element concentrations (i.e. < 50ppm).

Accuracy, the bias between the analysis and the true value depends to a large degree on the quality and assessment of calibration reference standards. Most researchers employ international standard rock powders when

TABLE 2.2
Repeatability on the Analytical Normalizer

Standard: G2 (Granite)

Element	No. Rep.	Time (sec.)	Mean CPS	Std. Dev.	Var.	Coeff. of Var.	Std. Error
SiO ₂	20	40	25712	75.6	5717	0.29	16.91
Al ₂ O ₃	20	40	3599	49.6	2456	1.38	11.09
Fe ₂ O ₃ t	20	40	12895	21.1	447	0.16	4.73
MgO	20	100	50	0.9	1	1.80	0.20
CaO	20	40	2375	11.1	123	0.47	2.48
Na ₂ O	20	100	156	6.1	37	3.91	1.36
K ₂ O	20	20	36509	44.6	1985	0.12	9.26
TiO ₂	20	20	7152	18.1	330	0.25	4.07
MnO	20	40	145	1.9	4	1.31	0.44
P ₂ O ₅	20	100	27	0.5	0	1.85	0.11

Standard: AGV-1 (Andesite)

Element	No. Rep.	Time (sec.)	Mean CPS	Std. Dev.	Var.	Coeff. of Var.	Std. Error
SiO ₂	20	40	21657	52.7	2781	0.24	11.79
Al ₂ O ₃	20	40	4606	58.9	3471	1.28	13.17
Fe ₂ O ₃ t	20	40	32058	37.6	1417	0.12	8.41
MgO	20	100	85	0.8	1	0.94	0.13
CaO	20	40	6158	12.7	162	0.21	2.84
Na ₂ O	20	100	159	1.4	160	0.89	0.31
K ₂ O	20	20	24561	31.3	981	0.13	7.00
TiO ₂	20	20	15771	31.1	970	0.20	6.97
MnO	20	40	311	2.1	5	0.68	0.47
P ₂ O ₅	20	100	91	0.6	0	0.66	0.13

calibrating instruments for geochemical analysis. A selection of these were used for the present study and are listed by source and generally accepted composition in Appendix B. Values in the tables are those listed by Abbey (1974, 1977) and Lachance (per.comm.). A discussion of the controversies surrounding accepted values is provided in the papers by Abbey.

Overall accuracy in concentration determinations is dependent upon the accuracy with which both peak and background can be determined. This factor is increasingly important as the sensitivity, or, lower detectability limit is approached, since, as the number of counts for a peak approach that of background, sensitivity similarly decreases. Thus, a researcher must select optimum counting times (see Tables 2.2, B.2) which will yield the required high levels of precision for most concentrations, yet sacrifice precision below a certain minimum concentration. Counting errors at these low concentrations could be reduced by higher overall counting times, but would not provide optimization on an automated spectrograph. This sensitivity is largely a function of counting statistics and Jenkins et al.(1973) have shown that, at low elemental concentrations, detection limits for certain precision depend mainly upon the counting times. In general, the coefficient of variation (V), or, relative standard deviation increases at lower counting rates. Jenkins discusses this phenomenon in detail, along with several examples.

For more detailed treatment of XRF precision, the reader is referred to the excellent treatment by Leake et al.(1970).

2.4 STATISTICAL EVALUATION OF DATA

Extensive use of computerized modeling was used to interpret geologic data. Programmes were developed by the author, and a series of packaged programmes was also used (Nie et al., 1975). For information on the statistical manipulation of data, the reader is referred to Nie et al.(1975), Davis (1973), Dixon et al.(1969) and Ostle (1969).

The geologic data in this study consists of analyses of 318 samples for 18 elements, relative abundances of 9 modal and 8 normative minerals, 9 rock types, 3 alteration intensities and other petrographic information such as rock color, penetrative deformation and primary fragmentation.

2.4.1 Correlation Analysis

Bivariant correlation allows a single number, the correlation coefficient, or, a value that summarizes the relationship between two variables, to be calculated. These coefficients indicate the degree to which variation (i.e. change) in one variable is related to variation in another. Such correlations summarize not only the strength of association between a pair of variables, but also allows a

simple means of comparison of the strength of relationship between one pair of variables and a second pair. Naturally, there is some loss of detail, with respect to tabulations or graphical plots, but as in any method of summarization the technique delineates major strengths and trends between the variables. The objective of correlation analysis, then, is to determine the extent to which variation in one variable is linked to variation in the other.

One method of assessing this strength of relationship is through the calculation of Pearson product-moment correlations for pairs of variables. Here, the Pearson correlation coefficient, r , is used to measure the linear strength between two interval-level variables and indicates both the closeness of fit of a linear regression line to the data, and, when r is squared, the proportion of variance in one variable, explained by the other. Variance is a measure of variability, or, lack of homogeneity in a variable. When analyses cluster close to the mean, the variance will be small and increases as the values spread out. Mathematically, r is defined as the ratio of covariation to square root of the product of the variation in two variables, X and Y , and corresponds to the formula:

$$r = \frac{\sum_{i=1}^N (x_i - \bar{x})(y_i - \bar{y})}{\left\{ \left[\sum_{i=1}^N (x_i - \bar{x})^2 \right] \left[\sum_{i=1}^N (y_i - \bar{y})^2 \right] \right\}^{1/2}}$$

where X_i = i th observation of variable X
 Y_i = i th observation of variable Y
 N = number of observations
 $\bar{X} = \sum_{i=1}^N X_i / N$ = mean of variable X
 $\bar{Y} = \sum_{i=1}^N Y_i / N$ = mean of variable Y

This formula can be restated by dividing the numerator by $N-1$ to show that the correlation coefficient can also be defined as the covariance in X and Y divided by the product of their standard deviations. The covariance in X and Y is defined as:

$$\frac{\sum_{i=1}^N (x_i - \bar{X})(y_i - \bar{Y})}{N-1}$$

The actual formula used in computing the correlation coefficients is:

$$r = \frac{\sum_{i=1}^N x_i y_i - (\sum_{i=1}^N x_i)(\sum_{i=1}^N y_i) / N}{\left\{ \left[\sum_{i=1}^N x_i^2 - (\sum_{i=1}^N x_i)^2 / N \right] \left[\sum_{i=1}^N y_i^2 - (\sum_{i=1}^N y_i)^2 / N \right] \right\}^{1/2}}$$

A matrix of correlation coefficients, for the elements analysed, was produced for each main stratigraphic area. Within each matrix, those variables with strong co-

relationship were noted and a cut-off value of 60 per cent was established as being the lower level of significance. From these matrices, a comparison could be made concerning those elements with strong concomitant variation. The matrices were subsequently used in factor determinations (see next section).

A second method of estimating the degree of correspondence between variables is by construction of scattergrams, as illustrated in Appendix D. This is really a visual display of the correlation of an entire population for two variables. Often, statisticians attempt to fit a line to such graphs, based on the "least-squares regression" technique. The method assumes that a best-fitting (regression) line can be constructed, with vertical distance of all points from the line minimized. Thus, for any point on a curved or straight regression line, the amount of error (incomplete accountability) would be the vertical distance from the point to the line. The general formulae for linear and curvilinear or polynomial regression lines, respectively, are:

$$Y = A + BX$$

$$Y = A + B_1X_1 + B_2X_2 + \dots + B_nX_n$$

where A is the Y co-ordinate (vertical) intercept
B is the slope of the line

When A and B are calculated by least squares regression, m is termed the regression coefficient. For most

distributions, it is unusual to find a regression line, especially a linear one, that exactly fits the data. A measure of degree of fit to the regression line is called for and is served, for linear regression by the Pearson product-moment correlation coefficient (r). When a poor fit occurs, r is close to zero; a close fit allows r to approach +1.0 or -1.0 (depending on the slope of the regression line). The value for r ($\times 100$) is included on each scattergram in Appendix D to show the degree of linear correlation. It should be noted, however, that this value in no way deals with any non-linear correlation. In such instances, curvilinear or polynomial regression would be required to best-fit a curved line to the data. For purposes of the present study, however, non-linear trends are simply compared to the previously mentioned "average" curves.

2.4.2 Factor Analysis

For capability of data reduction, one of the most powerful techniques is provided by factor analysis. This procedure creates a minimum number of new variables which are linear combinations of the original ones, such that the former contain the same amount of information. It is a foil, in this respect, to discriminant analysis, which, as discussed in the next section, derives functions relating to differences in the population. But the methods are complex

and, in places, include mathematical and statistical premises that are still controversial in theoretical, if not practical, aspects. Thus, the application of the various factoring techniques requires an awareness of their inherent shortcomings. Discussion of these problems as well as an explanation of the methods can be found in Joreskog, 1976; Davis, 1973; Kim, 1975; Rammel, 1967; and Rozeboom, 1966.

The intention of factor analysis is to determine an underlying pattern of relationships in the data, such that this new data may be reduced to a smaller set of "factors" or components which will account for the observed interrelations. Three main steps are involved in the calculations:

1. preparation of a correlation matrix
2. extraction of initial factors
3. rotation to a terminal solution

The first step involves the measurement of association for relevant variables. Here, the correlation can be made between variables (R-factor analysis), as in the present study, or between units such as rock groups (Q-factor analysis). A correlation matrix is the most efficient input for factor analysis and can be modified by adding or subtracting component variables.

The second step, constructing new variables based on interrelations in the data, may define the variables as

exact mathematical transformations of the data (Principal-component analysis), used in this study, or inferential assumptions on the source or structure of the variables (Orthogonal-component analysis).

Finally, the new set of factors which are not readily interpretable, are mathematically rotated about reference axes to emphasize variables with strong relationships and diminish the significance of lesser ones. Unfortunately, there are many ways to define the underlying dimensions in the same set of data and there is no unique and best accepted solution. A variety of rotational methods are possible, falling into two main categories, orthogonal (mathematically simple; pattern and structure matrices are identical) and oblique (empirically more realistic; different pattern and structure matrices).

Actual calculation of the final scores is complex and the methods and intricacies are to be found in the previously mentioned references. Suffice to say that, for this study, the approach taken was:

1. Pearson Product-Moment Correlation Matrix
2. Principal Component Analysis
3. Orthogonal Factor Rotation

The Principal Component method of factor extraction is the most widely accepted factoring method (Kim, 1975, p.480). Several rotational methods were applied to determine

A) Max	El.	B) Min
Li	Li	Li
Na	Na	Na
K	K	K
Rb	Rb	Rb
Cs	Cs	Cs
Ag	Ag	Ag
Cu	Cu	Cu
Pb	Pb	Pb
Bi	Bi	Bi
Te	Te	Te
Se	Se	Se
As	As	As
Sb	Sb	Sb
Sn	Sn	Sn
Ge	Ge	Ge
Al	Al	Al
Fe	Fe	Fe
Mn	Mn	Mn
Zn	Zn	Zn
Co	Co	Co
Ni	Ni	Ni
Cd	Cd	Cd
Hg	Hg	Hg
Ca	Ca	Ca
Sr	Sr	Sr
Ba	Ba	Ba
Pt	Pt	Pt
Au	Au	Au
Ir	Ir	Ir
Os	Os	Os
W	W	W
Mo	Mo	Mo
Ta	Ta	Ta
Nb	Nb	Nb
Th	Th	Th
U	U	U
Pa	Pa	Pa
Ac	Ac	Ac
La	La	La
Ce	Ce	Ce
Pr	Pr	Pr
Nd	Nd	Nd
Pm	Pm	Pm
Sm	Sm	Sm
Eu	Eu	Eu
Gd	Gd	Gd
Tb	Tb	Tb
Dy	Dy	Dy
Ho	Ho	Ho
Er	Er	Er
Tm	Tm	Tm
Yb	Yb	Yb
Lu	Lu	Lu

chemical factors as a whole (i.e. total) area to observe any differences in the final solutions. The results are portrayed in Table 2.3 , for two orthogonal and one oblique rotation. It would appear that, for the present application, the type of rotation is irrelevant except for a minor translocation of second and third order factors. Factor selection, however, remains unchanged.

For each of the main stratigraphic areas, factors were derived by using an orthogonal rotation (Varimax) on principal component factors. A compression of the resultant factors can be made from data presented and is discussed in Chapter 8.

2.4.3 Discriminant Analysis

Discriminant analysis attempts to statistically distinguish two or more groups by creating functions that will allocate new samples of unknown origin into one or two of the original groups. The researcher selects a collection of discriminating variables that will measure characteristics on which the groups are expected to differ. Then, by a complex mathematical procedure (see Cooley and Lohnes, 1971, p.243-250; Tatsuoka, 1971, p.157-164), the variables are weighted and linearly combined in various ways so that the groups are as statistically distinct as possible.

TABLE 2.3
Comparison of Three Rotation Methods in Factor Analysis

ROTATION METHOD	CORR.	FACTOR	COMPONENTS	% of VARIANCE
Varimax (orthogonal)	+	1	MgO, CaO, Ni	61
	-		SiO ₂ , Na ₂ O	
	+	2	Fe ₂ O ₃ , FeO, TiO ₂ , P ₂ O ₅	22
	+	3	K ₂ O, Ba, Rb	11
	+	4	Sr (Al ₂ O ₃)	7
Equimax (orthogonal)	+	1	MgO, CaO, Ni	61
	-		SiO ₂ , Na ₂ O	
	+	2	K ₂ O, Ba, Rb	22
	+	3	Fe ₂ O ₃ , FeO	11
	-		Sr, (Al ₂ O ₃)	
	+	4	TiO ₂ , P ₂ O ₅	7
Oblique	+	1	MgO, CaO, Ni	61
	-		SiO ₂ , Na ₂ O	
	+	2	TiO ₂ , P ₂ O ₅	22
	-	3	K ₂ O, Ba, Rb	11
	+	4	Sr, (Al ₂ O ₃)	7
* Components in parenthesis are marginal residual elements				

An attempt at discriminant analysis during the present study met with very limited success, possibly due to the selection of too many discriminating variables, used to obtain the discriminant functions. Low initial eigenvalues (an intuitive measure of the effectiveness of discrimination) were obtained, at the minimum 95 percent significance level, and, thus, classification could not be made with any degree of certainty.

Detailed procedures and further explanation of statistical techniques are contained in Klecka (1975, p.434-467) and Davis (1975, p.434-467).

Chapter 3

CLASSIFICATION OF VOLCANIC ROCKS

"-- the mountains must indeed be examined with the microscope" Sorby (1856)

3.1 INTRODUCTION

Investigation of geologic suites has, as in other scientific endeavours, required a system of classification as a means of ordering large and diverse groups of rocks. Pursuit of such a system, for igneous rocks, has taken many forms, based primarily upon three approaches: mineral content, chemical composition, and field or geologic relationships. The resulting frameworks have been largely systematic, since the exact magmatic processes are not yet sufficiently understood to permit the creation of a general genetic classification.

The classification of Archean volcanic rocks is often difficult because these rocks have almost invariably been metamorphosed, and most classification schemes have been devised for unmetamorphosed rocks. While some Archean volcanic rocks still have primary mineralogy and textures preserved (Jolly, 1974, 1975, 1976; Pearce, 1974; Pearce et al., 1974), most, including those at Bachelor Lake, are

products of higher grade, dynamothermal events which obliterate primary features. The petrography of these metamorphosed rocks is described by Moorehouse (1959,1970), Turner (1968) and Miyashiro (1968).

It is the writer's intent to review various classification schemes and determine the most appropriate one(s) for metamorphosed greenstone belts.

3.2 MINERALOGICAL CLASSIFICATIONS

All early classifications of igneous rocks were based on mineralogical parameters (Zirkel, 1893; Rosenbusch, 1906; Johannsen, 1939). While genetic implications were strongly emphasized in these early investigations, magmatic significances drawn from the petrography were not always accurately understood. Realization that composition in rock suites is gradational lead to the concept of rock "families" (Williams, Turner & Gilbert, 1954, p.35; Turner & Verhoogen, 1960, p.70; Huang, 1962, p.90; Carmichael, Turner & Verhoogen, 1974, p.32; and others). The families consist of members, or, rock types, which are defined in terms of fabric and essential mineralogy (eg. Table).

Unfortunately, many Archean terrains, including the present study area, contain rocks which have original mineralogy and textures transformed by regional metamorphism. Mineralogical schemes are, therefore, largely unworkable for these suites.

TABLE 3.1

Corren's (1969) Mineral/SiO₂ Classification of Igneous Rocks

	SiO ₂ in excess Quartz bearing				SiO ₂ saturated; most without quartz				Undersaturated in SiO ₂							
% SiO ₂ on average	75	69	67	60	62	58	56	50	46	55	44	41	53	40	30	
light minerals	Quartz and K-feldspar		dominantly Plagioclase		dominantly alkali feldspars		Feldspars dominantly ab < 50		plagioclase an < 50		Feldspathoids with felspar		without felspar		predominantly monomineralic constituents	
dark minerals	biotite, hornblende, pyroxene in part olivine										partly olivine		light		dark	
Plutonic rocks (Plutonites)	Granite Alkali granite	Granodiorite		Syenite Sodium- Syenite		Diorite		Gabbro Norite		Nepheline- Syenite Essexite		Anorthosite (plagioclase)		Peridotite (olivine pyroxene) Dunite (olivine)		
	Quartz diorite Tonallite Adamellite		Monzonite													
Extrusive rocks (Vulcanites)	Rhyodacite Rhyolite		Dacite		Trachyte with sanadine Latite Trachyandesite		Andesite		Basalt Alkali olivine- basalt and Tholeiitic basalt		Phonolite Nephelino- trophite* Nepheline- basanite* Limburgite with glass		Nephelinite Leucitite Melilitite			
anachimetaorphic	Quartz porphyry		Quartz porphyrite Quartz Keratophyre		Keratophyre with albite		Porphyrite		Diabase						Kimberlite Pierite (olivine, augite, transition to basalt)	
Glasses	Obsidian Pitchstone (>3% H ₂ O)										Sideromelane Palagonite with H ₂ O					
Dikes	Aplite and lamprophyre										Kersanite (K)		Camptonite (Na)		Monchiquite (Na)	

* Notes corresponding leucite rock.

lower counting rates. Jenkins discusses this phenomenon in detail, along with several examples.

- 18 -

3.3 CHEMICAL CALCULATIONS AND GRAPHICAL PLOTS

The influence of chemical parameters is evident in some early divisions of rock suites, following the observations of Harker (1896) and Becke (1903) (Correns, 1969, p.215), that alkaline rocks occur around the Atlantic Ocean and subalkaline (calc-alkaline) rocks around the Pacific. Later, Niggli (1931) subdivided the Atlantic suite into a majority with a preponderance of sodium and those of the Mediterranean area, containing abundant potassium. Terminology for these geographic clans varied somewhat, but all were attempts to classify suites in accordance with their chemistry, although rooted in mineralogy.

Chemical parameters have been treated in many different ways to help divide rocks into various types (i.e. recasting into minerals or plotting on variation diagrams). These are not truly chemical classifications, but, as will be seen in the next section, a combination of minerals and/or plots can form the basis for a chemical rock classification. Such charts have been used since petrochemical analysis became routine, and, while the variety of diagrams has increased, many of the early types have endured. Although the plots are useful simply for comparison of data, they are also of advantage, in some instances, in the division or subdivision of rock suites and environments. For this reason, they are included in the present chapter.

Parameters may include Niggli values, normative or modal minerals, oxide weight percent, ionic chemical values, or other parameters which serve the intended purpose. Whatever functions are used, variation diagrams depict regular changes in a sequence of rocks, corresponding to their magmatic differentiation. By manipulating the values assigned as ordinate and abscissa, many characteristics of the rocks can be displayed.

3.3.1 Peacock's Classification

Some rocks were found to lie in a zone of uncertain classification, such as those of Peacock's (1931) Icelandic suite. He attempted to find "natural, acceptable boundaries, if such exist" for rock series and used a silica based modification of the Harker-type diagram. According to his method (Fig. 3.1), quantitative classification was made by an alkali-lime index (i.e. the point of crossover of total lime and alkali, plotted vs SiO₂). While many major elements were now involved in classification, correlation was still made to the modal composition:

	<u>SiO₂</u>	<u>Mineral Character</u>
Alkalic	51%	Syenitic
Alk-Calcic	51-56%	Na Mafics (Px, Hbld rare)
Calc-Alkalic	56-61%	(Na & K) CaO (Hbld, Aug, Feld)
Calcic	61%	

Thus, four classes of igneous rocks were arbitrarily chosen by Peacock on the basis of his index and one (calc-alkaline) coined what would become a new magmatic series. This was the first plot by which a suite of rocks could be assigned to a magmatic series. It is, however, inoperable on single rocks or on multiple analyses of similar composition. Also, many tholeiitic suites from continental margins or oceanic islands are ruled calc-alkaline by the index. As such, Peacock recognized "no natural dualistic division" but rather a "gradual progression from normal to extreme alkaline types".

3.3.2 Niggli's Classification

While Peacock was working at the University of British Columbia, Niggli, at the University of Zurich, Switzerland, realized that it was difficult to make direct comparisons of chemical analyses from the weight percentages of constituent oxides. By his method, molecular quotients are calculated from the weight percentages $((Wt\%/MW) \times 1000)$ and are then compiled so that mutual chemical relationships can be shown graphically:

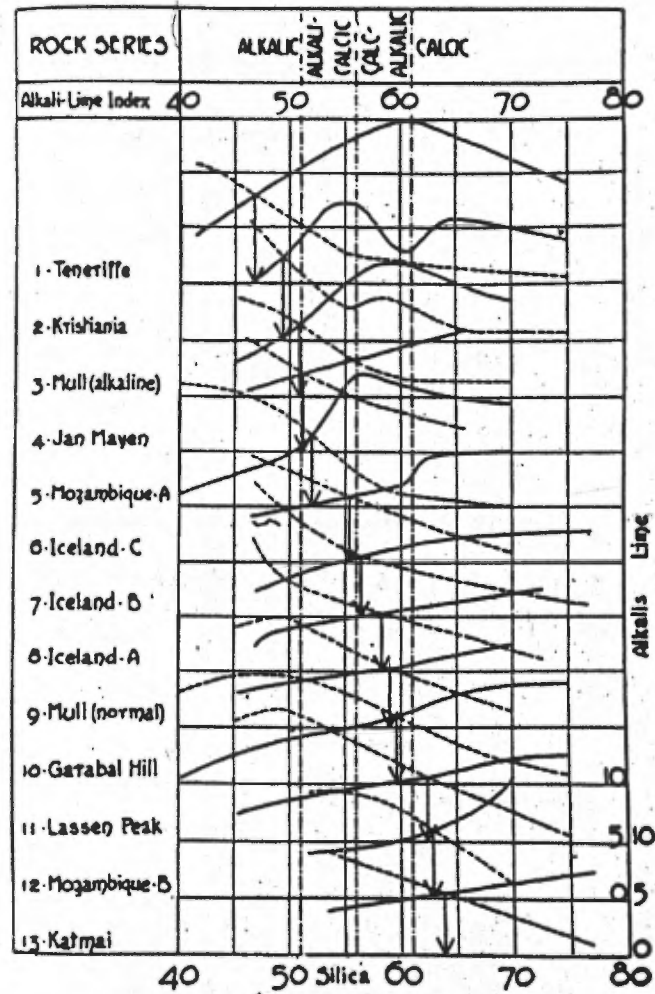
1. Mol.Quotient Calculated for:

al = Al_2O_3

fm = $FeO + MgO + MnO$ (incl. Fe_2O_3 as FeO)

c = $CaO + BaO + SrO$

alk = $K_2O + Na_2O + Li_2O$



Curves for $\text{Na}_2\text{O} + \text{K}_2\text{O}$ (full lines) and for CaO (broken lines) for thirteen rock series arranged in four groups according to the "alkali-lime index" (SiO_2 value at which $\text{Na}_2\text{O} + \text{K}_2\text{O} = \text{CaO}$).

Figure 3.1: Peacock (1931) Rock Series Classification

When A and B are calculated by least squares regression, m
is termed the regression coefficient. For most

- 22 -

2. Recalculate: $al+fm+c+alk = 100\%$

3. Si (and TiO₂, P₂O₅, etc.) calculated proportionately

4. $al:si = Mol.Quot. Al_2O_3/Mol.Quot. SiO_2$

5. Proportion K₂O: $k = K_2O/K_2O+Na_2O+Li_2O$

$MgO: mg = MgO/MgO+FeO+MnO$

An example is Niemann's 1958 calculation (Tab. 3.2) as reported by Correns (1969, p.218-220), for the Wurmberg granite in Germany. The molecular quotients, al, fm, c, alk, k, and mg, are known as "Niggli Values" and are plotted against si for comparison of large numbers of analyses. The method is limited in that silica remains a base function and not all elements are involved. It was a significant early attempt at manipulating large amounts of geochemical data, and is still commonly used in Europe.

3.3.3 CIPW Norms

Another method of recasting chemical analyses is the calculation of standard normative minerals. This common, and more versatile procedure, termed the CIPW norm after its originators, Cross, Iddings, Pirsson and Washington, was developed in the United States (1901-1902) by a new breed of chemical petrologists. Details of the calculation have been

TABLE 3.2
Niggli Values for the Wurmberg Granite, Germany (after
Correns, 1969)

	Weight %	Molecular number × 1000	Relative Numbers
SiO ₂	73.34	1221	si = 413
TiO ₂	0.13	1.6	ti = 0.5
P ₂ O ₅	0.12	0.85	p = 0.3
		130.7	al = 44.2
Al ₂ O ₃	13.32		
Fe ₂ O ₃	1.11	as FeO 13.9	
FeO	1.14	15.9	
MnO	0.017	0.2	36.2 /m = 12.2
MgO	0.25	6.2	
CaO	1.24		22.1 c = 7.5
Na ₂ O	3.05	49.2	
K ₂ O	5.42	57.5	106.7 alk = 36.1
		295.7	100.0
S	0.1		
H ₂ O ⁺	0.82		k = 0.54
H ₂ O ⁻	0.16		mg = 0.17
	100.21		c/m = 0.61
Corrected for S/O	-0.03		
	100.18		
Density	2.62		

described by Holmes (1921) and by Irvine and Baragar (1971) who include equations for a computerized formulation. Agreement between normative and optically determined minerals is, in general, quite good (Fig. 3.3). But since the norm, at best, expresses the mineralogy which could have crystallized from a magma at low pressure and relatively anhydrous conditions, correlation is poor for altered mineral assemblages. Thus, whenever possible, a complete modal analysis should be given for such samples, and the alteration products tied to the norm. Other disadvantages of the norm include lack of a micaceous phase, sensitivity to Na_2O , $\text{Fe}_2\text{O}_3/\text{FeO}$, and volatile change, and unacceptability of hydrothermally altered, inhomogeneous (porphyritic, fragmental, etc.), or undersaturated rocks. Nonetheless, for most volcanic rocks, the CIPW norm gives a fair approximation of the primary modal composition.

3.3.4 Harker Diagram

A rectangular plot forms the basis of this diagram, with weight percentages of each principal oxide plotted against SiO_2 as a common ordinate. A continuous increase in SiO_2 content during the evolution of a consanguineous magma series is an underlying presumption in the interpretation of this diagram. Such allowance is generally correct but exceptions can occur. The diagram, which has been used by a host of investigators for over 60 years, does serve to

TABLE 3.3
Mineral Composition and CIPW Norm - Wurmberg Granite

Norm minerals (CIPW) and symbols

Quartz	q	Wollastonite	Diopside	wn	Magnetite	mt
Corundum	c	Enstatite	di	en	Hematite	hm
K-feldspar	or	Ferroilite		fs	Ilmenite	il
Albite	ab	Forsterite	Olivine	fo	Apatite	ap
Anorthite	an	Fayalite	ol	fa	Pyrite	pr
Leucite	le	Acmite		ac	Calcite	cc
Nepheline	ne					
Kalsophilite	kp					

	SiO ₂ 121	TiO ₂ 1.6	P ₂ O ₅ 0.85	Al ₂ O ₃ 130.7	Fe ₂ O ₃ 6.9	FeO 18.9	MnO 0.2	MgO 6.2	CaO 22.1	Na ₂ O 48.2	K ₂ O 57.2	S 3.1	Mole- cular Number	Weight %
Quartz	630												630	31.8
Orthoclase	345			57.5							57.5		57.2	31.9
Albite	295.2			49.2						49.2			49.2	25.8
Anorthite	38.6			19.3					19.3				19.3	5.4
Corundum				4.7									4.7	0.5
Hypersthene	6.2					5.8	0.2	6.2					6.2	1.2
	6.0				6.9	6.9							6.0	1.6
Magnetite						1.6							1.6	0.2
Ilmenite		1.6											1.6	0.2
Apatite			0.85						2.8				0.85	0.3
Pyrite						1.6						3.1	3.1	0.4
														99.1
														H ₂ O ⁺ 1.0
														H ₂ O ⁻ 1.0
														100.1

Mineral composition of Wurmberg granite; comparison of modal analyses and norms based on chemical analyses

	Modal volume %	Calculated volume %	Calc. after CIPW-norm weight %
K-feldspar	33.0	33.2	32.0
Plagioclase (15% An)	31.5	31.4	31.2
Quartz	30.4	32.0	31.8
Biotite and chlorite	3.0	2.5	—
Ors	0.7	0.5	1.8
Residue	0.3	-0.4	0.4

* 1.2% hypersthene.

provide a grasp of the general chemistry of igneous rock series. It is moderately useful to contrast the chemistry of different petrographic provinces but is not well suited to rock subdivision within a particular province. Petrologists (primarily European) using Niggli values would plot al, fm, c and alk against si values. An example of the standard Harker-type plot is provided in Fig. 3.2 .

3.3.5 Larsen Diagram

Combination of elements along a single axis began with Larsen's (1938) significantly modified Harker-type diagram. Oxide percentages are plotted against an abscissa ($1/3\text{SiO}_2 + \text{K}_2\text{O} - \text{CaO} + \text{MgO} + \text{FeO}$), consisting of most of the major elements.

An advantage of Larsen's plot over the Harker diagram is increased linearity of the curves and thus improved correlation of chemistry with the presumed order of magmatic evolution. Otherwise, the advantages of the two diagrams are similar. An example of the standard Larsen diagram is provided in Figure 3.3 .

Nockolds and Allen (1953, 1954) modified the Larsen factor to demonstrate any absolute enrichment in iron and also to show the variation in minor and trace elements in relation to the major components. Their modified factor is $(1/3\text{Si} + \text{K} - \text{Ca} + \text{Mg})$ with traces plotted by weight percent. Figure 3.4 illustrates this type of plot.

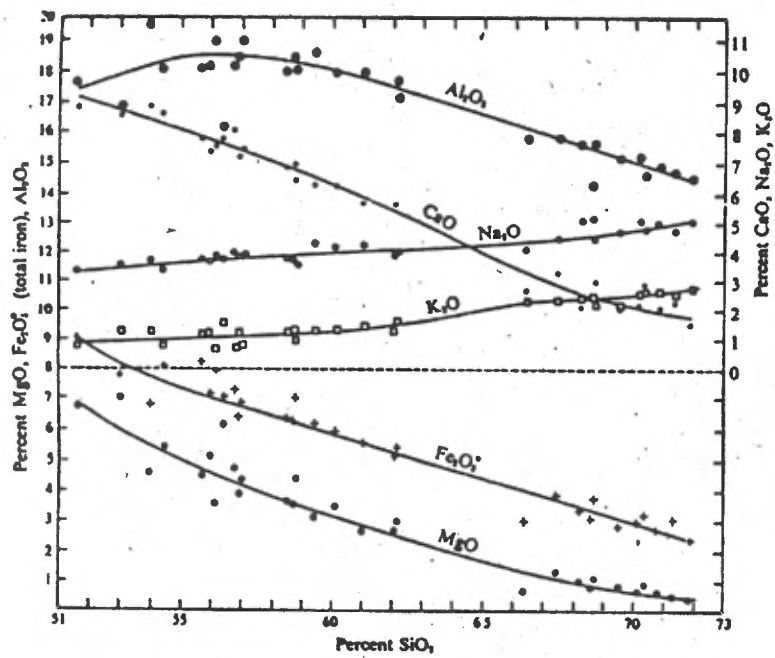


Figure 3.2: Harker-type Variation Diagram (after Barth, 1962)

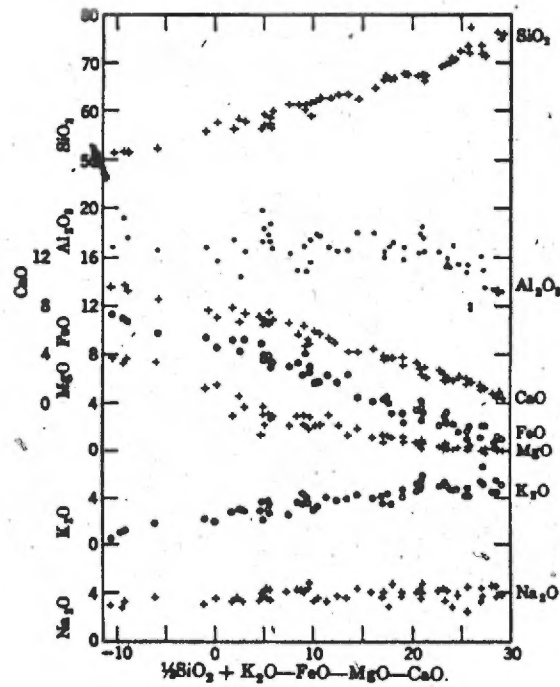


Figure 3.3: Larsen Variation Diagram, San Juan Mts. Colo.
(after Barth, 1962)

preserved (Jolly, 1974, 1975, 1976; Pearce, 1974; Pearce et al., 1974), most, including those at Bachelor Lake, are

- 29 -

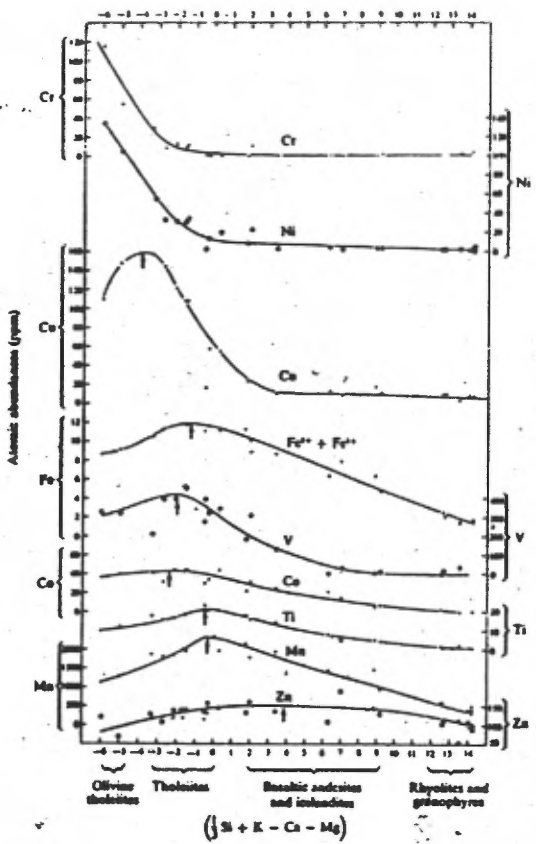
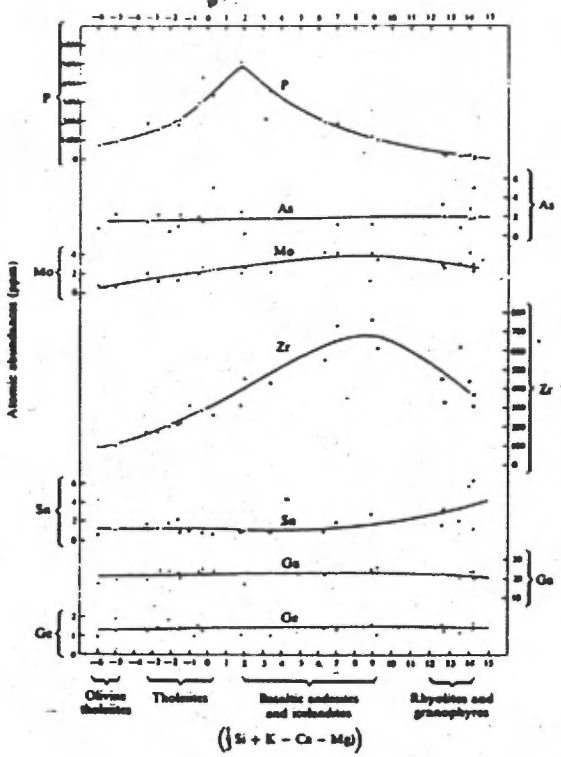


Figure 3.4: Nockold & Allen Diagram, Thingmuli Series (after Carmichael, Turner & Verhoogen, 1974)

metamorphism. Mineralogical schemes are, therefore, largely unworkable for these suites.

- 30 -

3.3.6 Alkalies vs Silica Diagram

This modified Harker diagram was used to great advantage by MacDonald (1968) in subdivision of alkaline and sub-alkaline rocks from Hawaii. Other workers, including Tilley (1950), Kuno (1968) and Irvine and Baragar (1971) have also used the diagram, although slightly modifying the boundary line. Numerous suites in the Irvine and Baragar paper were found to be correctly separated for at least 90 percent of the control data, and most suites were placed satisfactorily on a statistical basis.

Certain suites were less clearly defined. The Coppermine River lavas, for instance, have broadly tholeiitic characteristics, yet more than half the analyses fall in the alkaline field. For that reason, Irvine and Baragar suggest that normative plots are somewhat more reliable. Other authors have condemned the plot as unsatisfactory due to the relative mobility of the alkalies. But such criticism has not been justified with the exception of highly altered material. Indeed, the diagram has proven invaluable in identifying slightly altered volcanic rocks which appear fresh in hand specimen. It is for such use that the diagram has its greatest applicability (see Figure 6.1).

3.3.7 Al₂O₃ vs Normative Plagioclase Diagram

Division of the calc-alkaline and tholeiitic series is usually accomplished by the APM diagram (see section 3.4.10). However, this separation is less accurate for the more mafic members whose most prominent chemical difference, in each series, is their alumina content. Calc-alkaline (16-20% Al₂O₃) and tholeiitic (12-16% Al₂O₃) separation is well illustrated in the Al₂O₃ vs Norm. Plagioclase plot (Irvine & Baragar, 1971, p.535).

3.3.8 Color Index vs Normative Plagioclase Diagram

Subdivision of subalkaline rocks has, in the past, been based on color index (CI), plagioclase composition, silica or quartz content, or other petrochemical criteria. It has been found by many recent investigators that such rocks can be satisfactorily classified by a CI versus normative plagioclase plot with more certainty than using a single factor (i.e. Johannsen's (1937) division via plagioclase composition, or Shand's (1951) method using color index).

The diagram proposed by Irvine and Baragar (1971) requires both CI and normative plagioclase, resulting in sloped boundaries between rock types. The major disadvantage of the plot is similar to that of the Al₂O₃ versus normative plagioclase diagram, in strong dependency on Na₂O content ("error in the determination of Na₂O automatically increases about 8 times in relative weight the

calculation of normative albite, and errors in CaO amplify 5 times in normative anorthite" -- Church, 1975, p.258). Thus, location within the plot is extremely sensitive to both analytical error for sodium (common in some types of analysis) and to secondary alteration or metamorphism. However, extra care in both sampling and analytical technique can provide results suitable for this method of rock identification.

3.3.9 Al₂O₃ vs FeO/(FeO + MgO) Diagram

Most classification schemes do not have facility for the plotting of ultramafic and komatiitic type rocks. In recent years, increasing numbers of studies of these rocks, as well as a growing recognition of their relative abundance in many volcanic sequences has prompted a need for expanded classification.

Many ultramafic rocks have been routinely identified by modal mineralogy. Uncertainty arises, however, for medium to fine-grained, altered varieties, void of most original texture.

A suggestion, made by T.N. Irvine of the GSC, for separation of normal tholeiitic (iron-rich) rocks from those of komatiitic affinity, was adopted by several Canadian investigators of ultramafic suites (Arndt, 1975; Naldrett & Arndt, 1976; Naldrett & Goodwin, 1977; Naldrett & Cabri,

1977). It was found that a plot of Al_2O_3 vs $FeO / (FeO + MgO)$ (total iron as FeO) would give reasonable separation of the two groups (Figure 3.5) since:

"up to the stage at which plagioclase appears on the liquidus, alumina becomes steadily more concentrated in a magma crystallizing at crustal depths, with the result that alumina content of the magma is a rough guide to the extent to which crystallization has proceeded" (Naldrett & Turner, 1977, p.68.)

The $FeO / (FeO + MgO)$ ratio serves as an index of fractional crystallization but is susceptible, as in the previously discussed normative calculations, to the influence of prevailing oxygen fugacity and availability of oxygen during crystallization. Location of the major dividing line between the two groups was estimated through plotting many suites of Archean komatiites and iron-rich tholeiites from worldwide locations. Naldrett and Goodwin's (1977) horizontal boundary, at $Al_2O_3 = 16.5$ wt. percent, species of high Al_2O_3 content, while the short diagonal bounds a small zone of intermediate types.

Naldrett and Cabri (1976, p.1136) stressed that, in addition to the chemical requirements of low $FeO / (FeO + MgO)$ ratio for a given Al_2O_3 , a komatiite must have the spinifex or harasitic texture characteristic of ultramafic flows. In addition, they modified the original komatiite definition (Viljoen & Viljoen, 1969; Brooks & Hart, 1974)

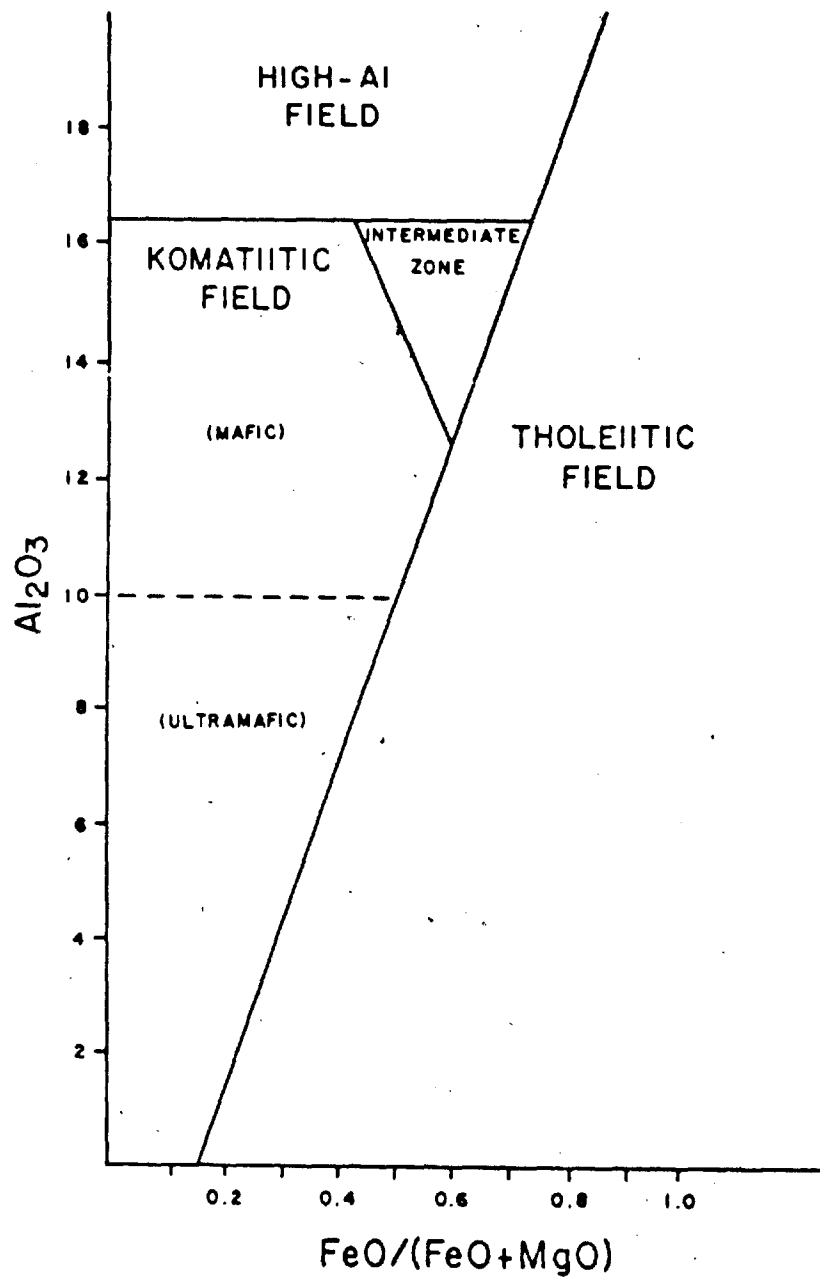


Figure 3.5: Al_2O_3 vs $FeO/(FeO+MgO)$ Diagram

which included $\text{CaO}/\text{Al}_2\text{O}_3$ greater than 1.0, to broaden the spectrum for similar rocks in other parts of the world. The matter of tholeiitic versus komatiitic series will be dealt with in a later section of this thesis.

During the present investigations of this diagram, samples were plotted not only for the Bachelor Lake area, but also from South Africa (Viljoen & Viljoen, 1969), Rhodesia (Bickle, 1975), Australia (Williams, 1972; Nesbitt et al., 1976; Halberg et al., 1972) India (Viswathan, 1974), and Canada (Naldrett & Goodwin, 1977; Gellnes & Brooks, 1974, and Arndt et al., 1977) in figure 3.6. It was noted that ultramafics associated with komatiites plot in the komatiitic field.

In general, mafic rocks (komatiitic basalts) plot above 10 percent Al_2O_3 and ultramafic rocks (pyroxenitic, peridotitic komatiites) fall below that threshold. It is suggested that this boundary be affixed a permanent part of the diagram, due to its general, worldwide applicability.

The excellent delineation of a wide range of Archean mafic and ultramafic rock types suggests that this diagram is well suited to their classification. It goes beyond many systems which do not account for ultramafic composition and is more selective than the few (i.e. Jensen Cation Plot (1976), etc.) that contain a general ultramafic region. The diagram would therefore make a worthwhile inclusion in a

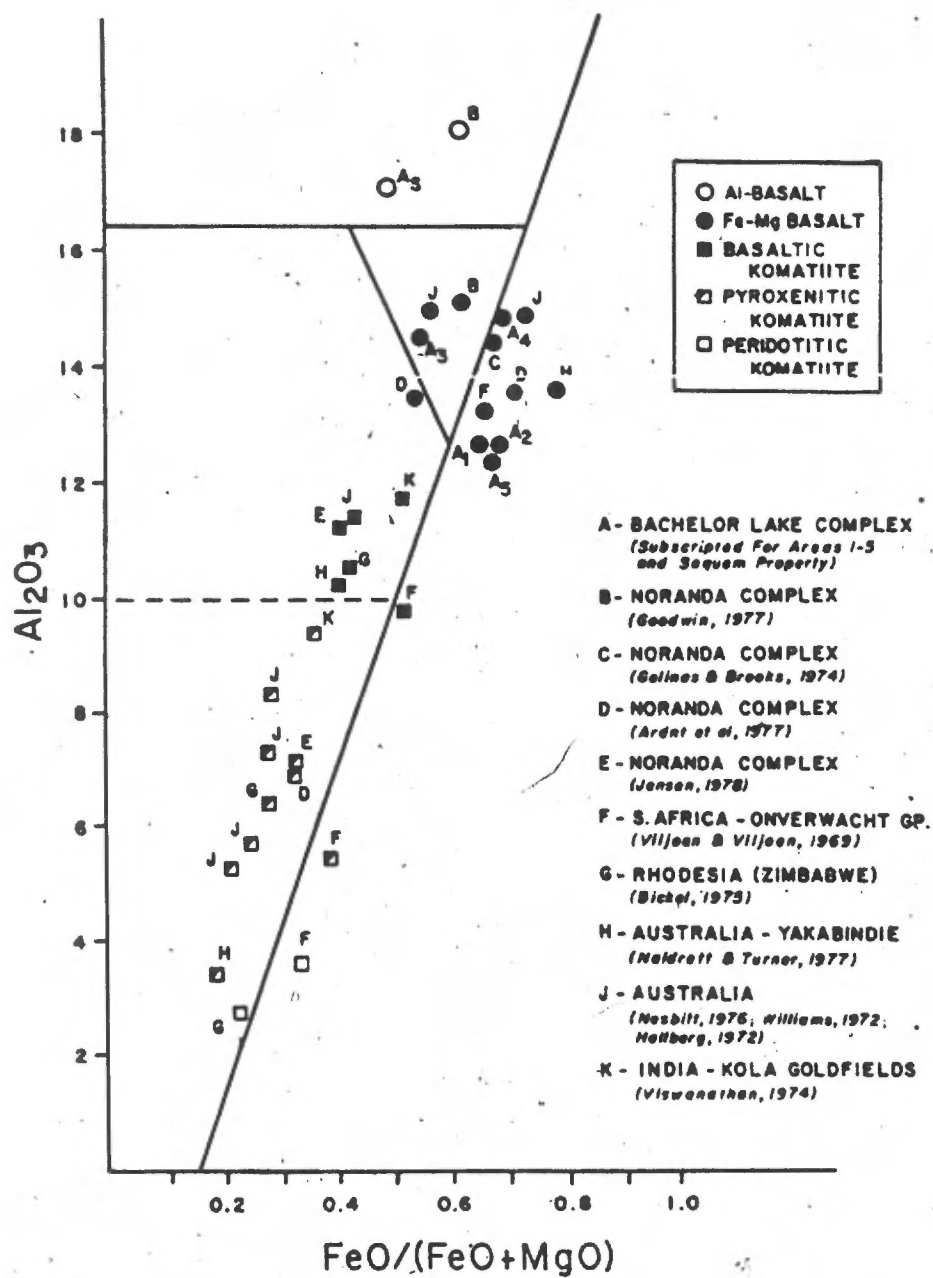


Figure 3.6: World Archean Mafic-Ultramafic Rock Suites on the Al₂O₃ vs FeO/FeO+MgO Diagram

classification scheme such as that of Irvine and Baragar (1971).

3.3.10 AFM Diagram

Volcanic rocks examined in early geochemical studies were comprised primarily of well-differentiated, calc-alkaline (see Ch.8) sequences. Later, investigators of suites which became known as tholeiitic or gabbroic series, showing little or no silica enrichment during differentiation, found that Harker and Larsen diagrams could not be used in comparing such rocks with those of calc-alkaline sequences. Thus, Wager and Deer (1939), during a study of the Skaergaard complex (representative of the former magma type), developed a triangular plot by recasting the most abundant constituents into three coordinates: A ($\text{Na}_2\text{O}+\text{K}_2\text{O}$), F ($0.8998 \times \text{Fe}_2\text{O}_3\text{t}$) and M (MgO). These factors correspond, respectively, to the least, intermediate and most refractory minerals. Theoretically, the rock composition trends toward or away from these poles, depending on the path and degree of magmatic evolution.

The AFM diagram is useful in separating suites of iron-rich (gabbroic or tholeiitic) and iron-deficient (calc-alkaline) rocks. But the correlation of such trends with evolution of a magma is circumspect and will be discussed later. The diagram does not involve all major elements, nor any traces, but the correspondence of two trends to

significant field data assures its value as an indispensable geochemical diagram. Illustration of the two fractionation trends is given in Figure 3.7 for calc-alkaline suites (Idaho and southern California batholiths) and a tholeiitic (Skaergaard complex) suite of extreme iron enrichment.

3.3.11 Pearce Diagram

More recently, triangular diagrams have been used to display a variety of chemical trends. A useful diagram has been provided by Pearce et al. (1975) for discriminating between oceanic and continental type basalts. By plotting 241 ocean floor and ridge basalts and 277 non-oceanic basalts on a TiO_2 - K_2O - P_2O_5 ternary diagram, they found that a dividing line, at 54.5% TiO_2 , 0% P_2O_5 and 79.6% TiO_2 , 20.4% P_2O_5 , separated 93% of the rocks into the proper field (Fig. 3.8). The division was confirmed by "further work with large numbers of analyses".

The authors emphasize that the diagram is effective only for primary basalts, and fractionated or alkaline rocks are not well discriminated. For this reason, all analyses are screened through an AFM diagram and an isoalkaline line of 20% used as the upper limit of acceptability.

The "Pearce" diagram is an effective means of discriminating between oceanic and non-oceanic environments.

	Gabbroic series	Calc-alkali series
Structural form	Stratified sill, lopolith, or funnel intrusion	Complex batholiths of massive steepwalled plutons, domes, or mushroom-shaped plutons
Structural environment	Nonorogenic; faulting dominant	Orogenic; both faulting and folding prominent
Number of intrusions	One or few	Multiple
Water content of the magmas	Low	High
Mean temperatures of differentiation	High to moderate	Moderate to low
Dominant character of mineralogy	Anhydrous gabbroic	Hydrous quartzofeldspathic
Type of differentiation	Absolute iron enrichment, no silica enrichment	Relative iron enrichment; strong silica enrichment
Contact effects	Modest thermal	Modest to profound thermal and metasomatic

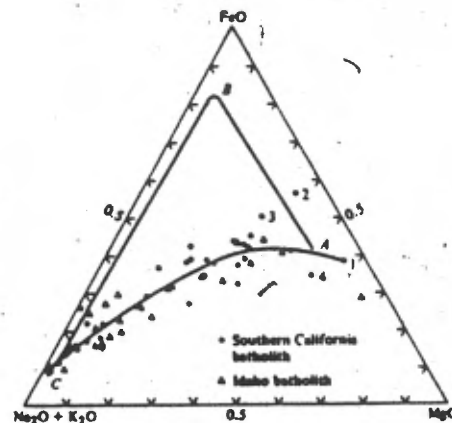


Figure 3.7: Calc-alkaline & Tholeiitic (Gabbroic) Trends a) Comparison of Features b) Location on an AFM Diagram (after Mueller, 1977)

Figure 3.4 illustrates this type of plot.

- 40 -

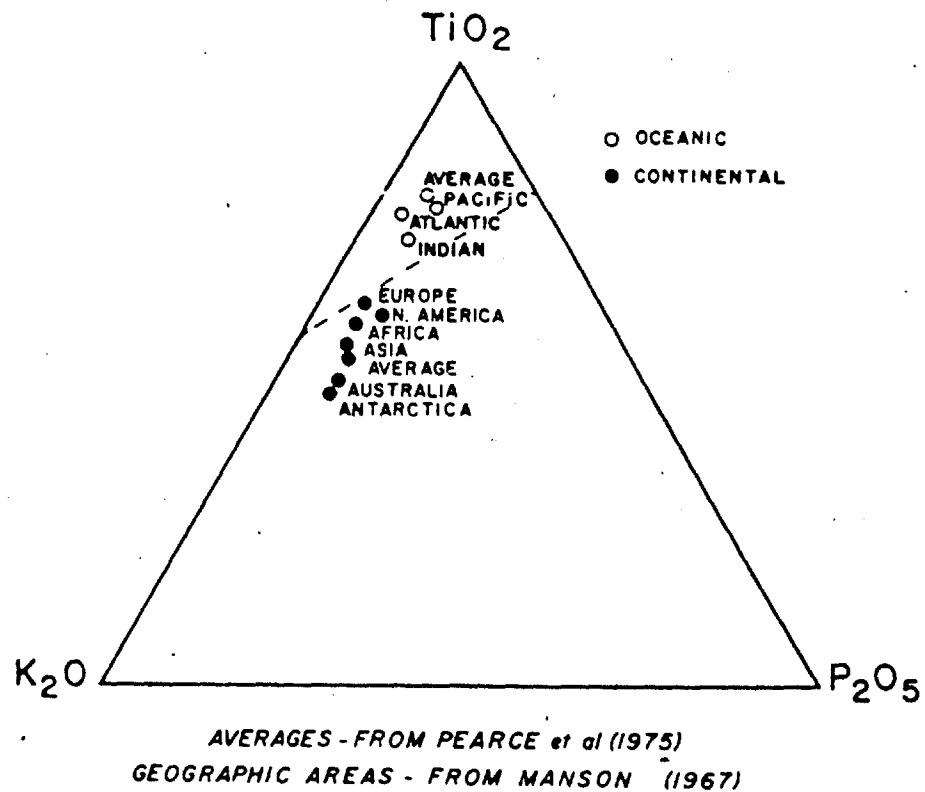


Figure 3.8: Pearce (1975) Tectonic Environment Diagram

As the authors point out, high degrees of weathering and/or alteration tend to move oceanic rocks into the non-oceanic field. However, altered or weathered rocks plotting in the oceanic field are unlikely to have a non-oceanic origin.

A selection of worldwide, average Archean basalts was plotted in the original paper and most fell in the oceanic field, suggesting an environment similar to present-day oceans. It was decided to use the diagram in the present study to inspect this tendency in the Bachelor Lake area, and also to determine if the pattern changes with position in the stratigraphic pile.

3.4 CHEMICAL ROCK CLASSIFICATION METHODS

3.4.1 Church-Murata Diagram

Many investigators have disparaged those variation diagrams which use only a small number of major elements. The criticism is somewhat justified in that the more elements used, the less noticeable are effects of analytical error and the better distinguished a rock becomes. But graphical representation of such complex systems is fraught with difficulty. Most proposed diagrams have had little success in delineating distinct fields for particular rock types.

Church (1975, p.259) lists the main chemical variations as changes in basicity, alkalinity and the relative proportions of alumina and silica:

	<u>Rhy, Trach, Phono.</u>	<u>Basalt</u>
Basicity: Fe-Oxides		
Magnesia	Low	High
Lime		

Alkalinity - varies inversely to basicity but also has an independent trend toward alkali enrichment for some basic rocks.

Al₂O₃ vs SiO₂ - increase in Al₂O₃ with respect to SiO₂ parallels alkali behavior in the rhyolite to phonolite trend. Also increased Al₂O₃ with differentiation.

Combining aspects of earlier Al₂O₃-SiO₂ based diagrams and alkali silica variation diagrams, Church adds an ordinate of basicity in a three-axis orthogonal plot ($\text{Na}_2\text{O} + \text{K}_2\text{O}$ vs $\text{FeO} + \text{Fe}_2\text{O}_3 + \frac{1}{2}(\text{MgO} + \text{CaO})$ vs $\text{Al}_2\text{O}_3/\text{SiO}_2$). Doubling the iron factor in the ordinate serves to polarize rocks of ultramafic composition and thus virtually eliminates their discrimination in the diagram.

Compositional fields of common volcanic rock types are shown in Figure 3.9. Data points were obtained from approximately 1500 analyses and contoured to include 2/3 of the total points for each rock type. The contours do overlap to some extent and Church suggests using intermediate rock names such as rhyodacite, basaltic-andesite, trachyandesite, etc., or descriptive terms (i.e. alkaline basalt, subaluminous andesite, etc.) where samples plot outside the contours. The method seems to work fairly

well except that, as previously noted, the contours represent only a majority of points for each rock type and therefore actual overlap is, in reality, much greater. The diagram does work well for the Cascade felsic volcanics, the Highwood phonolite trend, Skaergaard differentiates and volcanic rocks from Rice Lake, Manitoba, and the Canary Island volcanics (see Church, 1975, p.260-262).

The relatively good discriminating powers of this diagram suggest that it should be considered as a possible classification tool, but in conjunction with other diagrams for delineation of series trends, alkalinity and ultramafics.

3.4.2 Jensen Diagram

The Cation plot of Jensen (1976) is a rock classification scheme which uses Al_2O_3 , $(Fe_2O_3+FeO+TiO_2)$, and MgO recalculated as cation percent (Figure 3.10). Similarity to the AFM diagram is evident, except for the replacement of the occasionally mobile alkaline elements by the relatively immobile Al_2O_3 .

Jensen's intention was to produce a classification which would be directly related to the color of field specimens. To that end, he used cation percentages since "iron and titanium are heavy atoms with small volumes relative to atoms of magnesium and aluminum; cation

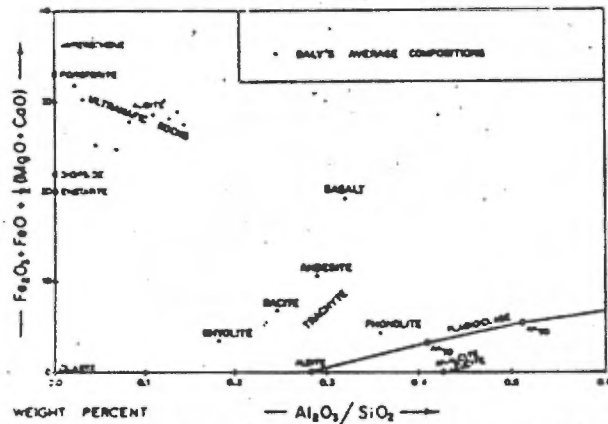


Figure 3.9a: TAS plot with modified ordian showing relative position of important silicate minerals and some of Daly's (1933) average rock compositions.

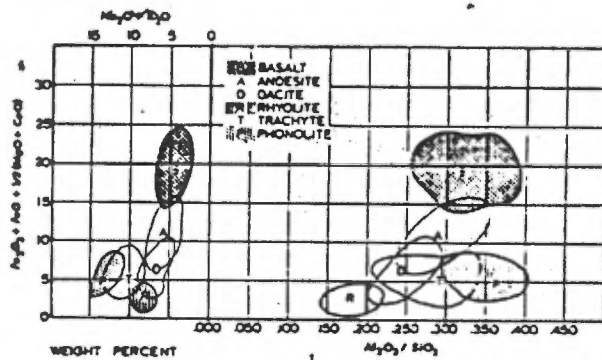


Figure 3.9b: TAS plot showing fields of variation of most common volcanic rocks; contours are inclusive of two-thirds of total points counted for each rock type. Letters designating rock types are positioned near Daly's (1933) averages.

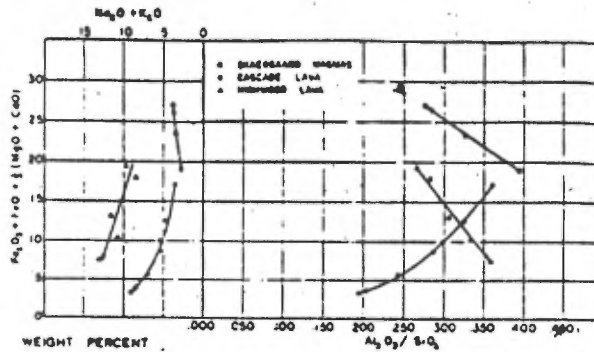


Figure 3.9c: TAS plot comparing well-known magma trends exemplified by Cascade volcanic rocks, Highwood magmas, and primary Silvegaard liquids.

Figure 3.9; Church (1975) Volcanic Rock Classification Diagram

percentages represent a volume measure that to some degree can be distinguished by the human eye". The color relationship is further emphasized by trends toward the iron-titanium apex. Light colored rocks generally have high proportions of Al_2O_3 (feldspars or their alteration products) or MgO (talc, forsterite, or Mg-amphiboles or Mg-pyroxenes) but become increasingly darker as iron and titanium content rise.

The logic of the method is sound and conforms to Jensen's goal of a chemical-field related system as an aid to stratigraphic interpretation. Classification boundaries on the plot were adjusted, during testing of over 2000 published analyses, to form an 85 percent or better correspondence with published rock names. For methods of locating boundary position, reference is made to the original paper (Jensen, 1976, p.2-3). A major point of concern is the very arbitrary division of rock types, based entirely upon regular intervals of Al_2O_3 content. This factor assumes a gradational increase in Al_2O_3 (probably in feldspar) as a magma is progressively differentiated, but is not supported by other Al_2O_3 variation diagrams (see Fig. 3.2). Nonetheless, Jensen indicates good correspondence with other classification schemes, including that of Irvine and Baragar (1971). The plot also shows a general differentiation trend for komatiitic-type rocks, an advantage not found in many other variation diagrams. The

Jensen Cation Plot provides a rapid method of classification, developed to include a correlation between hand specimen color and chemical composition. The relationship may hold for the low grade metamorphic rocks in some areas, but is unsuitable for rocks of higher grade, due to metamorphically-induced color changes.

Jensen parameters were calculated for all fresh Bachelor Lake rocks and plotted in Figure 3.11, using the rock names assigned by the scheme chosen for this project (see next section). Results show that separation of basalts from more differentiated rocks is quite good but greater overlap occurs between the more felsic varieties. It is evident, therefore, that only comparison of basaltic rocks can be made using the system of Jensen and the one selected for the present study.

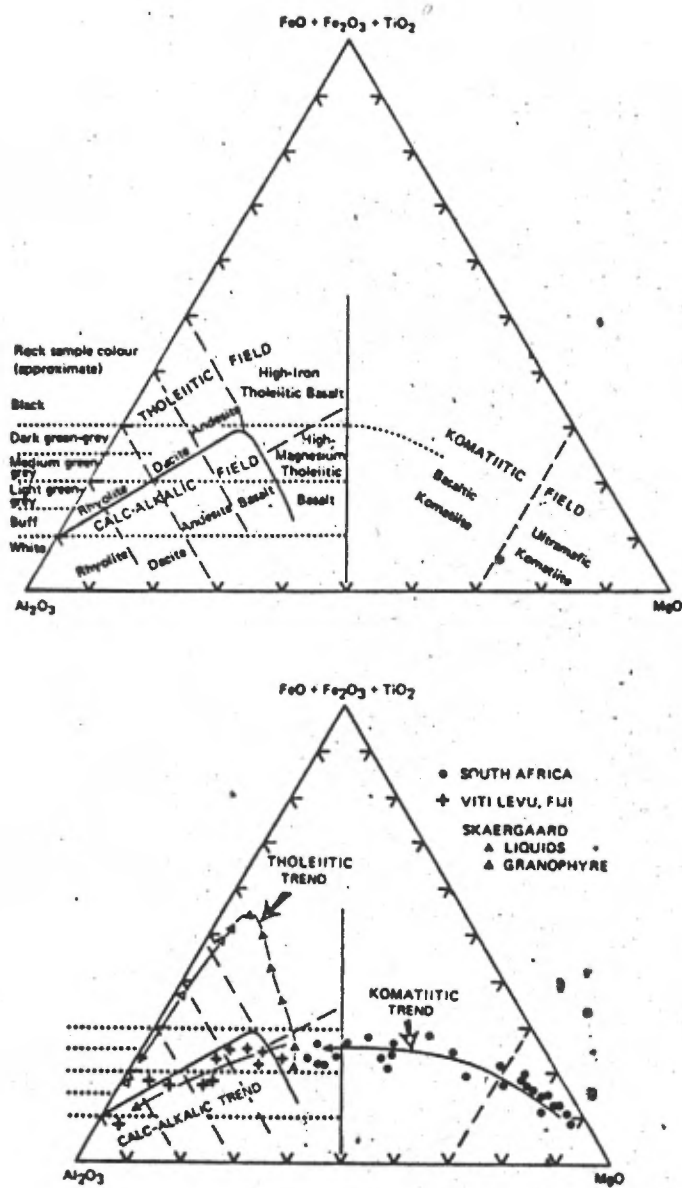


Figure 3.10: Jensen (1976) Volcanic Rock Classification Diagram

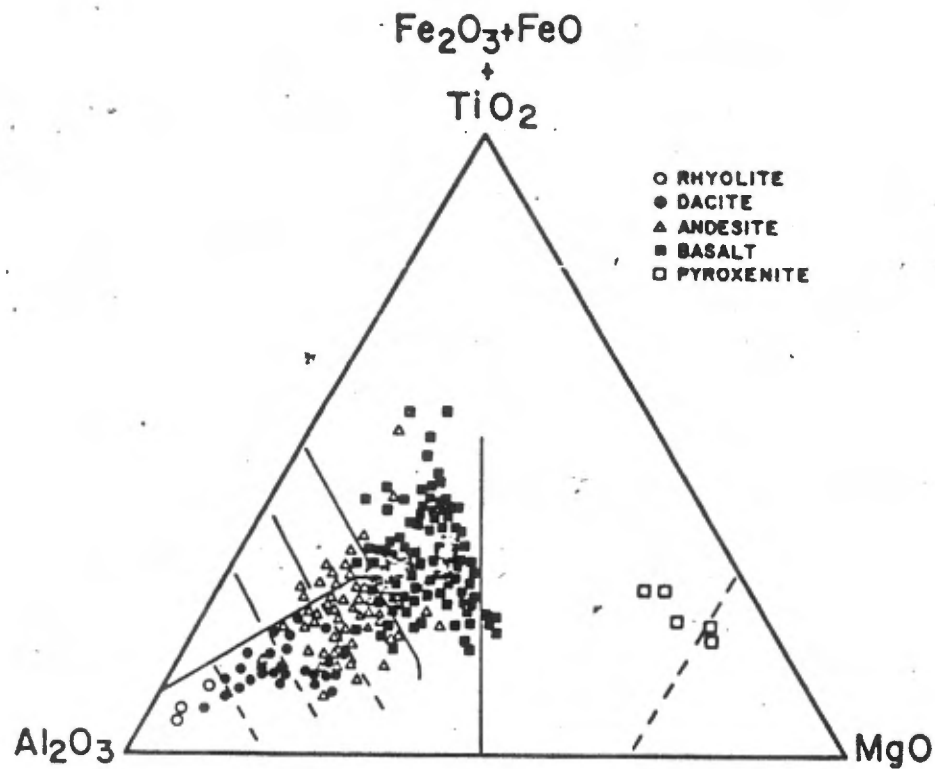


Figure 3.11: Distribution of Bachelor Lake Samples on the Jensen Diagram

3.5 CLASSIFICATION OF BACHELOR LAKE ROCKS

In 1966, Irvine, Baragar and Moorhouse, at the request of the Volcanological Subcommittee of the NRC, attempted to develop a classification scheme for volcanic rocks in Canada. The purpose was to standardize rock name terminology for Archean rocks and "to give chemical definition to conventional rock names" (Irvine & Baragar, 1971). The published results consist of a detailed, multi-graphic chemical classification. Although certain values derived by their methods must be viewed with caution, the system offers a versatile way of dealing with large numbers of geochemical analyses. For that reason, the Irvine-Baragar classification, with slight modifications, has been adopted for the present study.

The Irvine-Baragar scheme attempts to classify rocks through use of the CIPW norm which, they state, "gives a fair approximation of the mineral and modal composition of common volcanic rocks as crystallized at low temperatures under relatively anhydrous conditions". Here, the validity of anhydrous conditions may be questioned, especially with regard to typically hydrous calc-alkaline magmas, but the value of normative calculations, nonetheless, retains the merits as previously described.

The Irvine-Baragar approach divides simple, graphical plots which can distinguish and name different rocks

according to compositional fields that are consistent with current nomenclature. They note that their method has limitations due to "the difficulty of representing chemically complex systems on graphs and because --- long-standing rock names have not been used in a consistent way over the years. Minor compositional changes through metamorphism and/or hydrothermal activity are accounted for, assuming severely altered rocks are first eliminated. Oxidation of iron is corrected by setting an upper limit on Fe_2O_3 according to the equation: $3Fe_2O_3 = 3TiO_2 + 1.5$. If the analysis value is greater than this, the excess is converted to FeO , thereby giving a more undersaturated norm. Furthermore, volatiles are eliminated from the analysis before normative calculations and are used only to indicate the state of alteration of the rocks.

Norms are calculated by standard conventions and are expressed both by classical weight percent and by cation equivalents (molecular norm or 'Barth-Niggli katanorm'). While corresponding values of both methods are similar, the cation norm has been chosen by Irvine & Baragar as being better-suited to graphical projection and easier to recast for alternative combinations.

Many classification schemes, the present included, add genetic modifiers, such as tholeiitic or calc-alkaline, to the derived rock names in order to segregate similar rocks

with slightly differing characteristics. These inherent differences often have logical field relationships (e.g. Kuno, 1968) and are therefore valid. But they are often unsuitable for interpreting genetic significance. Thus, the series names are used simply because they appear to be natural divisions. The three main series: tholeiitic, calc-alkaline and alkaline are the most common and will be discussed in Chapter 8.

The Irvine-Baragar (1971) classification scheme first involves calculation of the CIPW normative minerals for each sample. The procedure, as discussed in section 3.3.4, can be rapidly accomplished by a short, fortran computer programme. Norms and geochemical data are then passed through a series of steps as illustrated in the flow sheet in Figure 3.12). If aegirine occurs in the norm, the rock is peralkaline and classified according to the method of Noble (1968). If the color index is greater than 75, the rock is ultramafic. Otherwise, it passes through the alkali-silica diagram to determine if any rocks are alkaline. Subalkaline rocks then pass to the Al_2O_3 vs Normative Plagioclase diagrams to determine if they are tholeiitic or calc-alkaline. If normative olivine is greater than 25%, the rock is then labeled a picritic basalt. Otherwise, it is classified by the Color Index vs Normative Plagioclase diagram as rhyolite, dacite, andesite or basalt. Finally, the rocks are evaluated for their relative potassium content

by the An-Ab-Or diagram. Equations for boundary lines in the above mentioned diagrams have been listed by Irvine & Baragar (1971, p.547-548). These greatly assist classification of the rocks in a computer programme, thus eliminating tedious plotting.

The classification scheme used in this study is essentially the same as that of Irvine & Baragar except that a silica screen was added to eliminate altered samples. Some specimens were found to possess abnormally high or low silica values for the correspondingly-derived rock name. Since silica tends to gradually increase through differentiation, within relatively narrow constraints for particular rock types, values lying outside these normal limits must be regarded skeptically. Such diachronisms do exist in the normal Irvine-Baragar derivations, but can be removed, for further study, through the use of a screen as displayed in Figure 3.13. Silica ranges used for individual rock types have been arbitrarily set to include most published values for that type and thus overlap the ranges of other categories to some extent. But since the screen serves only to remove erratic anomalies rather than prescribe identification, the method is deemed valid. In addition, ultramafic volcanic rocks can be further classified by the Al_2O_3 vs $FeO/(FeO + MgO)$ (Naldrett) diagram as described in a previous section.

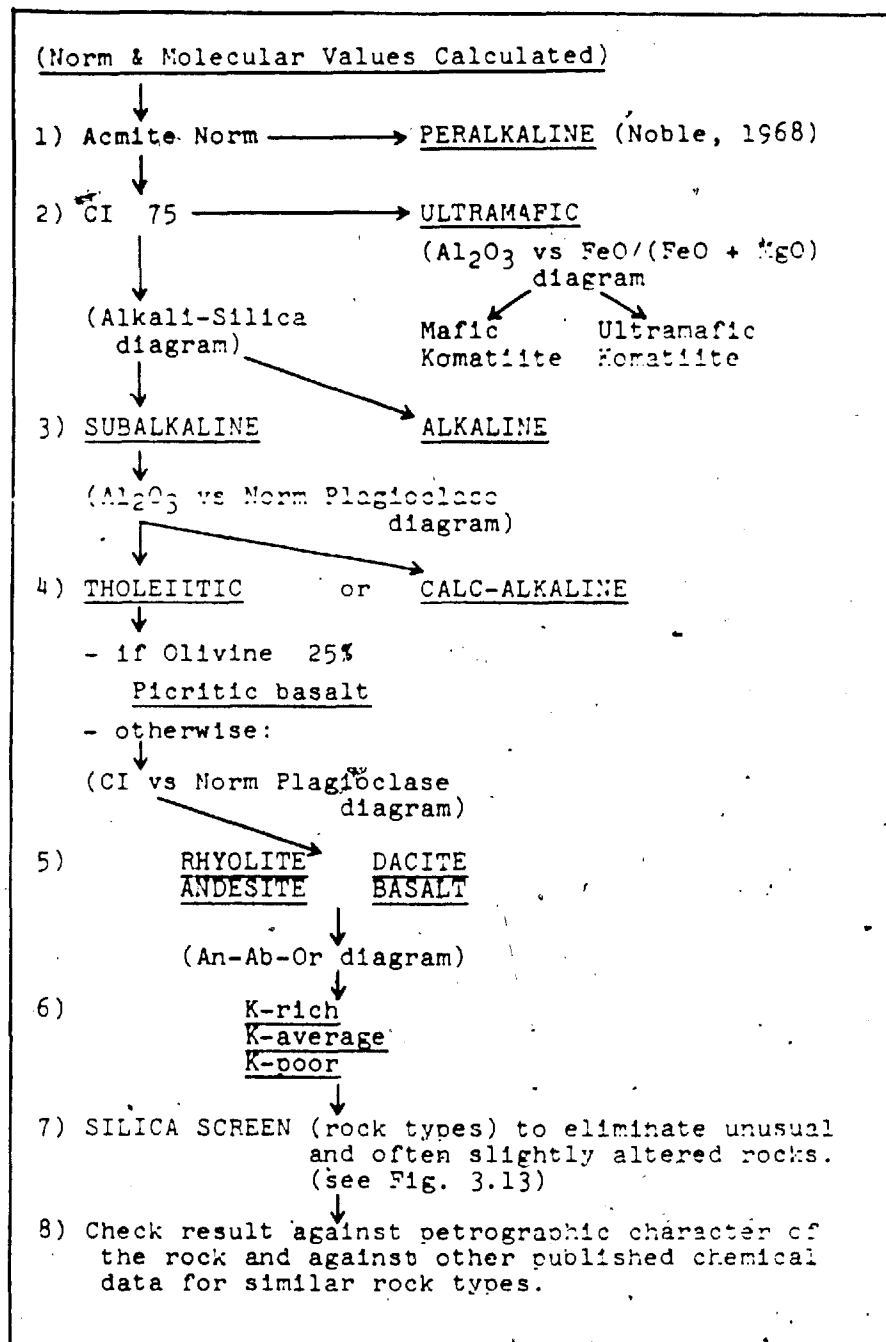


Figure 3.12: Modified Irvine-Baragar (1971) Classification Flow-Chart for the Bachelor Lake Suite

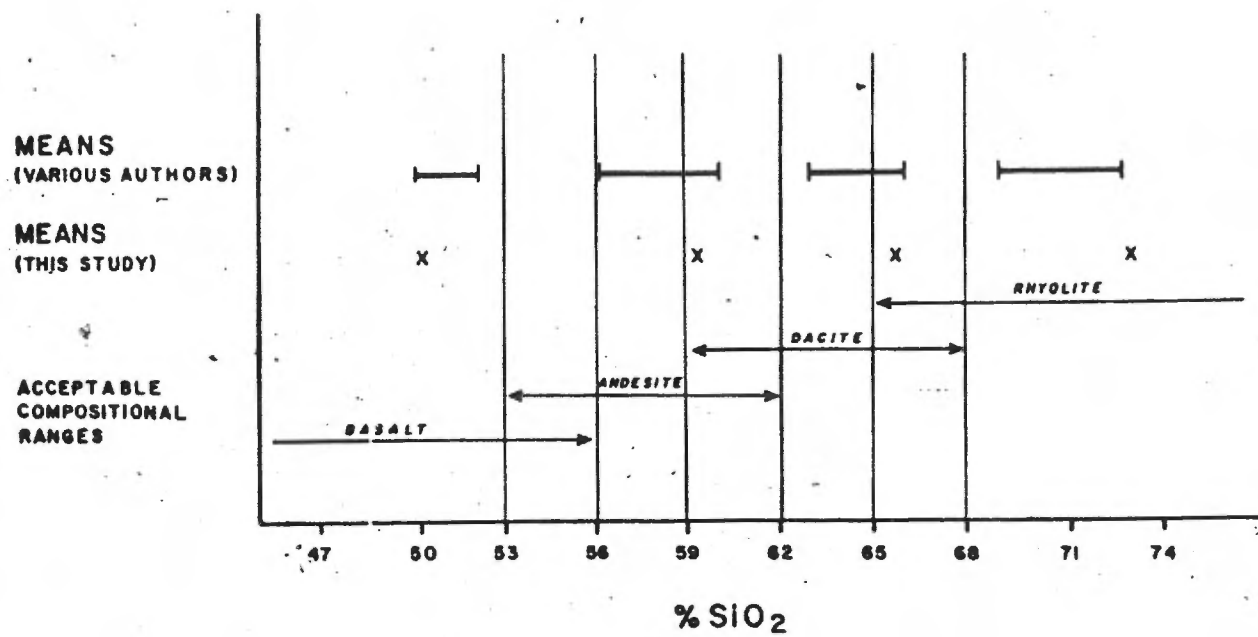


Figure 3.13: Silica Screen for Common Volcanic Rocks

3.6 SUMMARY OF CLASSIFICATION

Many techniques have been devised, using chemical data, to identify rock types, or to characterize magmatic suites. These include:

1. PEACOCK CLASSIFICATION - divides igneous rocks into four chemical classes but does not identify the rock type.
2. NIGGLI CLASSIFICATION - recasts chemical weight percent of oxides into molecular quotients, which are then compared for various rock types by plotting them against si. Use of si as a base function is questionable. Niggli classification does not identify rock types.
3. CIPW NORMS - calculation of normative minerals from chemistry and therefore an indirect "mineralogical" classification. Excellent correlation with optical mode but problems are caused by hydrous assemblages and Na₂O or Fe₂O₃/FeO changes. Provides the best developed approximation to primary modal composition.
4. HARKER DIAGRAM - shows general chemical relationships to igneous rock series, but assumes continuous SiO₂ increase during consanguinous magmatic evolution.

5. LARSEN DIAGRAM - similar to Harker diagram and may be superior in terms of a more complex abscissa and more linear elemental curves.
6. ALKALI-SILICA DIAGRAM - good division of most volcanic rocks into natural alkaline and subalkaline suites.
7. Al_2O_3 vs NORMATIVE PLAGIOCLASE DIAGRAM - good division of subalkaline volcanic rocks into tholeiitic and calc-alkaline series, especially for mafic rocks. Care is necessary to avoid altered samples which affect the plagioclase (Na_2O) factor.
8. COLOR INDEX vs NORMATIVE PLAGIOCLASE DIAGRAM - good division of subalkaline volcanic rock types. Similar problems, as above, with the plagioclase component.
9. APM DIAGRAM - good division of subalkaline volcanic rocks into tholeiitic and calc-alkaline series (especially for intermediate to felsic rocks). Useful for displaying Fe-fractionation trends but careful sample selection is necessary to avoid alkali alterations.
10. Al_2O_3 vs $FeO/(FeO + MgO)$ DIAGRAM - useful division of tholeiitic and ultramafic (including

komatiitic) volcanic rocks (poorly accomplished by most of the above diagrams).

11. PEARCE DIAGRAM - divides basaltic rocks, from some geologic provinces, into continental and oceanic types. Useful in illustrating the evolution of major volcanic sequences.

Several authors have combined one or more chemical schemes and/or variation diagrams into generalized, volcanic rock classification schemes:

1. CHURCH-MURATA METHOD - a good method of obtaining volcanic rock names. Based predominantly on post-Archean suites (Archean rocks have some notable chemical differences). Limited by lack of provision for alkaline-subalkaline, tholeiitic-calc-alkaline or ultramafic divisions. Some degree of overlap of rock-type fields.
2. JENSEN METHOD - primarily a simple, ternary plot of the major elements considered the least mobile under low to medium metamorphic conditions. Useful provision for correlation with color (i.e. ties in with a viable field classification). No provision for alkaline-subalkaline division but this could be accomplished by an alkali-silica diagram pre-screening. Somewhat arbitrary

division of rock types, based entirely upon Al_2O_3 content.

3. MODIFIED IRVINE-BARAGAR METHOD - CIPW norms are calculated and, together with geochemical data, are passed through a series of variation diagrams and mineral/chemical screens. The use of numerous diagrams, while more cumbersome than some other classification schemes, allows better discrimination of rock and series divisions than is possible with a single diagram. Addition of a silica screen significantly improves the removal of altered specimens. An improvement at the ultramafic end of the classification is necessary and can be accomplished with the Al_2O_3 vs $FeO/(FeO + MgO)$ diagram.

Analysis of the preceding discussion leads to the inevitable conclusion that no singular diagram or analytical method is capable of classifying all rock and/or series types. Chemical, mineral and textural parameters are much too diverse to allow subdivision by the limited factors included in one diagram. Furthermore, the inherent bias and apportionment in certain techniques serve to enhance some rock types while diminishing others. This polarization is important in the separation of particular groups but at the same time tends to eliminate others (see Church, 1975, p.260).

Chapter 4

REGIONAL GEOLOGY

Located in the southeastern part of the Superior tectonic province, the Abitibi orogenic belt is the largest, continuous volcanic belt in the Canadian Shield. This generally east-trending entity is approximately 750 km. long by 200 km. wide, and is tectonically truncated on the east by high-grade Grenville province rocks and on the west by the Kapuskasing subprovince.

Lithologically, it contains orogenic supracrustal rocks together with mafic and felsic plutons. In common with other Archean greenstone belts, the area possesses a long and complex history of Precambrian events, with geologic relationships often obscured by younger sedimentary rocks and glacial cover. It has been studied for many years (recently summarized by: Ayres (1977) and Goodwin et al. (1977, 1972, 1970)) and has yielded several hundred ore-producing properties, including Au-Ag, Cu-Zn-Pb-Ag, Ni-Cu, Fe, Mo-Bi, and asbestos deposits.

With the exception of questionable granitic basement material, the oldest rocks in the belt consist of series of mafic to felsic volcanic flows and pyroclastics. Basalt and

andesite flows and syntectonic mafic intrusions are common in lower stratigraphic sequences, often exceeding 12,000 m. thick, with dacites, rhyolites and pyroclastics becoming increasingly prominent in successively higher horizons. The latter lithologies seem to dominate a number of discrete volcanic centers with limited stratigraphic continuity, and constitute only about 5-20 percent of the regional volcanic assemblage (Goodwin, 1971; Goodwin and Ridler, 1970). The generalized mafic to felsic trend may be repeated, in whole or in part, to form a number of cycles.

Toward the top of, and generally structurally conformable with volcanic sequences, are immature clastic and/or chemical sediments. The former range from discontinuous, intercalated units to broad, regionally east-trending belts of up to 3000 m. in thickness. They are composed, principally of poorly-sorted greywacke-argillite, shale, conglomerate and lithic sandstone of turbidite association and compare closely, in mineralogy and chemistry, to the enclosing volcanics (excluding granitic conglomerate pebbles). Chemical sediments are, in contrast, usually thin and laterally continuous stratigraphic units, often forming important marker horizons. Most have varying amounts of iron-mineralization and are classified as oxide, carbonate or sulphide facies, according to the dominant iron mineral (Goodwin, 1973; Eugster & Chou, 1973). Often, the various types are transitional through a broad, basinal environment.

Mafic intrusions, occurring as sheets, sills and dykes, generally within the mafic volcanic sequences, are commonly differentiated into an ultramafic base with a mafic upper portion and are often difficult to distinguish from differentiated mafic flows. More voluminous mafic intrusions forcefully intrude the host volcanics which are thereby deformed and wrapped around the intruded mass.

Felsic intrusions occur as stock-like plugs and laccoliths within and between synclinal greenstone arms. Larger, batholithic plutons occur toward the margins of the orogen and may include some primitive basement material. While the felsic intrusions are commonly classified as granites, they encompass a variety of mineral-chemical compositions and merit considerable detailed study to more completely define their role in the formation of the orogen. Similarly, contact relations are not fully understood between these felsic bodies and the volcanics. Many are clearly intrusive, deforming and altering volcanic trends (particularly toward the center of the belt), while others may be coeval intrusive differentiates.

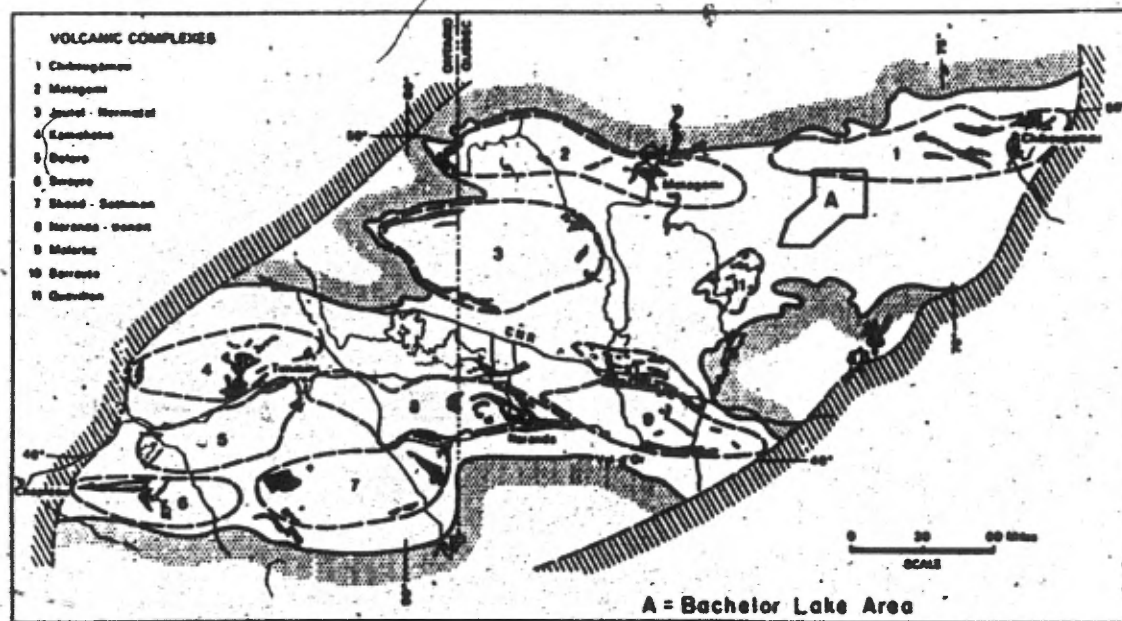
Dynamothermal tectonic events have overprinted most rocks in the Abitibi belt, producing low grade greenschist to amphibolite metamorphic mineral assemblages. Locally, however, certain areas seem to have escaped the regional effects and have endured to the present with only minor

burial metamorphic changes (Jolly, 1974; Rimsaite, 1974; Pearce et al., 1974). Conversely, in other localized settings, particularly in close proximity to intrusive bodies, the metamorphic grade may rise to upper amphibolite facies, with accompanying penetrative deformation. Typically, though, primary lava structures such as pillows, variolites, amygdules and flow and pyroclastic features endure, as do original, although mineralogically altered textures (Moorehouse, 1959, 1970). In sediments, graded bedding, facies change features and even soft-sediment deformational structures can often be observed.

Goodwin and Ridler (1970) have tentatively defined a number of ellipsoidal volcanic complexes (Fig. 4.1), each approximately 40-60 km. in diameter, which, they suggest, deviate from modern island arc settings due to compressional folding and foreshortening in a north-south direction. Overlying great thicknesses of mafic volcanic rocks are concentrations of felsic volcanics, each, representing a felsic eruptive center. Most precious and base metal deposits lie within or marginal to the felsic volcanic complexes.

Principal Au zones, often associated with carbonate-rich rocks, lie at the margins of volcanic complexes and have traditionally been interpreted as shear zones (Porcupine-Destor and Larder Lake "breaks") in intermediate

Figure 4.1: Volcanic Complexes - Abitibi Belt (after Goodwin & Ridler, 1971)



to felsic volcanics (Swayze, Matachewan, Kirkland Lake, Timmins, Cadillac, Malartic, and Val d'Or mining camps). A major east-trending Au zone extends intermittently from the Matachewan area on the west, through Kirkland Lake, Larder Lake, Noranda and Malartic, to Val d'Or on the east. A second prominent zone extends eastwards from Timmins through Duparquet and southeastward to join the first zone at Malartic. Smaller, discontinuous zones are widely distributed.

Principal base metal concentrations of the Cu-Zn-(Pb)-Ag type have direct stratigraphic relationships. Many lie at felsic-mafic transitions in upper parts of stratigraphic successions and thus define major target areas (Timmins, Noranda, Mattagami, Joutel and other, less prominent areas). Such deposits seem to be connected with processes of explosive, domal volcanic activity, as distinct from widely distributed felsic tuff zones and associated, non-economic mineralization. Ni-Cu sulfide deposits are generally connected with mafic-ultramafic rocks (Alexo, Texmont) and have been described by Arndt (1976, 1977), and Eckstrand (1972).

Chapter 5

GEOLOGY OF THE BACHELOR LAKE REGION

5.1 INTRODUCTION

The Bachelor Lake region is a volcano-sedimentary complex, downwarped into a major syncline with a regional ENE strike, except where locally modified by intrusive bodies (Fig. 5.1 & Map in back pocket). Felsic batholiths are common, adding structural complexity, especially on the south limb of the syncline. This has resulted in a number of narrow volcanic arms, running between the batholiths. Major faulting appears confined to the eastern part of the region.

The volcanic pile has been divided, on the basis of structural data, lithic proportions and petrochemical trends, into five major areas, each characterized by specific petrologic variations. Petrographic data has been summarized in table form and is found in Appendix C.

Rock types sampled in each area are summarized in Table 5.1. The 150m traverse sampling interval produced a collection that is probably representative of the relative abundance of rocks.

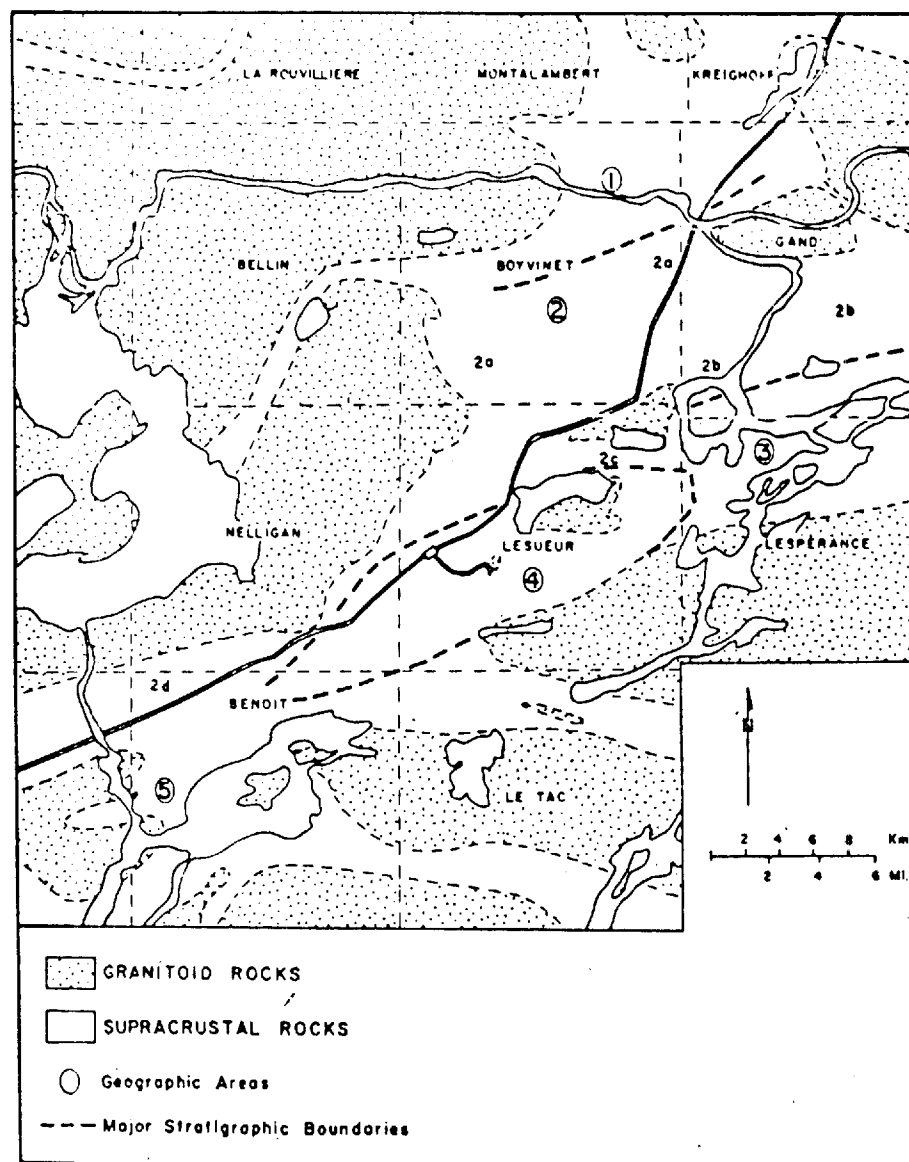


Figure 5.1: Simplified Geology of the Bachelor Lake Region

TABLE 5.1
Number of Samples of each Rock Type Collected in the
Bachelor Lake Region

	AREAS					
<u>ROCK TYPE</u>	1	2	3	4	5	TOTAL
Sedimentary	0	12	0	0	0	12
Rhyolite	1	0	0	1	1	3
Dacite	2	4	3	9	8	26
Andesite	1	10	11	16	15	53
Basalt	10	46	18	16	14	104
Pyroxenite	5	0	0	0	0	5

Subtotal	19	72	32	42	38	203

Highly Altered	2	7	4	5	8	26
*						

Total	21	79	36	47	46	229

* eliminated due to severe metamorphic
and/or alteration changes

5.2 AREA 1

Area 1 is located in Boyvinet and Gand townships in the northern part of the study area (Fig. 5.1 & Map 1). Thickness of this part of the pile is at least 7 km.

Samples were taken mainly from a traverse along the Waswanipi River in the northern part of Boyvinet township. Only 20 samples were taken, due to limited rock exposure. Sampling ended in the marginal granite batholith, but additional work further north, in Montalambert township, might succeed in reaching deeper levels in the pile.

Stratigraphy trends east-west through western Boyvinet township, where the belt pinches between two large batholiths, and swings northeast into the regional trend in northeastern Boyvinet, between other batholiths. Some shearing is noted in volcanics near the margins of these batholiths but faulting or topping features were not observed. The rocks consist primarily of mafic volcanics and ultramafic bodies. The ultramafic bodies are not present in stratigraphically higher areas, and their disappearance is the sole criterion for establishment of the boundary between Areas 1 and 2. Therefore, Area 1 may be considered as a conformable base to Area 2 but is treated separately because of the presence of these unique ultramafic bodies.

5.2.1 Ultramafic Intrusive-Cumulate Bodies

Due to their light green color and fine to medium grain size, the ultramafic rocks were identified as intermediate volcanic rocks during field mapping. Subsequent petrochemical study revealed their true nature, but not until field investigations were completed. Detailed assessment of their relationship to surrounding volcanics was therefore not noted.

These rocks consist almost exclusively of fine to medium grained pyroxene with interlocking texture. The grain cores are generally fresh but some degree of uranalitization of the rims is usually present. Some thin sections show alteration to hornblende. The amount of matrix is small and consists of plagioclase, calcite, minor chlorite, epidote and sphene.

5.2.2 Mafic - Intermediate Volcanic Rocks

Basalt, the most common rock type, is medium to dark green and shows little penetrative deformation or fragmentation. They are, for the most part, massive rocks, composed of equigranular, interlocking hornblende and plagioclase.

The hornblende usually contains a fresh core with a narrow outer rim of uranalite, giving the grains a feathery appearance. Plagioclase is generally fresh but contains

various proportions of granular epidote alteration. Infrequently, the plagioclase is altered to a very fine-grained dusty relic. Carlsbad twins are common, in contrast to the rarer polysynthetic twins, in many of which the twin planes are discontinuous.

The matrix, generally of minor volume, contains chlorite and minor amounts of epidote and fine-grained plagioclase. Sphene is common, often showing an opaque core and dusty, brownish margins. It occurs as both discrete grains and masses and as interstitial fillings between major silicates. Pyrite is a ubiquitous accessory mineral.

Intermediate volcanic rocks are scarce within this suite. Only one, relatively fresh specimen was examined. It consists of a few relic plagioclase phenocrysts, mostly decomposed to calcite and epidote, in a matrix of fine-grained plagioclase, quartz, calcite, sericite, and minor epidote, sphene and opaques. Most grains are aligned, suggesting a possible tuffaceous nature.

5.2.3 Felsic Volcanic Rocks

Only three, strongly altered samples of light to medium grey-green felsic volcanic rocks were found in Area 1.

Plagioclase phenocrysts are almost completely replaced by sericite, chlorite, and calcite, with minor epidote. They are enclosed by a fine-grained groundmass of quartz and

plagioclase with frequent and prominent streaks and patches of chlorite, calcite, and sericite.

Some degree of shearing seems to be present in these samples, resulting in a distinct lineation of the phyllosilicates and a preferred orientation of the remnant phenocrysts.

5.3 AREA 2

Supracrustal rocks in Area 2 lie conformably over those of Area 1 to the north (Fig. 5.1) and consist of approximately 10 km. of mafic to intermediate lavas with minor felsic volcanics. Actual stratigraphic thickness may be less than 10 km, since numerous minor synclines and anticlines were noted. This is the largest area in the field area, in terms of thickness and lateral extent. Stratigraphy conforms well to the regional northeast-southwest strike and dips steeply in most places.

The upper stratigraphic boundary was set at the erosional unconformity marked by deposition of clastic sedimentary wedges in Lesueur township. These zones seem to be laterally discontinuous, pinching out to the east and west, thereby making the upper limit of the area difficult to detect. The appearance of increasing numbers of felsic volcanoclastics indicates that the upper boundary has been crossed.

5.3.1 Mafic - Intermediate Volcanic Rocks

Three quarters of the rocks in Area 2 are tholeiitic basalts. For the most part, they are fine-grained, medium to dark green rocks and rarely greyish green. Fragmentation is uncommon but shows up as mafic breccias or, more commonly, as finely-laminated, dark tuffs.

The basalts are composed mainly of plagioclase and actinolite. The latter shows moderate pleochroism and occurs as feathery grains between plagioclase, either as single grains or radiating clusters and is not generally as abundant as plagioclase.

Hornblende, while less abundant than actinolite, is present as moderate to strongly pleochroic crystals. Normally fine to medium-grained, it becomes quite coarse-grained in some specimens. Crystal margins are rarely sharp or euhedral and are mostly replaced by uraltite, resulting in a feathery appearance. Progressive decomposition of former hornblende or, possibly pyroxene, into actinolite pseudomorphs is evident in some grains. Chlorite, as both penninite and clinocllore is a major matrix constituent.

Plagioclase may be fresh, but more often it is replaced to varying degrees by calcite and/or granular epidote. In some instances, entire replacement by calcite forms pseudomorphs after plagioclase, or recrystallized calcite rhombs. Less often, the plagioclase may be consumed by a

fine-grained, dusty replacement, possibly epidote. A further, although less common replacement is the appearance of small quantities of sericite. A few specimens contain skeletal, swallow-tailed laths of plagioclase, indicative of a quench-texture origin. The feldspars are almost always restricted to the matrix, although rare phenocrysts and microphenocrysts have been noted.

Quartz is present only in the matrix, except for rare thin veinlets. It is difficult to distinguish from plagioclase, due to fine grain size, but generally appears much less abundant than in the andesites.

Remnant pyroxene was noted in a few specimens, usually with wide replacement coronas of hornblende. These rocks are coarse grained and can be termed gabbroic. Pyroxene is not abundant, but may have been previously more common, as indicated by a few scattered hornblende grains, possibly pseudomorphic after the pyroxene.

Opaque minerals are relatively abundant in the basalts of this suite. When fine-grained, these minerals proved unidentifiable by optical or x-ray techniques. Pyrite is fairly common as distinct eu-subhedral cubes with relatively small grain size.

Andesites make up approximately one quarter of the rocks in Area 2, a significant increase over the lower

magnesian suite in Area 1. The andesites vary from medium to dark grey or green. Most samples are either massive or slightly sheared. Only a few brecciated or tuffaceous specimens were found.

Plagioclase is the dominant mineral in both matrix and phenocrysts. A majority of specimens contain plagioclase phenocrysts. In general, the proportion of feldspar phenocrysts to matrix is much larger than in the more felsic rocks. The grains are commonly twinned, either as single twins or as the more prevalent, polysynthetic twins. A few samples show possible evidence of quench texture, as described by Pearce (1974) and Pearce and Donaldson (1974), with swallow-tailed plagioclase laths. Most plagioclase grains are remarkably fresh and well-preserved. Where alteration has occurred, it is most often in the form of small patches of calcite, flecks of muscovite, or granular epidote. In specimens with more prominent alteration, the plagioclase is almost totally replaced by calcite and/or epidote. A few samples contain grains with a myrmekitic-like intergrowth of feldspar and quartz.

Quartz is relatively abundant as a fine-grained matrix constituent but is not common as phenocrysts.

Hornblende is present in many samples as relatively fine-grained, dispersed, subhedral crystals. They are weakly to moderately pleochroic and are occasionally

corroded with chloritic alteration. Actinolite is sometimes found as disseminated needles or as small felted aggregates but is not particularly abundant. Patches and streaks of chlorite are evident in most specimens, most commonly in the matrix. It occurs both as penninite, with anomalous blue polarization color, and the more common, greenish clinocllore.

Opaque minerals, of minor importance in these rocks, are most commonly found in shear or fracture zones and in samples which appear to be somewhat recrystallized during metamorphism. The predominant mineral is magnetite which occurs as fine, disseminated, granular grains, occasionally showing a slight tendency to form skeletal growth patterns. Much less abundant is the occurrence of ~~hemite~~ hematite which has been noted in a coarse-grained, eu-subhedral, skeletal form, adjacent to slightly recrystallized silicates.

5.3.2 Felsic Volcanic Rocks

Felsic volcanic rocks are scarce in this suite, although not as rare as in Area 1. They are widely dispersed throughout the area and usually form thin lenses surrounded by more mafic volcanic rocks.

Dacites, although still relatively rare in comparison with the mafic volcanics, are widely distributed. They are usually light grey-green, and generally maintain a cherty

appearance. Some of these rocks possess a lineation which may be either the effect of slight shearing or a primary tuffaceous banding.

Plagioclase is common in both matrix and phenocrysts and assumes dominance in the latter. The grains are often zoned and contain a variety of twin types, often in combination. Alteration of the plagioclase takes the form of fine grained dusty inclusions of possibly sericite, or granular epidote with minor calcite. Sericite and epidote are seldom found together in the same specimen.

Quartz is abundant in the matrix but is found only infrequently as phenocrysts and is always subservient to plagioclase. Sericite, together with chlorite, is found as streaks and grain clusters within the matrix and, occasionally, in fractures within plagioclase phenocrysts.

Actinolite is present in a few specimens as scattered needle-like grains in small, radiating clusters. Opaque minerals are not common in these rocks, although occasionally, a small amount of fine-grained magnetite or ilmenite (with a coating of leucoxene) and, less commonly, pyrite, is present as a very fine-grained, dusty opaque material. Magnetite is found in several specimens in fine to medium sized grains. Ilmenite was identified in a few rocks, notably those of more medium grain size. It is invariably skeletal in form and may have been present, but unidentifiable in smaller grains.

Sphene is an abundant mineral in these rocks. It occurs as either an irregular opaque with translucent margins or as an irregular, translucent, dusty grain, reddish brown in color.

Mafic minerals are generally absent, while quartz and feldspar are abundant as both matrix and phenocrysts. Frequently, the quartz phenocrysts are several millimeters in diameter and show as "quartz-eyes" in hand specimen. Sericite, calcite and epidote are moderately abundant as alteration products of plagioclase in some samples. Streaks of chlorite may be the altered remains of earlier amphibole or biotite.

5.3.3 Sedimentary Rocks

Sedimentary rocks were not examined in detail, during the course of present investigations, since they are not directly linked to processes of volcanism. However, most of the sedimentary rocks are derived from volcanic sources. Their presence and location within the enclosing volcanic suites, at specific stratigraphic positions, is of major significance in understanding the geologic history of the region.

5.3.3.1 Clastic Sedimentary Rocks

Two major bands of clastic sedimentary rocks are present, discontinuously, along the Bachelor Lake volcano-sedimentary belt. They are located north and south, respectively, of the major, regional synclinal axis and may therefore be stratigraphically equivalent (Fig. 5.1). These sedimentary units are located directly below the thickest part of the domal, calc-alkaline suite of Area 4.

The northern belt outcrops just south of Bachelor River in northern Lesueur township. It has a maximum thickness of 1200 m. over a poorly exposed length of about 3 km, with similar trend and dip to the enveloping volcanics. The northern contact may be fault-bounded along Bachelor River, since no outcrops were found to the north and since the linear course of the river may be fault controlled. Contact between the sediments and overlying volcanics in the southern part of the north belt is not exposed. Graham (1957) suggests that this contact is marked by the presence of angular boulders of basic lava with intercalated lava flows. As such, it is difficult to distinguish such angular clastic sediments from similar pyroclastic material often found in overlying strata, particularly in the eastern part of the north belt.

Rocks in the north belt consist of conglomerate with felsic (granite, aplite, feldspar porphyry, quartz) and

occasional mafic (greenstone) clasts, ranging in size from a centimeter to half a meter, in a greywacke matrix. Voluminous greywacke and lesser slate are also present, the former consisting of chlorite, hornblende, tremolite, epidote and sausseritized plagioclase, with minor quartz, mica, carbonates and opaques. The mafic nature of these sediments, with the exception of the felsic clasts, is thus evident and affirms their similarity to volcanic pyroclastic material. Intercalations with volcanic flows are frequent, particularly in the eastern part of the township, mapped by Dugas (1975), where "their sedimentary character is seldom obvious". Metamorphic effects have been noted by Graham (1957) immediately west of Bachelor Lake, where quartz-biotite gneiss and quartz-biotite-sillimanite gneiss are found near pink, granitic dykes.

The south belt of clastic sediments cuts the west end of Auger Lake in northern LeTac township. Here, the maximum exposed thickness is about 1000 m, exposed over 3 km, with similar trend and dip to the enclosing volcanics. The north contact, as well as the lateral extremities are mostly drift covered. Dugas (1975) finds no indication of the belt extending into the eastern half of the township. Graham (1957), working in the west, implied that a disconformity may exist between well-developed conglomerate and unexposed volcanics. Outcrops are slightly more abundant and lighter colored than in the north belt, but rock types are generally

similar. Conglomerate seems to be slightly more common and clasts are of slightly greater diameter. At a point 0.8 km. west of the mouth of Auger Creek, MacKenzie (1934) reports that "pebbles form more than 50 percent of the rock -- mostly of acid to basic volcanic material but there are some of massive, grey, hornblende granite and others of white and grey quartz -- granite pebbles are well-rounded and up to one foot diameter -- those of volcanic material are somewhat flattened -- matrix of fine-grained greywacke". He further notes that, to the north of these outcrops, two bands of similar conglomerate, each two feet wide, are interbedded with coarse-grained arkose.

5.3.3.2 Chemical Sedimentary Rocks

Chemical sediments, described as iron formations, chert bands, carbonated schists, and even shales, have been documented by various authors within the map area. These rocks are often discontinuous bands of fine-grained sediments, one to five meters thick, and up to tens of meters long. They have a distinct tendency to occur at or near the stratigraphic top of Area 2.

Approximately 500 meters northwest of Billy Lake in Lesueur township, diamond drilling by Chesbar Iron Powder Co. (formerly Chesbar Chibougamau Mines Ltd.), in 1960, indicated an iron formation up to 90 m. thick and 500 m. long. The country rock was reported to be an assemblage of

greywacke and conglomerate with thin layers of amphibolite. Earlier holes, slightly north, by McWatters Gold Mines Ltd., in 1958, intersected a graphitic horizon. A thinner band of iron formation, again composed of impure quartzite and magnetite, extends westward for 5 km. along the south shore of Billy Lake. It is generally less than 3 m. wide and contains minor feldspar, sericite and calcite.

Carbonated schist has been noted by Dugas (1975) as a 300.m. thick band, extending over 3 km, along the south shore of Billy Lake. It is composed of schistose, carbonated rock with interstratified, thin, iron formation bands, slate, and volcanic layers. Dugas suggested a volcano-sedimentary origin for this unit.

Iron formation is also present, to the southwest, in southern Bosse Township, as reported by Claveau (1953) and Blake (1953). In the course of regional mapping, they discovered impure quartzites and micaceous schists along the south shoreline of Waswanipi Lake. These bands were noted as being strongly drag-folded, in places, and commonly injected by coarse gneissic material in fold noses. They detected strong magnetic anomalies near the sediments and Claveau examined hornblende-bearing quartzites with up to 35 percent magnetite. He further suggested that the units might be extensive, due to the widespread magnetic anomaly. This description was followed up by Chesbar Chibougamau

Mines Ltd., in 1957, when it was staked, prospected and drilled, to outline a potential source of iron ore. The surveys (Dumont, 1957) revealed large "remnants of iron formation which have been positioned in irregular patterns by the intrusive action of the large batholith", within which they are contained.

5.4 AREA 3

Geologic relationships in Area 3 are somewhat enigmatic in relation to other parts of the pile. Field evidence (pillow tops, graded tuffs, etc.) quite clearly indicates that it lies on the south limb of the major regional syncline and is therefore stratigraphically equivalent to parts of Areas 2 and 4 (Fig. 5.1). Topping directions are scarce in this sequence, leaving the exact location of the synclinal axis uncertain. It is known, however, to lie somewhere between Short Lake and the east arm of Opawica Lake. More exact relationships are obscured by lack of detailed mapping and the presence of structural complexities.

Lowest stratigraphic units are cut off by large intrusive batholiths in southern Lesperance township. The sequence progresses upwards through a succession of predominantly mafic flows. On approaching the regional synclinal axis, mafic tuffs (possibly sheared flows, in part) and felsic volcanics appear. These felsic rocks are

by no means as abundant or stratigraphically thick as those in Area 4, but seem to represent a narrow (1 km) upper capping.

Limited mapping along the Opawica-Lichen Lakes system (Map 1 - rear pocket) indicates that the supracrustals follow the regional northeast-southwest trend, but swing to a more east-west direction in the eastern part of Gand and Lesperance townships. Very steep dips, common to the other areas, are maintained.

The linear and cross-linear pattern of river and lake systems suggests fault-bounded control, as is supported, along northeast-southwest trending waterways, by the presence of sheared volcanics.

Excellent access is provided by the water system into most parts of the area and good outcrop exposure is found along the banks of both islands and mainland.

5.4.1 Mafic - Intermediate Volcanic Rocks

Most volcanics within Area 3 are classified as mafic to intermediate rocks, and are traceable over relatively large distances, especially along shorelines, where most samples were collected. Vertical transitions in the pile are, however, difficult to detect, due to major lateral faulting at several stratigraphic intervals.

Basalts are the most common rock type and are dark grey to green, massive rocks with little penetrative deformation. Grain size is variable, with coarser varieties apparently more abundant lower in the sequence. These rocks have coarse, stubby plagioclase phenocrysts, in various stages of sericitization, and equally coarse chlorite and actinolite pseudomorphs, altered from the hornblende. The matrix is a combination of plagioclase, epidote, chlorite and medium to coarse-grained skeletal ilmenite. Between this base, and the andesite horizon, above, the basalts consist of fine-grained masses of epidote, calcite, plagioclase, chlorite and actinolite. The first two minerals are the altered products of plagioclase, little of which has been preserved. Where present, these feldspars are found as highly corroded laths and stubby prisms.

Andesites represent approximately one quarter of the rocks and are present mainly in a thin (1/2 km) band of long lateral continuity, located across the southwest arm of Opawica Lake. It is traceable, along strike, from the mainland through a series of islands, and thus forms a distinctive marker horizon. They are generally dark grey to green rocks and are normally massive, although some tuffaceous-like varieties do occur. Mineral lineations are common only in these tuffaceous samples and penetrative deformation is minor or absent.

Plagioclase is common both as phenocrysts and matrix constituents. Phenocrysts vary in size from 1.0 to 2.0 mm and commonly have margins and small interior patches altered to sericite and minor epidote. They are relatively fresh, however, and are seldom completely altered. Fine-grained plagioclase is abundant in the matrix.

Variable amounts of ragged actinolite, quartz, epidote, calcite and chlorite are found in the matrix, with the latter three being particularly abundant in narrow fractures. They are also common around the margins of plagioclase grains, which they appear to have altered. Mafic minerals are relatively uncommon and are represented only by a few altered (actinolite, chlorite) relics. Opaques are similarly uncommon, being present only as minute, dusty grains in the matrix.

Immediately above the andesite horizon, a thin, tuffaceous zone of basaltic composition is found. These rocks consist of fine-grained plagioclase and quartz with abundant chlorite and calcite seams. Higher in the pile, the basalts consist of dark green, fine-grained, generally massive rocks. The main components are plagioclase, quartz, chlorite, epidote, calcite and actinolite. Phenocrysts are rare, but, where present, consist of stubby plagioclase prisms, in random orientation. The uppermost basaltic units are tuffaceous and contain very fine-grained quartz,

plagioclase, epidote and abundant seams of chlorite and calcite.

5.4.2 Felsic Volcanic Rocks

Immediately above the mafic pile described above, is a zone of felsic flows, pyroclastics and intercalated mafic to felsic flows and fine tuffs. In this respect, it resembles the rock assemblage of Area 4. This upper zone appears to form a felsic capping on this part of the pile and is the uppermost, youngest unit. The regional syncline is presumed to lie somewhere in this zone, although insufficient detail is available to locate its exact position. Immediately north of Short Lake (Map 1 - rear pocket), the mafic pile of Area 2 tops to the south.

A series of fine-grained, grey, cherty volcanics outcrop on the west side of Opawica Island and consist of plagioclase phenocrysts in a fine-grained matrix of quartz, epidote, and minor chlorite. The phenocrysts are abundant and enclose very dusty (sericitic) plagioclase remnants.

Further east, one kilometer southeast of Short Lake, agglomeratic material has been described by Shaw (1939). He describes these rocks as containing "fragments of banded chert, diorite, andesite and a few rounded nodules of pyrite. The distribution of fragments in the agglomerate is very erratic -- pale, well-banded tuffs outcrop on the north

shore of Opawica Lake, south of Short Lake. They may be related to the agglomerates to the north -- ". But the units are not further described and more work is required to define the rock type and areal extent.

5.5 AREA 4

Area 4 contains the highest stratigraphic sequence in the study area, lying within the inner zone of the major, regional syncline. Boundaries for the unit have been defined, along regional strike, as the contact between the unconformity of Area 2 (i.e. sedimentary sequences east of Bachelor and Auger Lakes) and the overlying volcanics of the next major volcanic succession. The sedimentary rocks serve as major marker horizons and allow relatively accurate definition of the boundaries along strike, but the location of the boundaries at the eastern and western extremities of the area is less exact. Here, sedimentary units are absent, having pinched out closer to the core zone (i.e. central Lesueur township), and boundaries must be extrapolated along strike. Therefore, Area 4 forms an ovoid-shaped lens, pinching out to the east and west.

The rocks types in Area 4 are quite different from those in the underlying volcanic pile. For the first time, medium to coarse, fragmental volcanics become a prominent feature. Their scattered distribution, along with increasingly differentiated volcanic flows, is a major delineating feature of Area 4.

Intrusive bodies are present both as irregular, small (1km) and medium (5km) sized granitoid masses and semi-stratiform, medium-sized gabbro-diorite bodies.

5.5.1 Mafic-Intermediate Volcanic Rocks

While the abundance of intermediate to mafic volcanic rocks in this area is somewhat diminished by higher proportions of felsic lavas and pyroclastics, they nonetheless form a major portion of the pile. Detailed mapping by Graham (1957) and Descarreaux (1973) reveal that these rocks comprise at least three quarters of all volcanics in the central part of this area. The bottom of the sequence, exposed along Highway 113, begins as a massive to pillowed group of primarily mafic lavas and changes upward with the introduction of felsic flows and pyroclastics. But mafic volcanics continue to be found both interlayered and alternating with more felsic rocks, the former averaging twice the stratigraphic thickness.

It is significant that the proportion of andesite, relative to basalt increases in this area, although both are present throughout the whole study area. This fact is supported not only by the petrochemistry of the present study, but by also the works of Graham (1957), Van de Walle (1970), Dugas (1975), and Descarreaux (1976).

Basalts are most common in the basal units but occur throughout the sequence. East of the village of Desmaraisville they are frequently pillowed, topping south, and are probably equivalent to similar rocks in southeastern Nelligan township. At higher levels, the basaltic units are thinner. Most are dark green, fine-grained and relatively massive. They are almost invariably composed of felted masses of plagioclase, actinolite, chlorite, sericite and epidote. The plagioclase grains are lath-shaped and in various stages of decomposition with very fine-grained mottling. Mineral orientation and veining are both rare.

The andesites are medium to dark grey (less commonly greenish), fine-grained, and massive. None were observed to be pillowed but a few are brecciated. Mineralogically, they consist of plagioclase, hornblende, actinolite, chlorite, epidote, and sericite. Plagioclase phenocrysts are very common but their state of preservation varies from relatively fresh, slightly fractured grains to clouded pseudomorphs, to heavily chloritized and sericitized relics. The mafic minerals are often lath-shaped, with hornblende occasionally pseudomorphing pyroxene and in turn being replaced by actinolite. Fine, disseminated pyrite forms a majority of the opaques. Amygdules of calcite and lesser quartz become more abundant at progressively higher levels in the sequence.

5.5.2 Felsic Volcanic Rocks

Felsic volcanic rocks form approximately one third of the samples collected and are thought to represent a similar volume in the suite as a whole. As these felsic rocks are intercalated with more mafic volcanics, a specific "felsic" horizon is not apparent, although the proportion of felsic rocks increases toward the top of the volcanic pile.

Dacites constitute the largest proportion of the felsic volcanic rocks. Rock color is similar to the rhyolites, in massive flows, being light shades of grey-green to buff. In many instances, these rocks are fragmental, in the form of abundant cherty clasts bonded by a slightly darker, chloritic matrix. The massive flows consist predominantly of fine-grained quartz and plagioclase, the latter often being reduced to epidote and chlorite. Plagioclase phenocrysts are common in many of these flows and, while frequently fresh, are usually replaced to some degree by either granular epidote or, to a lesser extent, by sericite or calcite. In a few instances, plagioclase phenocrysts are almost entirely converted to a fine-grained, dusty epidote, leaving a cloudy but identifiable feldspar relic. Mafic minerals are uncommon, even as chlorite which, itself, is restricted to fracture planes.

Rhyolites are not a particularly common rock type, although they appear slightly more abundant than in the

lower suites. Rock color is essentially light, or more rarely, medium grey to green to buff. They are seldom deformed by post-depositional forces, but show occasional signs of primary, tuffaceous bedding. This bedding is difficult to confirm due to the fine-grained, siliceous character as observed in the "cherty" hand specimens.

Plagioclase is a common mineral in both phenocrysts and matrix. It is frequently fresh but more often altered to epidote and minor sericite, with the degree of replacement varying from granular cores to a pervasive, dusty relic. The phenocrysts are sometimes zoned and twinning usually occurs as simple carlsbad twins. The matrix plagioclase is very fine-grained, and is difficult to distinguish from the accompanying quartz. Quartz is predominantly a matrix mineral with phenocrysts being extremely rare. Streaks and patches of sericite may indicate replacement of fine-grained plagioclase. Parallel streaks of chlorite in the matrix may indicate the presence of either original bedding or post-depositional shearing. Mafic minerals are uncommon. Opaques are restricted to a few fine-grained pyrite cubes, as single crystals and in trains.

5.6 AREA 5

Area 5 lies to the south of the regional synclinal axis, which, in turn, appears to run parallel to and 1.5 km. south of Highway 113 (Fig. 5.1). Pillows top to the south

along the highway, but few topping directions are available to the south. Approximate position of the axis is suggested, however, by graded beds topping north, in the sedimentary units in southwest Lesueur township (i.e. the eastern extremity of Area 5). In addition, this position matches well with the axial trend established to the southwest in Mountain and Greve Townships.

The oldest rocks encountered in Area 5 were found south of Benoit Lake and are underlain by even older strata beyond the study area, to the south (Benoit and Ruelle townships). The rocks in this unmapped section are believed to comprise a north-topping base for the sequence, on the basis of government mapping to the southwest. Massive mafic volcanics are encountered south of Benoit Lake and merge into a thin (1 km) sequence of massive felsic flows in the center of, and parallel to the long axis of the lake. The strata reverts to massive mafic flows on the north shore of Benoit Lake and continues upward toward the synclinal axis.

The strike parallels the regional northeast-southwest trend except in proximity to batholithic intrusions. Dips are steep and flow units can commonly be traced for long distances, especially along Benoit Lake, where exposures are abundant.

The volcanic rocks are highly metamorphosed and deformed adjacent to the batholiths. Many samples were

eliminated from the geochemical study when they proved too highly altered. Such rocks are commonly veined with quartz and pink feldspar and were found up to one kilometer from the apparent batholithic margin. Tongues from several major bodies extend considerable distances from east and west into Benoit Lake, changing strike direction and metasomatizing the volcanics for distances of up to 1 km. It is believed that this type of alteration, which often takes the form of potassium-feldspar bearing veinlets, is widespread and has influenced a large proportion of nearby volcanics.

The penetrative nature of the batholith margins has undoubtedly altered the true stratigraphic thickness in the area. A rough estimate from a compilation of available mapping would suggest a stratigraphic interval of just over 20km, but more detailed structural mapping, especially to the south of the study area is required. It is also a point of bifurcation of the belt and should be the target of more regional study.

Area 5 comprises the western limit of actual sampling for this project and specimens were obtained along a more or less north-south traverse, perpendicular to stratigraphy, but with wide lateral sampling to confirm the strike.

5.6.1 Mafic - Intermediate Volcanic Rocks

With the exception of a narrow felsic band striking through Benoit Lake, all of the volcanic rocks in this area are mafic to intermediate. These dark, fine-grained rocks are traceable for many kilometers along strike, especially through the excellent exposures in and around the lake.

The base of the stratigraphic sequence was not reached since it lies south of the limits of the study area. The lowest unit examined is located along the southeast corner of Benoit Lake and is composed of a zone of andesitic lavas. These are grey to green, fine-grained rocks, possessing strong lineation in most samples. Stubby plagioclase phenocrysts are occasionally present, but are uncommon. Most specimens contain fine-grained quartz-plagioclase with numerous, parallel seams of chlorite and infrequent calcite. It is difficult to determine if these rocks represent tuffs or are simply sheared flows. These rocks probably correlate with volcanics found in the southwest arm of the lake, in Duplessis Township. Here, the rocks are not as strongly foliated but are similarly altered to sericite, chlorite and epidote. In addition, several basalts are present, containing less plagioclase and quartz, and much more chlorite which is pseudomorphic after hornblende. This lower unit proceeds upward into a felsic flow unit which will be discussed in the next subsection.

Above the felsic zone is found an alternating series of basalt and andesite strata. These units are traceable for several kilometers through shoreline exposures, although frequently disrupted along strike by intrusive bodies.

Basalts are dark green, often foliated rocks, containing fine-grained quartz, plagioclase, chlorite and actinolite. Many samples have fine-grained, parallel seams of quartz and/or calcite, suggesting moderate shearing and possible alteration. The basalts seem to be less deformed with increasing distance north of Benoit Lake, and become massive as the highway in the northeastern part of the township is reached.

The andesites are dark grey to green, fine-grained, moderate to strongly lineated rocks, composed of plagioclase, quartz, minor sericite, actinolite, calcite, epidote, and abundant chlorite, with lesser biotite, in parallel orientation. Phenocrysts are not common, but, where present, are in random orientation, with severely corroded margins. Mafic relics are present in the form of chlorite pseudomorphs. Many of these samples may be slightly recrystallized intermediate tuffs.

5.6.2 Felsic Volcanic Rocks

A narrow zone of massive, felsic volcanics lies approximately halfway up the stratigraphic column in this area. It trends through and along the long axis of Benoit Lake and forms a distinctive marker horizon, although overall trends are deformed by large intrusives.

All sites examined seem to consist of massive, fine-grained, grey volcanics, with overall "cherty" appearance. None appeared fragmental. Mineralogically, they contain fine-grained quartz, plagioclase, sericite, minor epidote, and infrequent chlorite and actinolite. Phenocrysts are present in some specimens, with quartz predominating over plagioclase, the latter having corroded rims. Some samples contain shear zones filled with narrow chlorite laths, while others have very thin quartz-calcite veinlets.

5.7 SUMMARY

The Bachelor Lake region is a synclinally downwarped volcanic complex. Mapping and petrographic study have shown the lower stratigraphy (i.e. Areas 1, 2 and the base of Area 3) to consist mainly of extensive, platform-type volcanic flows. A majority of these rocks are basalts, generally massive at the base of the pile, but becoming increasingly pillowed and amygdular in higher strata. The style of volcanism changes with upward progression into the domal sequence (Area 4 and extreme upper Area 3). There, the

proportions of intermediate and felsic rocks increase to the point where, together, they equal the abundance of mafic volcanic rocks. Within the domal sequence, pyroclastics, for the first time, become an important volcanic component, especially toward the top of the sequence.

Distinctive sedimentary units are relatively uncommon in this part of the Abitibi belt, but do occur at several key horizons. Chemical sediments occur as thin, cherty and occasionally graphitic and carbonaceous bands toward the top of the platform sequence. Clastic sedimentation is restricted to a wedge, pinching out east and west in the central part of the study area, and marks the upper margin of the platform sequence.

Most rocks in the Bachelor Lake region have been subjected to moderately high regional metamorphism. Descriptive petrography, in previous sections, has shown most samples to consist of altered assemblages with little primary mineralogy preserved. Mafic rocks typically consist of actinolite and/or hornblende (not as abundant and commonly uralitized), chlorite, plagioclase (often replaced by epidote, sericite or calcite) and minor sphene and opaque minerals. Intermediate rocks are similar but have lower proportions of mafic minerals and the proportion and size of plagioclase phenocrysts increases from that found in the mafic rocks. Felsic rocks contain mainly quartz and

plagioclase, the latter often being altered to epidote, calcite, or dusty inclusions. These rocks usually appear less changed by metamorphism than their more mafic counterparts.

Metamorphic grade is fairly constant throughout the region but does increase slightly (larger grain size) near large batholiths and within narrow volcanic arms running between batholiths (e.g. northern Le Tac Township - map in rear pocket).

Overall, regional metamorphic grade appears to lie in the upper greenschist to lower amphibolite facies, but the exact determination of this boundary is controversial (Winkler, 1976, p.75). Several petrologists (Turner & Verhoogen, 1960; Wenk & Keller, 1969; and Streck, 1969), following the work of Eskola (1939), suggest the sudden change from albite (An 0-7) to oligoclase or andesine (An 15-30) as the high temperature boundary for greenschist facies metamorphism of mafic rocks. This is supported by Winkler (1976, p.166) who cautions that the boundary, as defined by other mineral changes in pelitic rocks (such as the first appearance of cordierite or staurolite) may lie 20-40°C higher.

Only 35 of the Bachelor Lake rocks contained sufficient plagioclase to use the XRD method, outlined in section 2.3.3, for measuring An content. All of these samples fall

in the narrow range of An 14-28 (oligoclase), indicating that the rocks have undergone medium-grade (lower amphibolite facies) metamorphism.

Chapter 6

GEOCHEMISTRY

-- chemical analysis alone can never provide a basis for the genetic classification of rocks -- its real value is to supplement the evidence given by the microscope."

Shand (1927)

6.1 INTRODUCTION

A total of 318 rock samples from the Bachelor Lake region was analysed for 18 elements, giving a total of 5724 determinations. This large volume of data is treated in two ways.

First, in order to evaluate the geochemical characteristics of the region as a whole, analyses are plotted on the following variation diagrams: an alkali-silica plot; AFM plot; Church-Murata diagram; Pearce diagram; Naldrett Plot; and Harker variation diagrams. This enables comparison to be made with volcanic complexes in other regions of the world.

Second, to detect variations within the Bachelor Lake volcanic complex, variation diagrams are plotted for each of the five areas described in Chapter 5. The largest area, Area 2, is subdivided into four subareas.

A third method of examining the data was attempted, whereby sample analyses are projected onto three cross sections: an eastern, a central and a western section. This was done to identify geochemical trends across the volcanic belt. The considerable variation in element abundances, which exist even within one flow, obscured any trend that may exist across the belt. It was therefore found that by treating analyses by area, instead of along a traverse line, trends could be more easily identified.

The relationship between geochemical and petrographical data is discussed in Chapter 8. Chemical analyses for individual samples are tabulated in Appendix E. Element and selected ratio means and standard deviations for each rock type in the whole Bachelor Lake region and each of the five Areas are listed in Table 6.1. In addition, the coefficient of variation (i.e. Mean/Std.Dev, commonly expressed as a percent) has been calculated for each element and element ratio. The coefficient of variation (V), expresses the relative dispersion about the mean, and is useful as long as the mean is not close to zero.

TABLE 6.1
Geochemical Statistics for Bachelor Lake Data

	AREA 1																	
	Rhyolite			Dacite			Andesite			Basalt			Pyroxenite			Dacite		
	\bar{X}	s	V	\bar{X}	s	V	\bar{X}	s	V	\bar{X}	s	V	\bar{X}	s	V	\bar{X}	s	V
SiO ₂	74.37	-	-	65.80	0.21	3	60.70	-	-	49.41	2.13	4	56.24	2.50	4	66.63	2.06	3
Al ₂ O ₃	14.01	-	-	15.30	0.18	1	15.00	-	-	12.65	1.62	12	3.64	0.72	20	14.19	1.14	8
Fe ₂ O ₃	0.44	-	-	1.60	0.36	22	3.00	-	-	4.78	0.67	14	3.11	0.62	20	1.37	0.48	35
FeO	0.86	-	-	3.12	0.70	22	5.87	-	-	9.27	1.44	15	7.02	0.85	12	3.07	0.56	18
MgO	0.62	-	-	2.86	0.12	34**	2.22	-	-	7.28	2.17	30*	17.01	1.77	10	3.00	1.02	34
CaO	1.87	-	-	3.16	0.11	35*	4.67	-	-	9.65	1.38	14	8.09	2.02	25	3.73	0.37	9
Na ₂ O	3.52	-	-	4.40	0.61	13	4.16	-	-	2.59	1.09	42*	0.79	0.42	53*	4.22	0.82	19
K ₂ O	3.31	-	-	1.50	0.49	32*	1.23	-	-	0.09	0.03	33*	0.12	0.02	17	1.36	0.87	64
TiO ₂	0.97	-	-	0.55	0.12	21	0.84	-	-	1.05	0.43	40**	0.62	0.10	16	0.54	0.09	16
MnO	0.04	-	-	0.10	0.02	20	0.16	-	-	0.21	0.02	9	0.16	0.04	25	0.08	0.01	17
P ₂ O ₅	0.63	-	-	0.15	0.01	6	0.21	-	-	0.11	0.05	45*	0.03	0.00	0	0.14	0.02	14
S	0.02	-	-	0.01	0.01	100**	0.01	-	-	0.04	0.03	75**	0.01	0.01	100**	0.07	0.08	114
Ba	560	-	-	362	52	14	27	-	-	90	26	28	46	23	50*	268	38	14
Pb	59	-	-	35	6	17	25	-	-	1	1	100**	2	1	50*	32	16	50
Sr	85	-	-	236	38	16	248	-	-	237	125	52*	58	24	41*	272	55	20
Cu	4	-	-	11	4	36*	24	-	-	70	54	77**	60	84	140**	22	10	45
Zn	72	-	-	93	11	12	225	-	-	115	28	24	66	18	27	87	27	31
Co	9	-	-	25	24	96**	0	-	-	40	10	25	60	6	10	37	6	16
Ni	0	-	-	21	29	138**	7	-	-	92	87	94**	334	41	12	41	24	58
K/Rb	461	-	-	373	166	45*	408	-	-	684	323	47*	456	324	71**	349	74	21
Ba/Pb	7	-	-	10	3	30*	1	-	-	67	18	26	18	12	67**	10	4	40
Pb/Cr	0.75	-	-	0.15	0.05	31*	0.10	-	-	0.00	0.01	200**	0.03	0.02	67**	0.13	0.07	59
Ni/Co	0.0	-	-	0.6	2.8	133**	0.0	-	-	1.9	1.6	84**	5.5	0.5	9	1.2	0.7	58

\bar{X} Mean
s Standard Deviation
V Coefficient of Variation (%)

Coefficient of Variation: Moderate (30-60%) *
High (60% +) **

Dacite			AREA 2												AREA 3												Dacite		
n=4	s	v	n=4	s	v	n=10	s	v	n=6	s	v	n=3	s	v	n=11	s	v	n=18	s	v	n=1	s	v	n=1	s	v	n=1	s	v
66.63	2.06	3	66.63	2.06	3	57.23	2.38	5	49.04	2.38	4	65.63	1.75	3	59.57	2.79	4	49.70	2.54	5	72.09	-	-	64.32	1.2	-	64.32	1.2	-
14.10	1.14	8	14.19	1.14	8	12.93	2.10	16	12.86	1.10	11	14.52	1.55	11	15.96	2.12	13	14.91	1.91	12	12.30	-	-	13.37	1.2	-	13.37	1.2	-
1	0.48	34	1.37	0.48	35	3.77	1.42	43	5.16	1.10	23	1.45	0.51	35	1.98	0.31	15	3.90	0.91	23	1.46	-	-	2.19	0.5	-	2.19	0.5	-
3	0.56	8	3.07	0.56	18	7.37	3.18	43	9.87	2.62	20	2.84	0.76	27	3.93	0.55	14	7.26	1.98	27	2.83	-	-	4.25	1.2	-	4.25	1.2	-
3.73	0.37	0	3.00	1.02	34	4.94	2.07	41	6.96	1.93	27	2.09	0.92	44	5.02	1.44	28	8.13	2.47	30	1.19	-	-	2.35	0.5	-	2.35	0.5	-
4.22	0.82	10	3.73	0.37	0	5.42	2.37	43	8.74	2.12	25	6.36	1.36	21	6.13	2.19	35	9.90	1.90	19	2.06	-	-	5.21	1.2	-	5.21	1.2	-
1	0.87	64	4.22	0.82	10	3.85	0.83	21	2.65	0.14	27	2.96	0.63	21	4.43	0.79	17	2.21	1.21	54	4.42	-	-	4.35	1.2	-	4.35	1.2	-
0	0.00	16	1.36	0.87	64	0.42	0.45	91	0.22	0.09	131	2.02	0.72	35	0.43	0.22	51	0.41	0.48	117	1.73	-	-	0.24	0.5	-	0.24	0.5	-
0.08	0.01	12	0.54	0.00	16	1.05	0.64	61	1.27	0.46	88	0.33	0.12	36	0.49	0.12	24	0.78	0.39	50	0.39	-	-	0.77	0.5	-	0.77	0.5	-
0.14	0.02	14	0.08	0.01	12	0.18	0.05	27	0.24	0.05	20	0.12	0.07	58	0.11	0.02	18	0.18	0.02	11	0.09	-	-	0.15	0.5	-	0.15	0.5	-
0.07	0.08	114	0.14	0.02	14	0.21	0.08	38	0.12	0.16	50	0.11	0.03	27	0.11	0.03	27	0.10	0.02	20	0.07	-	-	0.18	0.5	-	0.18	0.5	-
8	38	14	0.07	0.08	114	0.07	0.06	85	0.07	0.09	128	0.02	0.04	200	0.01	0.02	200	0.02	0.03	150	0.02	-	-	0.06	0.5	-	0.06	0.5	-
2	16	50	268	38	14	235	123	52	135	114	77	400	76	19	150	78	52	138	115	83	350	-	-	244	1.2	-	244	1.2	-
272	55	20	32	16	50	11	12	109	5	6	120	47	12	25	10	8	80	7	11	157	35	-	-	22	1.2	-	22	1.2	-
22	10	45	272	55	20	175	146	74	147	73	49	152	12	73	268	102	38	184	65	35	191	-	-	221	1.2	-	221	1.2	-
17	27	31	22	10	45	41	30	73	74	36	48	10	6	60	23	23	100	39	33	84	25	-	-	25	1.2	-	25	1.2	-
17	6	16	87	27	31	122	55	45	129	38	29	94	38	40	69	22	31	96	18	18	110	-	-	189	1.2	-	189	1.2	-
41	24	58	37	6	16	20	19	67	45	8	17	35	9	25	42	6	14	51	9	17	19	-	-	33	1.2	-	33	1.2	-
349	74	21	41	24	58	65	44	67	82	53	64	56	41	73	99	60	60	150	98	65	26	-	-	34	1.2	-	34	1.2	-
10	4	40	349	74	21	415	159	38	409	225	55	356	76	21	476	233	48	463	251	54	419	-	-	344	1.2	-	344	1.2	-
13	0.07	59	10	4	40	34	19	55	39	31	79	9	3	33	30	30	100	27	15	55	9	-	-	11	1.2	-	11	1.2	-
12	0.7	58	0.13	0.07	59	0.08	0.07	83	0.04	0.04	117	0.31	0.10	32	0.03	0.02	61	0.05	0.05	117	0.31	-	-	0.15	0.5	-	0.15	0.5	-
			1.2	0.7	58	2.1	1.1	52	1.7	0.9	52	1.6	0.7	43	2.2	1.1	50	2.8	1.4	50	0.8	-	-	1.9	0.5	-	1.9	0.5	-

Dacite	n=7
1.2	1.2
1.9	1.9
2.19	0.5
4.25	1.0
2.35	0.7
5.21	1.1
4.35	1.2
0.94	0.4
0.77	0.2
0.15	0.0
0.18	0.0
0.06	0.0
244	
22	
221	1
25	
143	
33	
34	
344	
11	
0.15	0.1
1.0	0

AREA 4												AREA 5											
Rhyolite			Dacite			Andesite			Basalt			Rhyolite			Dacite			Andesite			Basalt		
n=1			n=2			n=6			n=16			n=1			n=8			n=15			n=14		
X	s	V	X	s	V	X	s	V	X	s	V	X	s	V	X	s	V	X	s	V	X	s	V
-	-	-	64.32	1.22	2	59.54	3.34	5	52.18	2.72	5	76.00	-	-	66.45	1.25	1	58.42	2.24	3	49.52	3.12	6
-	-	-	13.37	1.95	14	14.46	1.57	11	14.59	1.86	12	11.00	-	-	15.22	1.38	9	15.17	1.14	7	12.52	1.57	12
-	-	-	2.19	0.54	24	2.79	0.72	25	4.24	1.12	26	0.95	-	-	1.18	0.13	11	2.51	0.69	27	5.20	1.07	20
-	-	-	4.25	1.05	24	5.34	1.34	25	7.90	1.61	20	1.87	-	-	2.29	0.24	10	4.93	1.36	27	10.23	2.08	20
-	-	-	2.35	0.74	31*	3.96	1.23	31*	6.23	1.68	27	1.05	-	-	2.49	0.85	34*	3.91	0.96	24	6.58	1.64	24
-	-	-	5.21	1.13	21	5.50	1.42	25	7.31	1.97	26	1.29	-	-	4.03	1.27	31*	6.16	1.24	20	8.16	1.78	21
-	-	-	4.35	1.26	29	4.23	0.97	22	2.58	0.80	31*	5.43	-	-	4.96	0.54	10	4.54	0.70	15	2.67	0.85	31*
-	-	-	0.94	0.40	42*	0.86	0.55	64**	1.06	0.72	67**	1.00	-	-	1.51	0.59	39*	0.93	0.47	50*	0.31	0.29	93**
-	-	-	0.77	0.20	26	0.87	0.31	35*	0.92	0.18	19	0.19	-	-	0.42	0.09	21	1.01	0.56	55*	1.32	0.42	31*
-	-	-	0.15	0.03	20	0.19	0.04	21	0.25	0.10	40*	0.06	-	-	0.00	0.00	0	0.16	0.06	37*	0.32	0.18	56*
-	-	-	0.18	0.05	27	0.18	0.08	44*	0.15	0.04	26	0.03	-	-	0.10	0.02	20	0.20	0.12	60**	0.17	0.13	76*
-	-	-	0.06	0.07	116**	0.07	0.13	185**	0.05	0.09	180**	0.01	-	-	0.03	0.04	133**	0.04	0.03	225**	0.12	0.21	175**
-	-	-	244	63	25	295	127	76**	211	108	51*	190	-	-	339	89	26	314	137	41*	175	88	50*
-	-	-	22	8	36**	20	13	65**	25	16	64**	22	-	-	40	16	40*	29	13	46*	10	7	70**
-	-	-	221	152	68**	227	136	60**	192	144	75**	178	-	-	386	134	34*	360	137	38*	217	192	88**
-	-	-	25	9	36*	37	22	59**	32	24	75**	3	-	-	10	6	60**	37	15	50*	93	46	49*
-	-	-	143	55	36*	146	43	29	146	85	58*	73	-	-	74	14	18	104	25	24	146	46	31*
-	-	-	33	11	33*	38	16	42*	42	8	19	0	-	-	35	2	5	44	32	72**	48	40	83**
-	-	-	34	26	76**	61	47	77**	129	79	61**	32	-	-	36	23	63**	51	39	76**	88	51	58*
-	-	-	344	62	18	357	92	25	423	287	67**	377	-	-	310	47	14	275	68	24	233	102	43*
-	-	-	11	3	27	16	6	37*	15	24	160**	9	-	-	9	2	22	12	4	33*	19	6	31*
-	-	-	0.15	0.13	88**	0.12	0.07	63**	0.20	0.23	111**	0.12	-	-	0.12	0.07	98*	0.09	0.06	64**	0.06	0.04	77**
-	-	-	1.0	0.6	60*	1.5	0.9	60**	3.1	1.8	58*	0.0	-	-	1.0	0.6	60**	1.4	1.0	72**	2.2	1.1	50*

AREA 5												TOTAL BACHELOR LAKE REGION											
Dacite n=8			Andesite n=15			Basalt n=14			Rhyolite n=3			Dacite n=26			Andesite n=53			Basalt n=104					
X	s	V	X	s	V	X	s	V	X	s	V	X	s	V	X	s	V	X	s	V			
66.45	1.25	1	58.42	2.24	3	49.52	3.12	6	74.15	1.96	3	65.87	1.74	3	58.85	2.82	5	49.84	2.81	5	SiO ₂		
15.22	1.38	9	15.17	1.14	7	12.52	1.57	12	12.44	1.51	12	14.51	1.52	10	14.65	1.84	12	13.42	1.89	14	Al ₂ O ₃		
1.18	0.13	11	2.51	0.69	27	5.20	1.07	20	0.95	0.51	54	1.53	0.53	35	2.76	0.99	36	4.81	1.24	25	Fe ₂ O ₃		
2.29	0.24	10	4.93	1.30	27	10.23	2.08	20	1.85	0.99	54	3.07	0.97	32	5.36	1.92	36	9.19	2.31	25	FeO		
2.49	0.85	34	3.91	0.96	24	6.58	1.64	24	0.95	0.30	32	2.61	1.01	39	4.21	1.41	33	6.85	2.05	30	MgO		
4.03	1.27	31	6.16	1.24	20	8.16	1.78	21	1.74	0.40	23	4.23	1.26	30	5.76	1.63	28	8.66	2.20	25	CaO		
4.96	0.54	10	4.54	0.70	15	2.67	0.85	31	4.46	0.96	22	4.49	0.90	20	4.29	0.84	20	2.54	0.91	36	Na ₂ O		
1.51	0.59	39	0.93	0.47	50	0.31	0.29	93	2.01	1.18	59	1.36	0.63	46	0.77	0.50	65	0.44	0.57	120	K ₂ O		
0.42	0.09	21	1.01	0.56	55	1.32	0.42	31	0.22	0.16	73	0.55	0.18	33	0.89	0.46	52	1.10	0.49	44	TiO ₂		
0.00	0.00	0	0.16	0.06	37	0.32	0.18	56	0.06	0.03	50	0.07	0.06	86	0.17	0.05	29	0.25	0.11	44	MnO		
0.10	0.02	20	0.20	0.12	60	0.17	0.13	76	0.04	0.02	50	0.13	0.04	31	0.18	0.09	90	0.13	0.07	54	P ₂ O ₅		
0.03	0.04	133	0.04	0.03	225	0.12	0.21	175	0.02	0.01	50	0.04	0.06	150	0.05	0.09	180	0.07	0.11	157	S		
339	89	26	314	137	41	175	88	50	366	185	51	304	80	26	267	176	66	157	115	73	Ba		
40	16	40	29	12	46	10	7	70	38	18	47	33	15	45	20	13	65	10	14	140	Rb		
386	134	34	367	137	38	217	192	88	151	57	38	292	132	45	268	144	54	176	116	66	Sr		
10	6	60	30	15	50	93	46	49	10	12	120	17	10	59	33	21	64	63	42	66	Cu		
74	14	18	104	25	24	146	46	31	85	21	45	98	42	43	122	48	39	130	52	40	Zn		
35	2	5	44	32	72	48	40	83	6	10	167	34	10	29	38	23	61	45	17	38	Co		
36	23	63	51	39	76	88	51	58	19	17	89	36	23	64	62	46	74	101	71	70	Ni		
310	47	14	275	68	24	233	102	43	419	42	10	339	73	22	357	134	38	397	251	63	K/Rb		
9	2	22	12	4	33	19	6	31	9	0	0	10	3	30	19	15	79	29	27	93	Ba/Rb		
0.12	0.07	58	0.02	0.06	64	0.06	0.04	77	0.40	0.32	80	0.14	0.09	64	0.09	0.07	71	0.08	0.13	172	Rb/Sr		
1.0	0.6	60	1.4	1.0	71	2.2	1.1	50	0.2	0.4	200	1.0	0.6	60	1.6	1.0	62	2.2	1.3	59	Ni/Co		

6.2 WHOLE BACHELOR LAKE REGION

All of the volcanic rocks in the Bachelor Lake region, with the exception of altered samples, plotted in the subalkaline field of an alkali-silica variation diagram (Fig. 6.1). It is interesting to note that the modified dividing line suggested by Irvine and Baragar (1971), gives a much better boundary for the Bachelor Lake suite, since a number of samples fall between it and the original line of MacDonald (1968).

Elements which most closely monitor the changing nature of magmatic differentiation are represented on an AFM diagram and are plotted for all fresh samples in Figure 6.2 A. While widespread scattering is evident, trends are apparent for individual rock types. Basalts follow a tholeiitic trend, from the pyroxenite grouping near the MgO apex, towards the Fe₂O₃+TiO₂ apex. Intermediate to felsic rocks follow a calc-alkaline trend.

A further expression of differentiation trends is provided by the Church-Murata plot (Fig. 6.3). The Bachelor Lake rocks plot at lower alumina/silica values and have a slightly higher iron-magnesium-calcium index than the 1500 common volcanic rocks that were used by Church to construct the diagram. The mean of each rock type lies outside or close to the perimeter of the original 2/3 boundary curves of Church (1975). This may be due to a preponderance of

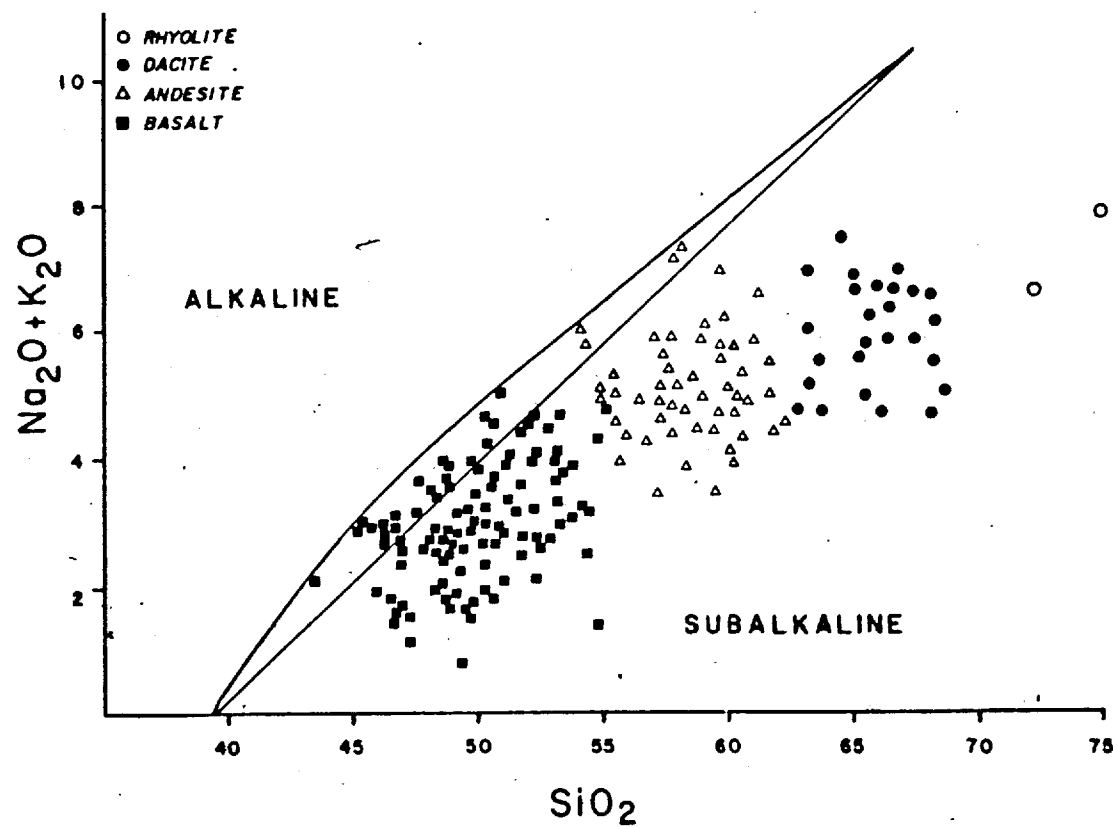


Figure 6.1: Whole Bachelor Lake Region - Alkali-Silica Variation For Fresh Rocks

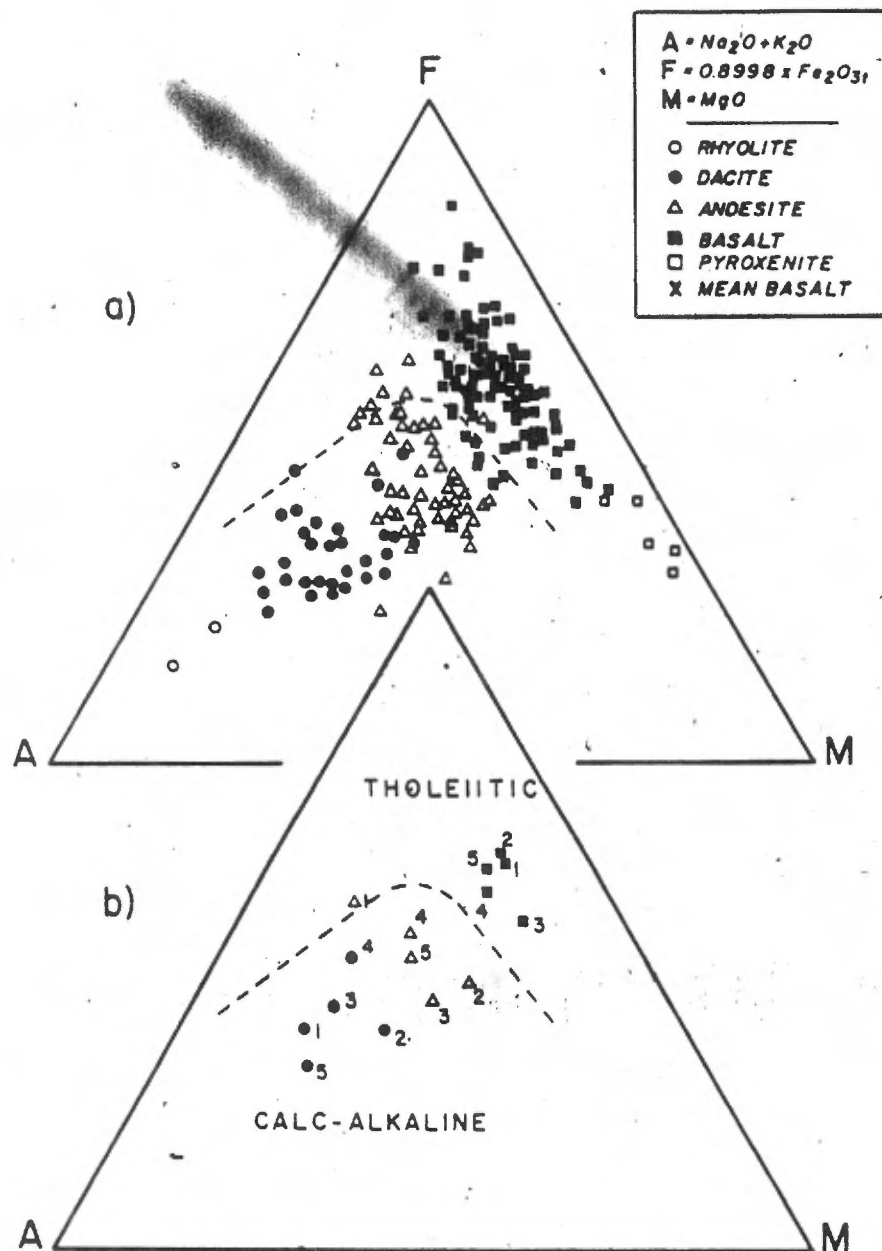


Figure 6.2: Whole Bachelor Lake Region - AFM Diagram a) All Samples b) Area Means

more modern, high Al rocks in the derivation of Church's original fields (see Fig. 6.6 & 6.7). The alkaline portion of the diagram correlates well for the Bachelor Lake rocks, for all rock types except basalt, which is slightly low in alkalies.

The TiO_2 -K₂O-P₂O₅ diagram of Pearce et al. (1975) (Fig. 6.4) reveals that most Bachelor Lake basalts fall in the oceanic field, although some trail into the continental field towards the K₂O apex. The mean for all samples falls inside the oceanic field.

As noted in Chapter 3, the plot of Naldrett et al. (1976) for $(\text{Al}_2\text{O}_3 \text{ vs } \text{FeO}/(\text{FeO} + \text{MgO}))$ was originally developed to distinguish between komatiitic and tholeiitic rocks. Although no komatiitic trend is present in the Bachelor Lake sequence, the diagram does serve a useful purpose in relating the alumina content of respective rock types to the iron-magnesium ratio. Plots for all basalts and pyroxenites are shown in Figure 6.5 A. Most basalts can be seen to lie in the tholeiitic field, with approximately one third lying across the main boundary in the intermediate zone and a few in the komatiitic field.

Harker diagrams provide a convenient plot of mean values for major elements in the various rock types (Fig. 6.6). Similar curves are provided in Figure 6.7 for Daly's (1933) and Nockold's (1954) average compositions for

volcanism changes with upward progression into the domal sequence (Area 4 and extreme upper Area 3). There, the

- 110 -

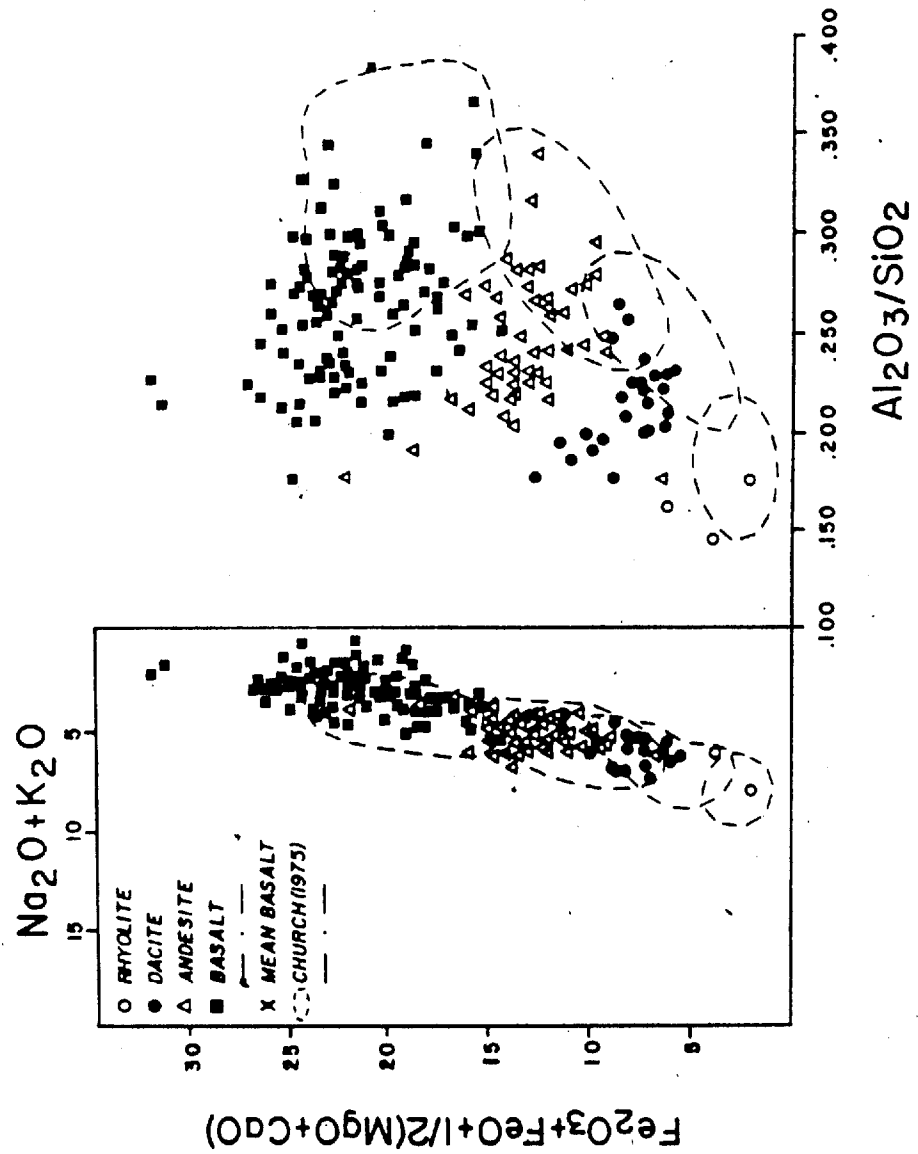


Figure 6.3: Whole Bachelor Lake Region - Church-Murata Diagram

- 121 -

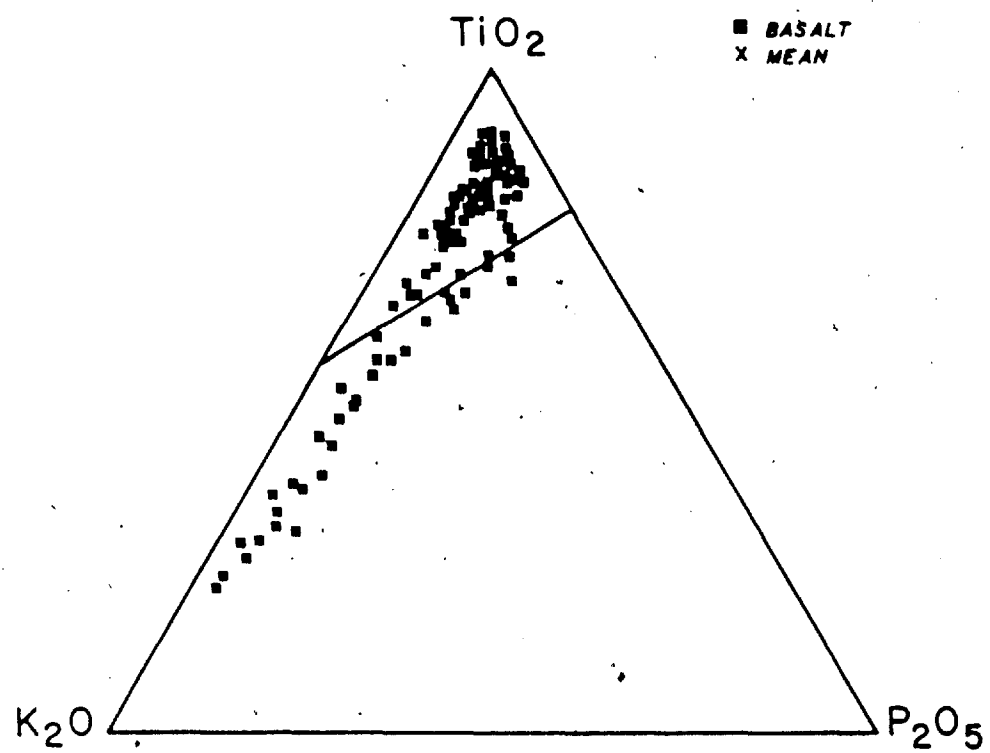
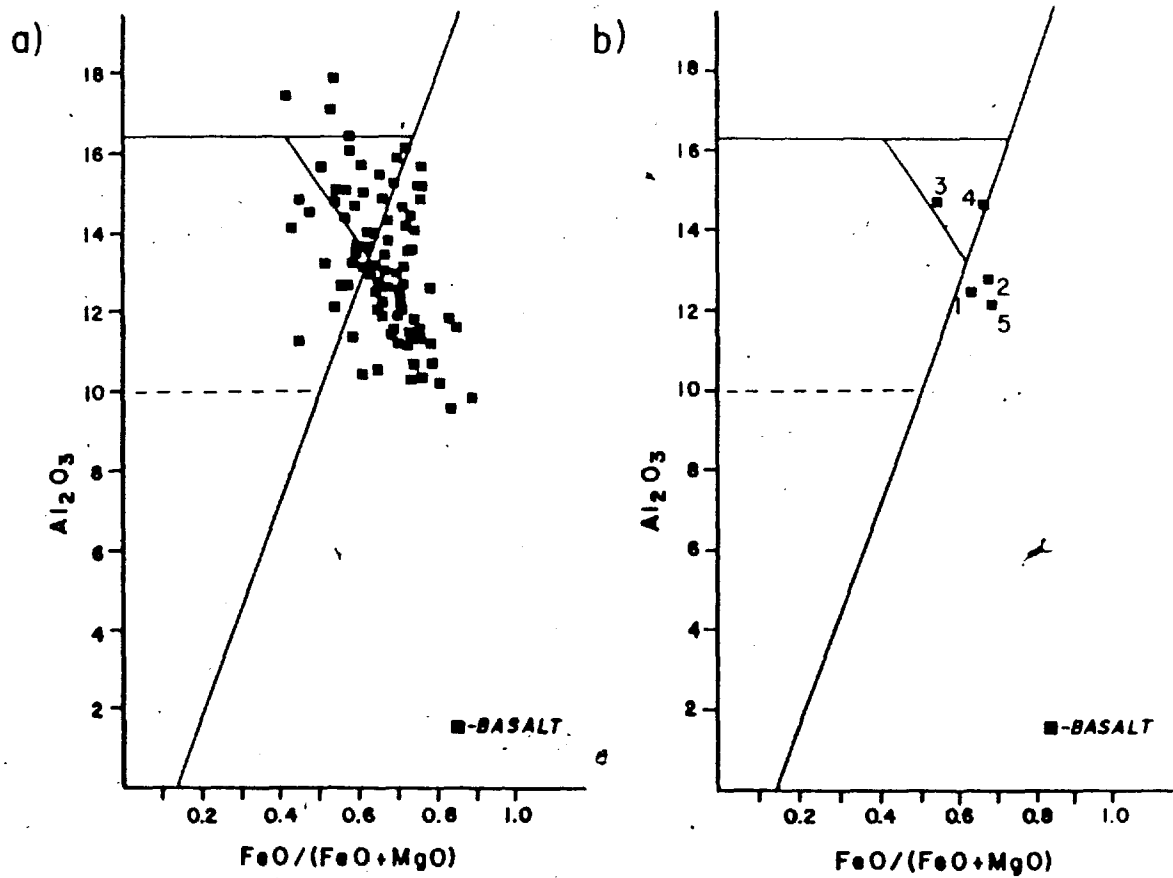


Figure 6.4: Whole Bachelor Lake Region - Pearce Diagram

Figure 6.5: Whole Bachelor Lake Region - Naldrett Plot a)
All Basalts b) Means for Geographic Areas



Phanerozoic rocks. The most obvious differences between the Bachelor Lake suite and these younger average rocks is the lower alumina and potassium and higher magnesium in the former.

To illustrate the range of values for all rocks, separate Harker diagrams were prepared for each element (Appendix D). Each diagram includes the mean value curves and a set of two standard deviation curves on either side of the mean. The latter allow statistical 95% inclusion limits to be placed upon the data, thereby excluding spurious values. The mean value line was chosen, as opposed to a regression line because each element does not have a linear relationship to SiO_2 during magmatic differentiation.

Similar Harker diagrams were prepared for samples from each of the five Areas in the Bachelor Lake region. The set of two standard deviation curves for the whole region is superimposed on each of these diagrams and is shown by dashed lines (Appendix D). In this way, the curves for each area can be compared with those for the region as a whole.

Where the mean for any one of these five Areas is $1/2$ a standard deviation above (or below) the mean for the whole region, the abundance of the element in that Area is considered to be above (or below) normal.

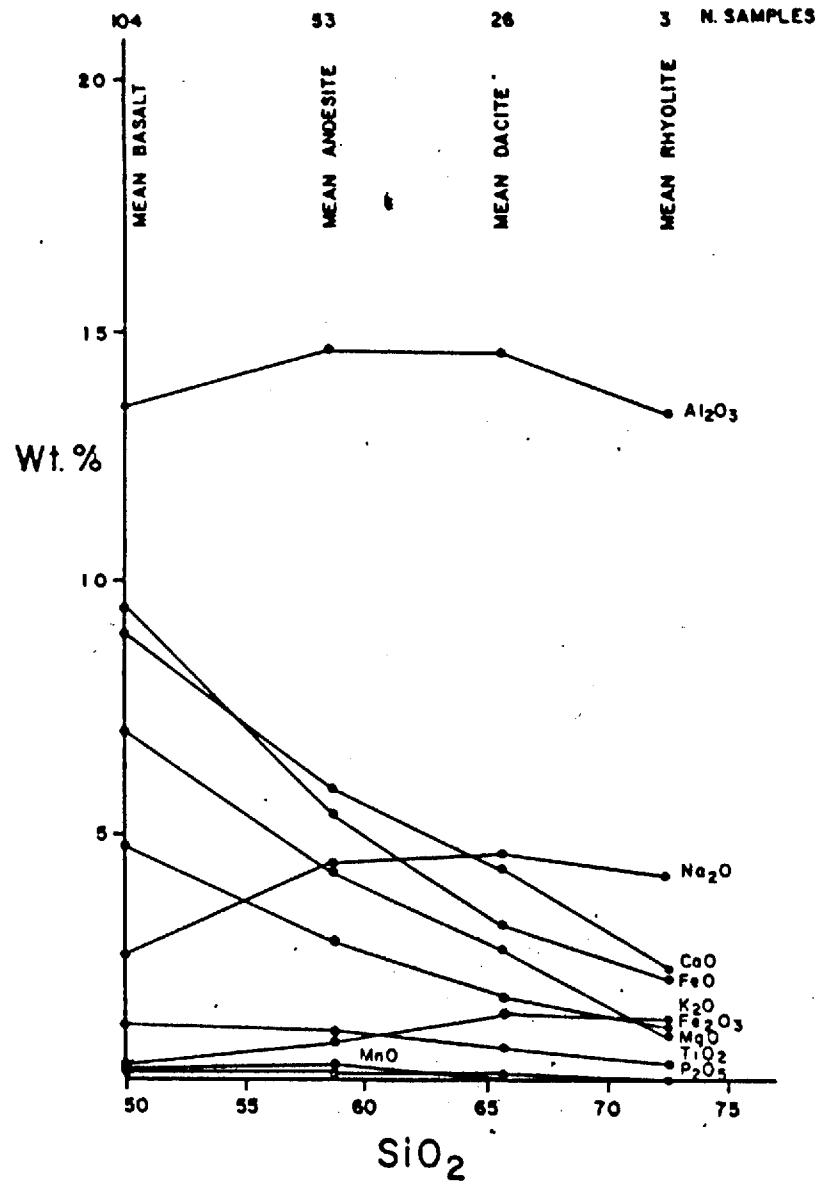


Figure 6.6: Whole Bachelor Lake Region - Harker Variation Diagram

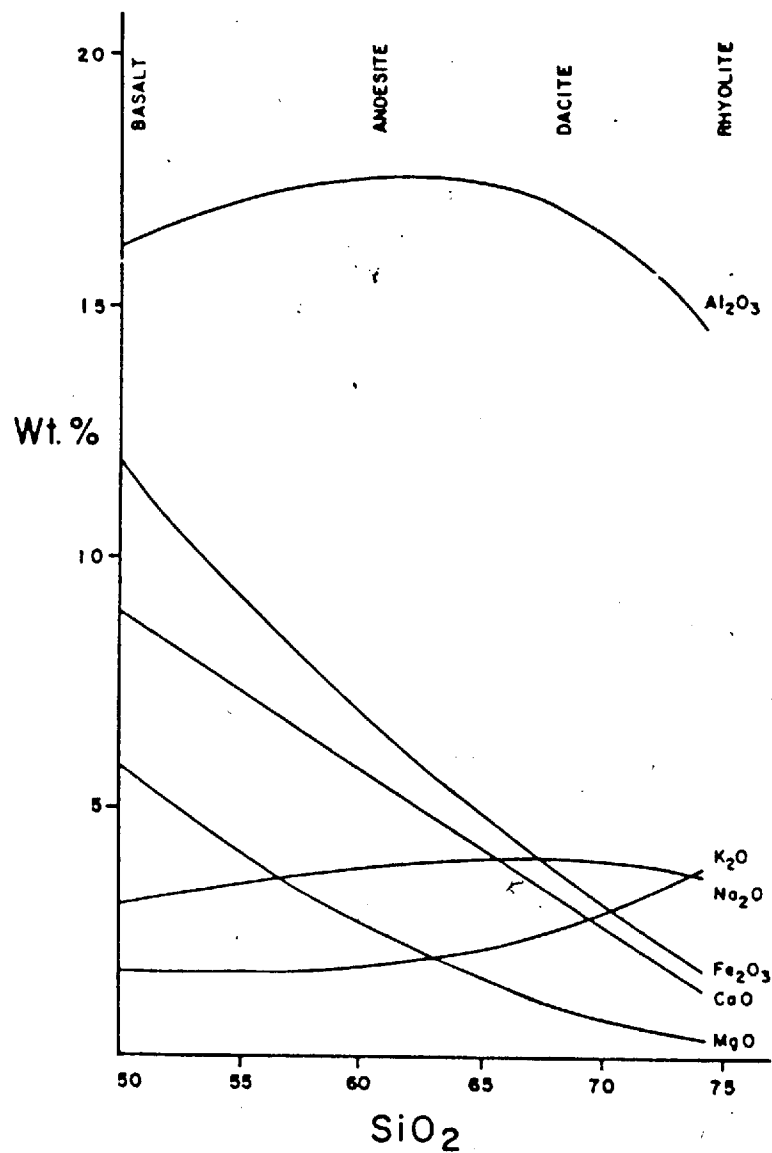


Figure 6.7: Harker Variation Diagram for Daly's (1933) & Nockold's (1954) Average Composition for Phanerozoic Rocks

1 OF 1

6.2.1 Area 1

Trends on an AFM diagram, for Area 1 (Fig. 6.8), show a distinctive tholeiitic pattern, from pyroxenites near the MgO apex through increasingly iron-rich basalts. The single andesite sample also plots in the tholeiitic field. The basaltic mean is low, in alkalies relative to all of the basalts in the study area (see Fig. 6.2 B).

The Church-Murata plot (Fig. 6.9) shows a distribution that is similar to the Bachelor Lake average, with alumina slightly lower for given silica and alkalies lower than normal.

All basalts in Area 1 fall in the oceanic field of the Pearce plot (Fig. 6.10). These rocks plot much closer to the TiO₂ apex than does the mean for all basalts in the Bachelor Lake Region (see Fig. 6.4).

The Naldrett plot (Fig. 6.11) reveals that the basalts lie in the tholeiitic field. The pyroxenites also lie in the tholeiitic field but with extremely low alumina values.

Harker diagrams, in Appendix D, indicate that the distribution of chemical elements, with respect to silica, is very similar to that of the whole Bachelor Lake region except for slightly low zinc, nickel and cobalt values, and a high K/Rb ratio.

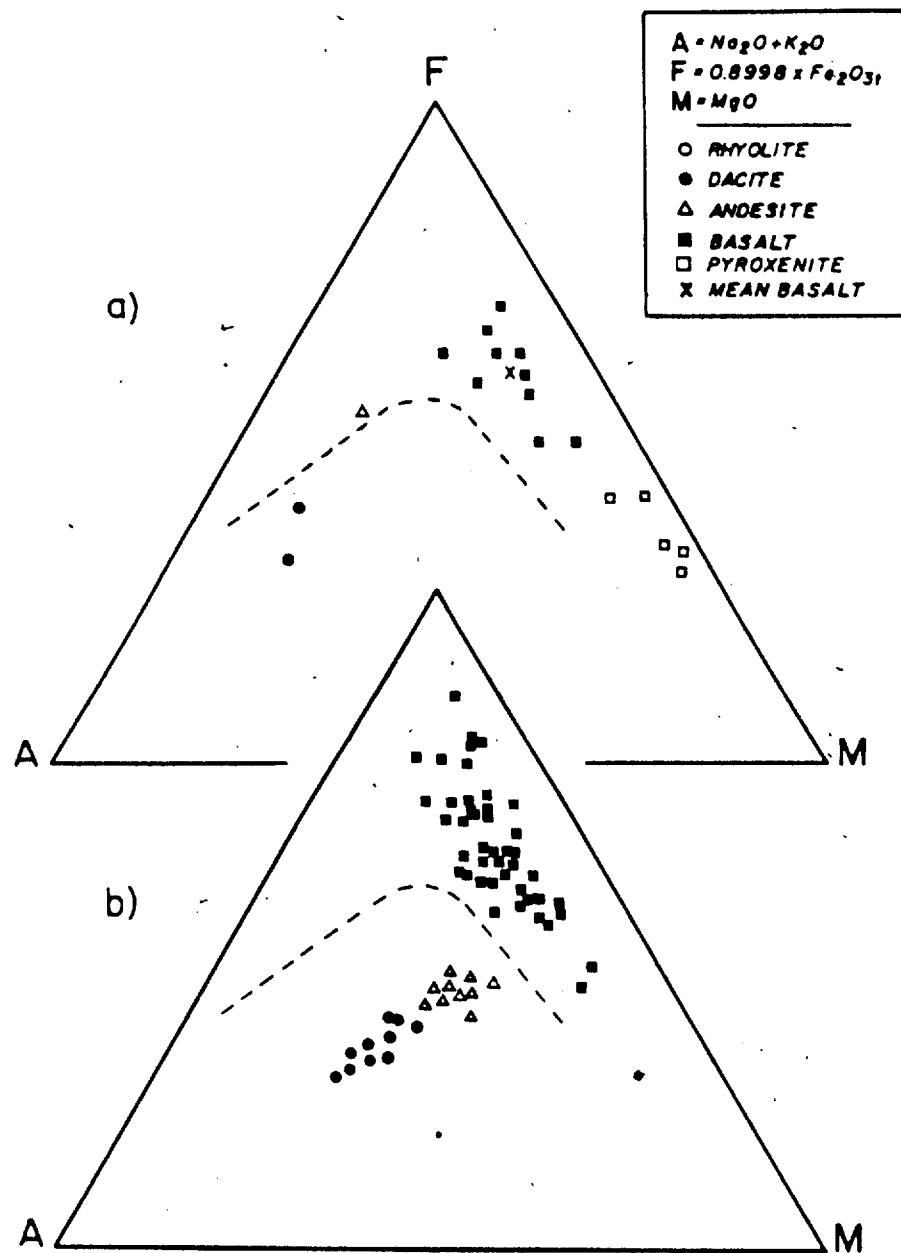
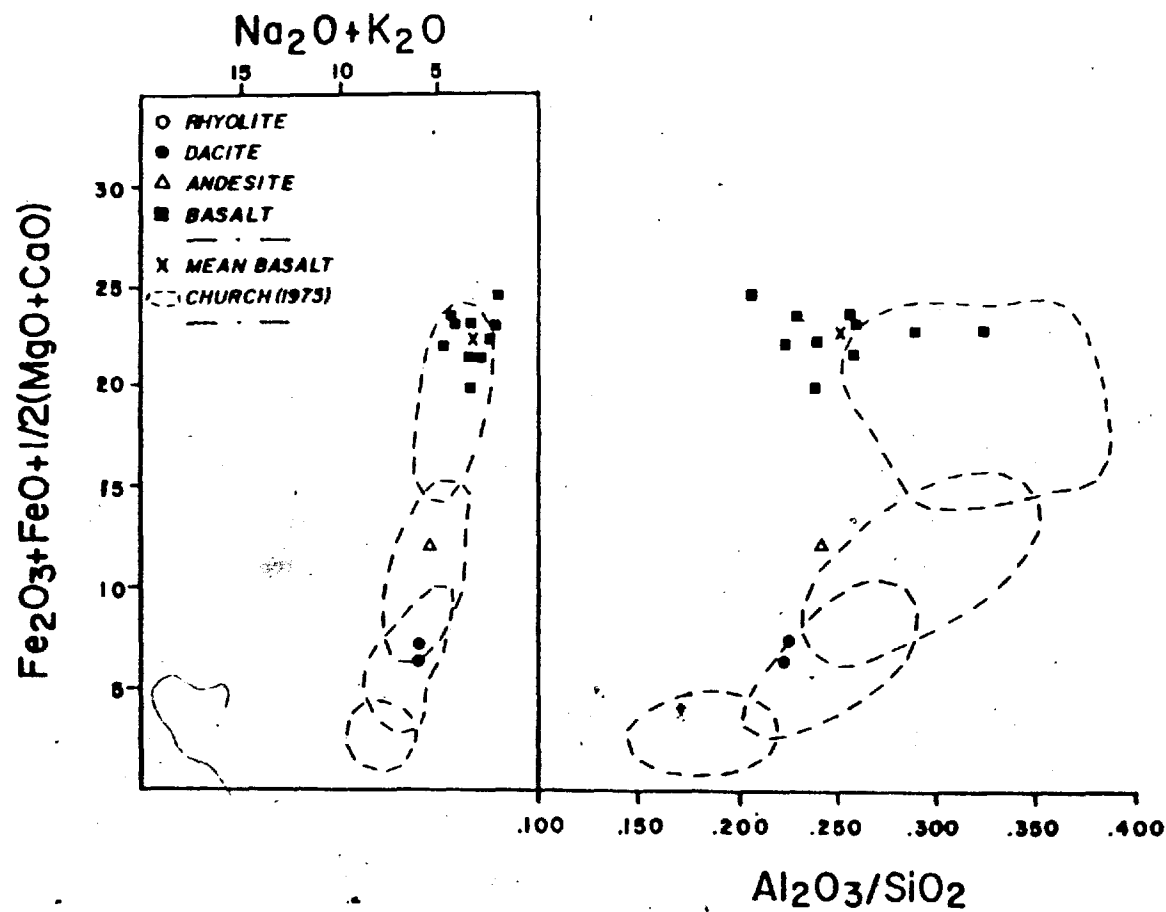


Figure 6.8: AFM Diagrams for a) Area 1 and b) Area 2

Figure 6.9: Church-Murata Diagram - Area 1



4054

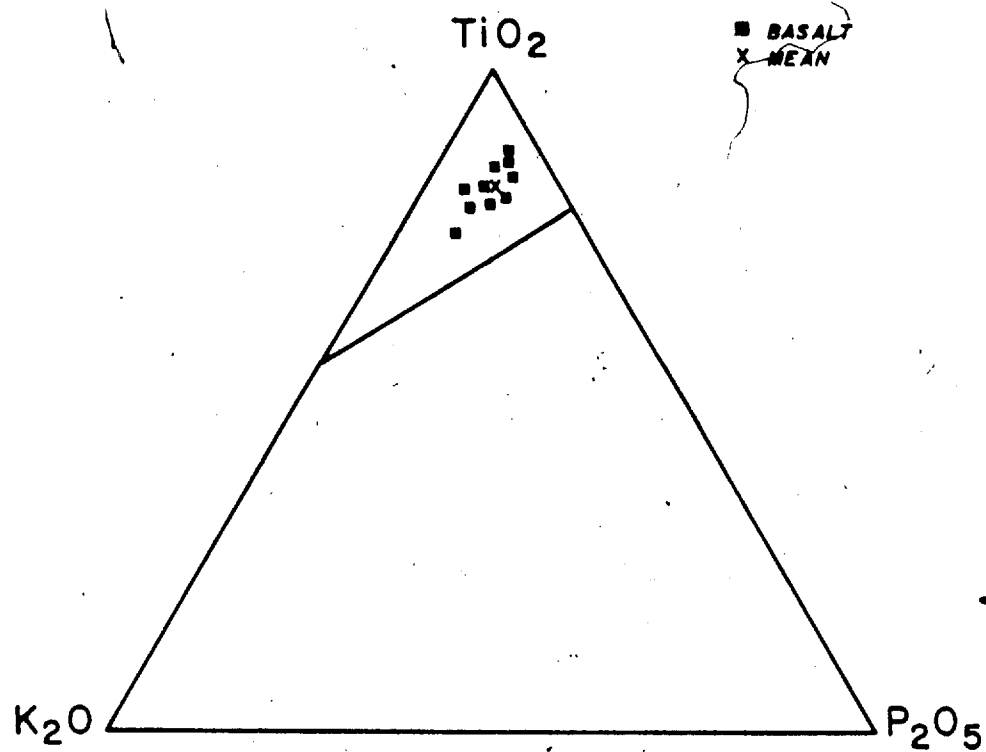
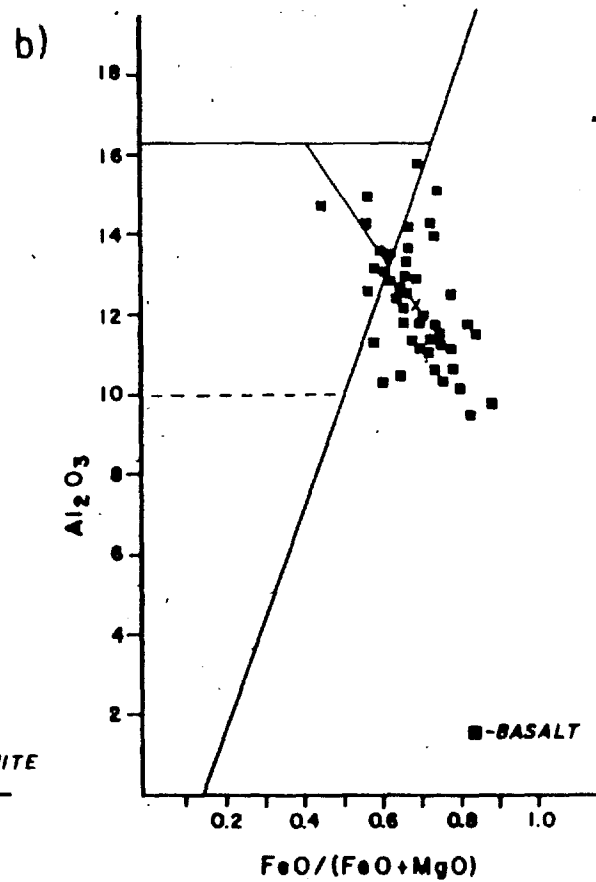
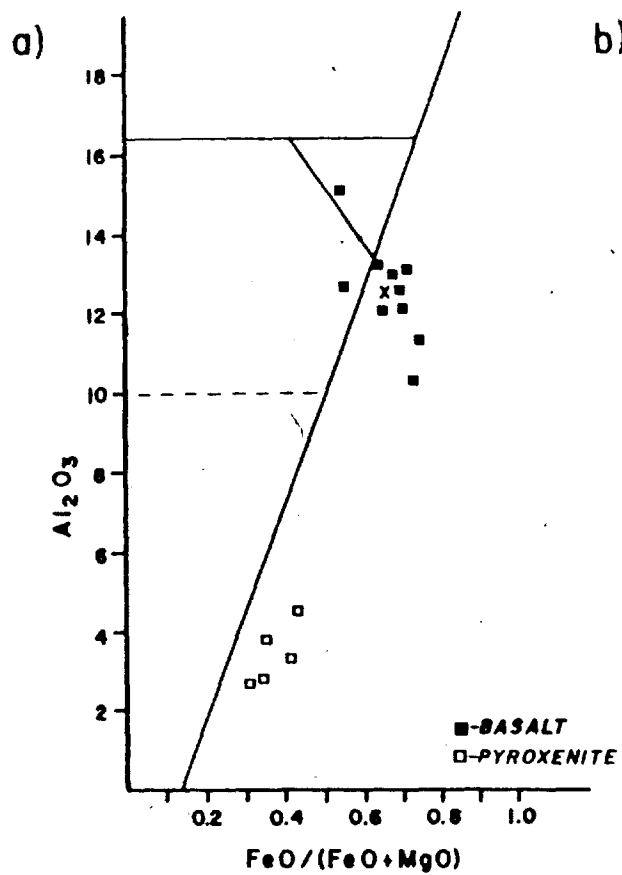


Figure 6.10: Pearce Diagram - Area 1

Figure 6.11: Naldrett Diagram a) Area 1 b) Area 2



6.2.2 Area 2

Geographically, Area 2 forms the largest unit and contains the largest number of sample stations. Because of this, the area has been broken down into four Subareas to check distributions both along and across the belt.

Subarea 2a is located in the southern half of Boyvinet and west central edge of Gand Townships, and consists of rocks which lie stratigraphically and immediately above those of Area 1 (Fig. 5.1 and map in rear pocket). Subarea 2b is found in the southern part of Gand Township. The rocks occupy a stratigraphic position between Subarea 2a and Area 3. Subarea 2c lies between Bachelor Lake and Billy Lake, in northeastern Lesueur Township, just below Area 4, and also includes a small part of eastern Nelligan Township. Subarea 2d, in northern Benoit Township, occurs at the western end of the study area and lies stratigraphically below Area 4.

Distribution on the AFM diagram (Figures 6.12, 6.13) reveals a distinct tholeiitic trend with a slight bias toward the iron apex. The mean basalt value for all of Area 2 lies near that of Area 1.

The AFM diagram for Subarea 2a (Fig. 6.12 A) shows that the mean value lies close to the overall average for Area 2. Further south, in Subarea 2b (Fig. 6.12 B), the mean is Mg-rich, while in Subarea 2c (Fig. 6.13 A), the mean is found

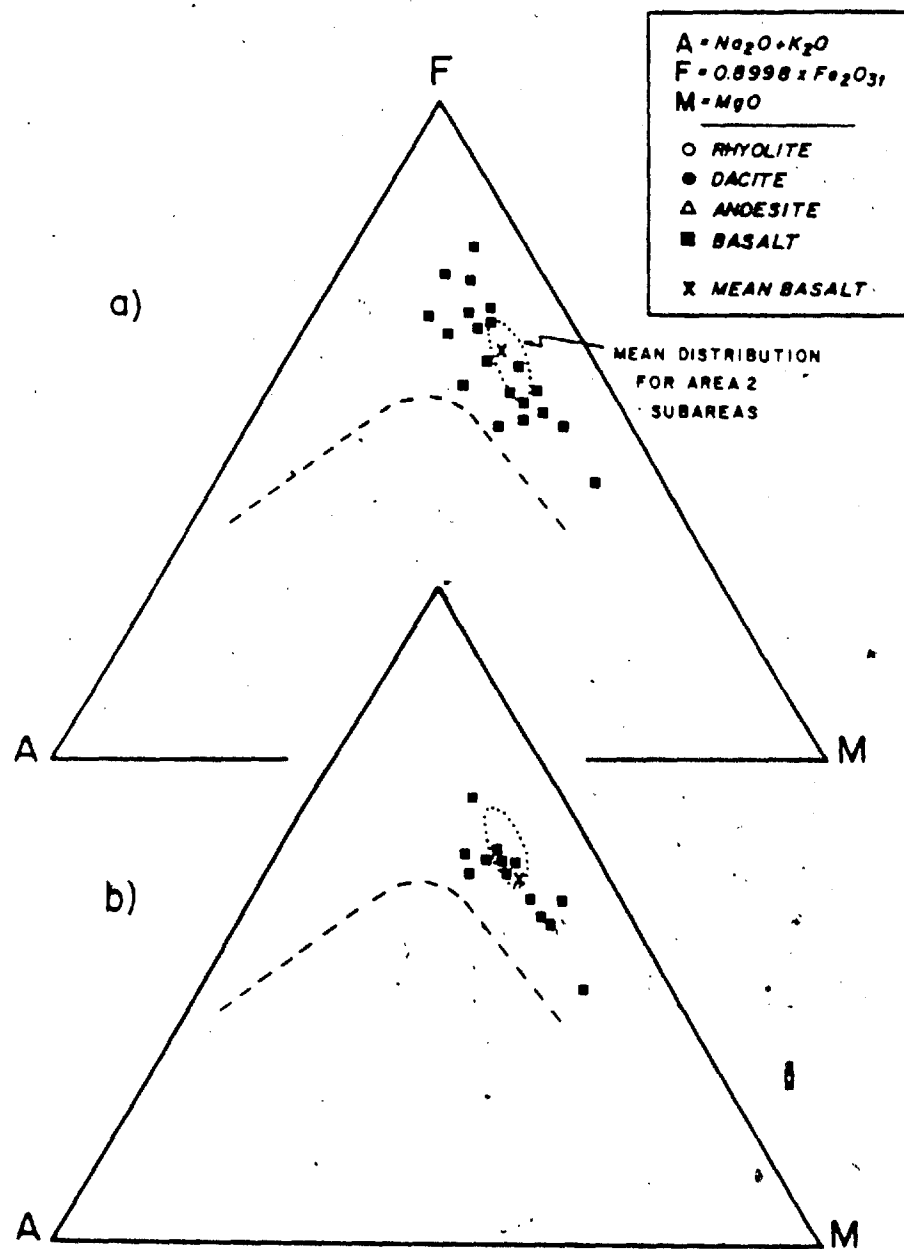


Figure 6.12: AFM Diagram - Subareas a) 2a b) 2b

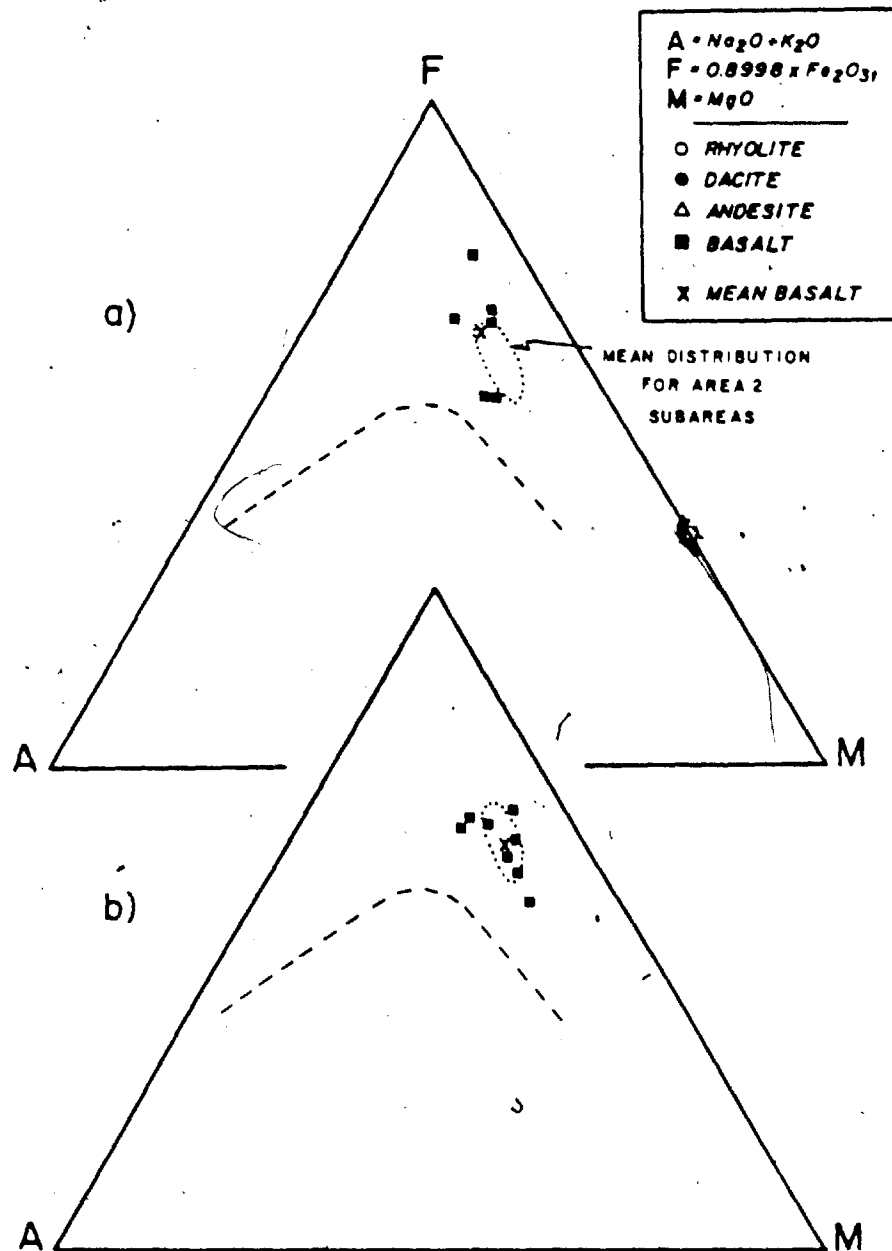


Figure 6.13: AFM Diagram - Subareas a) 2c b) 2d

to be Fe-rich. The mean for Subarea 2d (Fig. 6.13 B) is similar to Subarea 2a. The few differentiated volcanics in the area are all located in Subarea 2a and plot in a calc-alkaline trend.

Patterns for Area 2 volcanics in the Church-Murata plot (Fig. 6.14) show slightly low alumina values for given silica, above normal iron-magnesium-calcium index, and slightly low alkali values.

Almost all basalts, as well as their mean value, are classed as oceanic by the Pearce plot (Fig. 6.15 A). The few continental values are from widely scattered localities and do not represent a specific environment.

Basalts plot primarily in the tholeiitic field on the Naldrett plot with their mean lying close to that of Area 1 (Fig. 6.5). Samples from Subarea 2a (Fig. 6.16 A) contain less alumina, and are more iron-rich than any other Subarea except for 2c. Subarea 2b (Fig. 6.16 B) has the highest alumina values and is least Fe-enriched, with the mean lying on the main boundary line. Samples from Subarea 2c (Fig. 6.17 A) have high alumina and iron values, while those of Subarea 2d (Fig. 6.17 B) are intermediate.

Harker diagrams (Appendix D) indicate that elemental distribution is the same as that for the entire region. It could be argued that the heavy sampling in this area bias the averages.

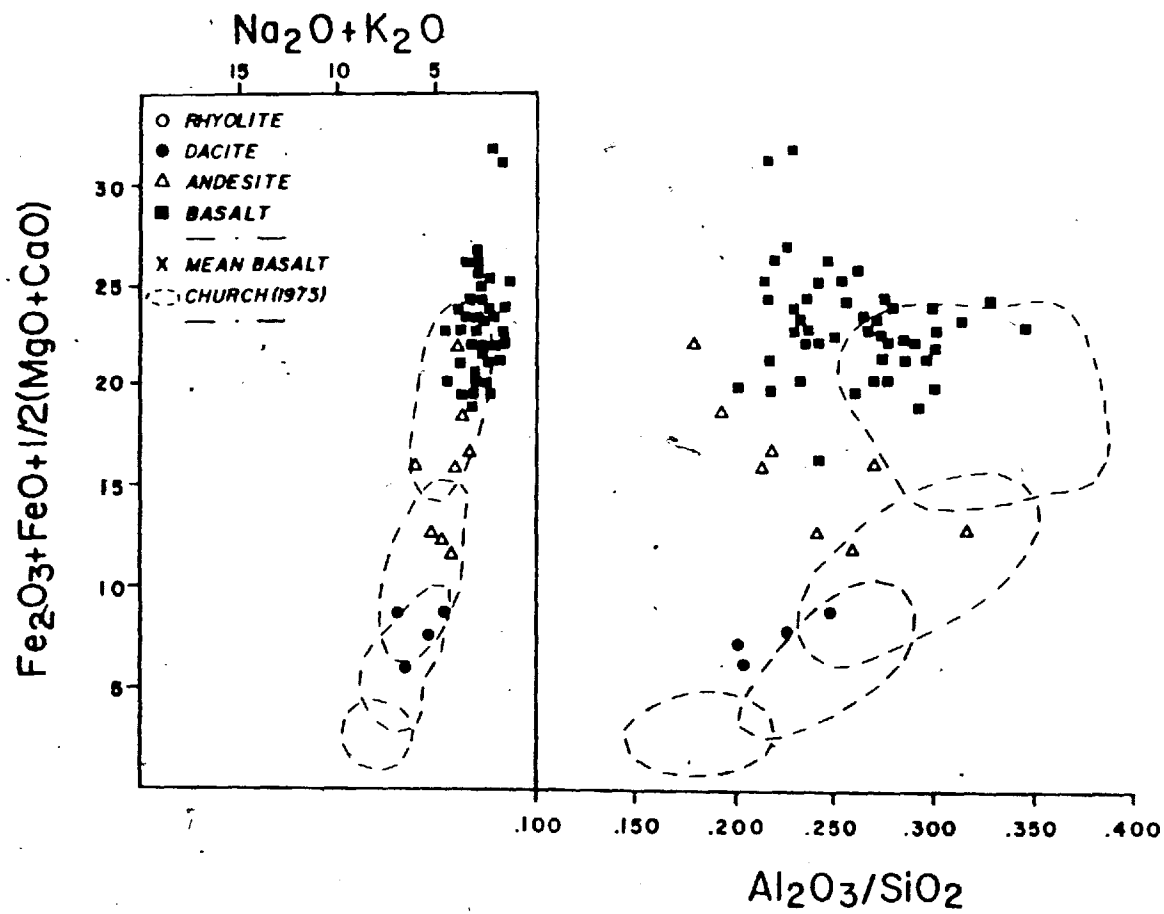


Figure 6.14: Church-Murata Diagram - Area 2

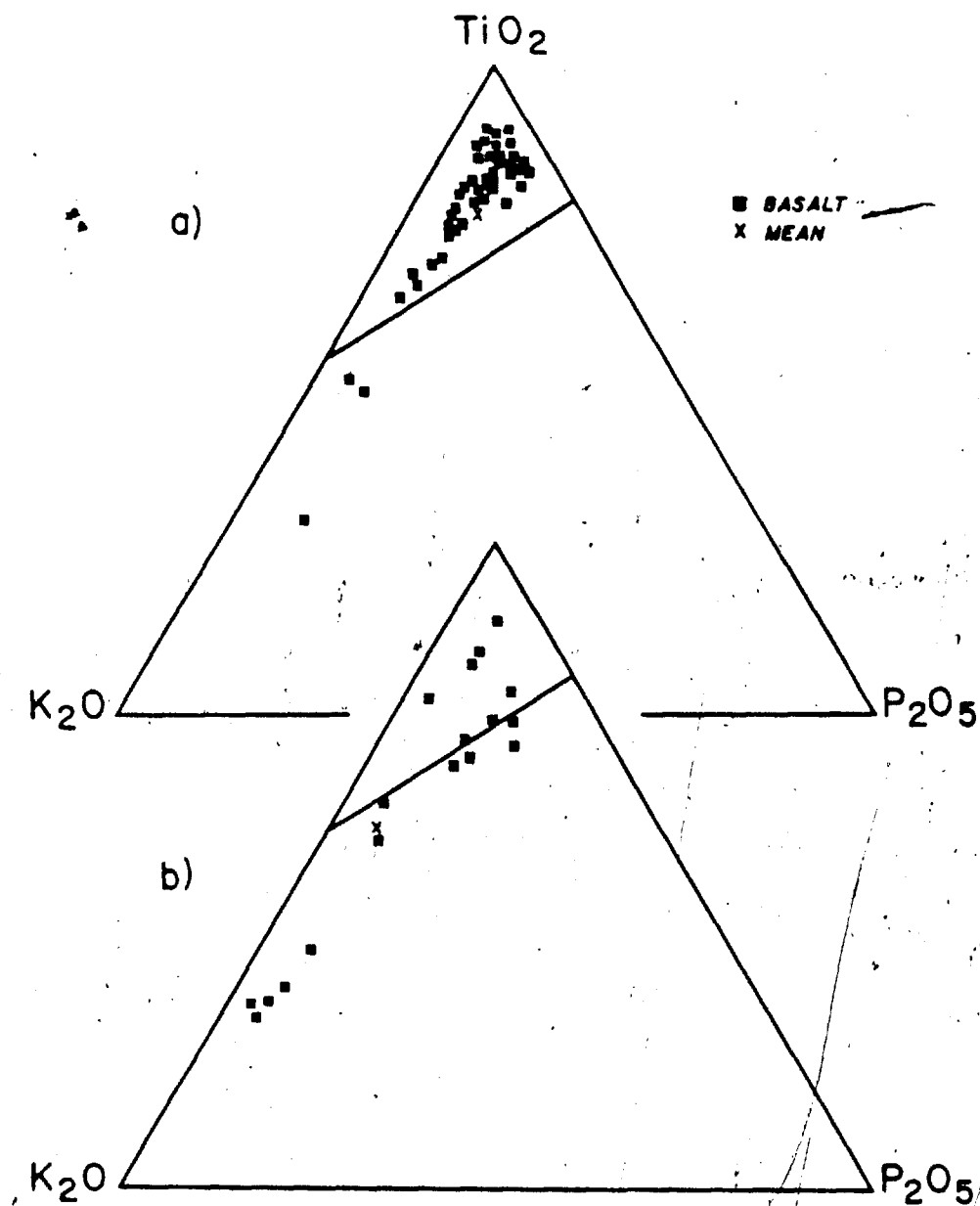
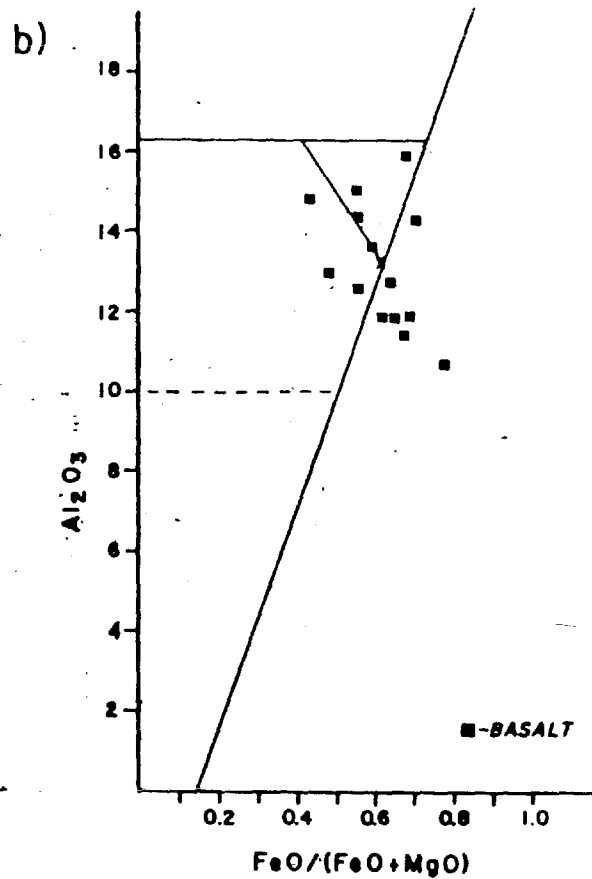
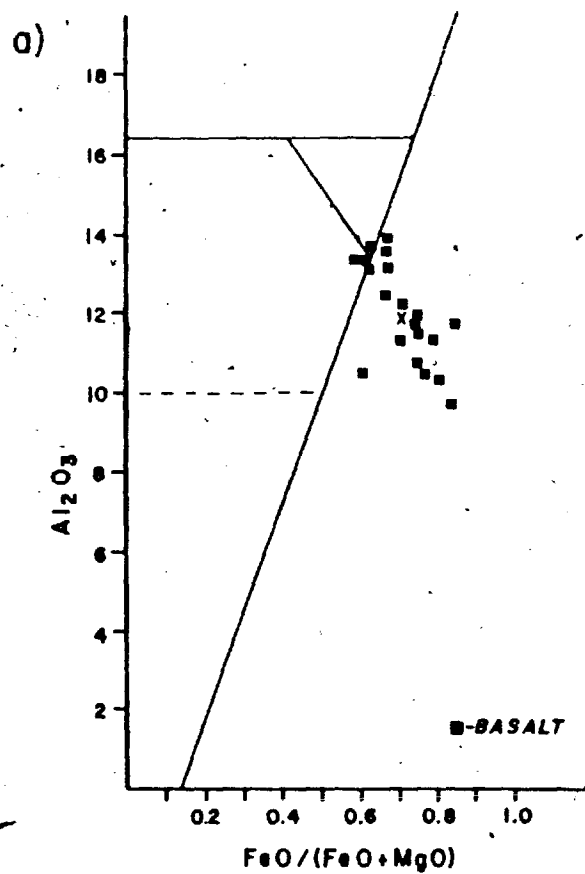


Figure 6.15: Pearce Diagram a) Area 2 b) Area 3

Figure 6.16: Naldrett Diagram - Subareas a) 2a b) 2b



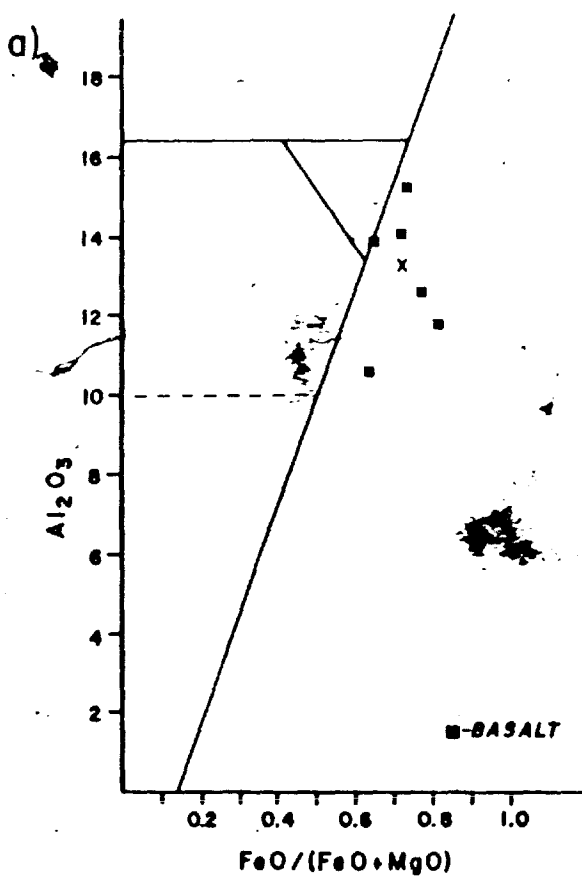
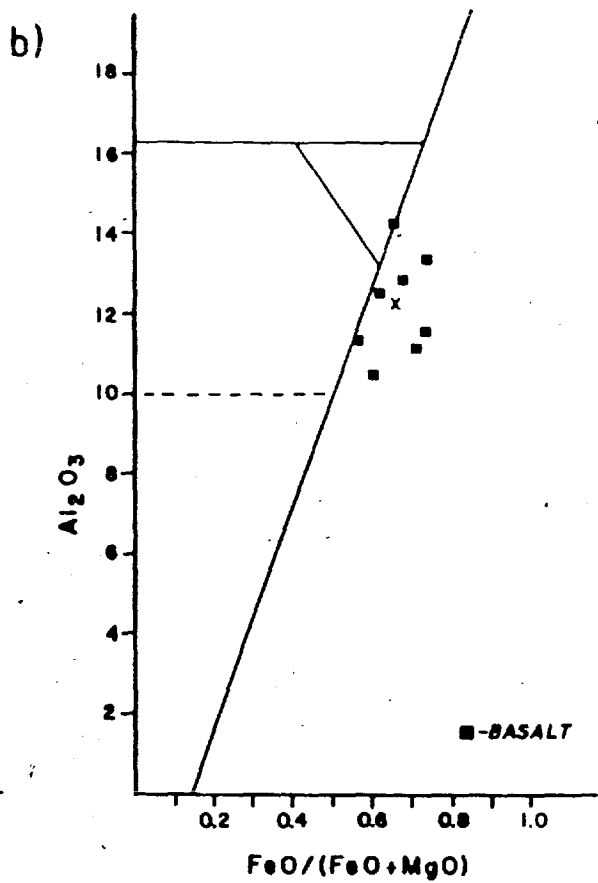


Figure 6.17: Naldrett Diagram - Subareas a) 2c b) 2d

6.2.3 Area 3

Area 3 appears at the eastern end of the study area and is fraught with the structural complexities outlined in Chapter 5. Excellent sampling intervals were achieved and are sufficient to reveal geochemical trends.

Both tholeiitic and calc-alkaline trends appear on the AFM diagram (Fig. 6.18 A), with the basaltic mean being more Mg-rich than that of any other area. The base of the pile, in the extreme south, contains Mg-Basalts alternating with a few Fe-rich basalts. A band of predominantly andesites occupies the central portion of the pile, and are overlain, toward the top of the sequence, by a calc-alkaline group of rocks.

The Church-Murata plot (Fig. 6.19) shows that Al_2O_3 is still slightly low for given SiO_2 but not as much as those for Areas 1 and 2. However, basaltic alkalies are still low.

Basaltic samples are classified as both oceanic and continental on the Pearce plot (Fig. 6.15 B) although many fall close to the boundary curve, as does the mean. Less potassic (i.e. more oceanic) basalts have a tendency for higher P_2O_5 .

The Naldrett plot (Fig. 6.20 A) shows that basalts for this area have quite high Al_2O_3 content and have the lowest

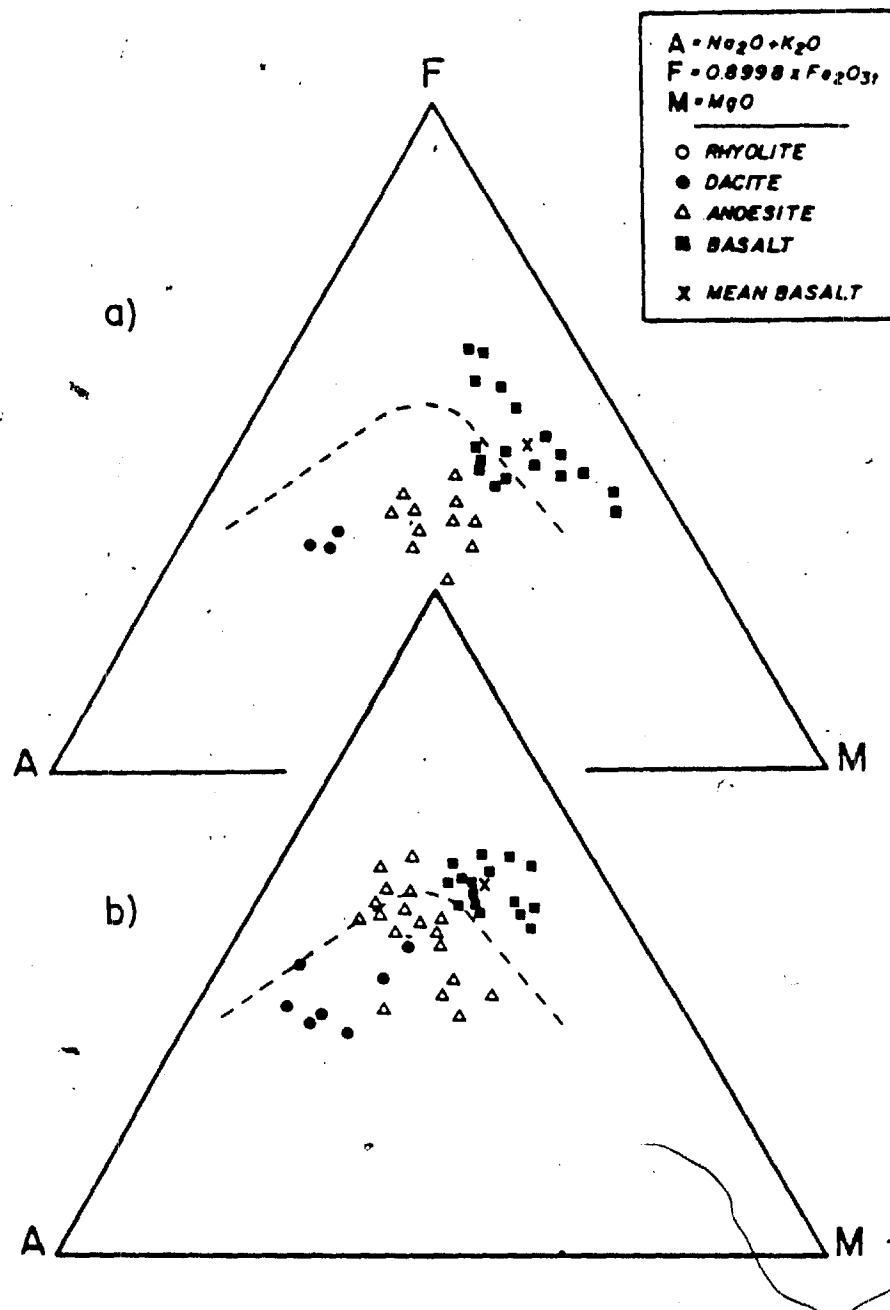


Figure 6.18: AFM Diagram a) Area 3 b) Area 4

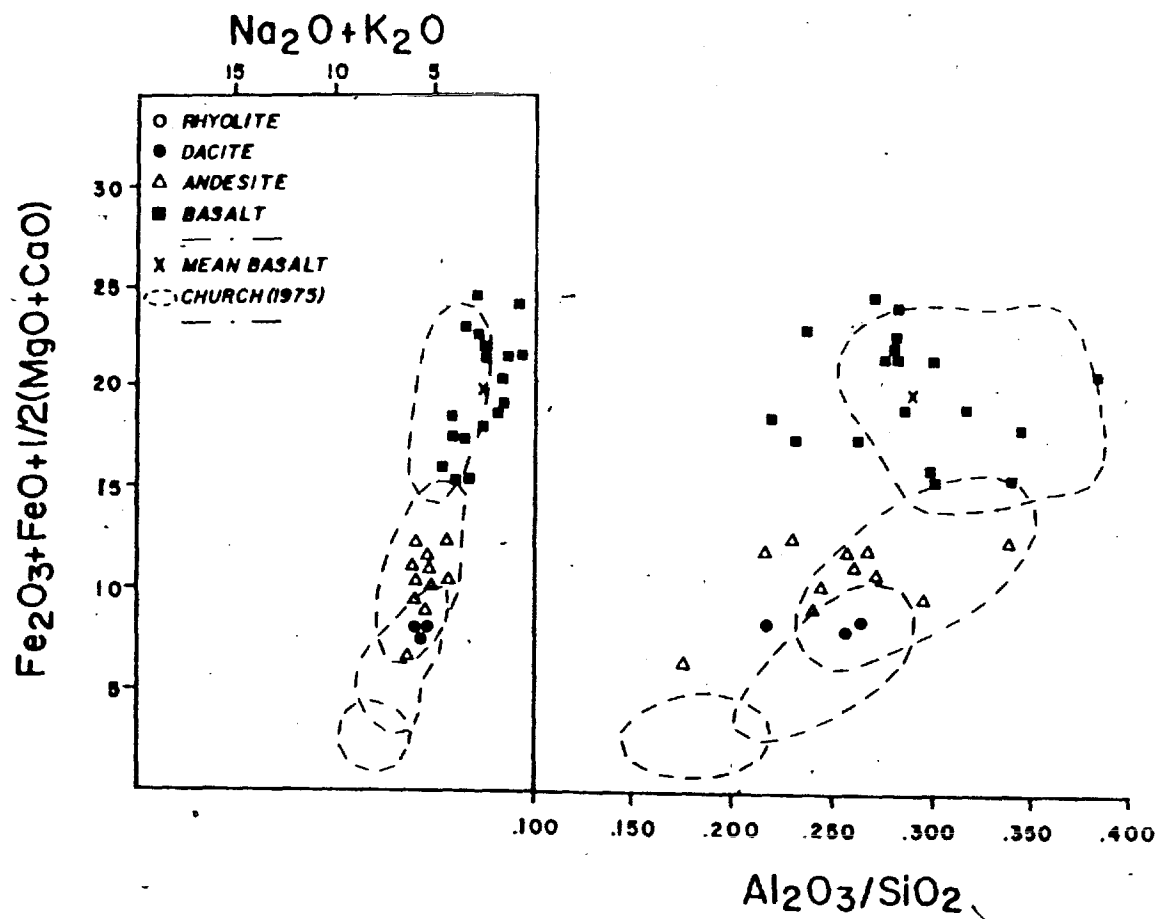


Figure 6.19: Church-Murata Diagram - Area 3

FeO/(FeO + MgO) ratio (Fig. 6.5) . Most samples lie in the uncertain triangular and high alumina fields. The mean lies in the triangular area and is furthest from the tholeiitic field of any area.

The modified Harker diagrams (Appendix D) indicate that Al₂O₃, CaO, MgO and Ni are high with respect to the regional average, while Fe₂O₃, P₂O₅, TiO₂ and Zn are low. Ni/Co is above average in the mafic rocks. Na₂O and Cu are very slightly below average.

6.2.4 Area 4

A plot of the AFM distribution (Fig. 6.18 B) shows a definite calc-alkaline trend. Basaltic rocks, which occur predominantly in lower parts of the domal sequence, form a relatively tight grouping (i.e. narrow FeO-MgO range) but have a more alkaline mean (Fig. 6.2) than all other Areas. Andesites are also most abundant in lower parts of the sequence, but form higher proportions in the upper strata, relative to basalts. The effects of differentiation on these intermediate rocks is seen in the wide FeO-MgO range. Dacites become a significant member of the upper strata, both as flows and pyroclastics. The AFM diagram indicates the roughly equal proportion of basalts to more differentiated rocks, and is largely a result of increases in the latter at higher stratigraphic levels.

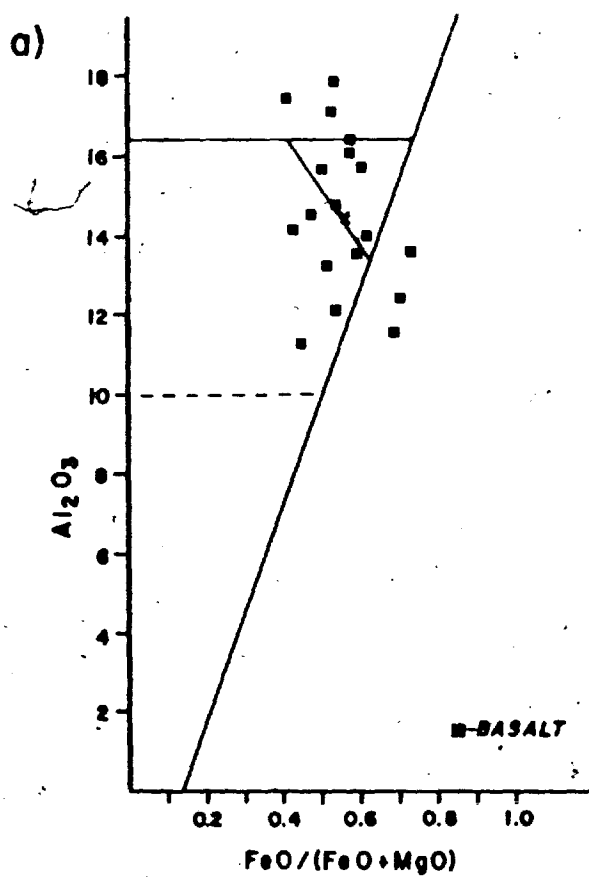
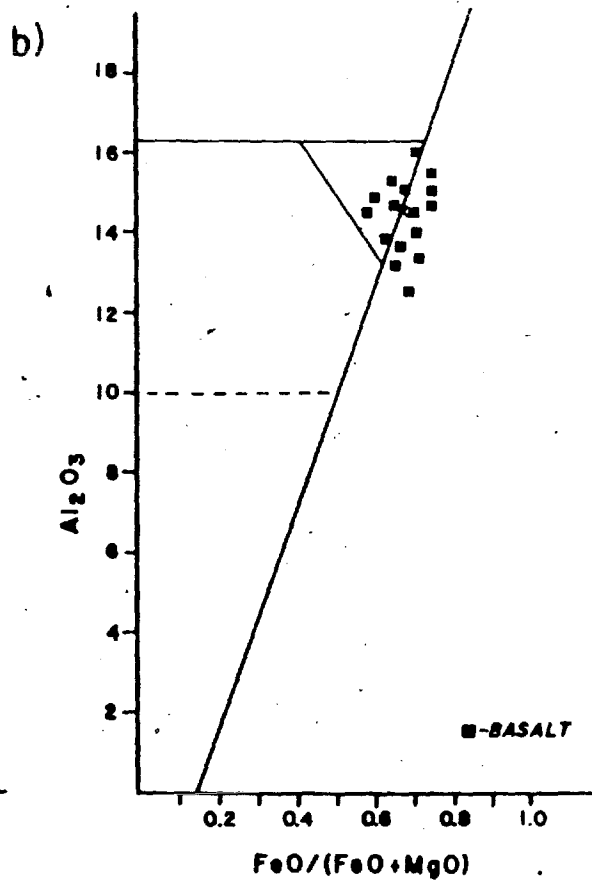


Figure 6.20: Naldrett Diagram a) Area 3 b) Area 4

On the Church-Murata plot (Fig. 6.21), Al_2O_3 is still slightly low for given SiO_2 but less so than in Areas 1 to 3, with means falling close to the 2/3 boundary curves. For the first time, alkali values, for all rocks, including basalts, are almost identical to Church's (1975) values and are within his boundary curves.

The Pearce plot (Fig. 6.22 A) suggests a continental environment, since virtually all basalts lie within that field. This is the first instance where basalts have such high K_2O (& low TiO_2) values as to lie solidly, with their mean, in this more "potassic" field.

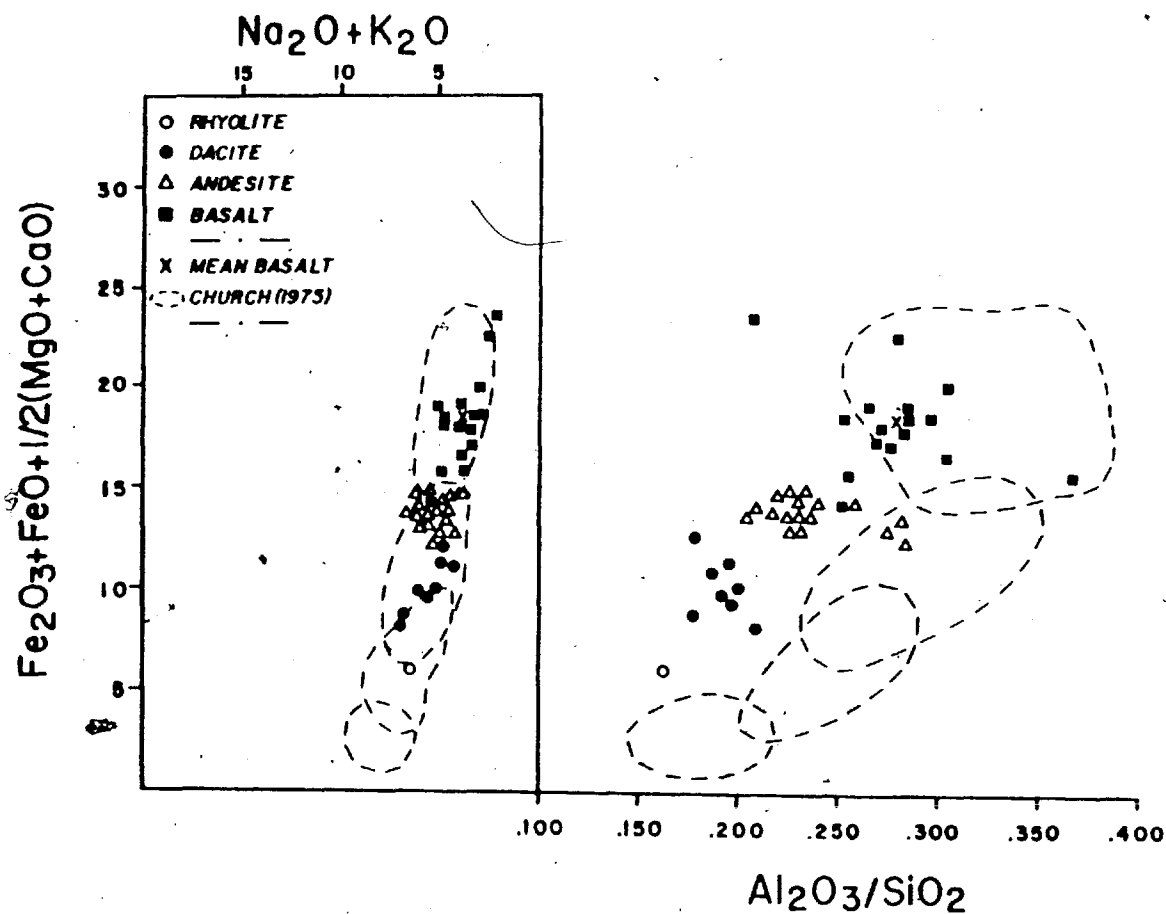
Sample location on the Naldrett plot (Fig. 6.20 B) shows basaltic distribution mainly between the tholeiitic and triangular fields.

Harker diagrams show that MnO and Zn are high and Sr and Sr/Ca are low, relative to the regional average. Na_2O and Ca are slightly below average in basalts, but near normal in the felsic rocks. In the mafic rocks, K_2O and Rb are high, but are below average in the felsic rocks.

6.2.5 Area 5

Area 5 appears only along the western end of the study area and is well represented by numerous sampling stations across the belt. While its relationship to other parts of the belt is somewhat uncertain, the area of sampling is

Figure 6.21: Church-Murata Diagram - Area 4



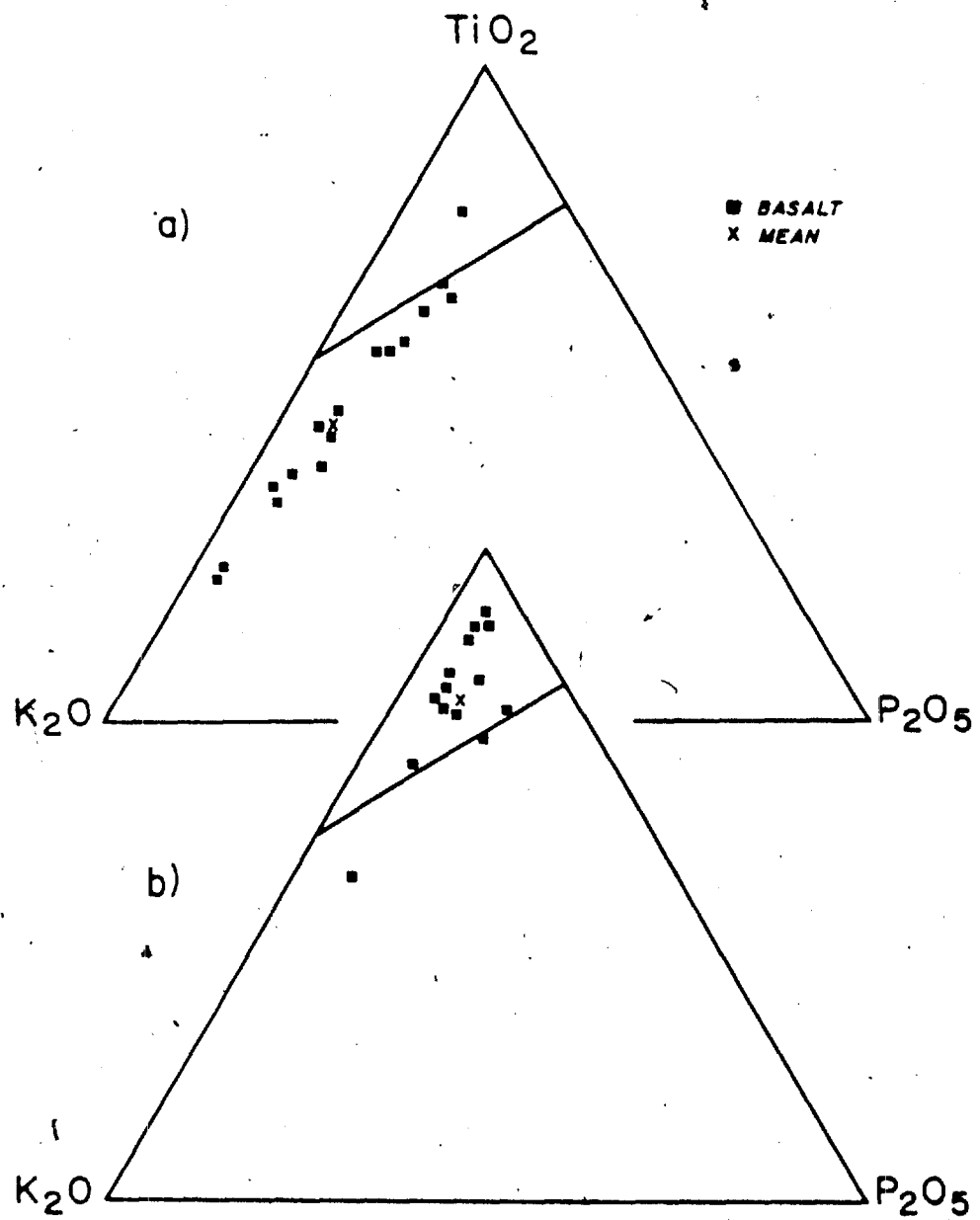


Figure 6.22: Pearce Diagram a) Area 4 b) Area 5

believed to represent a continuous vertical stratigraphic unit.

An AFM plot (Fig. 6.23) yields a pattern of calc-alkaline affinity, from the closely grouped basalts in the tholeiitic field, across the boundary toward the alkalic apex. The trend is almost a linear distribution between rock types and is a much different pattern from the tholeiitic-type basalts along the highway to the north.

The Church-Murata diagram (Fig. 6.24) reveals a pattern similar to much of the belt, with the characteristic low alumina and slightly low alkali range for basalts.

An oceanic environment is suggested for basalts by the Pearce plot (Fig. 6.22 B), with the mean solidly entrenched in that field.

Most basalts fall in the tholeiitic field of the Naldrett plot (Fig. 6.25).

Harker variations (Appendix D) indicate that statistical distribution of elements is very similar to that of the regional average. The only exceptions are unusually high Sr, and slightly low K/Rb. Cu is above normal in basalt, but near normal in the felsic rocks.

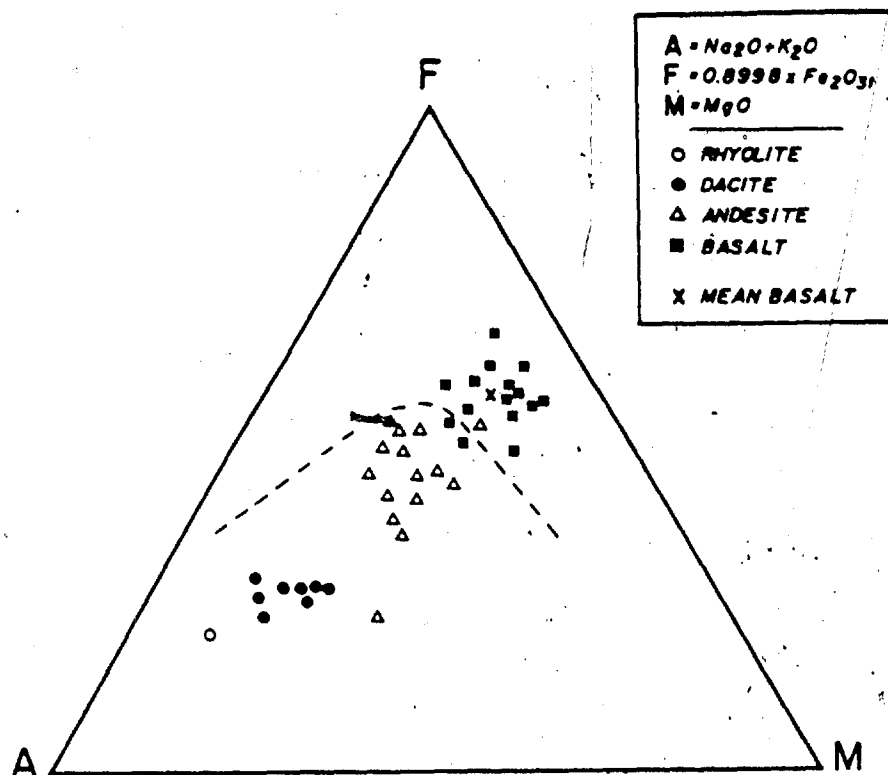
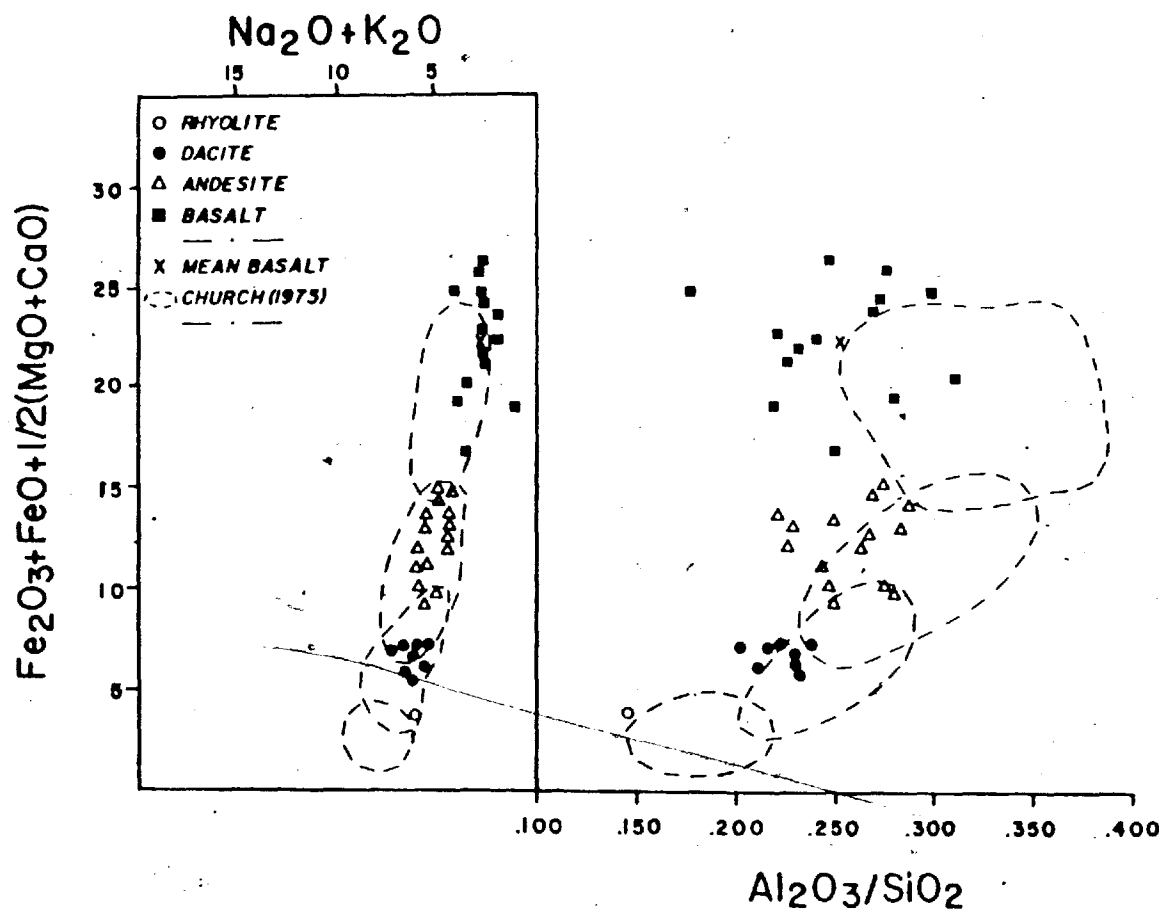


Figure 6.23: AFM Diagram - Area 5

Figure 6.24: Church-Murata Diagram - Area 5



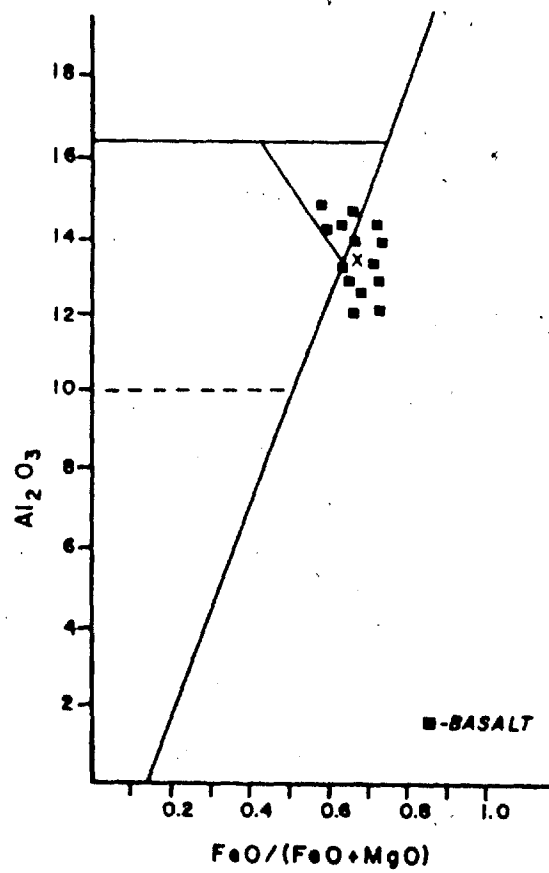


Figure 6.25: Naldrett Diagram - Area 5

6.3 GEOCHEMICAL SUMMARY

Geochemical trends and patterns, outlined in previous sections, have been summarized in Table 6.2. From this table, it is readily apparent that major differences occur between the geographic areas.

The platform sequence (Areas 1 & 2) consist mainly of tholeiitic rocks, characteristic of an oceanic environment. There are no major differences between any of the four Subareas in Area 2, although basalts in Subarea 2b are richer in Mg and are somewhat similar to the Mg-rich basalts in Area 3, immediately to the south. Subarea 2c basalts, which occur near the top of the platform sequence, are Fe-rich and may be the end-product of differentiation along a tholeiitic trend.

Rocks of the domal sequence (Area 4) are mainly calc-alkaline and are more typical of a continental environment (Pearce and Naldrett diagrams). Several elements are anomalous on Harker diagrams, Zn in particular becoming an important trace element.

Area 3 contains elements of both platform (tholeiitic trends, oceanic basalts, high MgO and Ni) and domal (calc-alkaline trends, continental basalts, high SiO₂) sequences and will be further examined in Chapter 8.

TABLE 6.2
Summary of Geochemical Variation Diagrams

AREA	AFM	CHURCH-MURATA	PEARCE	WADLRETT	HARKER
1	Tholeiitic Basalts	Low * High **	Oceanic Basalts	Tholeiitic. Pyroxenite high in FeO/FeO-MgO, unlike most Komatiitic flows.	Similar to regional average. Slightly low Zn, Ni, Co. High K/Rb.
2	Tholeiitic Basalts C-Alk. Int. to felsic rocks Subareas: 2c } high Fe 2a } 2d } 2b } high Mg	Low * High **	Oceanic Basalts	Tholeiitic. 2b } high Al, 2c, 2d } Mg 2a } low Al, 2b } high Fe	Similar to regional average.
3	Tholeiitic & C-Alk. trends.	(low)*	Oceanic & Continental Basalts	Widespread Tholeiitic to high-Al trends.	High Al ₂ O ₃ , CaO, MgO, MgC, Ni Low Fe ₂ O ₃ , TiO ₂ , P ₂ O ₅ , Zn Slightly low Na ₂ O, Cu
4	C-Alkaline trend for all rocks.	Low *	Continental Basalts	Tholeiitic basalts but with much higher Al than other Areas.	High MnO, Zn Low Sr, Sr/Ca Slightly low Na ₂ O, Cu in basalt. K ₂ O, Rb high in basalt, low in felsic rocks.
5	C-Alkaline trend for all rocks.	Low * Basilts have High **	Oceanic Basalts	Tholeiitic basalts.	High Sr, Sr/Ca Low K/Rb, Ba/Rb Slightly low Zn
* Al ₂ O ₃ /SiO ₂ ** Fe ₂ O ₃ + FeO + $\frac{1}{2}$ (MgO + CaO) With respect to regional averages					

Geochemical traverses for basalts were not particularly useful for displaying trends across the belt, probably due to structural complexities. Comparison using variation diagrams for geographic areas (as outlined in Chapter 5) proved more useful.

Chapter 7

MINERAL DEPOSITS

7.1 CONIAGAS MINES LTD. - BASE METAL DEPOSIT

7.1.1 Introduction

During extensive gold prospecting in the 1940's, a strike was made south of Bachelor Lake, by O'Brien Gold Mines Ltd. The subsequent rush to the area included Dome Exploration Co. (Quebec) Ltd., who, in the following year, 1947, discovered a lead-zinc-silver deposit, outcropping approximately a kilometer west of the gold prospect.

Delineation of the ore zone proved somewhat difficult, due to the remote location of the property. A winter road, south of present Highway 113, allowed a geophysical survey and 15,000' drilling programme to be carried out during 1948-49. Property location and drilling plan have been outlined by Graham (1957). The main highway and CNR line were constructed in 1957.

By 1952, the drilling programme had outlined a deposit of 365,000 tons of ore grading 13.55% Zn, 0.88% Pb and 10.50 oz/ton Ag. The property was purchased in 1955 by Coniagas Mines Ltd., who, in 1956, sunk a 1250', 3 compartment shaft and performed lateral development on five levels. Workings

were closed shortly thereafter, due to depressed metals markets.

The mine was finally brought into production in March, 1961, at 300 tons/day, when the shaft was dewatered and deepened to 1368', with 8 development levels. In addition, a small volume of high grade ore was removed by open pit excavation, north of the headframe. The mine yielded almost a million tons of ore, with a value of \$10,000,000 before a depressed market again forced closure in May, 1967.

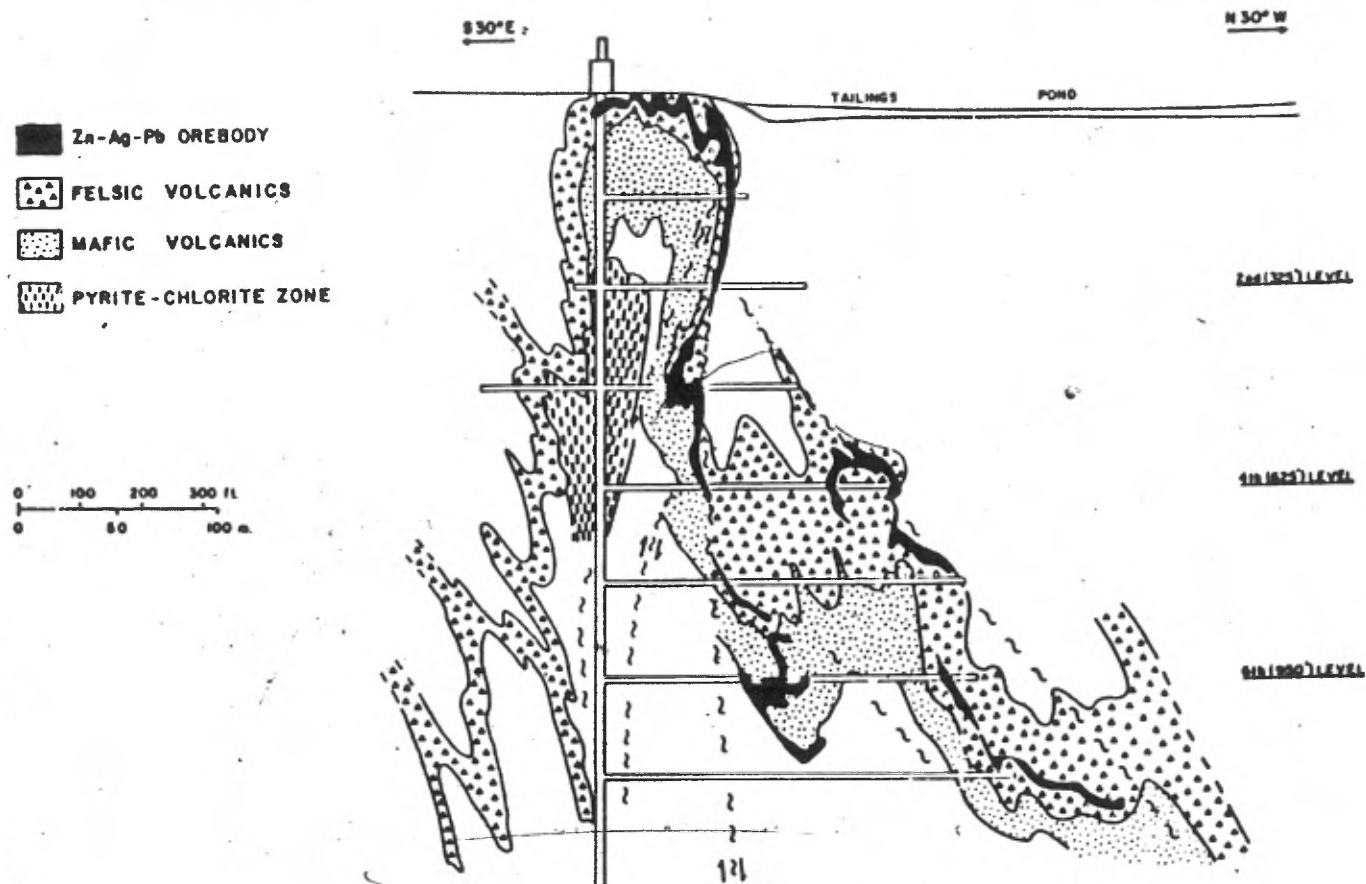
7.1.2 General Geology

7.1.2.1 Host Rocks

The northwest part of the Coniagas property is underlain by a large gabbro-diorite intrusion which extends several kilometers NE-SW (Map 1 - rear pocket). To the southeast, the mine series consists of bands of felsic pyroclastics (cherty tuffs, lapilli and lesser agglomerates), alternating with strata of more mafic tuffs and flows.

Ore lenses are contained almost entirely within one band of felsic pyroclastics (Fig. 7.1) which, itself, has been highly deformed. Due to the intense hydrothermal activity associated with the ore deposition, few of these enclosing rocks can be termed fresh.

Figure 7.1: Coniagas Mine Cross-Section (after Coniagas Ann. Rept., 1967)



7.1.2.2 Structure

The tightly folded nature of the host pyroclastics and enclosed ore zones appears to be a direct result of the Kenoran period of folding (Duquette, 1972). As a result, most strata have steep to vertical dip. Northwest of the mine series, pillow tops indicate beds topping south, while strata in Figure 7.1 indicate an anticline encompassing the ore zones. Thus, a synclinal axis must be present slightly northwest of the mine. Pillows, approximately two kilometers southeast of the headframe top north toward the Coniagas anticline, while slightly south of these pillows, other tops point south. Thus, two minor anticlines occur to the north of the regional synclinal axis. The Coniagas deposit is associated with the northernmost anticlinal structure. Mine maps show that the axis of this anticline strikes N60°W and plunges to the east-southeast.

Since the rocks hosting the ores have been folded into a tight anticline with secondary drag folding, it is not surprising that axial faulting has occurred near the main and secondary apices. This is most evident in the "main fault" which bifurcates the north and south anticlinal limbs. Shearing also cut the ore lenses, which had already been stretched by folding, but shear displacement was generally of small magnitude.

7.1.3 Orebodies

The Coniagas orebodies occur as stretched lenses within the enclosing, regionally folded felsic volcanics. Outcropping at surface, the ores undulate as a short series of normal, tight folds, before plunging steeply downward along the Main Fault and thence through a series of irregularly folded lenses to the 8th level of the mine (Fig. 7.1).

Ore, in situ on the edge of the open pit, consists mainly of massive pyrite, sphalerite, pyrrhotite, and galena layers interbedded with the felsic volcanics. Small amounts of galena and native silver have been reported by Duquette (1972) to occur, mainly along fractures, in cross-cutting lamphrophyre dykes.

No copper ore was found in the mine, although Graham (1957) reports a trace of vein chalcopyrite in polish section from the Northeast lens. This may be significant in that this lens is stratigraphically lowest of those delineated and may thus indicate the presence of a copper zone at greater depth.

7.1.4 Petrography

Little evidence of the relationship of host rocks to the ores can be made since workings were closed prior to this study, and all drill cores destroyed. A few samples

were collected from surface outcrops near the open pit (Fig. 7.2) and were therefore in close proximity to the ore.

The ore lenses are contained in felsic pyroclastics and outcrop at surface near the nose of a local fold. These hanging wall rocks have been termed tuff and agglomerate by Graham (1957) and massive to fragmental rhyolite with minor andesite and basic fragmentals, by Descarreaux (1973, 1976).

Outcrops closest to the open pit are formed by light grey, slightly cherty, fine-grained volcanics and invariably show patchy alteration in hand specimen. Thin section analysis reveals highly altered mineralogy with abundant epidote-sericite-(chlorite) patches in a fine-grained quartz-plagioclase matrix. Small plagioclase phenocrysts are occasionally present as well-terminated, euhedral grains, ranging from fresh to heavily sericitized. Plagioclase composition, based on the method described in section 2.3.3, ranges from An 16-28 (oligoclase). With the exception of quartz, all fine-grained matrix material has been severely decomposed. Pyrite is the main opaque mineral.

Stratigraphically above the felsic horizon (i.e. to the south and east), the rocks become more mafic. Mafic agglomerates are present in the nose of the fold, to the east of the headframe and continue south of, and parallel to the Quebec Sturgeon Mine road, for approximately 500 meters.

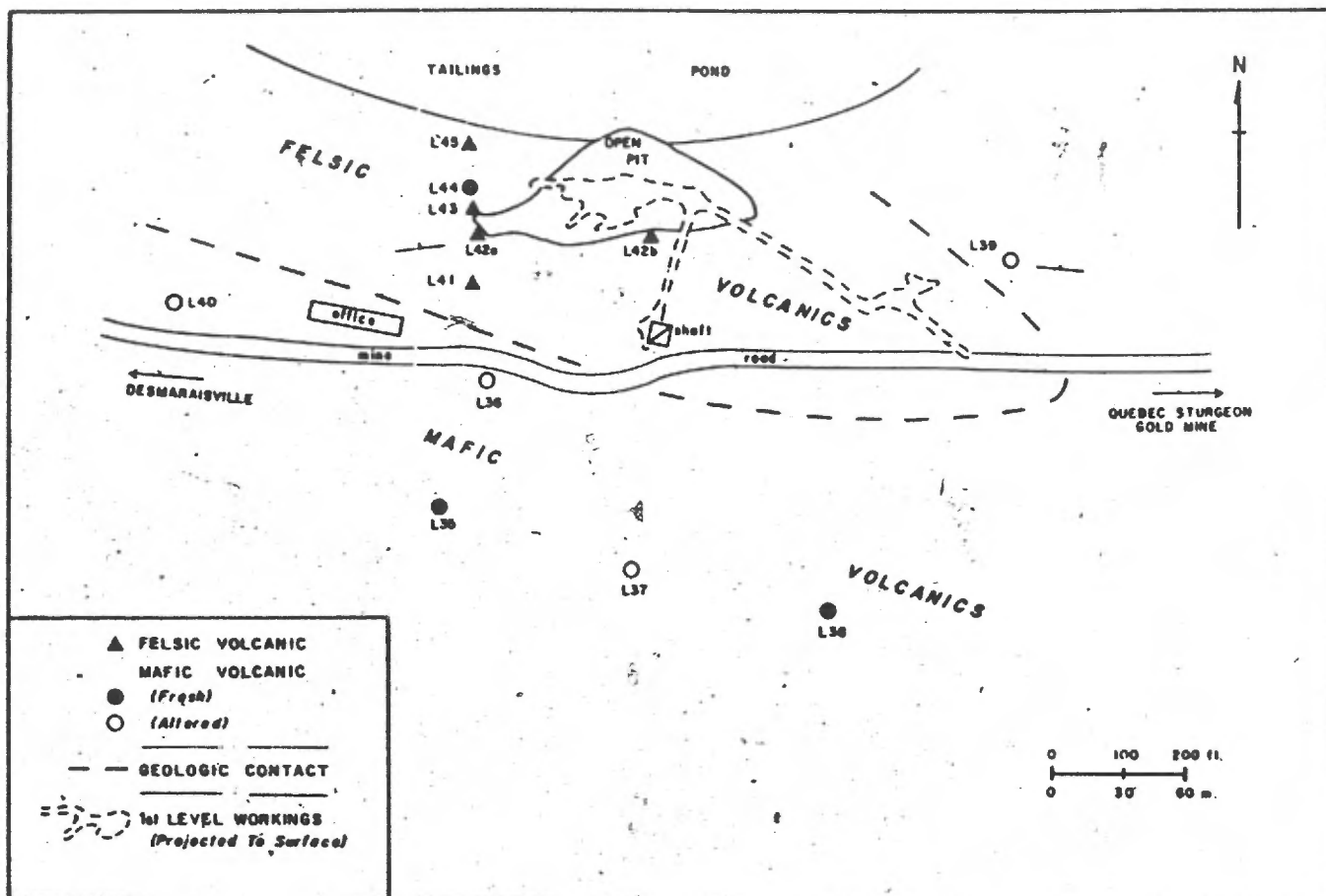


Figure 7.2: Coniagas Minesite - Sketch Plan & Sample Locations

They contain mafic fragments with abundant plagioclase phenocrysts and epidotized amygdules, in a grey-green, chloritic matrix with abundant plagioclase microlites. The low An content of these basalts (An 6-10) indicates that they have been albitized and can therefore be called spilites. A few felsic fragments are sometimes present. Other specimens contain mafic fragments cemented by a carbonate matrix.

Southeast of the headframe, several relatively fresh outcrops of grey to green basalt are present, containing fine-grained hornblende, actinolite, plagioclase and chlorite. In some samples, numerous augite crystals are found, with euhedral forms and slightly uraltized rims. The presence of fresh pyroxene is unusual in this volcanic belt, other than in the pyroxenites of Area 1.

7.1.5 Geochemistry

Samples near the Coniagas deposit are restricted to three, relatively unaltered mafic flows with minor agglomerate (L35, 38, 44), three altered mafic rocks (L36, 37, 39) and five altered felsic samples (L41, 42a, 42b, 43, 45) that are closely associated with the ore.

An alkali-silica diagram (Fig. 7.3 A) shows that most rocks lie in the subalkaline field. Altered mafic rocks show alkali enrichment.

Distribution on an AFM diagram (Fig. 7.3 B) indicates that the felsic rocks are similar to calc-alkaline dacites, with slight iron enrichment due to the presence of chlorite and pyrite. The relatively fresh mafic rocks resemble tholeiitic basalts.

In order to test the hypothesis that the altered basalts are significantly different from the fresher varieties, the two groups were compared by means of the Student's t and F tests (Tab. 7.1). A Kolmogorov-Smirnov (goodness of fit) test was performed, initially, and no indication of non-normality was found, despite the small numbers of samples in the groups. The degree of alteration is shown to be statistically significant, at the 95 percent confidence level, for the major factors in the sericitic alteration (i.e. K₂O addition, CaO depletion). Therefore, division of the basalts into two groups, for purposes of this discussion, is considered valid.

Mean, standard deviation and coefficient of variation (relative %) are provided, for the fresh and altered basalts, and the felsic pyroclastics, in Table 7.2. The coefficient of variation is most significant in that a large value indicates greater variation than elements with lower values. This greater variation can be due to the processes which occur during crystallization of the lavas (magmatic differentiation) or post-crystallization mobilization during hydrothermal alteration.

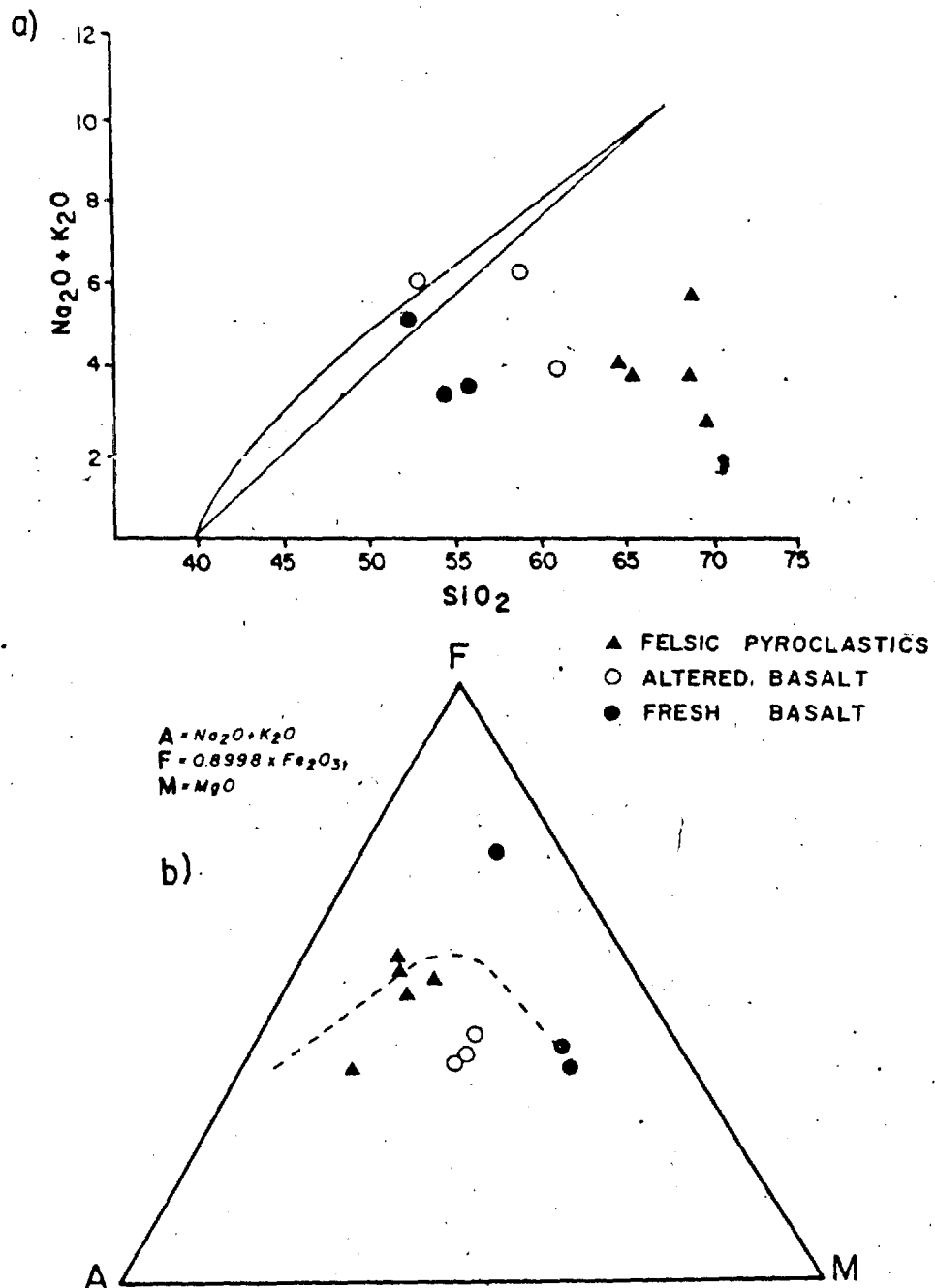


Figure 7.3: Coniagas Minesite Geochemistry a) Alkali-Silica
b) AFM Variation

TABLE 7.1

Significant Geochemical Differences Between Rock and Alteration Types a) Coniagas Minesite b) QSRML

a) CONIAGAS		b) QUEBEC STURGEON		
	Groups 1 & 2		Groups 1 & 2	3 & 4
SiO ₂		SiO ₂		
Al ₂ O ₃		Al ₂ O ₃		(*)
Fe ₂ O ₃		Fe ₂ O ₃		
FeO		FeO		
MgO	(*)	MgO		
CaO		CaO		
Na ₂ O		Na ₂ O		
K ₂ O	*	K ₂ O	(*)	
TiO ₂		TiO ₂		
MnO		MnO		
P ₂ O ₅		P ₂ O ₅		
S		S		
Ba		Ba		
Rb		Rb	*	(*)
Sr		Sr		
Cu		Cu		
Zn		Zn		
Co		Co		
Ni		Ni		
K/Rb		K/Rb		
Ba/Rb		Ba/Rb		
Rb/Sr		Rb/Sr	*	
Ni/Co		Ni/Co		

GROUP 1:

Relatively Fresh Basalts

GROUP 1:

Felsic Pyroclastic Rocks

GROUP 2:

Altered Basalts

GROUP 2:Potassically Altered Felsic
Pyroclastic RocksGROUP 3:

Mafic Volcanic Rocks

GROUP 4:Mica-Carbonate Altered Mafic
Volcanic Rocks* Significant at the 95% Confidence Level
as determined by F and Student's t tests

(*) Significant at the 99% Confidence Level

TABLE 7.2
Coniagas Geochemistry - Summary Statistics

	FRESH BASALT			ALTERED BASALT			FELSIC PYROCLASTICS		
	n=3			n=3			n=5		
	X	s	V	X	s	V	X	s	V
SiO ₂	54.14	1.56	2	57.51	4.25	7	67.39	2.36	3
Al ₂ O ₃	14.72	0.74	5	15.64	0.65	4	11.70	1.42	12
Fe ₂ O ₃	2.64	0.31	11	2.54	0.35	13	2.00	0.36	18
FeO	5.23	0.64	12	4.92	0.74	15	3.88	0.71	18
MgO	9.56	0.40	4	5.64	0.92	16	1.91	0.14	7
CaO	6.24	1.47	23	5.16	3.09	60**	6.44	2.28	35*
Na ₂ O	2.44	0.74	30*	4.90	1.68	34*	2.07	1.01	48*
K ₂ O	1.53	0.46	30*	0.53	0.39	74**	1.95	0.77	39*
TiO ₂	0.70	0.08	11	0.82	0.04	5	0.47	0.06	12
MnO	0.13	0.09	45*	0.15	0.04	26	0.28	0.05	17
P ₂ O ₅	0.14	0.03	18	0.09	0.06	69**	0.12	0.03	24
S	0.04	0.05	115**	0.04	0.05	129**	0.08	0.13	161**
Ba	259	141	54*	140	75	53*	171	37	22
Rb	24	8	35*	9	7	83**	45	19	43*
Sr	308	152	49*	140	53	38*	56	15	28
Cu	23	22	96**	31	13	42*	24	9	41*
Zn	126	23	17	93	8	9	1355	2714	200**
Co	43	3	8	35	8	24	94	171	182**
Ni	106	116	109**	55	31	56*	23	6	26
K/Rb	534	55	10	482	71	14	362	54	17
Ba/Rb	10	2	23	17	7	44*	5	4	82**
Rb/Sr	0.08	0.01	13	0.06	0.03	53*	0.89	0.44	49*
Ni/Co	2.1	2.7	126**	1.6	0.9	56*	0.5	0.6	101**

X Mean
s Standard Deviation
V Coefficient of Variation (%)

Coefficient of Variation: Moderate (30-60%) *
High (60% +) **

The very limited sampling makes it difficult to interpret the geochemical data. However, some apparent variations can be related to geological processes. The relatively fresh basalts show moderate variations in Na₂O, K₂O, Ba, Rb, and Sr, all of which may be due to incipient reactions between the basalts and heated sea water. The large variations in S, Cu, Ni and Ni/Co may be related to the mineralizing process. Thus, even the relatively fresh basalts, overlying the host pyroclastics, appear to have been altered to a minor degree by the hydrothermal processes.

Altered basalts show a significant decrease in MgO and K₂O and an apparent increase in Na₂O. These changes reflect the intense albitization and minor chloritization of these rocks. Decreases in Ba, Rb and Sr can also be related to albitization, while the decrease in Ni may be due to its release from ferromagnesian minerals during chloritization. In almost all cases, the relative variations (i.e. coefficient of variation) are higher in the altered basalts than in the fresher group.

As samples of fresh felsic pyroclastics were not seen near the Coniagas deposit, it is more difficult to determine which elements were added or removed. TiO₂ is normally one of the most immobile elements during hydrothermal alteration. If the TiO₂ content (0.47 wt.%) for the altered

pyroclastics has not changed, this value would indicate that the rocks originally had a composition between a rhyolite and a dacite, i.e. a rhyodacite (see Table 6.1). With the exception of Al_2O_3 , CaO and Na_2O , all of the other major elements are within about one standard deviation of the expected values for rhyodacite. The low Al_2O_3 and Na_2O , abundant CaO and moderately abundant K_2O is reflected in the abundant epidote and sericite. The very high variations in S, Zn and possible Co are due to reactions between the ore fluid and the felsic pyroclastic rocks.

7.2 QUEBEC STURGEON RIVER MINES LTD. - GOLD DEPOSIT

7.2.1 Introduction

Trenching of a quartz-veined prospect (see Graham, 1957, plate II), in the fall of 1946, by O'Brien Gold Mines Ltd., resulted in the staking of ground when modest gold-assay values were determined. The zone was traced for a length of "400 feet over an average width of 7.7 feet". On the basis of further trenching and diamond drilling, the company reported a deposit of 235,000 tons, grading 0.34 oz Au/ton, in late 1949.

Financing problems and a complicated series of litigations eliminated the possibility of O'Brien Gold Mines Ltd. bringing the property into production and development was suspended.

In 1961, Sturgeon River Mines Ltd. optioned the property and began a drilling programme which increased reserves to 480,000 tons averaging 0.326 oz Au/ton. A permanent road was extended to the minesite from the Coniagas property, in 1962, and Coniagas personnel, who were supervising the development work, agreed to process any recovered ore in their mill. During this period, the early surface trenches were cleared, expanded, and sampled in detail. Assay results show a narrow zone of high grade (over .50 oz Au/ton) ore over 60 meters in length with average width of 1 meter. Values of greater than 0.02 oz Au/ton were maintained, on average, over at least two meters width. The following year, nineteen claims and a management concession were obtained from O'Brien Gold Mines Ltd. and the shaft completed to 1111 feet, with 7 levels at 150' intervals (175'-1075'). However, little lateral development was performed. Development was suspended until 1972 when gold prices rose to \$60/tr.oz. The property was purchased and a new headframe and plant installed. Extensive lateral work brought reserves to 967,046 tons averaging .195 oz/ton (10% dilution).

With a rise from \$65 to \$120/oz in 1973, extensive development work began bringing reserves to 933,000 tons of .217 oz/ton to the 7th level. Gold, at \$180/oz in 1974-75 convinced the company to attempt production. By 1978, no production had begun, but estimated pre-production costs had risen to \$6.5 million (Northern Miner, Feb 9).

7.2.2 General Geology

The ore zone of the Quebec Sturgeon deposit is contained within a series of felsic pyroclastics and mafic lava flows, and strikes N70°E. It trends at approximately 90 degrees to the strike of the enclosing volcanics. To the east, the mineralized area adjoins and is underlain by the intrusive O'Brien granite stock.

Reporting on field work performed in 1949, Graham (1957, p.22) describes the country rock as "a formation of interbedded agglomerate and tuff striking N33°W and dipping 80°NE. Mineralization is said to be contained in a vein or series of lenses of milky quartz, up to one foot in width, lying along a narrow shear zone". This description of the surface expression of the deposit accurately conveys the broad relationships at depth.

During field work for the present investigations, the first level of the mine was examined and a series of 25 samples taken across the trend of the ore zone (Fig. 7.4) to determine alteration effects on the host rocks. These specimens transgress two major rock types, mapped by mine personnel as felsic pyroclastics (samples L83 to L98) and greenstone (L99 to L107).

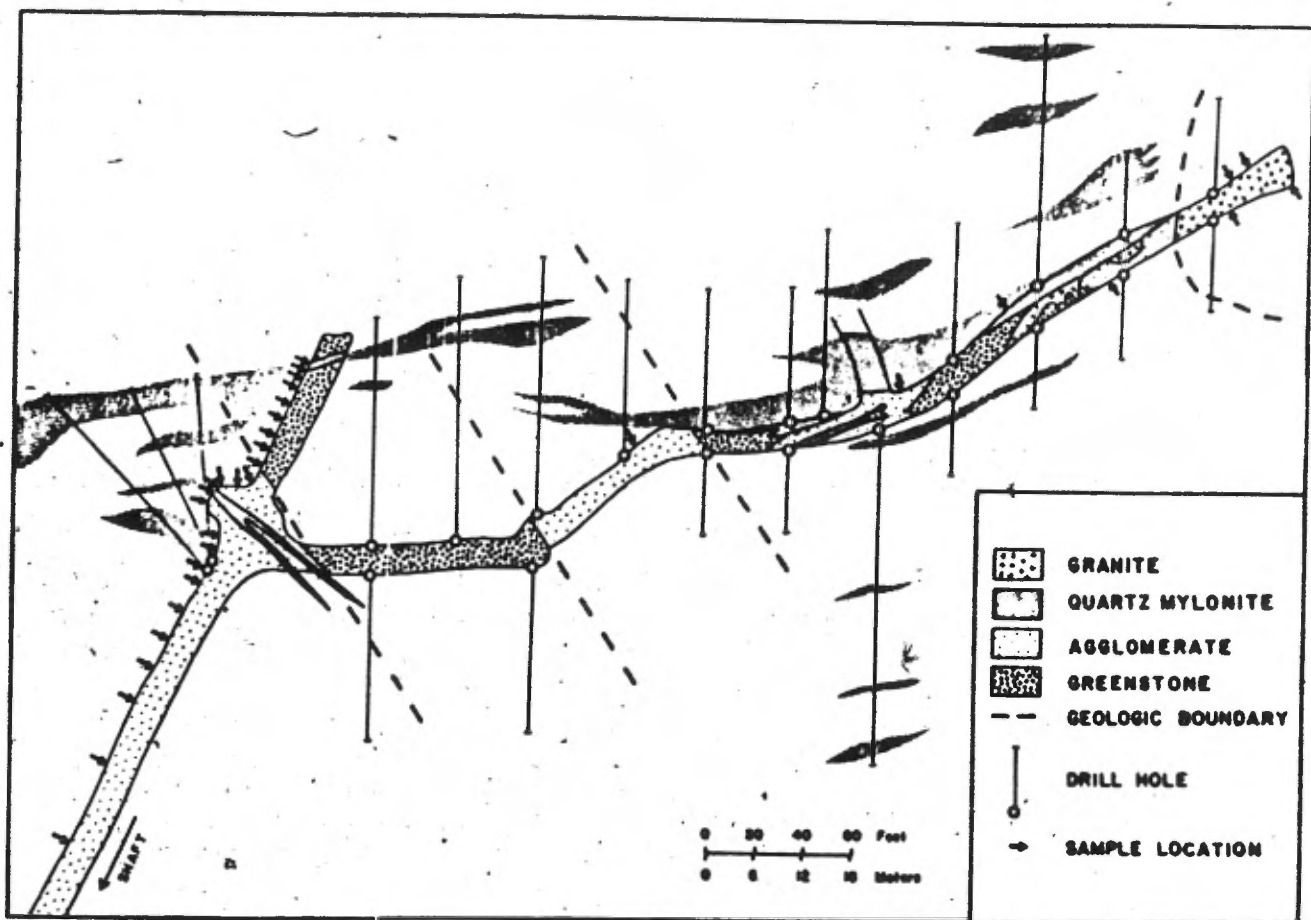


Figure 7.4: QSRM Gold Deposit - 1st Level Plan

7.2.3 Orebodies

Ores at the Quebec Sturgeon property are contained in a series of irregular but generally east-west trending veins, lying in close proximity to the O'Brien granitic stock. The veins pinch and swell into lens-shaped stringers along this trend.

Mine geologists have termed the vein material "mylonite", a broken, altered, and impregnated material, consisting of wallrock fragments and quartz-carbonate matrix. Samples of the vein, as observed in thin section, appear to be heavily impregnated with irregular quartz stringers, frequent carbonate and abundant pyrite. Extremely intense alteration of the wall rock fragments to a fine-grained quartz-sericite mass accompanies the quartz deposition. Such strong and pervasive decomposition is indicative of intense hydrolitic activity.

7.2.4 Petrography

Host rocks at the Quebec Sturgeon deposit are felsic pyroclastic rocks and associated mafic volcanics. All rocks are more or less sheared.

The felsic rocks contain mainly fine-grained, quartz-plagioclase grains. Plagioclase phenocrysts are common and, while not abundant, are dispersed through the matrix. Mafic minerals are conspicuously absent, even as relics, with

chlorite being present only as thin streaks and wisps along fractures. Mineralogically, these rocks could be termed dacites.

Most felsic rocks show some degree of shearing and are cut by 1-5mm wide, pyrite-bearing quartz veinlets. This deformation appears to increase progressively as the ore vein is approached, at which time the quartz veining becomes quite pronounced.

A short distance north of the main ore vein, the rocks become a darker green color and have thus been termed "greenstone" by mine geologists. They are much less sheared than the felsic rocks and are void of quartz veining and plagioclase phenocrysts. In essence, they are dark, fine-grained and slightly foliated by parallel orientation of chlorite and actinolite grains, which form up to 30 percent of the mode. The remainder is formed by plagioclase, quartz, sericite and minor epidote. At the northernmost sampling location, a smaller ore vein was encountered. Collection beyond this point was prevented by backfill.

It should be noted that accurate classification of rocks in proximity to the ore veins cannot be made with certainty. They have been deformed and subjected to varying degrees of hydrothermal activity. This alteration can be divided into two types:

1. PROPYLITIC ALTERATION

The felsic rocks contain quartz, plagioclase and abundant epidote. Plagioclase is oligoclase (An 12). Mica and/or carbonate are minor or absent.

The mafic rocks contain abundant actinolite, plagioclase, quartz and epidote. Plagioclase is oligoclase (An 16-24). Minor biotite but little or no carbonate is present.

2. CARBONATE-POTASSIC ALTERATION

In felsic rocks, the common, higher grade alteration minerals are sericite and/or biotite and carbonate (dolomite). Epidote may be present but is much less common than in propylitically altered samples. The An content of plagioclase varies from 10-28.

In the mafic rocks, biotite and/or sericite are moderate to abundant and there is little or no epidote. Plagioclase in the rocks is albite to oligoclase (An 6-20), except within 2 meters of the gold-quartz veins, where An drops to near 0.

Alteration appears to be strongly controlled by the shearing, and alteration increases toward the ore. This

increase is shown by greater alteration of the matrix, increased sericitization of plagioclase phenocrysts and, in a few rocks, by the appearance of a pinkish hue, suggesting potash feldspar addition. Albitization is restricted to within about 2 meters of quartz-carbonate filled shear zones, while potassic alteration (sericite and/or biotite) forms a wider halo. These alteration patterns strongly suggest that alteration occurred at the time of and probably by the same mechanisms as that of ore deposition.

7.2.5 Geochemistry

Sampling at the Quebec Sturgeon deposit was restricted to samples along a first level crosscut and drift. Twelve felsic pyroclastics were collected, four of which had undergone propylitic alteration (see section 7.2.4) and the remainder containing a more intense, potassic alteration. Ten mafic volcanics were examined, half of which were propylitized and the remainder containing a stronger, carbonate-potassic alteration.

All samples, with the exception of those immediately adjacent to the ore veins, plot as subalkaline on an alkali-silica plot (Fig. 7.5 A). Mafic volcanic rocks, within 1.5 m. of the veins lie in the alkaline field, indicating strong potassium enrichment, while the remainder are subalkaline.

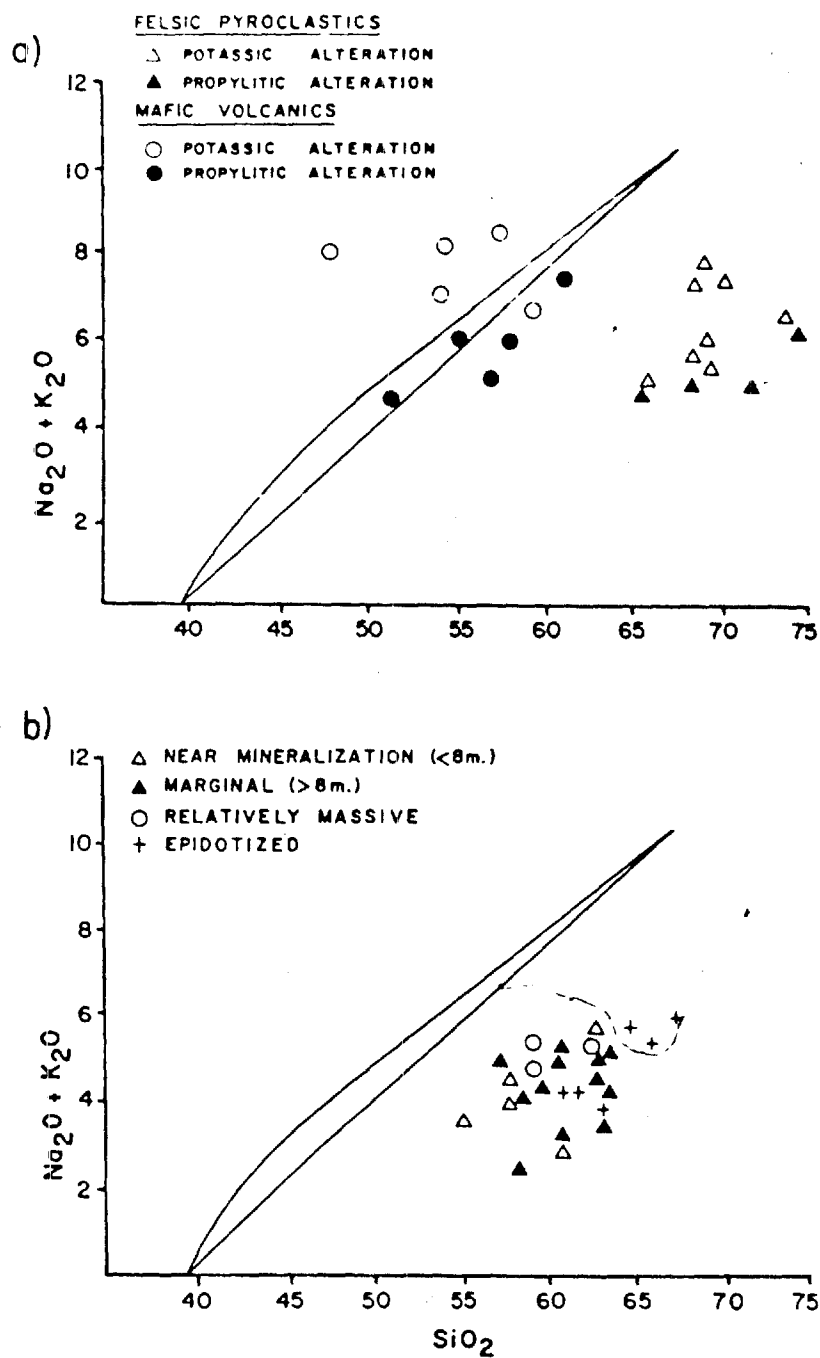


Figure 7.5: Alkali-Silica Diagrams a) QSRML b) Soquem Properties

α

All samples lie along a calc-alkaline trend, within the calc-alkaline field on an AFM diagram (Fig. 7.6 A), strongly polarized toward the A-apex. This position is reasonable for felsic rocks but is unusual for "greenstones", which must therefore have suffered alkali-enrichment.

As with the Coniagas suite, checks for significant differences in chemical composition between propylitized and carbonate-potassic altered rocks were done using Student's t and F tests (Table 7.1 B). Again, a Kolmogorov-Smirnov (goodness of fit) test was performed prior to these tests and no significant departures from normality were noted, despite the small numbers of samples in each subgroup.

Mean, standard deviation and coefficient of variation are provided for each rock and alteration type, in Table 7.3

The felsic rocks have geochemistry similar to a fresh, average rhyodacite (i.e. between rhyolite and dacite in Table 6.1) for Area 4, within which the deposit is located. However, the least altered samples (those showing propylitic alteration) contain slightly less Al_2O_3 , Na_2O , Sr, and Co, and slightly more K_2O and S than similar, average, fresh rocks. In addition, the coefficient of variation for iron (Table 7.3) is considerably greater than in fresh rocks. These features are consistent with low grade propylitic alteration.

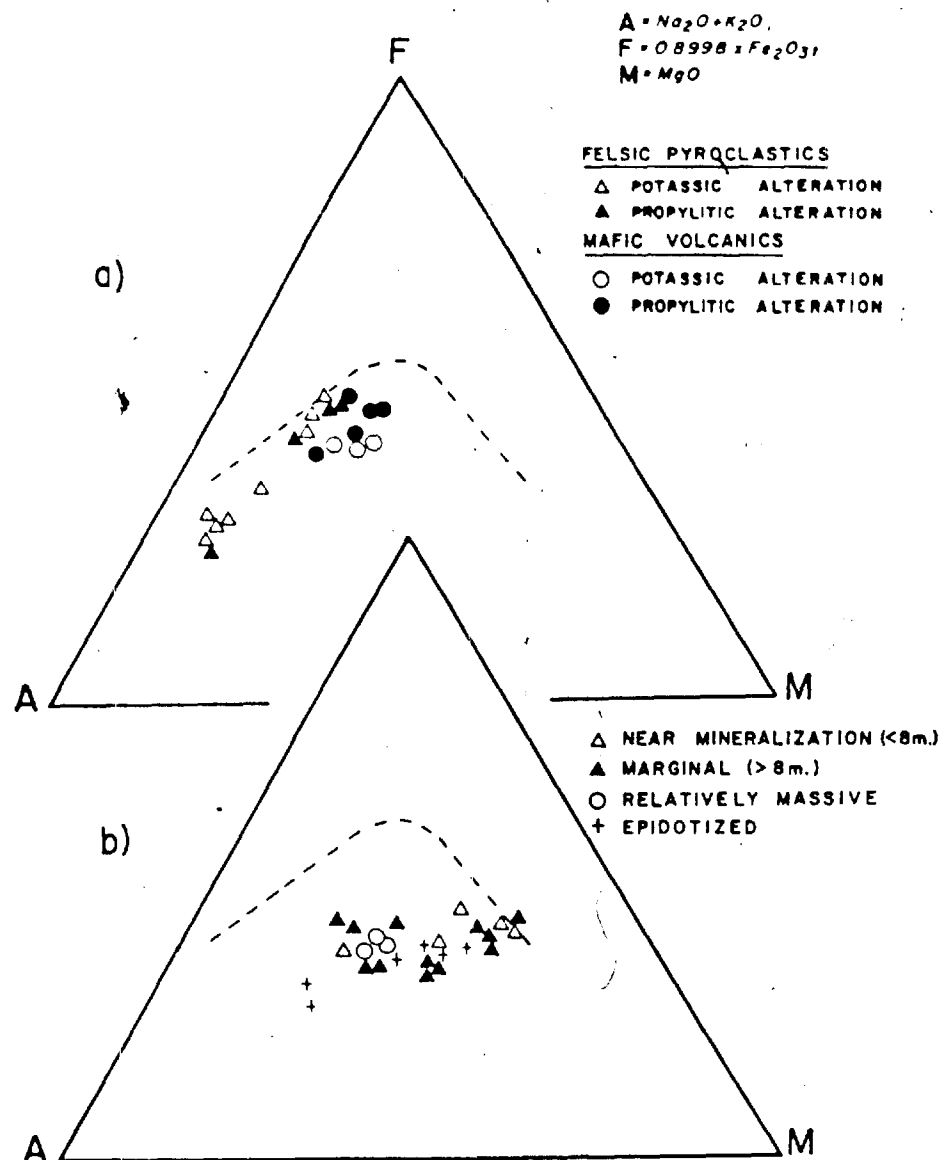


Figure 7.6: AFM Diagrams a)QSRML b)Soquem Properties

TABLE 7.3

Quebec Sturgeon Geochemistry - Summary Statistics

	FELSIC PYROCLASTICS						MAFIC VOLCANICS					
	Less Altered n=4			Potassic Alt. n=8			Less Alt. n=5			Carb-Potassic Alt. n=5		
	X	s	V	X	s	V	X	s	V	X	s	V
SiO ₂	69.97	3.86	6	69.13	2.20	3	56.49	3.45	6	54.38	4.31	7
Al ₂ O ₃	11.81	0.24	2	12.44	1.09	8	16.20	0.91	6	13.29	1.06	8
Fe ₂ O ₃	1.79	0.69	39*	1.57	0.56	35*	2.75	0.26	9	2.92	0.34	11
FeO	3.46	1.38	40*	3.07	1.04	34*	5.33	0.51	10	5.69	0.64	11
MgO	1.75	0.57	32*	1.42	0.41	28	3.61	0.49	14	3.99	1.17	29
CaO	3.44	1.45	42*	3.52	1.57	44*	6.40	3.04	47*	8.30	2.18	26
Na ₂ O	3.99	0.65	16	3.62	0.94	26	3.02	1.72	44	4.34	1.27	20
K ₂ O	1.37	0.47	34*	2.84	0.90	17	2.12	1.20	56*	3.39	0.74	21
TiO ₂	0.51	0.15	29	0.52	0.11	22	0.94	0.14	15	0.91	0.13	14
MnO	0.13	0.06	45*	0.11	0.05	47*	0.17	0.04	21	0.21	0.05	27
P ₂ O ₅	0.12	0.04	32*	0.10	0.03	35*	0.17	0.03	15	0.15	0.02	19
S	0.16	0.19	117**	0.16	0.08	52	0.02	0.01	27	0.61	0.50	82**
Ba	325	100	31*	332	83	25	372	363	97**	290	113	39*
Rb	30	12	40*	58	15	26	52	23	44*	107	20	19
Sr	111	28	25	108	33	29	157	43	27	228	75	33*
Cu	16	8	54*	30	17	58*	19	7	41*	63	46	74**
Zn	140	62	45*	112	51	45*	131	11	8	136	26	19
Co	14	17	122**	15	17	119**	16	16	103**	29	14	50*
Ni	24	5	27	26	6	26	59	23	40*	47	38	81**
K/Rb	388	154	40*	417	84	20	316	58	18	263	35	13
Ba/Rb	11	3	33*	5	1	23	6	3	44**	3	1	40*
Rb/Sr	0.29	0.12	40*	0.59	0.22	37*	0.35	0.19	55*	0.50	0.15	30*
Ni/Co	0.4	0.4	100**	0.4	0.4	114**	4.0	3.8	95**	1.5	0.6	45*

X Mean
s Standard Deviation
V Coefficient of Variation (%)

Coefficient of Variation: Moderate (30-60%) *
High (60% +) **

Table 7.1 shows that the most significant differences between propylitic and carbonate-potassic alteration of felsic rocks are the increases in K₂O, Rb and Rb/Sr ratio of the latter. Table 7.3 also indicates that these are the only elements that show significant changes, and is undoubtedly due to the intense sericitization. Despite development of abundant dolomite, no significant increases in CaO or MgO occur. The sources of these elements in dolomite is apparently from the breakdown of epidote and chlorite.

Chemistry of the mafic volcanic rocks is similar to a fresh, average basaltic-andesite (i.e. between andesite and basalt, in Table 6.1) for Area 4. The propylitically altered samples contain slightly less Sr and slightly more Al₂O₃, K₂O and Rb than similar average fresh rocks, consistent with a very low degree of sericitization.

Table 7.1 shows that there is a significant decrease in Al₂O₃ and increase in Rb, in the more intensely altered (carbonate-potassic) samples. Table 7.3 indicates that K₂O, S and possibly CaO have also increased, while SiO₂ may decrease. All of these changes are consistent with sericitization of feldspar and deposition of carbonate and pyrite. Some silica, released during sericitization, may be removed and deposited in the quartz-rich ore zone.

The lower coefficients of variation for K₂O, Rb and K/Rb in the more intensely altered rocks suggests that these rocks equilibrated with a homogeneous K₂O and Rb-rich ore fluid.

7.3 SOQUEM Lté. - BASE METAL PROSPECT

7.3.1 Introduction

Earliest recorded exploration in northwestern LeTas township was performed by McIntyre Gold Mines Ltd. in 1949. This included mapping and a certain amount of trenching.

In 1951, ground was acquired by Decary Minerals Corp. Ltd. who later became Empire Oil and Minerals Inc. The company initiated a 17,000' drilling programme in 1951-52 and was followed, in 1956, by an additional 11,000'. In conjunction with the drilling, mapping and preliminary geophysical surveys indicated zinc mineralization within pyroclastic volcanics.

No further work was performed in this area until a property evaluation report was compiled by H.J. Bergman in 1965. A number of claims containing the mineralized ground were purchased by J.J. Martell in 1970, who then conducted an EM survey.

The claims, along with those of H. Belanger, were optioned by Soquem Lté in 1971 and twenty miles of survey line were cut and followed by vertical loop and IP surveys

in 1972. Access to the claims was made by a winter road which proceeds south from the Coniagas Mine road and thence by a trail to the center of the property. A total of 18,682' of core was recovered from a 1972-73 drilling programme and at that time, a detailed map was compiled by R. Doucet.

A final, unpublished company report (Doucet, 1973) suggested that while known reserves were not economically exploitable at that time, further regional exploration in the same and surrounding townships could result in further discoveries. To date, no further work has been done on the property, except that all drill core has been collected and stored at the company's office at the Louvem Mine, near Val d'Or.

7.3.2 General Geology

Rocks on the Soquem property consist of volcanics, in close proximity to large, felsic batholiths to the north and south. As such, they form a small arm, branching off from the main greenstone belt.

A majority of rocks in the area have been classified as pyroclastic (Doucet, 1973), with alternating strata composed of tuff (1-32 mm), agglomerate (32-256 mm) and lesser intermediate to mafic lavas. Fragments are described as acidic in a darker, chloritic matrix. A few outcrops of

dacite were reported in the northeastern part of the property. All fine-grained fragmentals (tuffs) were found to be strongly foliated.

The property was not examined during the present study, due to extremely high water conditions, but a number of Soquem drill cores were examined. A representative selection, across strike and through a one kilometer distance, was provided at 35m intervals. Sample and drill hole locations are plotted on the geologic property map (Fig. 7.7). All holes were drilled to the north.

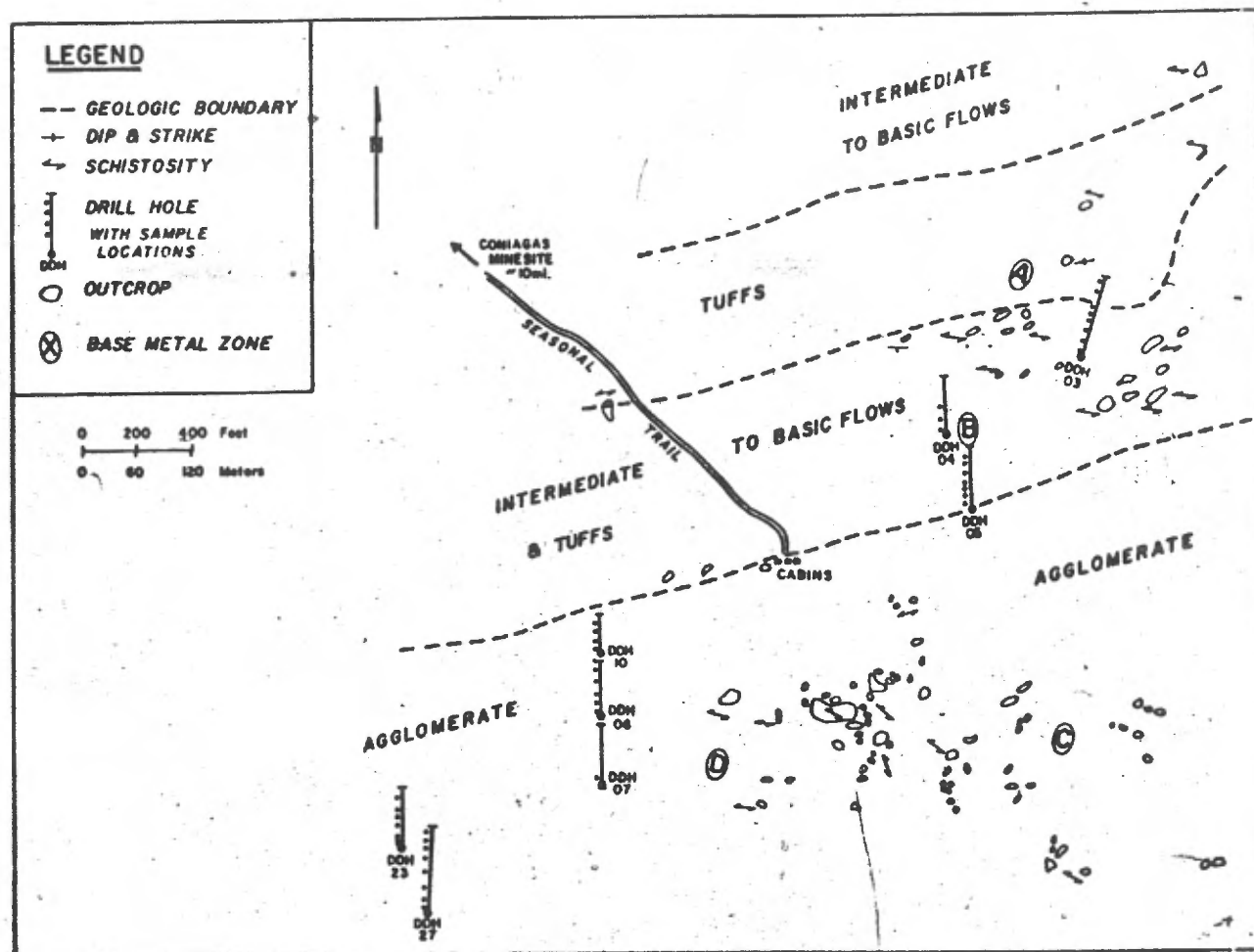
Rocks sampled from the cores traverse both country rock and several zones of Zn(Cu) mineralization.

7.3.3 Orebodies

Drilling programmes during 1951-52, 1956 and 1972-73 succeeded in delineating several potential ore zones, and are summarized by Doucet (1973). Locations of the main mineralized zones are illustrated on the geologic property map (Fig. 7.7).

The stratigraphically highest, "A", zone contains 260,000 tons averaging 3% Zn and <1% Cu. Most of the mineralization is contained in two NW-SE trending lenses and occurs primarily as vein-fillings and lesser disseminated material. The absence of stratiform sulphides and the trend of mineralized lenses across the local strata at a steep angle may be significant and will be discussed in Chapter 8.

Figure 7.7: Soquem Property Map



Mineralization of the "B" zone, directly below the "A" zone, is of minor volume and is not considered important in overall ore calculations. Zones "C" and "D" are the lowest stratigraphic sulphide occurrences and contain 35,000 and 33,000 tons, respectively, of approximately 2.5% Zn and minor copper. Overall tonnage of these Zn-Cu zones is too low to warrant further development.

7.3.4 Petrography

Samples taken along the semi-continuous drill traverse pass through zones of base metal mineralization, whose presence was expected to impose some degree of alteration on the host volcanics. Thin section analysis shows that most samples have been subjected to intense shearing and high degrees of alteration. A few specimens were found to be relatively fresh and are considered as background for this small (1km. square) area.

The high degree of deformation and alteration in these rocks poses a problem for their classification. Most, if not all, samples appear to be dacitic in composition. Evidence comes from the fact that all have extremely uniform TiO_2 content (a generally immobile element during alteration) and are on strike with the dacite horizon in Benoit Township (Area 5). In addition, four samples of sheared dacite occur 3 km, along strike, to the east.

Samples within 8 meters of mineralization (Group 2) were invariably found to contain abundant carbonate, sericite and chlorite. They are also highly sheared. Samples more than 8 meters from mineralization were divided into three groups:

1. GROUP 2. Highly sheared rocks, similar to those near mineralization, except that sericite is not abundant. Carbonate and chlorite are moderate to abundant and the rocks contain little or no epidote.
2. GROUP 3. Similar mineralogy to those near mineralization but much less intense alteration and are not as highly sheared (massive to slightly sheared). This group may be the closest approach to background of any rocks in the area.
3. GROUP 4. Massive to moderately sheared rocks (from one unit - DDH-05) which contain abundant epidote.

Petrographic examination revealed one dominating factor: that all rocks have been sheared and altered to some degree. Most specimens contain carbonate, accounting for 3-10 percent of the mode. All plagioclase grains have anorthite content near An 6 and therefore have been albitized.

The most massive rocks (Group 3) are found mainly in DDH-10. They are porphyritic, with plagioclase phenocrysts, slightly altered to sericite, embedded in a fine-grained, quartz-plagioclase-(chlorite) matrix. Calcite rhombs are present in some specimens, but alteration is generally of a lower intensity than in other parts of the Soquem property.

Specimens from other drill holes are more strongly sheared, often containing chlorite schlieren. The most intense shearing is usually accompanied by high degrees of sericitization, often aligned into parallel bands which weave between lenses of fine-grained matrix material. It is possible that this wrapping effect is what caused Doucet (1973) to term the horizon "agglomerate", but no evidence of primary, coarse-fragmental material is present in thin section. Plagioclase phenocrysts are relatively uncommon in these rocks (possibly all decomposed) but where present, are frequently partially replaced by sericite. More common is the replacement of plagioclase to calcite, which is often more abundant than sericite. The carbonate is disseminated through the rocks both as irregular masses and as euhedral rhombs. - It is also commonly associated with quartz, in irregular veins.

Shearing and alteration generally increase toward zones of sulphide mineralization. Accompanying these changes is an increase in sericite and/or carbonate at the expense of

plagioclase. These alteration products are, however, present even in the freshest specimens, as disseminated grains in pressure shadows around phenocrysts.

7.3.5 Geochemistry

All samples shown in Fig. 7.7 were chemically analysed. Those with greater than one percent sulphur were excluded from further study, due to their extreme change in compositions. Since a large proportion of the rocks have been severely altered, the plots are not expected to show primary distribution, but are useful in comparison with local and regional trends and to visualize the state of alteration.

All rocks plot as subalkaline on an alkali-silica diagram (Fig. 7.5 B) but no grouping is discernable. An AFM diagram (Fig. 7.6 B) shows most samples within the calc-alkaline field but, again, no groupings are present. In general, they lie in the andesite-dacite fields.

It is difficult to interpret the significance of all chemical differences because some may be due to original inhomogeneities in the rocks. This is particularly true for rocks in Group 4, whose TiO_2 content (normally the least mobile element during hydrothermal alteration) shows considerable variation. For this reason, comparisons will only be made between Groups 1, 2 and 3. Of these three

groups, Group 3 appears to be the least altered. It will therefore be compared with the other two groups.

Significant differences are evident (Table 7.4), at the 95% confidence level, between the fresher, relatively massive rocks of Group 3 and the more altered and sheared Groups 1 and 2. Group 1 is statistically different in Na₂O, K₂O, MnO, Sr, Zn and Rb/Sr, while Group 2 is different in Al₂O₃, TiO₂, MnO and S. Therefore, both are considered valid divisions.

Mean, standard deviation and coefficient of variation are provided for elements in each group in Table 7.5, and distinct geochemical patterns are evident.

Group 2 rocks, on average, contain higher MgO, MnO and S, and lower Al₂O₃ than rocks of Group 3. This is consistent with the slightly higher degree of chloritization in these more intensely sheared rocks. In addition, the TiO₂ content of Group 2 rocks is slightly lower than in Group 3, suggesting that the former are marginally more felsic. S and, perhaps, Zn are also slightly higher in Group 2, as a result of minor sulphide deposition from hydrothermal solutions entering along shear planes.

A considerable change in chemical composition occurs in the rocks within 8 meters of mineralization (Group 1). These rocks contain higher K₂O, Ba, Rb, K/Rb and Rb/Sr

TABLE 7.4

Significant Geochemical Differences Between Rock and
Alteration Types in the Soquem Deposit

	GROUPS 1 & 3	GROUPS 2 & 3
SiO ₂		
Al ₂ O ₃		*
Fe ₂ O ₃		
FeO		
MgO		
CaO		
Na ₂ O	(*)	
K ₂ O	*	
TiO ₂		*
MnO	*	*
P ₂ O ₅		
S		*
Ba		
Rb		
Sr	(*)	
Cu		
Zn	(*)	
Co		
Ni		
K/Rb		
Ba/Rb		
Rb/Sr	*	
Ni/Co		

GROUP 1: <8m. from mineralization

GROUP 2: >8m. from mineralization & Sheared

GROUP 3: >8m. from mineralization & Relatively Massive

* Significant at the 95% Confidence Level
as determined by F and Student's t tests

(*) Significant at the 99% Confidence Level

TABLE 7.5
Soquem Property Geochemistry - Summary Statistics

	GROUP 1			GROUP 2			GROUP 3			GROUP 4		
	n=5			n=12			n=3			n=6		
	\bar{X}	s	V	\bar{X}	s	V	\bar{X}	s	V	\bar{X}	s	V
SiO ₂	58.87	2.89	5	60.97	2.15	3	60.25	1.89	3	64.03	2.56	4
Al ₂ O ₃	17.68	1.74	10	16.46	1.54	9	18.60	0.37	2	17.31	2.23	13
Fe ₂ O ₃	2.30	0.50	22	1.81	0.30	17	1.69	0.15	9	1.54	0.37	24
FeO	4.54	0.94	21	3.54	0.59	16	3.30	0.31	9	3.01	0.73	24
MgO	6.63	2.29	34*	5.24	1.85	35*	3.83	0.31	8	4.47	1.56	35*
CaO	3.11	1.04	33*	5.29	1.53	29*	5.35	2.94	55*	4.42	1.17	26
Na ₂ O	1.43	0.68	47*	3.06	0.91	29*	3.63	0.28	8	3.53	1.10	31*
K ₂ O	2.65	0.54	24	1.17	0.54	46*	1.44	0.47	32*	1.32	0.55	45*
TiO ₂	0.56	0.06	11	0.46	0.05	10	0.54	0.02	4	0.46	0.15	33*
MnO	0.51	0.25	50*	0.18	0.07	43*	0.04	0.04	100**	0.12	0.10	84**
P ₂ O ₅	0.11	0.02	14	0.10	0.26	25	0.11	0.01	9	0.11	0.03	24
S	0.09	0.15	165**	0.08	0.11	145**	0.00	0.01	—	0.01	0.02	183**
Ba	535	151	28	373	154	41*	345	39	12	324	85	26
Rb	58	18	31*	26	9	38*	34	9	28	29	12	44*
Sr	107	38	36*	213	65	30*	284	30	11	210	55	26
Cu	37	21	58**	31	33	107**	21	9	43*	14	15	110**
Zn	708	126	18	294	247	84**	143	78	55	137	39	29*
Co	38	2	8	39	2	5	38	1	2	37	1	4
Ni	146	86	60**	116	40	35*	72	10	14	82	45	56*
K/Rb	379	30	8	358	52	14	346	19	6	364	18	5
Ba/Rb	9	4	51*	15	6	42*	10	2	21	11	2	22
Rb/Sr	0.59	0.25	41*	0.13	0.05	39*	0.12	0.05	37*	0.15	0.08	53*
Ni/Co	3.6	1.9	53*	3.0	0.9	32*	1.9	0.3	15	2.2	1.1	54*

GROUP 1: Near Mineralization (<8m.) & Sheared

GROUP 2: > 8m. from Mineralization & Sheared

GROUP 3: > 8m. from Mineralization & Relatively Massive

GROUP 4: > 8m. from Mineralization & Heavily Epidotized (sheared to massive)

\bar{X} Mean

s Standard Deviation

V Coefficient of Variation (%)

Coefficient of Variation: Moderate (30-60%) *

High (60% +) **

ratios and lower Na₂O, CaO and Sr, reflecting the high degree of sericitization. In addition, increases in MgO, MnO and possibly FeO, relative to rocks of Group 3, is due to chloritization. Higher Zn ~~and~~ slightly higher Cu accompanies the sericitization, as sulphide grains, probably deposited from the same hydrothermal solutions.

All rocks on the Soquem property have been highly dolomitized. MgO contents are considerably higher than average fresh rocks (Table 6.1), possibly as a result of interaction with seawater during alteration. On the other hand, CaO contents are high, but not appreciably above average, suggesting that calcium in the dolomite was provided from redistribution in the rocks during alteration.

Chapter 8

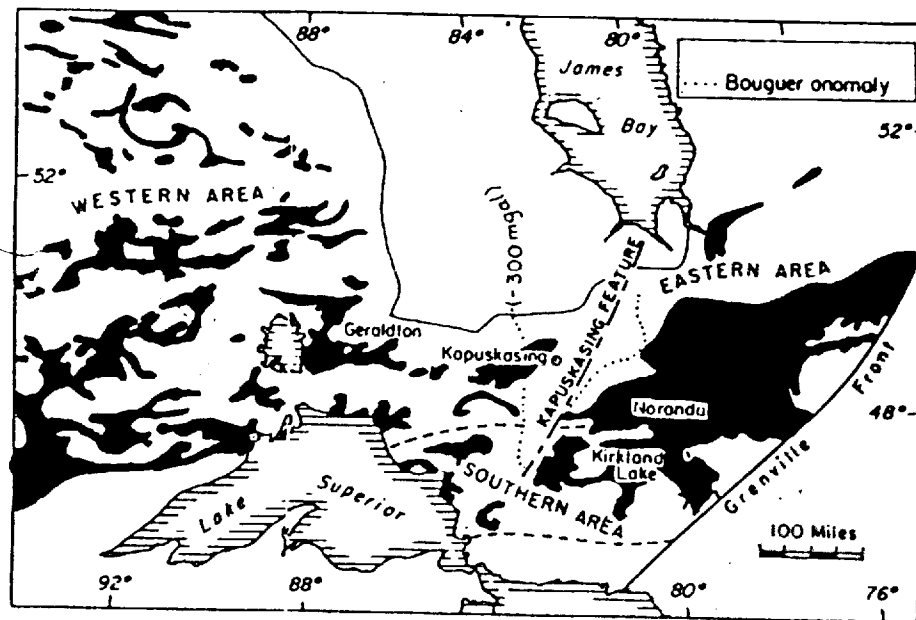
DISCUSSION

"Ultimately, it will probably be field relations --
that will be diagnostic of tectonic environment"
Brooks & Hart (1974)

8.1 INTRODUCTION

Archean volcanic belts in the Superior Province are contained in large, low metamorphic grade, E-W trending subprovinces or superbelt (Stockwell, 1964) and are separated by similarly trending, high-grade superbelt (Wilson et al., 1976, 1977; Goodwin, 1977; Gorman et al., 1978). The eastern and western Superior Province is separated by a north-northeast trending structural lineament, the Kapuskasing gravity high, on either side of which (Fig. 8.1), features of the volcanic belts are quite different (Goodwin, 1972; Hutchinson, 1971; Kalliokoski, 1968). For this reason, comparisons of the Bachelor Lake region to other areas will be mainly restricted to terrains east of the lineament. Detailed comparisons with Archean volcanic belts on other continents will be similarly restricted since they are unlike Canadian sequences in all but the broadest features (Jolly, 1977, p.328).

Figure 8.1: Relationship of Volcanosedimentary Belts to the Kapuskasing Feature (after Kallio Koski, 1968)



Regional relationship of volcanic-sedimentary belts (black) granitoid rocks (white) to the Kapuskasing feature.

This chapter attempts to draw conclusions from the data presented in preceding chapters and thus form a hypothesis for the evolutionary history of the Bachelor Lake region.

8.2 STRATIGRAPHY

The Bachelor Lake Area has been shown by this study to form a northeast-trending synclinal zone in the eastern Abitibi greenstone belt. As such, it represents a small portion of an extensive Archean terrain, traceable beyond the study area to the northeast and southwest, but truncated to the north and south by intrusive batholiths. Descriptions of parts of this area are provided by Dresser et al. (1944), Grenier (1967), and Duquette (1968), and suggest, by macro-structural patterns, that the area is a typical, downwarped, interior trough. Examination of the supracrustal sequence, therefore, provides an appreciation of the evolution of the area and possible extrapolations to other parts of the belt.

Geologic setting of the Bachelor Lake area is illustrated in the map in the rear pocket, on which the rock types have been plotted. The volcanosedimentary sequence is estimated at approximately 25 km. vertical thickness, although structural complexities may have exaggerated the true thickness. This estimate is, however, of similar magnitude to other reported parts of the Abitibi belt, such as the Noranda area (18 km. - Goodwin, 1972) and the

Timmins-Kirkland Lake area (35 km. - Jensen, 1976). It should be noted that the base of the stratigraphic sequence was not reached in the study area and could be the subject of further work.

The volcanosedimentary pile has been divided into Areas through the reasons cited in Chapter 5. The lowest stratigraphy, Areas 1, 2 and lowest parts of 3 & 5, consist predominantly of mafic to intermediate volcanics and are roughly traceable through the length of the study area. They form a platform sequence, produced by largely quiescent volcanism. Higher in the stratigraphy (Area 4 & upper parts of 3 & 5), a greater proportion of more differentiated volcanics and pyroclastic rocks are found. These rocks are confined to a domal sequence, centered on Lesueur township and pinching out to the east and west, and a minor band in Benoit and LeTac townships. It is within this upper part of the sequence that the major ore occurrences are found.

The rocks of Area 1 are considered to be products of a deep water environment, due to the absence of vesicular flows. The unique feature of this part of the pile is the presence of light-green, pyroxenitic bodies. They have undergone only minor greenschist facies alteration. While contacts with enclosing basalts were not seen, the unusual geochemical composition of surrounding rocks suggest that the pyroxenites are cumulates within thick flows.

Morphological change is evident with increasing height in the pile. The lowest 4-5 km. of Area 2 are massive and similar to Area 1 (which is not observed in the west due to batholithic intrusion), and then pillowed lavas commence to frequently alternate with massive flows. Vesicular lavas (preserved as amygdular calcite fillings) also become more common in the upper strata. These features strongly suggest that the depositional environment had changed to much shallower water.

A further feature in the uppermost parts of the platform sequence (Area 2) is the appearance of the first distinctive sedimentary horizons. These appear initially as chemical sediments, including several facies of iron formation. It is significant that the oxide facies iron formation appears due north of Bachelor Lake and progresses eastward through carbonate and finally sulphide facies. This is the same sequence represented regionally and considered to define shelf to basin bathymetry (Goodwin & Ridler, 1970, p.5). Above the oxide iron formation and alternating lava flows, the top of the platform sequence is approached and clastic sedimentation (greywacke, conglomerate) begins. This is the first appearance of abundant clastic accumulation and is present only in position directly below the domal sequence of Area 4. It occurs on both sides of the regional syncline and pinches out laterally. It must be concluded that this 10-15 km.

east-west zone was a basinal trough at the time of deposition and that adjacent terrain was at least slightly subaerial, to provide an erosional environment for the detritus. The presence of clastic sedimentation reveals an unconformity at the contact of the wedge and the platform sequence.

The highly mafic rock types and lack of shallow-water depositional features suggest that most of Area 3, which is on the south limb of the regional syncline, is equivalent to at least the deepest levels of Areas 1 and 2. In such case, insufficient volcanic accumulation is present to mirror the sequence on the north limb. An explanation is suggested by the extensive fault zones parallel to the strike of the volcanics. These faults are illustrated by the linear pattern of lake and river systems and by sheared volcanics along these waterways. It is proposed that the faults represent thrust planes along which the strata of Area 3 slid, resulting in tectonic thinning of this part of the pile.

In the central part of the study area, a domal pile of volcanosedimentary material is found, immediately above the clastic wedge of the upper platform sequence. It is the uppermost stratigraphic sequence and contains the regional synclinal axis. This pile contains the first appreciable quantities of pyroclastic rocks, as well as increased

proportions of felsic and intermediate flows (see Table 6.1). The presence of pyroclastics in a 4 km. thick sequence that pinches out, laterally, is evidence of a frequently explosive volcanic center, located in west-central Lesueur township.

The upper strata of Area 5 also contain an abundance of felsic volcanic rocks but these occur almost exclusively as massive flows. They are therefore products of a more effusive, quiescent volcanism than those in Area 4.

During the past decade, the stratigraphy of many Archean terrains has been documented on a regional scale. In the Abitibi belt, detailed mapping has been performed mainly within 100 km. around established mining camps.

In the Noranda region the sequence begins with the Munro and Bowman Groups (mainly mafic and ultramafic lava flows), progressing upward into the Garrison-Kenojevis Group (mafic to intermediate lavas and, very rarely, ultramafic lavas), to the upper, Noranda-Misema or Blake River Group (mafic to felsic lavas, felsic pyroclastics; ultramafic lavas absent) (see Naldrett et al., 1977; Jensen, 1978; Gelinas et al., 1977; Jolly, 1977, 1975; Spence, 1975; Baragar, 1968). A similar sequence has been mapped, along regional strike, in the Val d'Or region, to the east (Imreh, 1976; Latulippe, 1972, 1976). There, the lowest, Lamotte-Vassan and Dubuisson Groups (mafic to ultramafic rocks of

the antiquated, Lower Malartic classification) are probably equivalent to the Munro-Duparquet Group at Noranda, the Jacola Group (mafic to intermediate rocks) equivalent to the Kenojevis Group, and the Heva Group (mafic to felsic lavas of the old, Upper Malartic Group) coinciding with the Blake River Group.

To the north, in the Matagami region, a basal ultramafic sequence has not been observed, possibly because of limited regional mapping. An ultramafic section does occur, however, north of the Joutel-Porier mining camp, a few tens of kilometers to the south. From published data (Roberts, 1975; Sharpe, 1968), the lowest known sequence at Matagami is the Wabasse Group (mafic to felsic lavas), overlain by the Watson Lake Group (predominantly felsic lavas and pyroclastic rocks). A similar sequence occurs at Chibougamau, to the east of Matagami, where, in the Roy Group, the D'Obatagamu formation (mafic lavas) underlie the Wachonichi formation (mafic to felsic lavas and felsic pyroclastic rocks) (Gobeil, 1980; Allard, 1972).

Thus, the gross stratigraphies of many volcanic complexes in the Abitibi belt are strikingly similar. While the lowest group, rich in ultramafic lavas does not always seem to be present, this may be more apparent than real. The existence of such primitive lavas has only been recognized in recent years, in areas where much detailed

mapping and chemical analysis has been performed. Similar basal units may therefore be found in other regions upon further studies. However, the middle and upper groups, in most Abitibi piles, proceed from a platform sequence, of predominantly mafic lavas, to an upper domal sequence of mafic to felsic lavas and pyroclastic rocks, the latter two varieties becoming more abundant with higher stratigraphic position in each sequence.

This upward, stratigraphic progression of rock types toward increasingly differentiated varieties has been well-documented in the Canadian Shield (Goodwin & Ridler, 1970; Goodwin, 1971; Wilson & Morrice, 1977) and in other volcanic belts throughout the world (Windley, 1973; Anhaeusser, 1971; Goodwin, 1971; McCall, 1971; Viljoen & Viljoen, 1969). Abundant information has been gained from the upper parts of these sequences since many domal, felsic pyroclastic-bearing sequences contain a majority of Archean ore deposits. Much work remains to be done, however, to determine the stratigraphy and structure of intervening areas, between volcanic complexes.

8.3 PETROLOGY

Pervasive, low to medium grade regional metamorphism has altered most original mineralogy, in the Bachelor Lake region, to secondary assemblages. These changes make petrographic interpretation extremely difficult and it is

often necessary to rely on normative mineral calculations to establish primary trends. Especially useful in this respect is the ratio of normative quartz to normative olivine, since these calculated minerals are strongly indicative of the extent of fractionation in basalts.

As noted by Turner & Verhoogen (1960, p.209), high SiO₂ and low MgO and alkalies favor the appearance of quartz in the norm. Fractionation along a tholeiitic trend, from MgO-rich to MgO-poor results in the disappearance of olivine from the norm and appearance of quartz. Therefore, the normative quartz/olivine ratio should increase as fractionation progresses. This is in general agreement with discussions by Carmichael, Turner & Verhoogen (1974, p.455), Frey (1974, p.5515) and Ringwood (1975, p.123-138).

The normative quartz/olivine ratios for rocks in the Bachelor Lake Areas, that were classified as basalts using the modified Irvine-Baragar scheme and the Jensen scheme are listed in Table 8.1. Note that the ratios are nearly identical, regardless of the classification scheme used.

8.3.1 Platform Sequence

Basalts toward the base of Area 3, thought to be the oldest lavas in the Bachelor Lake region, are less mafic than the basal sequence of many Abitibi complexes, although, as previously explained, the lowest rocks of this sequence

TABLE 8.1
Quartz-Olivine Normative Ratios For Bachelor Lake Areas

AREAS	MODIFIED IRVINE-BARAGAR CLASSIFICATION	JENSEN CLASSIFICATION		
	Basalt	Fe-Basalt	Mg-Basalt	Av. Basalt
1	3:1	3:1	---	3:1
2	1:1	2:1	1:3	1:1
3	1:1	2:1	1:1	1:1
4	3:1	3:1	4:1	3:1
5	2:1	5:1	1:2	3:1

were not reached. Metamorphic processes have reduced most original mineralogy, with mafic minerals surviving as chlorite-amphibole-sphene masses and plagioclase partially altered to epidote or sericite masses. Relic textures are much less frequently preserved than in some other regions. Observable proportions of mafic to felsic alteration relics, however, indicate that very mafic basalts are common at the base of the sequence but become less mafic upward and begin to include a few intermediate and felsic rocks.

Areas 1 and 2 form a sequence of mainly basaltic and andesitic lavas with mineralogy similar to the central portion of Area 3.

The platform sequence (Areas 1, 2 and 3) has roughly equal abundance of quartz and olivine normative basalts. Both varieties alternate, upward in the sequence, with no particular pattern, thereby suggesting primary magmatic fluctuations. Such alternations may have resulted from varying degrees of partial melting and/or effusion through multiple vents in the thin, unstable Archean crust.

Basalts of Area 1, though near the base of the platform sequence, have an unusually high quartz:olivine ratio. This is probably due to removal of MgO through crystal settling of early-formed pyroxene, which accumulated to form the proxenite bodies.

The preservation of essentially fresh clinopyroxene, seems incongruous in a region which is almost devoid of fresh rocks. The pyroxenites do not possess textures of ultramafic flows, but neither are they necessarily younger than the surrounding volcanics, since contemporaneous ultramafic rocks are known from other, highly altered settings. Imreh (1976, p.62) describes well-preserved ultramafic rocks in the base of the Lower Malartic sequence (Lamotte-Vassan Group) near Val d'Or. A further example is the presence of fresh peridotites and pyroxenites in the highly metamorphosed Thompson belt of Manitoba (Paktunc, 1980, per.comm.). Baragar (1972, p.131) states that mafic sills containing fresh pyroxene and olivine are common in the lower parts of greenstone belts.

Similar differentiation trends are observable in less metamorphically altered platform sequences, such as the Noranda region (Jolly, 1975, 1977; Goodwin et al., 1977; Gelinas & Brooks, 1974). There, olivine and Ca-rich plagioclase appear to be the earliest crystalline phases, followed by clinopyroxene and Fe-Ti opaques. Thus, the liquidus for this platform sequence appears to be olivine and plagioclase, with clinopyroxene and Fe-Ti opaques added when the liquid reaches intermediate composition. Jolly's (1977, p.319) crystallization sequence:

OLIVINE + PLAGIOCLASE; CLINOPYROXENE + OPAQUES;
ORTHOPYROXENE

is supported by experimental phase data on mantle compositions, crystallized at low confining pressures. An extremely significant observation was the fact that, through an increase of only a few kilobars pressure, orthopyroxene becomes an early crystallizing phase and thus lead Jolly to the conclusion that these magmas underwent fractionation at shallow levels (see also: Winkler, 1967, p.131).

8.3.2 Domal Sequence

A dramatic change occurs in the transition from the platform to domal sequences. In addition to their less mafic nature, the basalts are less abundant (see Fig. 5.1) with respect to intermediate and felsic rocks. Extruded with these latter rock types are significant volumes of pyroclastic and brecciated material, indicative of a more fluid-rich magma.

A large increase in the quartz-olivine normative ratio (Fig. 8.1) is evident for basaltic lavas and suggests that this magma is much less enriched in the more mafic components than that of the platform magma.

Mineral data from the domal sequence of the less highly metamorphosed Noranda volcanic complex shows that the

earliest basaltic lavas contain olivine, clinopyroxene, plagioclase and Fe-Ti opaque mineralogy (Jolly, 1977), with orthopyroxene being, again, a late crystallizing phase. Thus, the liquidus for this magmatic sequence appears to be:

OLIVINE + CLINOPYROXENE + PLAGIOCLASE + FE-TI OPAQUES;
CLINOPYROXENE

and is supported by experimental data similar to that in the platform sequence.

The presence of clinopyroxene as an earlier liquidus phase necessitates a higher pressure in the magma chamber (Eggler, 1974). Clinopyroxene, therefore, suggests formation of the magma at deeper levels. This is supported by the pervasive presence of Fe-Ti oxides in all domal sequence rocks, a feature enhanced by high water or oxygen pressures (Osborn, 1962). These oxides are generally absent in the mafic members of the platform sequence, and, taken with other evidence, mentioned above, illustrates the importance of fluid pressure in domal sequence volcanic rocks.

8.4 GEOCHEMISTRY

Chemical variation within the Bachelor Lake volcanic pile is reflected in the petrographic changes, previously described, for specific rock types at various stratigraphic

levels. However, the chemical trends give a more intuitive view of the magmatic evolution and suggest reasons for preferred stratigraphic ore mineralization.

Interpretation of the chemical trends is aided by statistical analysis, especially the data-reducing features of factor analysis. The summary in Table 8.2 was obtained by combining the chemistry and mineral data sets. Many of the component loadings in the summary are the same as when the chemistry was factored separately (Table 8.3), showing that chemistry is dominant in the mineral-chemical analysis.

The component variables are members of the input data which, when sorted by factoring procedures, are ranked into stronger to weaker factors, in the order in which they account for the variability. pattern. They can then be interpreted in terms of geologic significance, which is aided by the offsetting positive and negative correlations in each factor. Percentage of variance, or, contribution of each factor is useful in comparison of similar component variables in the different geographic Areas. Residual factors are those with minor geologic significance but which do account for a small amount of the overall variation.

8.4.1 Platform Sequence

Many platform sequences have recently been subdivided into two major units, a lower, mafic-ultramafic dominated

TABLE 8.2
Factor Analysis Summary - Mineralogy & Chemistry

AREA	FACTOR	CORR.	COMPONENT VARIABLES	GEOLOGIC FEATURE	% of VARIANCE
1			Too Few Cases --- No factors possible		
2	1	+	Fe ₂ O ₃ , FeO, TiO ₂ , Zn	Differentiation	35
		-	SiO ₂ , Al ₂ O ₃		
	2	+	CaO, Co, Ni	Differentiation	20
		-	P ₂ O ₅		
	3	+	Cu, Chlor	Cu-metasomatism	12
		-	Rb		
	4	+	Deform, Fragn	Post-Depositional Tectonics	7
	5-10	+	Ba, Horn, Feld, Carb, Ep	Single Residuals	27
		-	Pyx		
3	1	+	Fe ₂ O ₃ , FeO, MgO, CaO, MnO, Co, Ni	Differentiation	39
		-	SiO ₂ , Feld, Na ₂ O		
	2	+	K, Rb, Altern, Mica	Sericitization	15
	3	+	TiO ₂ , Horn	Differentiation	13
		-	Quartz, Carb		
	4	+	S, Cu, Act	Cu-metasomatism (?)	8
	5	+	Deform, Fragn	Post-Depositional Tectonics	7
	6	+	Ba, Sr	Residual	6
	7-9	+	Zn	Residuals	13
		-	Horn, Ep		
4	1	+	Fe ₂ O ₃ , FeO, CaO, MnO, Co, Ni, Actin	Differentiation	35
		-	SiO ₂ , Na ₂ O		
	2	+	Al ₂ O ₃ , MgO	Differentiation	19
		-	SiO ₂ , Altern, Quartz		
	3	+	K, Rb, Zn	Metasomatism	12
	4	+	TiO ₂ , P ₂ O ₅	Residuals	10
	5-8	+	Ba, S, Sr, Cu, Deform, Fragn	Residuals	21
5	1	+	Fe ₂ O ₃ , FeO, MgO, K ₂ O, MnO, Ni, Co, Altern, Chlor, Quartz	Differentiation	42
		-	SiO ₂ , Al ₂ O ₃		
	2	+	Na ₂ O, Ba, Rb, Sr, Mica	Cu-metasomatism	28
		-	Fe ₂ O ₃ , Cu		
	3	+	CaO, Hbl	Residuals	9
	4	+	TiO ₂ , S	Residual	6
	5-7	+	Deform, Fragn, Actin, Carb	Post-Depositional Tectonics	15

TABLE 8.3
Factor Analysis Summary - Chemistry

AREA	FACTOR	CORR.	COMPONENT VARIABLES	% of VARIANCE
1			Too Few Cases --- No factors possible	
2	1	+	Fe ₂ O ₃ , FeO, TiO ₂ , Zn	47
	2	+	K ₂ O, Ba, Rb	26
	3	+	MgO, CaO, MnO	13
	4	+	MgO, Co	8
	5	+	Cu	6
3	1	+	MgO, Co, Ni	56
		-	SiO ₂ , Na ₂ O	
	2	+	Fe ₂ O ₃ , FeO, TiO ₂ , MnO	
	3	+	K ₂ O, Ba, Rb	
	4	+	S, Cu	
	5	+	Sr	6
4	1	+	Fe ₂ O ₃ , FeO, MnO	45
		-	SiO ₂ , Na ₂ O	
	2	+	K ₂ O, Rb, Zn	
	3	+	TiO ₂ , P ₂ O ₅	
	4	+	Al ₂ O ₃ , MgO	
		-	SiO ₂	12
	5	+	S, Cu	9
5	1	+	Fe ₂ O ₃ , FeO, MgO, CaO, Ni	65
		-	SiO ₂ , Na ₂ O, K ₂ O	
	2	+	Al ₂ O ₃ , K ₂ O, Ba, Rb, Sr	
		-	Fe ₂ O ₃ , FeO, Cu	
	3	+	P ₂ O ₅ , S	10
	4	+	TiO ₂ , MnO, Co	8

(Magnesian) series, and an upper, mafic rich (Tholeiitic) series (Jensen, 1978, 1976; Jolly, 1977, 1975; Goodwin et al., 1977; Arndt, 1976; Naldrett et al., 1976; Nesbitt et al., 1976). While the mineral and chemical differences between these units are not as obvious as the change to the domal sequence, they are, nonetheless, distinct. The changes are usually gradual and somewhat erratic, due to interlayering of rock (basalt-dacite-basalt) and series (tholeiitic, calc-alkaline, etc.) types.

Rocks of the magnesian, basal unit have been described in other regions (Viljoen & Viljoen, 1969; Brooks & Hart, 1974; Arndt, 1976; Naldrett & Turner, 1977; Naldrett & Goodwin, 1977; Arndt et al., 1977) as containing substantial volumes of ultramafic lavas. These flows are characterized by high MgO (10-40%), Ca/Al₂O₃, Ni (>150 ppm), Cr (>150 ppm) and low FeO (10-15%), Al₂O₃ (4-15%), TiO₂ (<1%), FeO/(FeO + MgO) (<0.65) and alkalis (K₂O <0.15%), as well as a characteristic "spinifex" texture. These rocks are further subdivided into basaltic, pyroxenitic and peridotitic, as discussed in section 3.4.8, and form a distinctive field on the Naldrett plot. It has been pointed out that these ultramafic lavas are interlayered with mafic and, more rarely, intermediate volcanic rocks.

In the Bachelor Lake region, no true komatiites have been found (lack of textural criteria) but some very mafic

flows have been found in the basal section of Area 3. These flows have chemistry similar to the least ultramafic komatiite rocks and fall in the "komatiitic" field on the Naldrett plot (Fig. 6.20). Thus, a very mafic-ultramafic base seems to be present, and is supported by the chemical factor analysis (Tables 8.2 and 8.3) for Area 3. There, the mafic components in Factor 1 (MgO, Ni, Co) are inversely correlated with felsic components (SiO₂, Na₂O) and account for over half the total variance.

Slightly higher in the stratigraphy (i.e. central Area 3, and Area 1), and interlayered with the sequence described above, rock chemistry changes to a more iron-rich, magnesium-depleted composition, characteristic of the tholeiitic magma series. Here, MgO has decreased (4-10%), in the mafic rocks, while FeO (12-18%), TiO₂ (>1%) and alkalis (K₂O = 0.15-0.35%) have all increased with respect to the magnesian sequence. Al₂O₃ remains fairly constant (10-14%), except for the ultramafic bodies in Area 1. The transition to a tholeiitic trend is confirmed by chemical factor analysis (Fig. 8.2 and 8.3) in Area 2. FeO-TiO₂ have become accountable for a far greater proportion of the total variance than in the more mafic-ultramafic components, such as MgO, Ni and Co. These changes can be explained by either magma fractionation, or lower degree of partial melting.

The compositions for rocks in Area 2 agree well with values listed for tholeiitic sequences in the references cited above. They are indicative of relatively primitive magmatic material. In addition, trace element compositions have also changed, usually following the tendency of ionic substitution for major elements. Thus, Ba and Rb increase following large cations such as K₂O; Zn, Cu and S increase, probably as independent sulphides, and Ni and Co decrease, mirroring the MgO decline. Unfortunately, many studies fail to include trace element information making comparative data relatively scarce. Limited published trace element information (Baragar, 1977; Goodwin, 1977; Larson & Webber, 1977) tends to confirm the platform data.

Several authors (Jensen, 1976, 1978; Jolly, 1975, 1977; Church, 1975) have disparaged the use of alkali values in variation diagrams as well as in general geochemical trends, citing high elemental mobility. The low and constant alkali values in these mafic lavas preclude their contamination by seawater reaction or metamorphic mobilization. Conscientious sampling techniques on large numbers of specimens eliminates this problem, except for very local, isochemical changes.

Workers harbouring an alkali anxiety may prefer a diagram excluding these phases, in lieu of the "more stable" elements. Both the Naldrett and Jensen diagrams (Fig. 3.5

and 3.10) are useful for this purpose, the former being more suitable for mafic and ultramafic volcanic rocks. The value of such diagrams in evaluation of stratigraphic field data is well illustrated by the plots in Chapter 6 and by a comparison with similar volcanic complexes in other regions.

Such diagrams are available for the Noranda complex (Fig. 8.2). There, a majority of data points from the basal, magnesian suite (i.e. Munro-Bowman-Hwyll groups) fall in the "komatiitic" field, with the few interlayered tholeiitic rocks lying in the tholeiitic to intermediate basalt fields. Basalts in the upper platform sequence (i.e. lower Garrison Group) fall in the tholeiitic to intermediate field, while the highest platform stratigraphy (i.e. upper Garrison Group) contains considerably more intermediate and numerous alumina-rich rocks. This progression in the platform sequence forms a dramatic illustration of the major chemical trends involved in the MgO to FeO-rich and finally independent, Al₂O₃-rich transitions. Similar, although less detailed results have been documented for other Archean platform sequences (see Fig. 3.6). Naldrett plots for the Bachelor Lake platform (Fig. 6.11) are also strikingly similar to the Noranda complex, except for the minimal magnesian suite.

Rocks of the platform sequence, Areas 1, 2 and 3, form a unimodal SiO₂ distribution, strongly skewed to the left

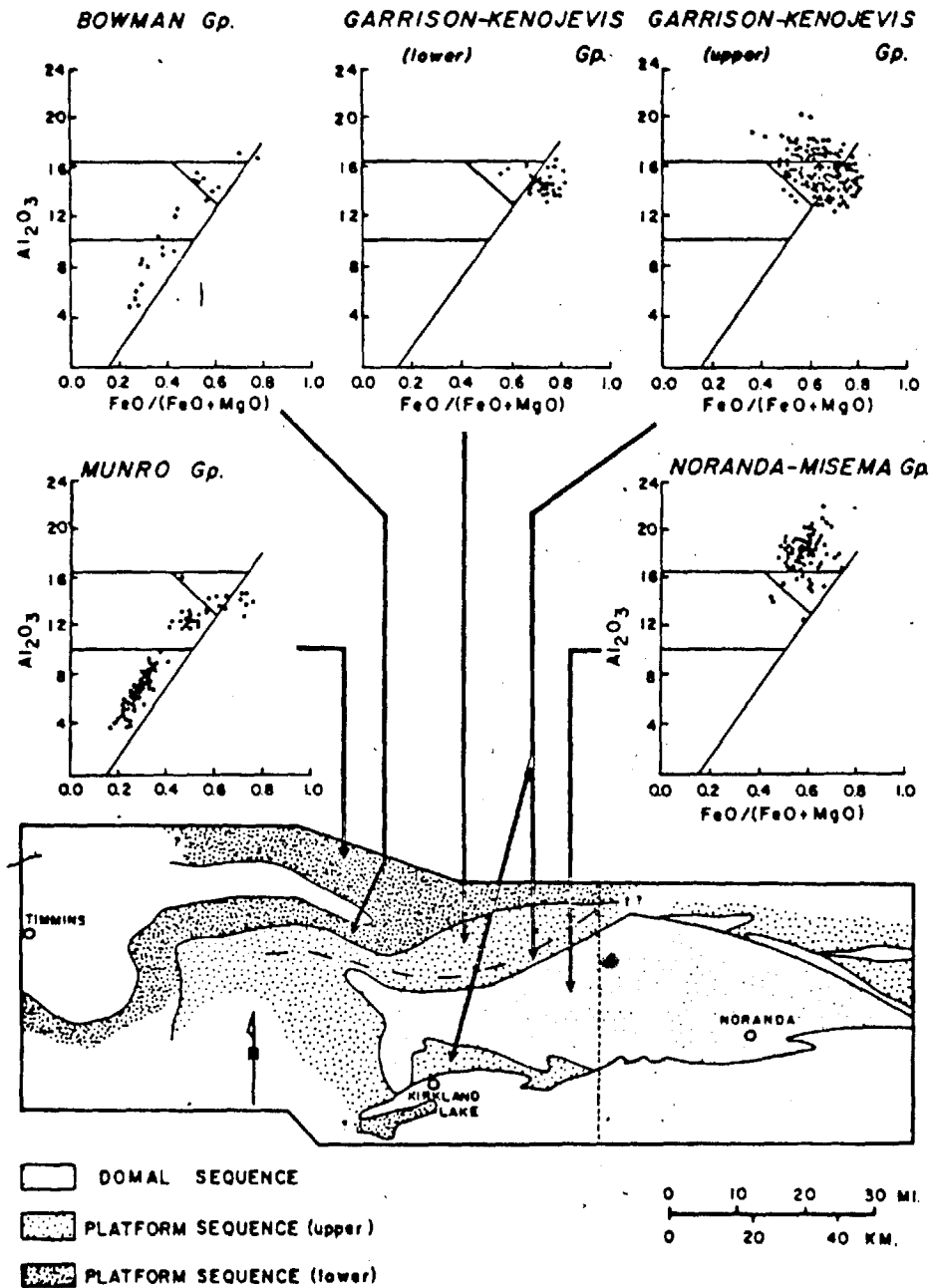


Figure 8.2: Major Chemical Trends in the Noranda Complex

(Fig. 8.3 A). In this respect, it is similar to other platform sequences, such as the average Abitibi groups and the Proterozoic Burin Group of Newfoundland (Fig. 8.3 C,D). These lognormal distributions are common in such primitive volcanic piles which contain a predominance of mafic-ultramafic rocks.

8.4.2 Domal Sequence

Rocks of domal sequences are perhaps the best documented of any Archean strata, since they contain the majority of economic mineralization. The transition from tholeiitic rocks of the upper platform sequence is suddenly apparent in the calc-alkaline dominated chemistry, but as in the lower stratigraphic sequences, some interfingering (in this case with tholeiitic flows) is maintained. These chemical trends are overshadowed, to some degree, by the increased abundance of intermediate to felsic rock types. However, the changes are most apparent when considering basalts, thereby allowing comparison with lower sequences.

Most noticeable is the cessation of the tholeiitic, iron-enrichment trend. In fact, averages of both iron (11-12%) and magnesium (5%) decrease considerably in these basalts, with a slightly smaller Fe/Mg ratio than in the tholeiitic sequence. A further important change is an increase in alumina (15-17%) and alkalies ($K_2O > 0.50\%$).

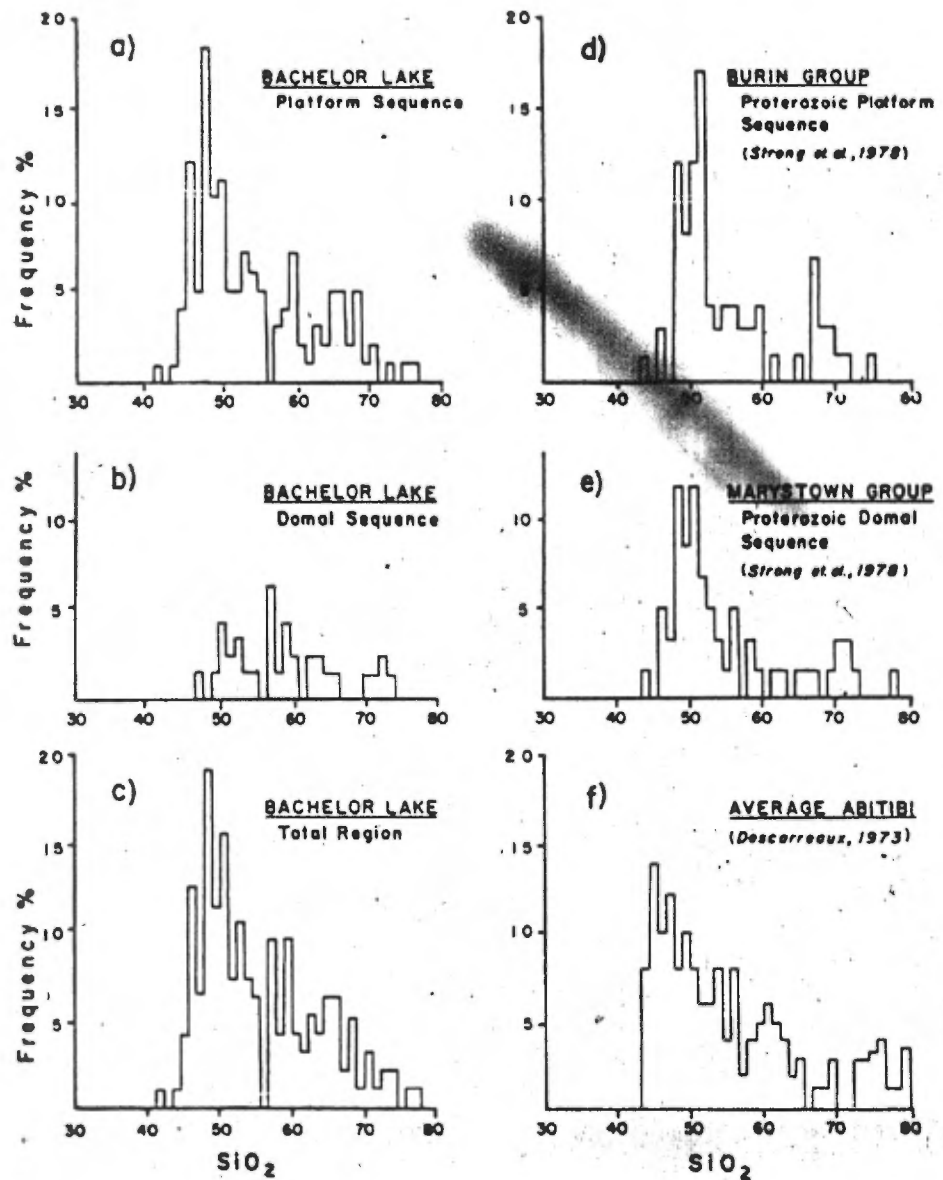


Figure 8.3: SiO₂ Frequency Distribution for Selected Volcanic Sequences

relative to both iron and magnesium. These trends are clearly shown on the AFM and Naldrett plots in Chapter 6 and result in continental classification on the Pearce plot. Alkali values in basalts of the domal sequence continue to increase from the base to the upper strata. Trace elements closely follow major element trends, with Ba (>200 ppm) and Rb (>20 ppm) increasing with K₂O.

Factor analysis component groupings (Tab. 8.2 and 8.3) show that the FeO-TiO₂ dominance, present in the upper platform sequence, is considerably reduced, with FeO now a substantially weaker component loading and TiO₂ shifted to a third factor of minor significance. As in the lower sequences, differentiation is still the most important factor, governing about half the overall variation.

Silica distribution for rocks in the domal sequence (i.e. Area 4 and extreme upper Area 3) forms a unimodal pattern, very slightly skewed to the left (Fig. 8.3 B). The lower frequency of mafic rocks questions the method of sampling and stratigraphic division, since some other areas, such as the Proterozoic Marystown Group of Newfoundland (Fig. 8.3 E) retain logarithmic distribution for the domal sequence. However, the unconformity between the Bachelor Lake platform and domal sequences seems to be a logical stratigraphic division, and sampling procedures were carefully standardized.

These features all suggest that the domal sequence is a more evolved, primitive-continental sequence, containing increased volumes of intermediate and felsic rocks. It is similar in chemistry to other Abitibi regions including Noranda. Figure 8.2 shows the lower Fe/Mg ratio and higher Al₂O₃ distribution of Blake River (Domal) basalts, relative to the corresponding platform sequence.

8.5 A MODEL FOR THE EVOLUTION OF THE BACHELOR LAKE REGION

8.5.1 The Crust in the Early Archean

The nature of pre-greenstone terrain is controversial and poorly defined. It is a subject beyond the scope of this study, but is important in considerations of the tectonic evolution of these volcanic belts. Many authors, particularly those in the northern hemisphere (Windley & Bridgewater, 1971; Goodwin, 1972; Windley, 1973; Kroner, 1976; Bald, 1977; Baragar & McGlynn, 1977; and Gorman et al., 1978) have provided convincing arguments that the early Archean crust (i.e. 3.8 - 3.5 by) developed an upper sialic layer upon which the younger (i.e. 3.5 - 2.5 by) volcano-sedimentary sequences were deposited. The older units are preserved as high-grade tonalitic gneisses/plutons and amphibolites, due to polycyclic mobilization. Thus, the basic assumption for the model of greenstone belt evolution, proposed herein, is that the crust contained an extensive sialic component at the time of greenstone deposition.

Another, commonly accepted assumption, is a much thinner crust than in later eras. This crust was rendered fairly supple by its lesser thickness and by the greater heat flow due to radioactive and gravitational energy releases. The formation of granite-greenstone terrains may have helped to decrease the upper geothermal gradient, allowing a more stable thickness of crust.

8.5.2 Greenstone Belts

Any model proposed for the formation of greenstone belts must account for common features found in these supracrustal regimes throughout the world. It must, however, be flexible enough to allow the inherent differences in each belt.

Most greenstone belts consist of distinct metavolcanic and metasedimentary assemblages as previously described. The sequence of a magnesium-rich, sometimes komatiitic, basal member, overlain by a tholeiitic group and followed, in turn, by a calc-alkaline upper group is extremely common but is not found in all regions due to incomplete preservation of the volcano-sedimentary pile. The proportion of sedimentary rocks is variable, forming narrow horizons in some regions and major belt components in others. The supracrustal units form synformal structures which lie between extensive granite and gneissic bodies.

8.5.3 The Model

8.5.3.1 Creation of a Platform Sequence

Mafic and ultramafic volcanic rocks, present in the lowest part of greenstone cycles were probably erupted through a tensional fracture in the primitive crust, with distribution of fissures controlling the geometry of surface volcanism. Few fissures would provide a low shield volcano due to the very low magmatic viscosity, interflowing with other volcanoes produced some distance away. More abundant local fissures would produce greater volumes of lava and thus increase the vertical thickness of the pile. Composition of these initial flows would depend upon the depth of rifting (i.e. depth of tapping into and composition of that part of the upper mantle), the degree of partial melting, and the speed of ascent and level of emplacement of the magma.

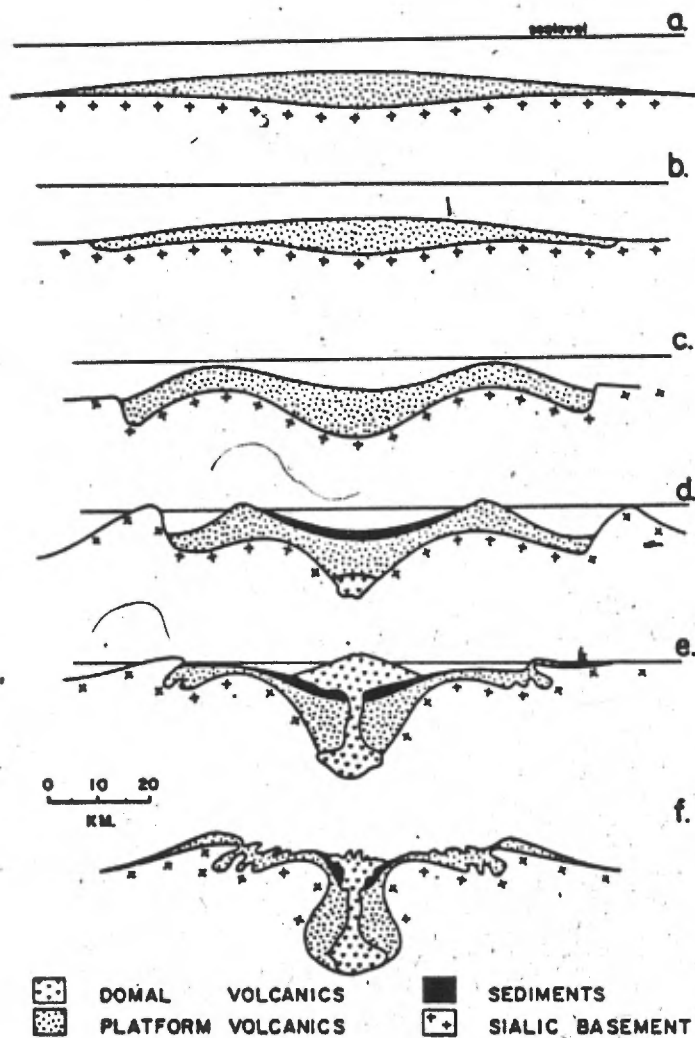
Due to the greater density of mafic-ultramafic rocks (SG = 2.9 - 3.3) overlying the presumed sialic crust of tonalitic composition (SG = 2.7) some depression of the crust must have inevitably occurred via gravitational forces. Greatest depression would occur closest to the centers of volcanic effusion, thereby keeping the rift active. A buildup of material at the outer edge of the volcano (and possibly from nearby volcanoes) may have caused marginal subsidence. Continued subsidence of the central portion of the pile, due to additional volcanic

accumulation, would result in further weakening of the basement and creation of a central basin. This situation represents the tectonic regime in effect during the formation of the lower, platform sequence in the Bachelor Lake region (Areas 1, 2 and 3).

Evolution of the greenstone belt, to this point, is similar to that envisaged by Gorman et al. (1978) in the early stages of their model (Fig. 8.4). Their discussion, based upon the tectonic-density modelling of Ramberg (1971, 1973), indicates that the marginal subsidence of the complex caused centripetal and upward mobilization of the basement into plutonic domes. These tonalitic plutons could be generated by partial melting of garnet-amphibolite/eclogites or from remobilized crust.

Further central subsidence would lead to some degree of lateral shortening and a steeper topographic gradient toward the center of the basin. The depression of a thick pile (10-15 km) of dense volcanics, as well as the underlying sialic basement, into the deeper crust may account for the hiatus in volcanic activity.

This cessation of volcanism, as described in section 5.3.3. is shown initially by the appearance of thin-bedded chemical sediments, intercalated with tholeiitic volcanics and finally a 1-2 km. thick clastic wedge. The wedge, found in NW and SW Lesueur Township, on either side of the



- a) Subaqueous deposition of Platform sequence volcanics.
- b,c) Additional volcanic accumulation and depression of the pile via gravitational instability. Note lateral shortening and progression to shallow water deposition.
- d) Erosion of exposed landmass to produce elastic wedge. Base of pile is further depressed and partially melts to form a calc-alkaline magma. Note lateral compression.
- e) Continued partial melting forms more magma and creates the Domal (subaqueous and subaerial) sequence. Lateral compression continues.
- f) Final tectonic expression (i.e. pre-erosional surface).

Figure 8.4: Schematic Illustration of Greenstone Belt Evolution (mod. after Gorman et al, 1978)

regional synclinal axis, has been noted to pinch out east and west. Deposition of such coarse clastics, including cobbles and boulders of granitoid composition, implies a reasonably close source area, with deposition aided by the steeply sloping central basin. The elongate nature of the clastic wedge suggests that the original basin was elongated in a NE-SW direction, since there is no indication of later structural elongation.

8.5.3.2 Creation of a Domal Sequence

Depression of supracrustals and underlying sialic basement into deeper crustal regions eventually leads to their melting and remobilization. This activity forms the "inverted-mushroom" of Gorman et al. (1978), causing the partial melting of garnet-amphibolite at depth, thereby producing calc-alkaline volcanism within the center of the basin (see Yoder & Tilley, 1962; Green & Ringwood, 1966, 1967; Best, 1969; Green, 1972; Cawthorn & O'Hara (1976)). This does not imply that volcanism becomes entirely calc-alkaline, for tholeiitic lavas continue to be extruded and intercalated. Rather, extrusives of calc-alkaline volcanics, andesites in particular, become more frequent and volumetric components of the pile. As the calc-alkaline magma differentiates, felsic rocks, including pyroclastic varieties, become more abundant.

Late plutonic rocks are also products of the calc-alkaline magmas. In the Bachelor Lake region, these include synorogenic gabbro bodies in eastern and western Lesueur Township and late granitoid bodies near Bachelor and Billy Lakes (Map - rear pocket). Gorman et al. (1978) suggest that contemporaneous basement uplift forms large plutonic structures (the "gregarious batholiths" of MacGregor, 1951) which further compress the volcanic pile and, through erosion, provide detrital sediments to the central basin. The present study, however, indicates that some basement remobilization began earlier than their proposed final stage, since much sedimentary detritus was transported before and during the early stages of calc-alkaline volcanism.

8.5.3.3 Evolution of Greenstone Belt Magmatism

Archean volcanic complexes display the same magmatic progression, from magnesian to tholeiitic to calc-alkaline, in the evolution of the Bachelor Lake and other volcanic piles. While not completely preserved in all regions, the transition is ubiquitous, and evidence for a genetic link between the magmas must be considered.

The magnesian magmatic series is always oldest and production of such lavas requires a high degree of partial melting in the mantle (Viljoen & Viljoen, 1969; Green, 1972, 1975; Brooks & Hart 1972, 1974). It is difficult, however,

to bring a peridotitic magma to surface without crystallization, since the liquidus phases would constantly struggle to separate.

Melting could be achieved at 1600-1700°C under deep level (200 km), anhydrous conditions (Arndt, 1976; Wyllie, 1971) and must then rise adiabatically to crustal levels. The instigating factor for the initial melting is controversial and suggestions have included removal of crustal material and shock penetration of the mantle by meteorite impact. Timing of major meteorite showers is somewhat displaced from the period of Archean ultramafic production, however (Naldrett, 1973) and a more plausible explanation may be melting over conductive mantle plumes and subsequent rift-tapping (Naldrett and Turner, 1977, p.90).

The need to retain a proportion of the ultramafic cumulus, lest the magma fractionate to a mafic composition, requires rapid and probably turbulent ascent. To this end, several authors (Green, 1972, 1975; Brooks & Hart, 1972, 1974; Arndt, 1976; Naldrett and Turner, 1977) have proposed a diapiric ascent of the magma. Naldrett and Turner (1977, p.92-95) have produced convincing arguments that the process must include a multi-stage or possibly continuous removal of interstitial liquid, thereby removing garnet, the densest phase, and extruding basalt. This, in addition to the high temperature, maintains positive buoyancy and allows the melt

to rise near surface where it consists of 65-70% olivine crystals and 30-35% melt. Future studies expanding on sketchy rare-earth trace element data (see Sun & Nesbitt, 1978; Hawkesworth & O'Nions, 1977; Naldrett & Turner, 1977; Nisbet et al., 1977; Condie, 1976) may improve this part of the model.

It is unclear if the ultramafic magmas described above are parent to the overlying tholeiitic sequences (once fractionated), but it is a strong possibility for at least part of the sequence, once the ultramafic components are extruded. Few ultramafic flows occur in the tholeiitic sequence, suggesting a cessation of ultramafic volcanism. However, ultramafic intrusions, such as the bodies in Area 1 at Bachelor Lake, may be connected to the once-diapiric chambers. In any case, new tholeiitic magmas are probably added to the volcanic regime, as discussed in section 8.3.2. Gravity subsidence of the basinal structure would carry partially hydrated crustal material a short distance into the crust where a relatively low degree of partial melting would produce tholeiitic magma (Kushiro & Yoder, 1969). Major element and mineral composition of this material should be fairly close to that of the final, fractionated stage of the magnesian magma. Studies of rare-earth element data may, again, prove useful in delineating parentage of these rocks.

One parameter of tholeiitic lavas in the Abitibi belt is quite certain: the lavas fractionated at shallow depth (Naldrett, 1970; Baragar, 1972; Jolly, 1972, 1975). The latter author explains this phenomenon by the absence of early orthopyroxene. Abundant experimental evidence indicates that pressure above a few kilobars precipitates this phase at an early stage of fractionation (see also: Winkler, 1967, p.131).

Transition to the calc-alkaline magmas, dominant in the domal sequence, has been described in previous sections as sudden and distinctive. One reason for the rapid change in the Bachelor Lake region is that, during transition of the magma series, a hiatus in volcanism occurred and may therefore have limited transitional lavas. This cessation is marked by the clastic sedimentary wedge, described in Chapter 5.

It must be remembered that the central Basin continued to subside, as discussed in previous sections, bringing quantities of hydrous supracrustals deeper into the crust. Higher water content in these rocks allows considerably lower melting temperatures and decrease in the degree of partial melting. It would be expected, therefore, that all rock types would be less mafic (i.e. lower FeO, MgO; higher Al₂O₃, alkalis) than the platform sequence.

The increased water content in calc-alkaline magmas has further importance since it leads to termination of the iron-enrichment trend present in the tholeiitic series. Jolly (1975,1977) cites experimental evidence that higher fO_2 allows rapid production of Fe-Ti oxides, yielding Fe depleted liquids. In addition, consumption of Fe by clinopyroxene also prevents iron-enrichment. Additional evidence for the increased water content in the magma is provided by a parallel increase in more felsic and pyroclastic rocks.

Chemical trends on most variation diagrams provide relatively smooth curves for many elements. For example, Al_2O_3 and alkalis tend to increase for each rock type, at higher stratigraphic levels, while MgO , Ni and Co correspondingly decrease. These patterns suggest magmatic evolution but are complicated by the interfingering of both rock and magma series types, especially near the contacts of the three main sequences. This is true even for detailed, small-scale, petrochemical studies such as that of Larson & Webber (1977) in the central part of the Noranda region.

Growth of the pile is thus gradational and, rather than the evolution of a particular magma, the volcanic complex is seen as a progression in vertical tectonic style, possibly with numerous volcanic sources of one or two magma series operating concurrently. Naturally, these developments are

preserved only because of increased stabilization of the crustal structure.

8.5.4 Structural Features of Greenstone Belt Orogenesis

Orogenic processes during late-stage formation of greenstone belts placed severe strain upon the supracrustal rocks and some evidence of adjustment to those forces has been preserved. Explanation of these tectonic features helps to interpret present relationships within the belts.

The orogenic modelling experiments of Ramberg (1971, 1973) have shown that, for the conditions previously cited, most forces are compressive. Basement mobilization at the margins of the belt are most intense, with the strain released in recumbent folds and, finally, high angle thrusting along bedding planes. The degree of thrusting is dependent upon the magnitude of marginal mobilization but is always directed to the center of the synclinal pile.

Faulting appears in Area 3 of the Bachelor Lake region, where it is displayed by the regularity of the Opavica Lake drainage system, parallel to the bedding. These were originally considered strike-slip faults, until petrochemistry revealed the area as the most mafic suite in the entire study region. This was surprising in view of its close position to the regional synclinal axis. In the central part of the region (Area 4), similar stratigraphy

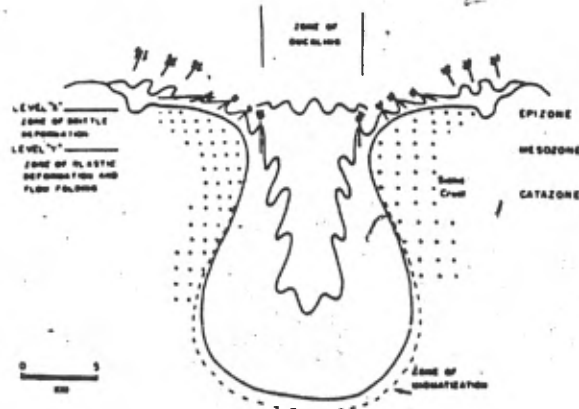
occurs on both sides of the axis, whereas in the east, the predominantly tholeiitic lavas of Areas 1 and 2 are mirrored by a much more mafic sequence in Area 3. The hypothesis of northward thrusting in the latter is supported by a few narrow bands of calc-alkaline andesites within the predominantly magnesium-rich basalts. These andesites are interpreted as remnants of higher stratigraphic slices caught up in the displacement. The northern limit of thrusting occurs at the Gand-Lesperance township boundary, north of which stratigraphy appears very similar to Area 4 to the west. These include the characteristic felsic lavas and pyroclastics as well as calc-alkaline intermediate lavas. The entire sequence, however, appears displaced to the north by NNW-trending faults.

Toward the center of the volcanic pile; the compressive forces were less severe and are represented by less intense isoclinal folding. Several minor synclinal features are shown in the map in the rear pocket. Annhaeusser (1974) suggests that, in this part of the tectonic regime, high angle thrust faults tend to shear out anticlines. The degree of isoclinal folding is more apparent in detailed underground structural mapping at the Coniagas minesite (Fig. 7.1).

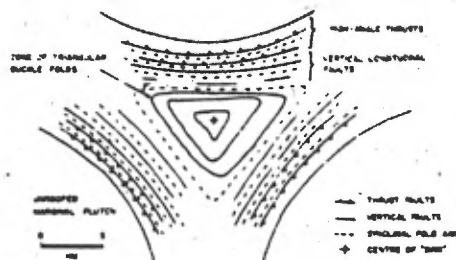
A schematic illustration of this type of orogeny (see Fig. 8.5) is provided by Gorman et al. (1978), and suggests

the appearance, in plan, of greenstone belts eroded to various crustal levels. The plans involve a high degree of basement mobilization, perhaps similar to some of the arcuate belts in the western Superior Province. However, allowing for a less intense deformation, as in the Abitibi belt, they do resemble some of the features of the Bachelor Lake region. Similar structural features have been reported by Wilson et al. (1977, p.361) in the western Superior Province.

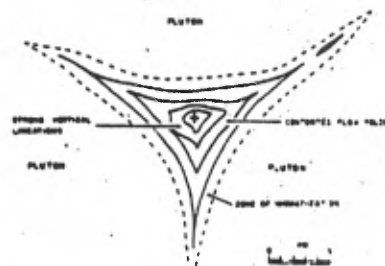
Gorman et al. (1978, p.33) state that thrusting in greenstone belts is rarely reported, but do cite a few worldwide examples, including two in the western Superior Province. An indication of thrusting in the Noranda region (Cadillac break) is also mentioned. It is proposed by Gorman that both the Porcupine-Destor and Larder Lake-Cadillac fault systems represent similar high-angle thrusting since both systems dip steeply toward the center of the basin (Jolly, 1975, p.201). Other, possibly similar, systems in the Abitibi belt are illustrated (Fig. 8.6) by Kalliokoski (1968) and Jolly (1976). The lack of recognition of these systems as gravity-induced, thrust sheets may lie in the absence of detailed structural mapping and scarcity of petrochemical evaluation of the stratigraphy.



1. Structures expected near the centre of the subiding greenstone belt. The attitude of faulting changes from high-angle reverse to subvertical and longitudinal near the central "sink". Buckling may be present in the upper sequences of the greenstones. At depth, plastic deformation predominates.



2. Plan view of level "X" in 1 after basement remobilization showing the original symmetry of the greenstone belt due to "claw-pot" plutons, which are partially unroofed. Due to faulting, synclines predominate in the greenstones, giving way to a zone of triangular buckle folds above the "sink".



3. Plan view of level "Y" in 1 after basement remobilization. At this level (near the cataplexis) the rocks are metamorphosed to amphibolite-facies with antiform flow-folding and prominent vertical lineations. The margins of the greenstones have reacted with the surrounding plutonic material to form a zone of megacrysts.

Figure 8.5: Structural Features formed by Greenstone Belt Orogenesis (after Gorman et al, 1978)

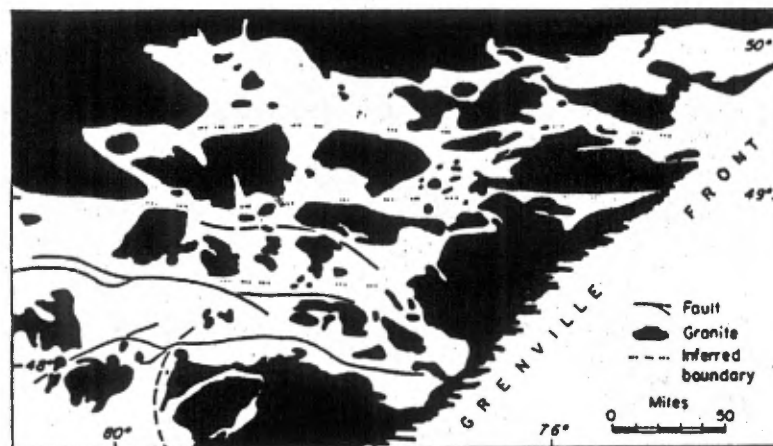
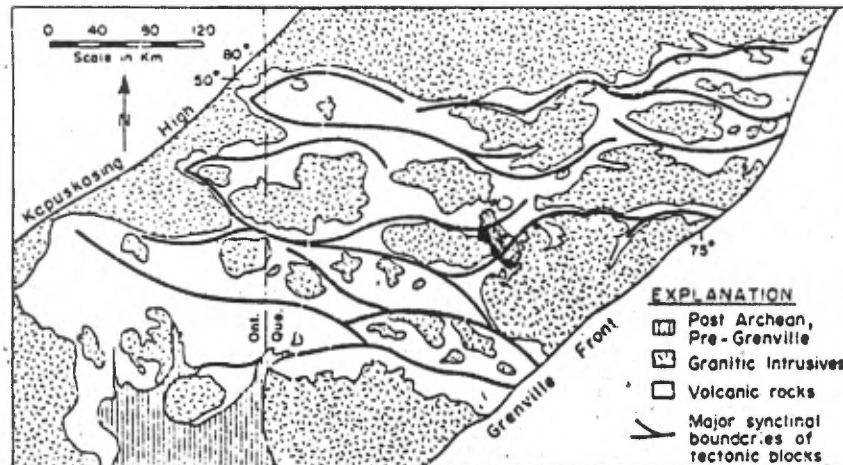


Figure 8.6: Major Fault Systems in the Abitibi Belt a) Jolly, 1976 b) Kalliokoski, 1968)

8.6 RELATIONSHIP OF OREBODIES TO ARCHEAN VOLCANIC BELTS

8.6.1 Ore Deposits of the Lower Platform Sequence

Major occurrences of Ni-sulphides have been documented, in recent years, as intimately associated with specific host rocks (Eckstrand, 1972; Naldrett, 1973; Arndt, 1976, 1977; Naldrett & Turner, 1977; Arndt et al., 1977; Wilson et al., 1976, 1977). Although they may occur in a wide variety of tectonic environments (Naldrett, 1973), a majority of important Ni-sulphide concentrations in Archean greenstone belts are found within lower platform sequences, and, in particular, with the most ultramafic rock types. These are the ultramafic bodies of Naldrett's class 1-(ii), occurring in "orogenic belts" and tied to contemporaneous, eugeosynclinal volcanism (i.e. prior to major folding). The scarcity of ultramafic rocks in the Bachelor Lake region virtually precludes this ore type, but their common presence in other regions makes them an important feature in greenstone belt evolution.

Potential reserves of this type of ore are provided by Naldrett (1973, p.4-6) and illustrate the superior volume of production plus reserves in the Australian and South African shields, with respect to the Canadian shield. The reason for this disparity must be investigated, in view of the apparently common occurrence of suitable rock types and magnesian sequences in Canada.

One strand of evidence for the lack of major Canadian nickel deposits of this type is provided by an observation of Arndt (1976, p.647). He states that, although the mafic-ultramafic rock assemblage of Munro Township has many similarities to those of regions with Ni-sulphides, no ultramafic rocks with greater than about 36% MgO are present. Numerous references are cited and show that highly olivine-rich rocks are host for most of these deposits, especially those of the Eastern Goldfields region, in Australia (see Naldrett & Turner, 1977). Naldrett & Gasparri (1971) and Eckstrand (1972) describe some of the small, Ni-sulphide bodies in the southern Abitibi belt and, while relating that some of these have nearby spinifex-textured flows, all the sulphides are contained in the more massive ultramafic bodies, as basal intercumulus depositions. However, little published whole-rock geochemistry is available for these host rocks. The nature of the metal-host association must lie in the formation of highly ultramafic lavas.

Most Ni-sulphide deposits are considered to form from emplacement of a sulphide magma, generally in intimate association with an ultramafic host silicate melt. Assuming that the sulphur is derived from a primary mantle source, it would be necessary to tap (see subsection 8.5.3.3) deep nickel and sulphur bearing levels (300+ km). This can be achieved only by a deep, 50-70% partial melting of pyrolite

(primitive mantle composition - Green & Ringwood, 1967) and long, adiabatic rise before separation of the partial melt and refractory residuum. Lesser partial melting (30-40%) or higher crustal melting would produce only a basaltic magma (Green, 1972; Naldrett, 1973), incapable of Ni-sulphide mineralization. Arndt (1976, p.650) cites evidence that the Munro lavas were, in fact, of initial pyroxenitic composition. This could have resulted from either a lower degree of partial melting or fractionation of the olivine-rich magma, but, in any case, they were more evolved than the peridotitic magmas associated with Ni-sulphide deposits. High degrees of partial melting, following a rapid diapiric rise will ensure a molten state for the sulphides, thereby allowing their solution in the silicate melt and eventual co-effusion. It is probably the original depth of diapir formation and subsequent rapid ascent to surface that determines if a magma will contain suspended Ni-sulphides.

It has been suggested (Naldrett, 1973, p.10) that the preponderance of Ni-sulphide ores in the Archean and early Proterozoic was caused by sulphur depletion of the mantle during these eras. Sulphides present would tend to concentrate in partial melts, leaving a sulphur-depleted mantle after successive partial melting. In a similar context, it may be useful to note that greenstone belts with larger and more abundant Ni-sulphide deposits (Australia, South Africa) have been noted to form earlier (3.0-3.5 by)

than the less Ni-rich Canadian belts (2.7-2.9 by), possibly resulting from this time-oriented sulphur depletion.

A useful indicator of potential mineralization in these mafic-ultramafic sequences lies in metal ratios of the host rocks (Table 8.4). Average $\text{Cu}/(\text{Cu}+\text{Ni})$ ratios associated with Naldrett's class 1-(ii) bodies are very low (Australia: 0.062; Rhodesia & South Africa: 0.048), reflecting the primitive, magnesium-rich host magmas. The tendency for this ratio to increase in rocks from peridotite to norite is well known and may therefore be a gauge of magmatic evolution. For instance, the less primitive nature of the Munro Township sequence has a strikingly higher ratio (0.226) and is even higher for more evolved (i.e. less ultramafic) bodies (Naldrett, 1973, p.4-6). Metal ratios for rocks hosting small, Canadian Ni-sulphide deposits of this type have not been published. The increasing importance of copper, relative to nickel, in less ultramafic bodies is supported by a few small Cu-Fe sulphide bodies (e.g. Potter and Potterdoal mines in Munro Township) in some lower platform sequences.

Significance of the above discussions to the Bachelor Lake region may be questioned, in view of the previously mentioned scarcity of ultramafic (i.e. lower magnesian suite) rocks. However, a few specimens collected in the lowest stratigraphic units of Area 3 are chemically

TABLE 8.4
Selected Metal Ratios for Potential Host Rocks of Ni-
sulphide Deposits

AREA	Cu/Cu+N1	Zn/Zn+Cu	Cu	N1	Zn
1	0.432	0.622	70	92	115
2	0.468	0.642	73	83	131
3	0.210	0.681	44	166	94 ^m
4	0.171	0.885	21	102	161
5	0.514	0.610	93	88	146
Bach. Lk. Average	0.361	0.683	60	106	129
E. Goldfields *	0.062				
S. Africa *	0.048				
Av. Abitibi *	0.226				
* Naldrett (1973, p. 4-5)					

equivalent to basaltic komatiites and thus have mafic-ultramafic affinities.

Mean basalt values for Area 3 (Table 6.1) are the most mafic (i.e. high MgO, Ni, Co, CaO, Sr; low FeO, TiO₂) in the region. This is supported by the strong component loadings of these elements in the chemical factor analysis (Tables 8.2 and 8.3). Of particular importance in the factored chemical components is the very high proportion of variance (within the first factor) of Ni and Co, with subordinate Cu (factor 4) and residual Zn. Furthermore, Cu/(Cu+Ni) ratios in Area 3 basalts (Table 8.4) are lower than anywhere in the platform sequence and similar to Naldrett's values for lower Abitibi sequences. They are probably too high to be significantly nickel-bearing, but are important in that they increase upward in the stratigraphy and thus indicate an evolving magma.

Features described above for the lower Bachelor Lake stratigraphy provide evidence of a magnesian sequence which has been encountered at the lowest stratigraphic level in the present study. Future mapping may encounter deeper levels in the pile and further delineate this sequence.

8.6.2 Ore Deposits of the Upper Platform Sequence

Metallic mineral concentrations in the thick, predominantly tholeiitic volcanic successions of the upper

platform sequence rarely form economic mineral deposits (Wilson, 1976, 1977). Reasons for this may include the low volatile content of magmas and lack of localized heat sources near surface, resulting in the absence of an enduring geothermal system.

The transition from ultramafic volcanism in the lower platform sequence to mafic effusion in the upper platform sequence removes the availability of nickel sulphides, as discussed in the last subsection. Tholeiitic volcanism may result from either fractionation of the previously formed ultramafic magmas, or lesser degree of partial melting to produce new magma sources (or a combination of both). In any event, deep mantle tapping does not occur. Conversely, the volcanic pile has not evolved sufficiently to produce deposits as found in the upper, domal sequence.

Mean basalt values for Area 2 (Table 6.1) show that, relative to the lower platform sequence, nickel has decreased but both copper and zinc are significantly increased. Similar conclusions are provided by the $Cu/(Cu+Ni)$ ratio (Table 8.4) which is higher for Area 2, thereby revealing a more advanced magmatism. Increases in both zinc and copper maintain $Zn/(Zn+Cu)$ ratios at levels similar to the lower platform sequence.

Support is lent to these trends by chemical factor analysis (Tables 8.2 and 8.3). It is significant that

nickel and cobalt have fallen from the first to second factor, while zinc has become one of the component variables in the first factor. Copper, however, seems to be a residual factor. Both copper and zinc tend to increase upward in the stratigraphy of Area 2.

Explanation of the trends, described above, can be found in the nature of magmatic evolution of upper platform sequences. As explained in section 8.5.3, density inversion created by mafic-ultramafic rocks of the lower platform sequence would cause a depression of the upper crust into the lower crust and upper mantle. Partial melting would then produce basaltic magmas. Since the crust, at this time, had presumably evolved to some degree of sialic geochemistry (see section 8.5.1), zinc and copper, among other elements, would be expected in greater abundance in the newly-formed magmas. Increases in abundances of these elements would be expected as increasing volumes of material were added to the pile, thus continuing subsidence and the recycling process.

The above process is gradual, however, with no mechanism available to concentrate the metals. Only a few minor ores are formed, such as the Maybrun deposit, Ontario (Wilson et al., 1976, p.14). There, chalcopyrite occurs interstitially to basalt pillows. Other, minor concentrations are present in upper platform sequences as

scattered showings and prospects of sub-economic importance (see Grenier, 1967; Duquette, 1970). Further evolution of the volcanic complex is required to concentrate these elements.

8.6.3 Ore Deposits of the Domal Sequence

8.6.3.1 Introduction

Ore deposits accompanying the transition to the dominantly calc-alkaline volcanism in this sequence would be expected to be markedly different from those of the lower magnesian and tholeiitic-rich volcanism and associated tectonics. Here, the metals which became increasingly abundant, upward in the platform sequence (Zn and Cu, among others) become sufficiently concentrated, for the first time, to form massive sulphide deposits. These are represented, in the Bachelor Lake region, by the Coniagas orebody and, with less certainty by the Soquem prospect. It is proposed that this final stage of greenstone belt evolution is essentially a recycling stage, possibly begun in the upper part of the platform sequence, and concentrating, by hydrothermal leaching of previously formed crustal material.

8.6.3.2 Coniagas Massive Sulphide Deposit

Common features of this type of ore deposit have been well documented (Hutchinson, 1973, and others 1971, 1973;

Sangster, 1972, 1980; Mennard, 1973; Spence, 1975) and only a brief review is necessary for comparison with the Bachelor Lake ores:

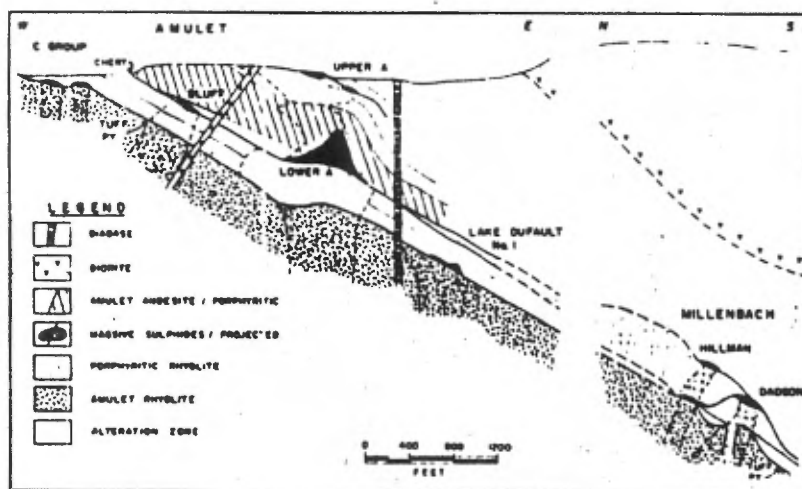
1. Occur within a domal volcanic complex (30 km. in diameter).
2. Ore deposits tend to occur in clusters (one or two large deposits and numerous smaller ones) within the domal complexes.
3. Associated with the loci of abundant felsic volcanic rocks, usually at or near the upper part of a mafic to felsic volcanic succession.
4. Ores are conformable with the enclosing stratigraphy.
5. Individual deposits contain, on average, 6 million tons of ore, grading 6% combined base metals.
6. Metals, in Archean deposits, occur in a rough ratio of 4:1:<1 for Zn:Cu:Pb.
7. Prominent metal zoning, in undeformed deposits, with a barren pyrite top, underlain by a sphalerite-galena-pyrite unit, which is usually banded parallel to the host rocks, followed by a chalcopyrite-rich base.

8. Distinctive alteration zone beneath the ore deposit, usually accompanying a stringer ore zone with fracture-filled host rock.

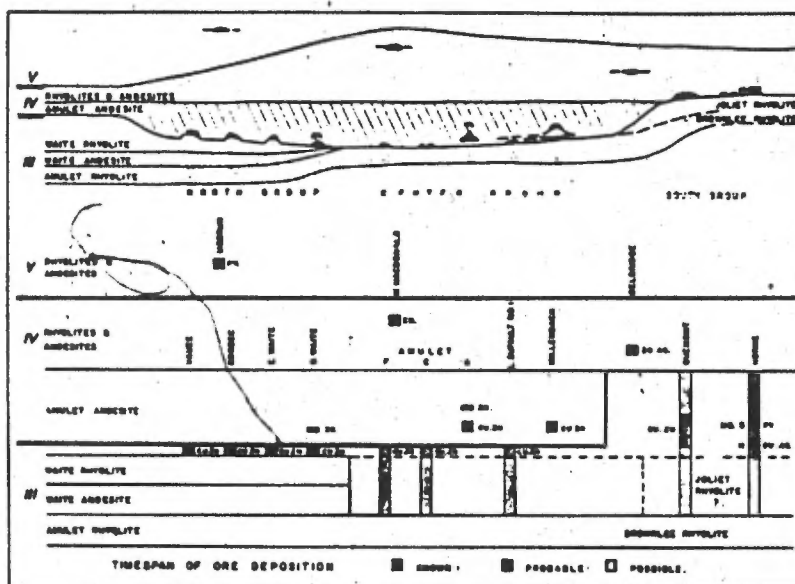
Many of these features are illustrated by Figure 8.7, showing the geology of some deposits in the Noranda region.

Description of the Coniagas orebody, in Chapter 7, revealed many of the above characteristics. The general environment is similar (i.e. within a large, domal complex, containing abundant intermediate and felsic volcanic rocks. However, the deposit appears to be unique in that despite intense local exploration, it is the only concentration of economic massive sulphides.

Coniagas ores occur within the upper part of a mafic to felsic succession (Fig. 7.1), and are conformable to the host rocks. Ore volumes are low, with respect to average Canadian deposits of this type (see Sangster, 1980) but this may be explained in terms of the metal ratios (Zn:Cu:Pb = 13:0:1). During mining in the mid 1960's, when metal markets were highly volatile for base metals, the company excavated much of the extremely rich zinc ore, but depressed metals markets forced closure before all known reserves were removed. Little deep exploration of the intensely isoclinally folded deposit had been carried out and, thus, undetermined copper-rich ores may lie at depth (see section 7.1.3). Thus, the metal ratios of removed ore may reflect



Composite sections, E-W through Amulet C and A deposits (Price, 1953) and N-S through adjacent Millenbach deposits (Simmons et al., 1973) modified by removal of most intrusions.



Top: Diagrammatic N-S section showing stratigraphic position of ore deposits, drawn to show general morphology at the time of deposition of the copper-zinc ores. Bottom: Representation of the known, probable, and possible time spans in which sulfides were deposited.

Figure 8.7: Geology of Ore Deposits - Noranda Region (after Spence & deRosen Spence, 1975)

only the upper, zinc-rich zone. Future exploration of deep levels has been proposed by company personnel, should economic conditions prove feasible, and might result in discoveries which would increase orebody tonnage and balance the grade.

8.6.3.3 Speculations on the Genesis of Massive Sulphide Ores

Volcanogenic massive sulphide deposits, once considered as hydrothermal replacement bodies, are now commonly considered to have formed, subaqueously, by fumarolic activity. Base metals are seen to have been carried from depth by hydrothermal brines, upward through aquifers, now evident as stringer zones and alteration pipes, and deposited on the sea floor (Kinkle, 1966; Hutchinson et al., 1965, 1971; Sangster, 1972). However, the reason for these ores occurring in the particular setting of the calc-alkaline, domal sequence, described earlier, rather than in the lower stratigraphic positions, has not been well documented. It is suggested that the present location and original source of base metals is a product of the tectonic style of the domal sequence.

Formation of massive sulphide ores requires a process of metal concentration and transportation more effective than that which moderately increased copper and

zinc values in the upper platform sequence. Following the model developed in section 8.5.3, gravitational and lateral depression in the central part of the platform sequence eventually leads to a large volume of supracrustal rocks being downthrust toward the mantle. This is the earliest known process to carry large volumes of relatively water-rich, moderately evolved rocks down to mantle depths. The effects are predictable: increased water content lowers rock melting temperatures and water, released by metamorphic reactions, mixes with overlying pore fluids and begins to circulate and dissolve a variety of elements. Solutions will probably become brine-rich, since alkali elements are most soluble, and will preferentially concentrate geochemically scarce trace elements (Skinner and Barton, 1973; Barnes et al., 1967). Concentration of metals by leaching from a volcanic pile has been proposed by other investigators (Anderson, 1969; Boyle, 1959; Kinkle, 1965). These brines would be confined by overlying impenetrable strata, either natural or hydrothermally sealed: see Hodgson & Lydon, 1977, p.103). The premise of metals being obtained by leaching of the volcanic pile, as opposed to coming from the mantle, is supported by isotope studies (Krauskopf, 1967).

Transport and deposition of hydrothermal solutes has been lucidly described by Barnes, 1967 and Skinner and

Barton, 1973. Hodgson & Lydon (1977) suggest that in a caldera (i.e. domal) environment, the most favorable conditions for release of hydrothermal fluids occurs during resurgent doming. Permeability of the cap rock is greatest at this stage, due to collapse fracturing of the early caldera.

Similar processes acting in other regions of high heat flow are seen as the reason for clustering of sulphide orebodies and similarities in metal tonnages and ratios, as described by Sangster (1980, p.78).

8.6.3.4 Guides to Base Metal Exploration

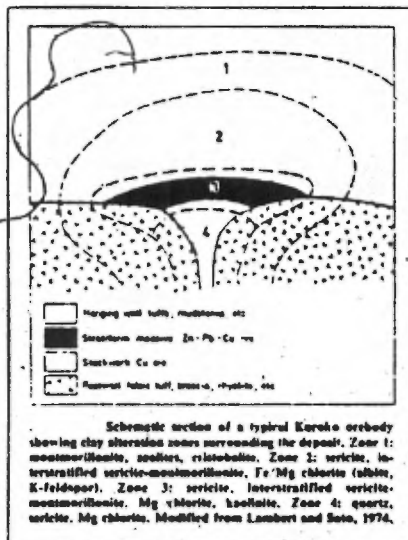
Surface expression of massive sulphide orebodies is not restricted to the relatively local extent of the metallic ores or closely associated geophysical anomalies. Hydrothermal fluids, which carried the metals to their emplacement, spread beyond the immediate conduit to produce an alteration halo of decreasing intensity, outward from the highly modified alteration pipe. The latter, intense alteration has been documented in the footwall rocks of most massive sulphide orebodies, but the extent of the lower grade, outer alterations have only been studied in a few cases (Gilmour, 1965; Meyer & Hemley, 1967; Hutchinson & Hodder, 1972; Franklin et al., 1975). The alteration sequence, from periphery to core, appears to be propylitic; quartz-sericite : chloritic and has therefore been compared

to patterns in porphyry copper deposits. The importance of hydrothermal alteration associated with base metal mineralization is shown in the factor analysis summary (Tab. 8.2 & 8.3), where elements associated with sericitization (K, Rb) are found, together with Zn in the same factor, for the first time in the volcanic pile.

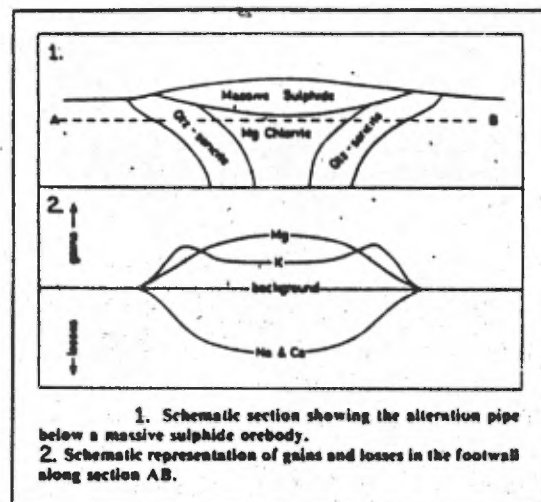
In the case of an orebody, such as the Coniagas deposit, where footwall rocks are concealed by intense folding, the question arises as to whether geochemical anomalies can be detected in hanging wall rocks. A few documented cases have been found to have such alterations (Fig. 8.8 a) (see Gilmour, 1965, p.71-72 and Govett & Goodfellow, 1975), but Sangster (1972) indicates that hanging wall alteration is rare. A sampling traverse over the Coniagas deposit (Fig. 7.2) showed intense mineral and chemical changes in these rocks and anomalous metal values. It therefore seems apparent that fumarolic activity continued to occur after deposition of the next volcanic succession began. Similar features may be present in other deposits if studies look beyond the secondary metamorphic overprint.

Studies have been made, alluding to the many similarities, albeit in different tectonic styles, between massive sulphide and porphyry copper deposits (Hutchinson & Hodder, 1972; Sawkins, 1973). Investigators of porphyry

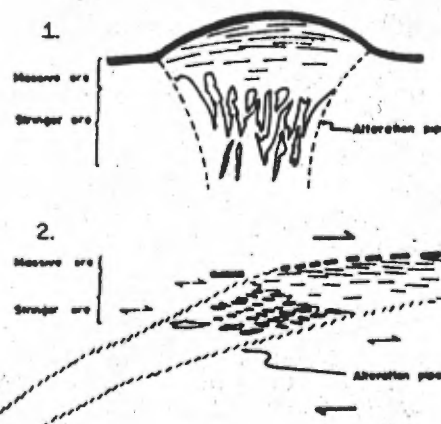
a)



b)



c)



1. Schematic diagram illustrating main geological features of an undeformed volcanogenic massive sulphide deposit.
2. Same deposit as 1 but modified by shearing in the sense shown by heavy arrows above and below the orebody.

Figure 8.8: Wallrock Alteration in Massive Sulphide Deposits a), b) (after Gannicott et al, 1979) c) (after Sangster, 1976)

copper deposits (Armbrust et al., 1971; Oyarzum, 1974; Olade & Fletcher, 1975) have determined that Rb and Sr, in conjunction with alteration studies, prove valuable pathfinder elements. Rb and Rb/Sr ratios increase progressively inward in hydrothermal alteration zones, following increases in potassic and phyllic alteration, whereas Sr decreases in the same direction, from high values in peripheral propylitic and argillic alteration. These pathfinder halos are often much larger than those of the major elements.

Outcrop exposure at the Coniagas deposit is too scarce to provide adequate lithogeochemical analysis for these minor element patterns. The limited traverse (Fig. 7.2) does, however, provide an indication that Rb is anomalous in the central zone, while Sr increases toward the periphery, even in the weak, hanging wall alteration. Of greater significance is the result of factor analysis on all fresh rocks of the domal sequence (Area 4 in Table 8.3). Zinc becomes a factor second only to the dominant differentiation factor and is a co-factor of positive correlation with K₂O and Rb. This is interpreted as direct correspondence of zinc mineralization with hydrothermal alteration, as opposed to metals which have no associated hydrothermal alteration (e.g. Area 2).

8.6.4 Ores of Uncertain Stratigraphic Location

8.6.4.1 QSRML Gold Property

Gold ores of Quebec Sturgeon River Mines Ltd. are unlike either the magmatic-cumulus, Ni-sulphide deposits or strataform and stratabound, massive sulphide ores, described in previous sections. The gold occurs in discordant veins, crossing the stratigraphy at high angles and has some aspects of hydrothermal emplacement.

Geochemical and petrographic data suggests that the host rocks are andesitic to dacitic, with relatively narrow hydrolytic alteration halos around the ore veins. Several features suggest that less intense alteration is more widespread. It has been shown (section 7.2.4) that parallel shearing becomes less intense outward from the ore veins but is present, to some degree, in most local rocks. This shearing is accompanied by sericitization which also decreases outwards. Quartz and albitization occurs near the veins. In addition, the K/Rb ratio increases away from the ore, revealing a Rb halo.

Gold mineralization of discordant, quartz-vein type occurs in many environments in greenstone belts (i.e. from lower to upper sequences) but is almost universally associated with areas of structural and lithologic complexity. There is obviously a strong structural control for the emplacement of the ore, but the metal source remains

problematical. Various authors have suggested that gold ores formed initially as exhalative sedimentary (Ridler, 1975; Hutchinson et al., 1971, 1975; Fryer et al., 1979), granitic (Ferguson, 1966), or ultramafic (Pyke, 1975; Imreh, 1976) metal components. Whatever the source, the gold has been mobilized (see Anhaeusser, 1976; Fyfe & Henley, 1973) and concentrated by hydrothermal solutions. These solutions may be produced by heating of near surface waters at a local heat source, by dehydration of rocks during metamorphism, and/or through partial melting of the source rocks and separation of an aqueous phase from the resulting magma (Hutchinson et al., 1971; Sawkins, 1972, p.389; Skinner, 1973, p.187). Genetic factors require further study.

8.6.4.2 Soquem Base Metal Property

Sub-economic sulphide deposits have been described for the Soquem property, in northwest LeTac Township (section 7.3). They are contained in a narrow volcanic arm, between large regional batholiths, which follows along strike to the massive felsic lavas in central Benoit Township (Area 5) (Map - rear pocket). Structural detail between Area 5, the Soquem property and Area 4 is extremely scarce. The Area 5 - Soquem property sequence may, in fact, be a second, albeit smaller, domal sequence of similar stratigraphic position to Area 4. Much additional detailed structural mapping remains to be done to confirm or refute this position.

Host rocks for the sulphides have been described by Doucet (1973) as fine to coarse felsic and intermediate pyroclastics. This study has shown the rocks to be intensely sheared and altered (section 7.3.4) varieties of the massive felsic and intermediate lavas of Area 5 (section 5.6). Fragmental textures in these rocks seem to be of dynamo-metamorphic origin. Alteration is much more intense and pervasive than would be expected from normal hydrothermal processes associated with sulphide ore emplacement. This may be a result of penetrative deformation by the nearby batholiths and subsequent percolation of hydrothermal fluids. The alteration becomes extreme upon approaching the ore veins, suggesting superposition of regional alteration upon the syngenetic, ore-related alteration.

Variation diagrams suggest that most rocks lie in the normal dacite-andesite fields, as opposed to normative calculations which make them much more mafic. Both Al_2O_3 and K_2O , major components in many variation diagrams, are much higher than normal, and are due to the very high sericite content. Al_2O_3 may not be enriched, however, since removal of SiO_2 , (i.e. from plagioclase decomposition) would cause an apparent increase in the alumina. Relative immobility of TiO_2 allows comparison of that oxide with rocks in other Areas and indicates that most of these rocks are in fact, dacites. This is supported by the lack of mafic minerals.

Soquem mineralization is of minor volume and will probably be sub-economic for many years. The volcanic succession in Area 5 is puzzling in its relationship to sequences in the northeast. It is a progressively differentiated group of lavas where the mafic rocks are chemically similar to lower platform sequences, but central felsic rocks and metallic mineralization resemble domal successions. Further efforts will be required to sort out the relationships in this bifurcation point in the volcanic belt:

Chapter 9

SUMMARY AND CONCLUSIONS

9.1 CONCLUSIONS

1.

X-ray fluorescence spectroscopy has developed into a rapid method of whole-rock geochemical analysis. Improvements in XRF techniques, during the present project, have allowed the analysis of large numbers of samples which are essential for checking systematic variations. An understanding of the limitations of the techniques is useful in evaluating the data.

2.

Commonly used classification schemes are largely unacceptable for use with Archean volcanic rocks. Mineralogical schemes are unworkable and current chemical methods do not accommodate the range of composition or degree of alteration of these early crustal rocks.

The present study uses a workable scheme, based upon that of Irvine & Baragar (1971) but requires the addition of a silica screen to remove rocks with unusual compositions. In addition, a

modified Al_2O_3 vs $\text{FeO}/(\text{FeO} + \text{MgO})$ (i.e. Naldrett-type) diagram is useful for mafic-ultramafic rocks.

Development of a universal system of classification, agreed upon by a consensus of researchers, is essential if valid comparison of results are to be made between different studies. It is also necessary to allow meaningful computation of local and regional average rock compositions and geographic and stratigraphic volumes.

3. Attempts to display petro-chemical variations using cross-sectional traverse plots, in the manner of Baragar (1968, 1972), Wilson et al. (1976, 1977), and others, proved unsuccessful. Many of these earlier works dealt only with the extreme upper platform and domal sequences and did not encounter the structural complexities of thick platform sequences.

This study found that systematic variations could be better presented, by tabulations and plotting on selected variation diagrams, groups of samples from successive stratigraphic intervals. Division of the pile into such intervals can be

accomplished by field data, supported by laboratory work. This method much better illustrates the trends in magmatic evolution than do plots of stratigraphic traverses, which tend to be erratic because of tectonic overprinting.

4.

The Bachelor Lake complex is typical of many Abitibi volcanic piles, in being a synclinally downwarped belt with a lower platform and upper domal sequence of, overall, progressively differentiated rock types. These sequences have been divided by structural and petrochemical methods, described petrographically in Chapter 5 and geochemically in Chapter 6. Ore deposits have then been examined within these settings (Chapter 7).

Evolution of magmatism in the pile is confirmed by both petrography and chemistry. Relic mineralogy shows that basalts, the most common rock type, become become less mafic upward in the stratigraphy, a fact substantiated by their normative quartz:olivine ratios. Transition to the domal sequence shows that, in addition to a proportionately lower volume of basalts, they are also less mafic.

Parallel trends are confirmed in basaltic chemistry as the averages of elements most susceptible to fractionation processes (i.e. SiO_2 , MgO , FeO , TiO_2 , alkalis) show less mafic upward tendencies. Of particular importance in confirming the chemical trends is the use of factor analysis which statistically supports the field and petrographic divisions of the platform (lower magnesian, upper tholeiitic trends) and domal (calc-alkaline trend).

5. Development of greenstone belts, as exemplified by the Bachelor Lake region, is seen as an evolutionary process, through change in magmatic and tectonic styles.

Initial volcanism of the magnesian suite (i.e. lower platform sequence) may have been instigated by mantle processes and aided by crustal rifting. Diapiric rise prevented undue fractionation at depth. The lavas, become less ultramafic with late fractionation. Petrochemical trends are complicated because magmas from different vents lying in close proximity may have formed from different degrees of partial melting and/or fractionation.

Volcanic deposition progressed to shallower water conditions and, finally, became subaerial, allowing erosion to produce a coarse clastic wedge in subsiding basins. Field evidence suggests that the volume of material in platform sequence flows gradually decreased to the point where, during clastic sedimentation, it consisted of very minor, thin flows.

As large quantities of water-rich crustal rocks were carried down by gravitational instability, the style of magmatism changed. Relatively low melting temperatures would cause partial melting of these relatively wet rocks and diapiric rise to a lower pressure regime, following an adiabatic cooling curve.

6.

The change to calc-alkaline volcanism in the domal sequence, barring a few intercalations from waning tholeiitic platform volcanism, is much more dramatic than the gradual transition from magnesian to tholeiitic volcanism in the platform sequence. Intermediate and felsic flows become much more prevalent, with respect to basalts, but distinct chemical changes are present even within the latter mafic rocks. A decrease in the Fe/Mg ratio results in disappearance of the tholeiitic

trend and alkali values increase from the base to upper domal strata. In addition, alumina values increase and trace elements closely follow major element trends.

These features suggest that the calc-alkaline "series" is formed by cannibalistic recycling of previously deposited and slightly hydrated rocks, rather than being a primary magma or a differentiate of a tholeiitic or other magma type. This could account for the fact that intermediate and felsic rocks are much more common and extensive in calc-alkaline suites, which may be fractionated at high level from a less mafic source than the tholeiitic magma suites of the platform sequence. In this sense, formation of the domal sequence is seen as a process of crustal stratification, with recycling causing an early, upward concentration in incompatible elements. It also represents an increasing degree of upper crustal evolution since these domal rocks approach a more continental composition (i.e. higher K₂O, Al₂O₃, relative to Fe₂O₃ and MgO and smaller Fe/Mg ratio).

7.

The Bachelor Lake region lies in close proximity to other greenstone complexes (Noranda,

Val d'Or, Matagami, Chibougamau) but contains rocks with a higher, overall, degree of regional metamorphism. The reason may lie, not in deeper burial, but the fact that the belt is much narrower than other regions and may therefore have absorbed a proportionately higher degree of strain. Supporting evidence is found in the narrow arm of volcanics which contain the Soquem base metal prospect. There, the belt decreases in width to a narrow zone of highly sheared rocks which often give the ores an appearance of structural control.

Since most original mineralogy and textures have been obliterated, the extrapolation of such data from the nearby Noranda complex is useful for placing constraints on the nature and emplacement of magmas.

8.

Metallic mineral concentrations are closely tied to this evolutionary process. Nickel minerals occur mainly with the most ultramafic and primitive rocks in the lower platform sequence, and then disappear as these magmas are depleted. Copper then becomes predominant in the middle and upper platform sequence but only rarely forms economic concentrations. It is present, to some

extent, in the magnesian suite, but is predominant in the tholeiitic suite. Then, as recycling processes begin in calc-alkaline volcanism of the domal sequence, hydrothermal processes begin to concentrate copper and zinc mineralization.

Exploration for metallic minerals in greenstone belts must be directed toward the magmatic environment in which they form. Ni-sulphide ores occur in basal sequences as cumulates of the most ultramafic flows. Arndt (1976, p.649) describes lateral exploration methods once a favorable horizon has been found. Hydrothermal ores, on the other hand, are not intimately tied to the rocks in which they are found, although they do occur at preferred lithologic horizons. Due to extensive alteration processes near the channelways in which they form, large alteration halos can be found by combined mineral and chemical rock surveys. This has been demonstrated to occur in both hanging wall and footwall rocks of massive sulphide deposits and parallel to veining in gold-vein type deposits. These haloes are not easily detected during exploration, especially since the outer and widest, propylitic alteration is often masked by later metamorphic overprinting. Use of the

statistical techniques, outlined in the text, are successful in separating hydrothermally altered samples from those that are relatively fresh (i.e. background).

9.2 SUGGESTIONS FOR FURTHER WORK

1. Further mapping to determine the nature of deeper volcanic horizons (i.e. delineate the basal magnesian suite in the lower platform sequence).
2. Extended mapping beyond the study area to determine the relationship of the Bachelor Lake region to other domal complexes and, most importantly, to the geology of intervening areas. The latter, part is critical to the interpretation of greenstone belt evolution, for most studies are concentrated near the domal complexes and little correlation is possible.
3. Detailed examination of the ultramafic bodies in Area 1 and determination of their relationship to the enclosing volcanics.
4. A study of the composition of intrusive bodies around and within the Bachelor Lake volcanic belt, to determine the possible existence of basement material and to determine if the smaller intrusive bodies may be subvolcanic feeders.

5. Determination and study of rare-earth element (REE) data for rocks at progressive stratigraphic levels in the Bachelor Lake. This information would provide valuable constraints on the methods of magma genesis, discussed in the text. In addition, sulphur isotope study of sulphides on the Soquem property and Coniagas deposit would assist speculation on the source of the sulphides.

Appendix A

PREPARATION AND ASSESSMENT OF PELLETS

The following is a discussion of the analytical procedures that were used in this study.

A.1 PREPARATION OF PRESSED POWDER PELLETS

The most serious problem involving the use of powders is the particle effect, the phenomenon where fluorescent intensity is proportional to the degree of physical homogeneity (Claisse & Sampson, 1962; Bernstein, 1962).

Shalgosky (1960; p.134) has suggested that the effective depth of penetration of x-rays is only a few thousandths of a centimeter and it therefore becomes evident that preparation of the specimen surface is of utmost importance. This surface must be as homogenous as possible to give consistent results. Sample powder must be carefully prepared in grinding and adequately mixed to avoid induced heterogeneities.

Powders should be ground so that particle size is much less than the critical depth to avoid large particles masking smaller ones. Satisfactory results are best obtained by standardizing grinding and pelletizing

procedures. Particle effects are minimized if grinding reduces grain size to 200 mesh (74 μ) or less (Note: Overgrinding may induce heterogeneity due to differential hardness of grain types), and if the sample is rotated during analysis. Particle size range should be similar in both standards and unknowns.

A.2 FUSION AS AN ALTERNATIVE TO PRESSED POWDERS

A Multi-sample, automated Claissé fusion apparatus and torrablé Mettler weighing scale were added to the XRF laboratory at the University of Ottawa in 1978. Excellent results have been reported by Hartree (Per.Comm.).

As a check on results obtained from pressed powder pellets, fused pellets were prepared from nine of the powdered samples. The technique involves fusion of 1.5gm sample powder with 4.5gm Lithium tetraborate ($\text{Li}_2\text{B}_4\text{O}_7$), 0.5gm Lithium Carbonate (Li_2CO_3 lowers the melting temperature of the flux), and a small amount of Ammonium Nitrate (to maintain oxidizing conditions in the presence of sulphides or sulphates). Samples are fused in platinum crucibles and molds, or, in the presence of high sulphides, in carbon molds.

This technique successfully removes the particle size effect and diminishes inter-element absorption and enhancement. The latter, however, is accomplished by having

a high flux to sample ratio (ie. high dilution: 10:1 to 100:1) which often leads to decreased sensitivity, especially at low elemental concentrations. It has been found that the problem is partially resolved by maintaining a low ratio (3:1). The interelement and enhancement effects, lamented by Czamanske (1966) can then be eliminated by a series of absorption coefficient corrections. These have been calculated by de Jongh (1975) or can be computed as described in Appendix B. They are essential for accurate determination using either fused discs or pressed powders.

It is suggested that, in future, major elements should be determined by fusion techniques, due to better defined calibration curves. But powder methods are only slightly less reliable for major elements and superior, in many instances, for traces, especially over restricted concentration ranges.

As evidence of the satisfactory nature of the powder method, a comparison of results on selected Bachelor Lake rocks is provided in Table A.1

	L12			LE9			L55			L75			L100b			N9			Q29			Du3			Po2a		
	F(1)	F(2)	P	F(1)	F(2)	P	F	P		F	P		F	P		F	P		F	P		F	P		F	P	
S102	48.84	49.00	53.14	67.98	67.79	69.05	65.57	65.24	61.81	63.92	73.81	73.48	48.10	48.75	49.55	49.54	75.51	76.00	66.68	68.11							
Al2O3	16.18	16.13	14.65	12.89	12.85	12.35	14.66	14.01	14.20	12.84	13.85	13.14	17.31	16.25	13.48	11.63	11.68	11.00	15.41	14.26							
Fe2O3	13.02	13.14	13.10	3.54	3.56	3.40	6.36	5.52	4.15	7.85	0.91	1.21	11.78	12.31	15.80	17.44	3.27	3.03	4.51	4.16							
MgO	4.49	4.61	5.18	1.73	1.67	2.61	1.40	2.07	2.19	1.98	0.00	0.51	5.11	5.56	6.07	7.27	0.58	1.05	2.56	3.28							
CaO	10.74	10.80	6.91	3.71	3.70	4.31	3.76	3.80	5.48	6.21	0.86	1.09	12.47	11.45	7.16	6.91	1.19	1.29	3.66	3.54							
Na2O	2.57	2.57	2.92	5.67	5.69	5.97	5.02	5.52	4.92	3.86	5.20	5.14	2.91	3.27	2.91	3.08	4.96	5.43	4.16	3.76							
K2O	0.99	0.99	1.05	0.40	0.40	0.35	1.18	1.30	0.89	0.82	4.35	4.58	0.17	0.16	0.05	0.08	1.02	1.00	1.00	0.88							
TiO2	1.01	1.01	1.04	0.30	0.30	0.33	0.93	0.95	0.61	0.68	0.03	0.02	0.79	0.84	1.77	1.48	0.18	0.19	0.40	0.52							
P2O5	0.17	0.16	0.17	0.07	0.09	0.09	0.18	0.16	0.17	0.18	0.00	0.03	0.04	0.00	0.18	0.19	0.00	0.03	0.12	0.12							
MnO	0.21	0.20	0.19	0.12	0.12	0.12	0.13	0.13	0.15	0.18	0.01	0.00	0.21	0.22	0.28	0.29	0.07	0.06	0.08	0.08							
S	0.00	0.01	0.01	0.01	0.01	0.01	0.01	0.02	0.18	0.20	0.05	0.09	0.00	0.01	0.13	0.09	0.00	0.01	0.00	0.01							
Ba	146	153	170	237	235	219	306	322	274	282	354	282	60	83	67	110	224	190	227	230							
Cr	1622	1636	nd	2457	2393	nd	1730	nd	2690	nd	1213	nd	1077	nd	738	nd	1693	nd	1806	nd							
Zr	86	88	nd	98	88	nd	141	nd	156	nd	52	nd	45	nd	112	nd	411	nd	133	nd							
Gr	226	232	218	562	487	455	255	223	170	166	172	160	175	159	144	140	214	178	285	272							
Pb	25	23	23	6	10	12	37	34	16	24	74	70	2	5	0	0	21	22	23	24							
Zn	132	134	120	160	166	160	100	88	120	131	32	37	106	73	151	180	91	73	87	82							
Cu	nd	nd	5	nd	nd	17	nd	15	nd	27	nd	4	nd	48	nd	174	nd	3	nd	18							
Mn	92	91	93	53	53	37	20	23	87	86	10	0	112	103	39	53	15	32	44	20							
TOTAL	98.22	98.86	98.40	96.78	96.52	98.68	99.46	98.79	99.10	98.79	99.26	99.35	99.05	98.87	97.51	98.12	98.73	99.14	98.93	98.83							
F = Fusion P = Pellet nd = not determined																											
														Majors in % Traces in PPM													

Comparison of XRF Data using Fused Discs and Pressed Powder Pellets

TABLE A.1

Appendix B

CORRECTION OF ANALYTICAL DATA

Ideally, all energy of excited electrons is discharged as fluorescence, in XRF analysis, but in fact, several factors serve to mask the theoretical calculations and cause inaccuracies in the energies recorded,

B.1 CORRECTION FOR BACKGROUND EFFECT

The contribution by background to count rates was removed from element intensities by a computer programme designed to calculate net intensities. For major elements the programme allows the background-under-peak value to be calculated by a single satellite background reading (where background is level), by linear interpolation from two satellite background readings (where background slopes linearly) or by a polynomial (Newton-Gauss) interpolation from four equispaced background readings. Correction is also made for blank/contamination readings and for K-beta interference from appropriate elements.

B.2 CORRECTION FOR INTERELEMENT INTERFERENCES

The most common interferences result from overlap of spectral lines. Many of these lines can be resolved by using specific operating parameters as suggested in Tables 2.1 and B.2. Several of the more serious problems are discussed below.

Spectral interference is a minor problem for major element analysis but is important for such determinations as phosphorous-calcium. Here, addition to the count rate occurs through reflection of the second order calcium peak, but is resolved by use of a germanium (GE) analysing crystal.

For certain elements, the normal K-alpha lines are not practical for measurement. In the case of barium, the 2-theta angle is too low for significant intensities and measurement must therefore be made on the L-series lines. Even there, minor Ti-K-alpha interference is present, indicating better resolution is to be obtained from beta radiation.

Elements within a few atomic numbers of an element being analysed, when present in the matrix, may accentuate the intensity of its peak. An example is the Co-K-alpha line (1.791A) which is accentuated by the nearby Fe-K-beta line (1.757A). Certain parameters such as a long collimator and scintillation counter can aid resolution, although decreasing the intensity.

TABLE B.2
Suggested Operating Parameters (after Allman & Lawrence,
1972)

ATOMIC NUMBER	ELEMENT	ANALYTIC LINE	TUBE	COLLIMATION	CRYSTAL	PREFERRED COUNTER WINDOW	X RAY PATH	TYPE OF COUNTER	REMARKS
11	Na	K α	Cr	480 μ	Gypsum or K.A.P. or Rb.A.P.	2 μ Polycarbonate 3 μ Flashed Mylar	Vac	Flow	Thinner windows on flow counter will improve count rates.
12	Mg	K α	Cr	480 μ	ADP or K.A.P. or Rb.A.P.	2 μ Polycarbonate 3 μ Flashed Mylar	Vac	Flow	
13	Al	K α	Cr	480 μ	P.E. or K.A.P.	3 μ Flashed Mylar 6 μ Flashed Mylar	Vac	Flow	
14	Si	K α	Cr	480 μ	P.E. or K.A.P.	3 μ Flashed Mylar 6 μ Flashed Mylar	Vac	Flow	
15	P	K α	Cr	480 μ	P.E.	3 μ Flashed Mylar	Vac	Flow	
19	K	K α	Cr. or W	480 μ	P.E.	6 μ Flashed Mylar	Vac	Flow	
20	Ca	K α	Cr. or W	480 μ	P.E.	6 μ Flashed Mylar	Vac	Flow	
22	Ti	K α	W	100 μ	LiF ₂₀₀ or LiF ₂₂₀	6 μ Flashed Mylar	Vac or Air	Flow	Ti suffers interference LiF ₂₂₀ gives better separation, but is not obtainable with some spectrographs.
25	Mn	K α	W or Au	480 μ	LiF ₂₀₀ or LiF ₂₂₀	6 μ Flashed Mylar	Vac or Air	Flow or Saint	Flow counter gives similar count rate but lower background. Dead time is a problem with high counts.
26	Fe	K α	W or Au	100 μ	LiF ₂₀₀	6 μ Flashed Mylar	Vac or Air	Flow or Saint	Flow counter has lower background. Dead time is a problem. Air path normally selected wherever possible for convenience.
16	S	K α	Cr	480 μ	PE	2 μ PolyCarbonate	Vac	Flow	Recent developments with this window on Flow Counters may improve the detection limits.
17	Cl	K α	Cr	480 μ	PE	2 μ PolyCarbonate 3 μ Flashed Mylar	Vac	Flow	
24	Cr	K α	W or Au	100 μ	LiF ₂₀₀ or LiF ₂₂₀	—	Air	Saint	
27	Rb	K α	W Mo Au	100 μ	LiF ₂₀₀ or LiF ₂₂₀	—	Air	Saint	
38	S	K α	W Mo Au	100 μ	LiF ₂₀₀ or LiF ₂₂₀	—	Air	Saint	
39	Y	K α	W Mo Au	100 μ	LiF ₂₀₀ or LiF ₂₂₀	—	Air	Saint	
40	Zr	K α	W Mo Au	480 μ	LiF ₂₀₀	—	Air	Saint	
55	Ba	L α	W	100 μ	LiF ₂₀₀ or LiF ₂₂₀	6 μ Flashed Mylar	Vac or Air	Flow	Heavy elements may suffer interference from transition elements.
57	La	L α	W or Au	480 μ	LiF ₂₀₀ or LiF ₂₂₀	6 μ Flashed Mylar	Vac or Air	Flow	If concentrations are suspected they must be checked.
58	M	L α	W or Au	480 μ	LiF ₂₀₀	—	Air	Saint	
82	Pb	L α	Mo or W	480 μ	LiF ₂₀₀	—	Air	Saint	

In general, parameter optimization should be made where interferences are suspected and, if the matrix is totally unknown, it should be scanned to semi-quantitatively determine the composition.

B.3 CORRECTION FOR MASS ABSORPTION

In the simplest case, all energy of an absorbed x-ray goes into kinetic energy of a photoelectron and thence into the potential energy of an excited atom. The resultant secondary, fluorescent radiation would produce maximum intensity of the characteristic spectrum. For a pure element, then, its measured intensity would be equal to the maximum fluorescent intensity, multiplied by its weight percentage and absorption would be controlled wholly by the element. However, in multielement samples, measured intensity of the characteristic x-ray line depends not only on the mass concentration of an element but also upon the nature and abundance of other constituent elements.

In relation to the element being analysed, lighter elements will absorb less and heavier elements more. Therefore, if lower atomic number elements are present, relatively more characteristic radiation will emerge from the sample than is directly attributable to the element's weight fraction. Conversely, elements of higher atomic number will produce a negative effect. A certain degree of cancellation will occur in a mixed sample but the overall

absorption will probably be skewed in one direction or the other. Unless correction is made, non-linearity enters the calibration curve as heavy elements in a light matrix cause an upward bulge and visa versa. The effect of absorption and incident wavelength on count rates is shown in Table B.3.

Calibration would not be difficult in cases where standards were compositionally very similar to unknown samples, but lack of sufficiently well-analysed standards over a systematic compositional range and the normal diversity of rock-element composition, create a more complex situation.

In this project, mass absorptions for major elements were calculated and programmed directly into the net intensity programme. Since major elements create most of the absorption in a sample (certain exceptions) and since they are usually analysed as oxide weight percentages, the total mass absorption of the elemental oxides is required to correct for absolute abundances of the trace elements.

Since each element has a specific absorbing effect (μ) on radiation, proportional to its density, then a mass absorption factor can be found for that element at a certain radiant wavelength. Using absorption values published by Victoreen (1949), Heinrich (1966), Champion et al (1968), and de Jongh (1975), the mass absorption coefficient for the

A) Wavelength (Å)	Background intensity (counts/sec)		B) Matrix	Mass absorption coefficient (g/cm ²)	Background intensity (counts/sec)
	observed	calculated			
2.50	72	240	MgO	8.0	640
2.10	96		Al ₂ O ₃	9.0	640
2.00		300	SiO ₂	10.1	640
1.93	120		85% SiO ₂ 5% Fe ₂ O ₃	13.1	570
1.84	280		90% SiO ₂ 10% Fe ₂ O ₃	16.1	510
1.50		410	80% SiO ₂ 20% Fe ₂ O ₃	22.2	480
1.43	280		K ₂ CO ₃	26.1	480
1.25	407		70% SiO ₂ 30% Fe ₂ O ₃	35.2	390
1.20		520	CaO	37.7	390
1.17	456		60% SiO ₂ 40% Fe ₂ O ₃	41.3	350
1.04	586		Fe ₂ O ₃	70.4	320
1.00		630			
0.92	713				
0.83	873				
0.80		790			
0.78	896				
0.71	1226				
0.60		1080			
0.53	1576				
0.51	1604				
0.50		1290			
0.49	1706				
0.40	1626	1590			

TABLE B.3
Variation of Count Rate with Wavelength & Matrix (after Salmon, 1964)

element is obtained as the product of the mass absorption times the specific wavelength value. The major elements, analysed as oxides, necessitate the addition of an oxygen mass absorption factor. The final absorption is therefore obtained through the equation:

$$\mu_{\text{oxide}} = \mu_{\text{el.}} \times \frac{K_a}{\text{el.}} + \mu_{\text{O}} \times \frac{K_a}{\text{O}}$$

For elements under consideration in this study, oxide absorptions are shown in Table B.4. These values were then entered in a short Fortran programme which calculates mass absorption on major element percentages for all samples.

Oxide Coefficients Used for Mass Absorption Correction

TABLE B.4

	Na	Mg	Al	Si	P	K	Ca	Ti	Mn	Pb
Rb	6.20	6.90	7.80	8.60	9.60	29.10	28.90	31.50	55.20	55.50
Sr	5.30	5.90	6.60	7.30	8.20	24.80	24.80	27.00	47.40	47.50
S	844.10	947.60	1048.00	1142.40	1279.20	426.40	483.20	587.90	895.20	940.90
Co	39.10	43.80	48.90	53.70	60.20	178.20	175.90	190.40	331.40	46.20
Ba	133.20	100.70	166.10	182.00	203.80	595.50	585.60	95.20	146.40	153.70
Cu	25.80	28.90	32.30	35.50	39.80	99.90	116.90	126.70	220.80	221.60
Zn	21.10	23.60	26.40	29.10	32.60	97.20	96.10	104.20	181.90	182.50
Ni	31.60	35.40	39.50	43.50	48.70	144.60	142.80	154.70	269.50	270.40

B.4 CONSTRUCTION OF CALIBRATION CURVES

Following application of the necessary correction procedures, calibration curves were constructed as a basis of determining samples of unknown composition. Count ratios or net intensity measurements of a group of known standard samples (Table B.5) are plotted against their accepted values, for respective elements, to form a roughly linear curve. Composition of the unknown specimens can then be determined by applying their count ratio or net intensity to the curve.

A thorough discussion of calibration techniques is provided by Leake et al (1970) and reference is made to their paper for assistance and criticism of the methods. A few comments are sufficient to assess the curves used in this study (Figures B.1). Not all calibration curves are strictly linear and for this reason, "best-fit" lines have been applied to some distributions. A curve may fail to pass through the origin if background is too high, if particle effects are present, if interference occurs from another element, if incorrect standard values are used, or if rock matrix (and therefore mass absorption) changes over the range of calibration. Proper sample preparation removes much of the particle effect, interelement corrections can be applied and standards covering the expected range of unknowns removes the matrix problem. Thus, the only unaccounted factor is background, which can be ignored if standards and unknowns have similar matrix.

	SiO ₂	TiO ₂	Al ₂ O ₃	FeO	MnO	MgO	CaO	Na ₂ O	K ₂ O	Sum	LOI	Si	Ti	Al	Fe	Mn	Mg	Ca	Na	K	Sum	LOI	Si	Ti	Al	Fe	Mn	Mg	Ca	Na	K	Sum	LOI
SiO ₂	69.19	17.11	59.72	52.72	54.85	40.68	42.15	69.96	75.85	38.39	72.31	52.49	62.69	57.61	56.69	56.67	63.03	55.28	62.17	42.74	47.11	58.48	58.87										
Al ₂ O ₃	15.35	15.19	17.22	14.87	13.68	0.29	0.73	14.51	12.51	10.25	14.25	14.66	16.57	17.41	17.22	16.30	14.73	15.64	15.19	16.43	19.43	9.24	12.25										
Fe ₂ O ₃	2.47	4.33	6.84	11.11	13.52	0.60	0.28	2.86	1.33	12.98	2.21	9.08	5.94	7.00	7.77	8.91	6.27	9.80	6.20	11.56	9.54	7.78	5.94										
MgO	0.77	0.16	1.55	1.63	3.49	49.83	43.63	0.95	0.03	13.35	0.76	7.80	1.86	1.07	0.91	1.16	1.20	3.71	1.25	8.27	2.70	1.98	2.57										
CaO	1.98	2.32	5.00	11.98	6.98	0.15	0.53	2.45	0.69	13.87	2.15	9.31	5.11	2.85	1.80	2.58	2.73	6.04	3.42	12.25	9.37	11.59	9.49										
Na ₂ O	4.04	2.90	4.31	2.15	3.29	0.01	0.01	3.55	3.05	3.07	3.37	2.80	4.40	7.10	8.81	6.79	5.58	5.25	5.52	2.96	5.79	1.47	4.47										
K ₂ O	4.52	5.53	2.93	0.64	1.68	0.00	0.00	4.03	4.76	1.41	3.92	1.42	1.24	4.19	4.57	4.32	4.31	2.60	4.02	1.27	2.94	2.81	4.06										
SiO ₂	0.50	0.66	1.05	1.07	2.22	0.03	0.01	0.38	0.08	2.61	0.25	1.17	0.59	1.23	0.73	1.51	0.68	1.46	0.73	2.52	1.64	0.38	0.13										
FeO	0.04	0.04	0.10	0.17	0.19	0.11	0.12	0.09	0.05	0.20	0.06	0.16	0.11	0.24	0.03	0.31	0.16	0.22	0.16	0.18	0.23	0.40	0.32										
SiO ₂	0.14	0.28	0.50	0.14	0.33	0.00	0.00	0.12	0.01	1.05	0.09	0.26	0.14	0.29	0.13	0.24	0.07	0.50	0.07	0.14	0.35	0.22	0.19										
SiO ₂	0.00	0.04	0.01	0.01	0.04	0.00	0.01			0.04			0.01																				
SiO ₂	1850	1390	1200	160	680	2	0	850	22	1050	450	490	640																				
Pb	179	250	67	21	47	0	0	175	390	45	185	40	33																				
Cr	480	230	660	190	330	0	0	300	10	1350	185	440	390																				
Cu	85	98	84	86	120	45	36	75	80	160	36	83	220																				
Zn	11	35	63	110	19	7	33	14	12	70	3	53	47																				
Co	6	7	17	50	37	135	110	5	2	50	6	39	13																				
Ni	6	9	17	78	13	430	2510	7	3	270	7	135	13																				
TOTAL	99.48	99.35	99.44	97.99	99.99	99.94	95.74	99.04	99.21	97.52	99.46	99.48	98.80	98.99	98.69	98.84	98.76	98.63	98.73	98.71	99.12	98.32	98.13										

* Majors & Traces from Abbey (1974, 1977)
Majors in %; Traces in PPM

** Leachman (per. comm.)

TABLE B.5
International Rock Standards

Lab	Country	Std	Rock Type
USGS	Boston, Va.	G2	Granite
		GSP-1	Granodiorite
		AN-1	Andesite
		B1	Diorite
		FCP-1	Basalt
		ITS-1	Gabbro
		FCC-1	Peridotite
CH2O	Nancy, France	JA	Granite
		GN	Granite
		BN	Basalt
Q2	Greenwich, Conn.	JG1	Granodiorite
	Japan	JB1	Basalt
W2	Dodona, Tanzania	T1	Tonalite
Carmichael		W34	
		W52	Phenocryst
		W16	Neph. Trachyte
		W1C1	
		W1C2	
		W1C3	
		W1C4	
		W1C5	
		W1C6	
		W1C7	
		W1C8	
		W1C9	
		W1C10	
		W1C11	
		W1C12	
		W1C13	
		W1C14	
		W1C15	
		W1C16	
		W1C17	
		W1C18	
		W1C19	
		W1C20	
		W1C21	
		W1C22	
		W1C23	
		W1C24	
		W1C25	
		W1C26	
		W1C27	
		W1C28	
		W1C29	
		W1C30	
		W1C31	
		W1C32	
		W1C33	
		W1C34	
		W1C35	
		W1C36	
		W1C37	
		W1C38	
		W1C39	
		W1C40	
		W1C41	
		W1C42	
		W1C43	
		W1C44	
		W1C45	
		W1C46	
		W1C47	
		W1C48	
		W1C49	
		W1C50	
		W1C51	
		W1C52	
		W1C53	
		W1C54	
		W1C55	
		W1C56	
		W1C57	
		W1C58	
		W1C59	
		W1C60	
		W1C61	
		W1C62	
		W1C63	
		W1C64	
		W1C65	
		W1C66	
		W1C67	
		W1C68	
		W1C69	
		W1C70	
		W1C71	
		W1C72	
		W1C73	
		W1C74	
		W1C75	
		W1C76	
		W1C77	
		W1C78	
		W1C79	
		W1C80	
		W1C81	
		W1C82	
		W1C83	
		W1C84	
		W1C85	
		W1C86	
		W1C87	
		W1C88	
		W1C89	
		W1C90	
		W1C91	
		W1C92	
		W1C93	
		W1C94	
		W1C95	
		W1C96	
		W1C97	
		W1C98	
		W1C99	
		W1C100	

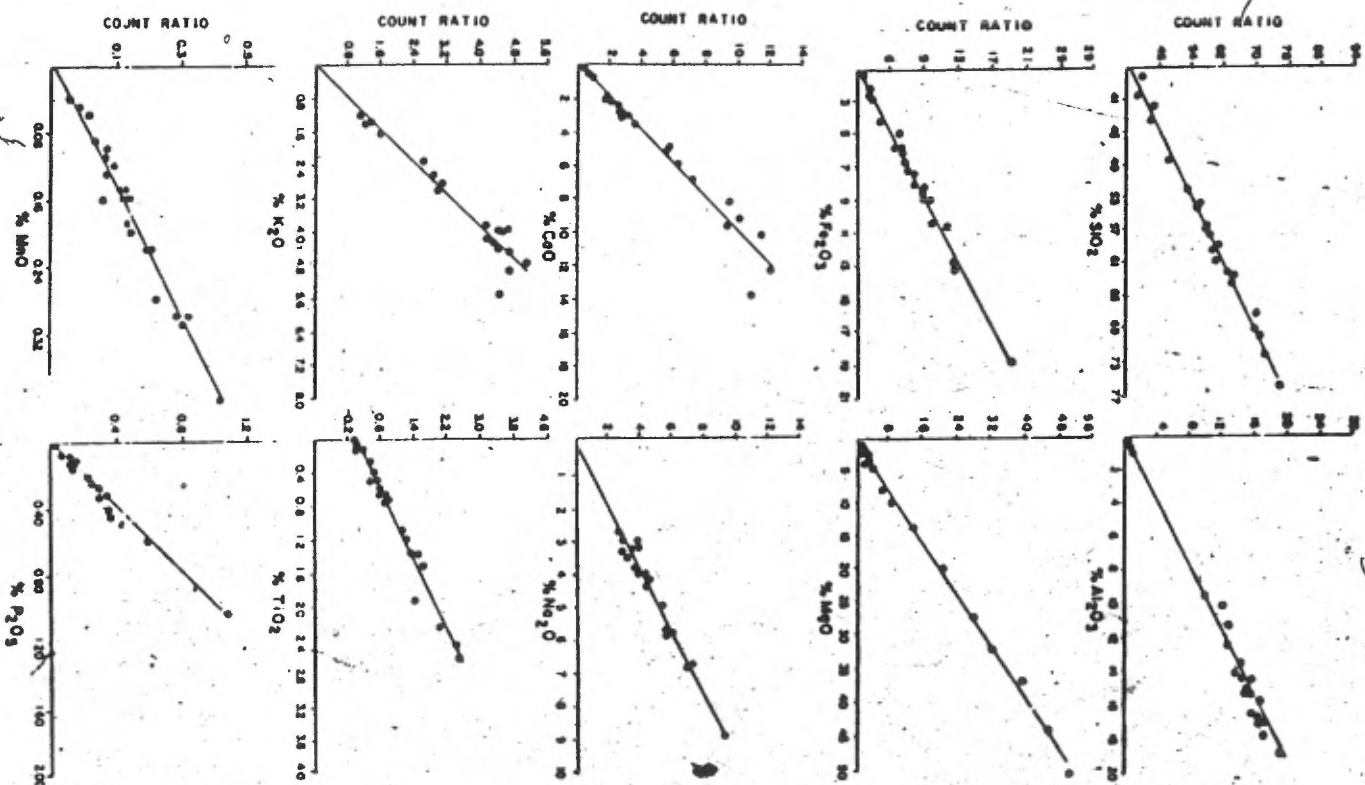
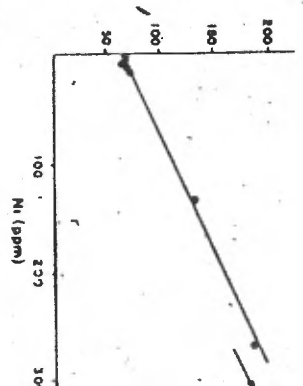
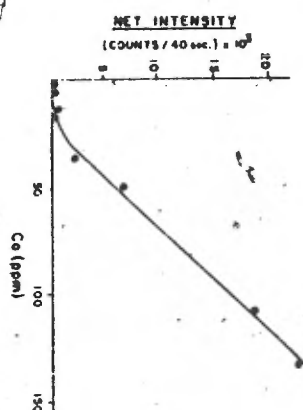
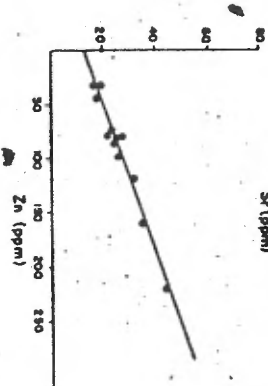
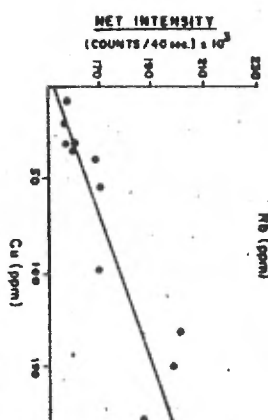
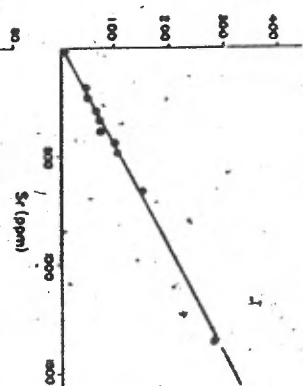
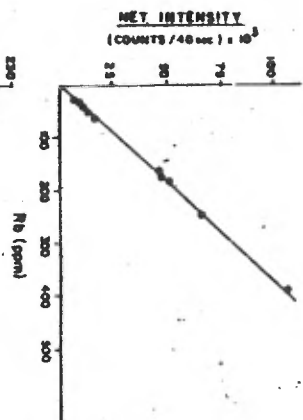
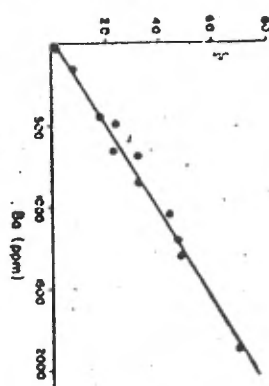
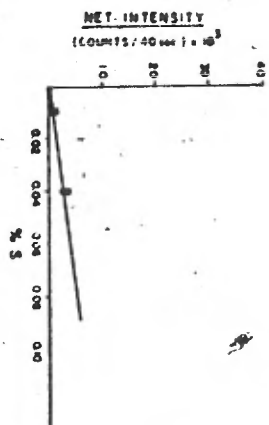


Figure B.1: Calibration Curves Used in This Study



Samples beyond the range of the standards must be extrapolated and values therefore indicate order of magnitude rather than absolute quantities. The amounts, however, are proportional to each other and thus represent relative concentrations.

COLUMN 7 : PRESERVATIVE DEFORMATION
- DEGREE OF POST-SOLIDIFICATION PHYSICAL MODIFICATION

- 0 - ABSENT-MINOR
- 1 - MODERATE
- 2 - INTENSE

COLUMN 8 : PRIMARY FRAGMENTATION:
- DEGREE OF FRAGMENTATION OF PRIMARY, SOLIDIFIED
ROCK MATERIAL

- 0 - MASSIVE
- 1 - FRAGMENTAL (RED-CS PYROCLASTICS, CLASTIC SEDS,
BRECCIAS)
- 2 - OTHER (HEATED TUFFS, SLIGHTLY SHEARED ROCKS
TO SCHISTS)

COLUMN 9-16 : NORMATIVE MINERALOGY
- DEDUCED MODE FROM MODIFIED-CIPW INVERSE/BARAGAN
SUBPROGRAMME
- DATA RECORDED IN ROUNDED WEIGHT PERCENT:

COLUMN	SYMBOL	MINERAL
9)	Q	QUARTZ
10)	Or	ORTHOCLASE
11)	Ab	ALBITE
12)	An	ANORTHITE
13)	Px	PHYCROCLASE

14)	Fe	Fe	OLIVINE
15)	Ca	Ca	CLINOPHASE
16)	Mg	Mg	FE-OXIDE PHASES

COLUMN 17-21 : NORMATIVE RATIOS + DEDUCED INDICES

- 16) AN OF PLAG - CALC AS AN/AN+AB (WT %)
- 17) COLOUR INDEX
- 18) RG OF PYROCLASTS - CALC AS RG/RG+AN (WT %)
- 19) DIFFERENTIATION INDEX
- 20) CRYSTALLIZATION INDEX

COLUMN 22-30 : MODAL MINERALOGY
- BASED ON WHOLE ROCK IED ANALYSIS AND SUPPORTED BY
DETAILED THIN SECTIONS AND SINGLE CRYSTAL IED

- 22) PYCROCLASE
- 23) TRICLINIC/ACTINOLITE
- 24) MONOCLINIC
- 25) CLINOPHASE
- 26) QUARTZ
- 27) PLAGIOCLASE
- 28) NICA
- 29) CARBONATE
- 30) EPIDOTE

- 3 DIGIT CLASSIFICATION:

- A) ABUNDANCE 0 - ABSENT
1 - MINOR
2 - MODERATE TO ABUNDANT
- B) PYROCLASTS VS GROUNDMASS 0 - ABSENT
1 - MODERATE
2 - MAJORITY - PYRO
- C) ALTERATION 0 - ABSENT
1 - MODERATE TO INTENSIVE
2 - MODERATE TO EXTENSIVE

1	2 3 4 5 6 7 8	9 10 11 12 13 14 15 16	17 18 19 20 21 22 23 24 25 26 27 28 29 30 31 32 33 34 35 36 37 38 39 40 41 42 43 44 45 46 47 48 49 50
L1	9 0 6 0 2 0 1	10 3 33 15 24 0 0 0 3.1	30 29 0 5 55 27 000 211 000 211 221 222 111 111 111
L2	9 0 7 0 1 0 0	6 2 21 30 34 0 0 0 3.6	57 40 0 6 29 45 000 211 000 211 111 211 000 111 211
L3	9 0 4 0 2 0 0	3 3 37 14 24 0 0 0 3.7	27 29 0 7 52 27 000 000 000 111 000 211 000 211 000
L4	9 0 7 0 1 0 0	10 3 24 29 28 2 0 0 3.6	54 34 0 5 37 0 00 211 000 111 211 000 000 211
L5	9 0 7 0 1 0 0	3 8 13 30 42 0 0 0 3.8	60 48 0 5 21 46 000 211 111 211 000 211 000 000 111
L6	9 0 6 0 1 0 0	16 4 35 17 23 0 0 0 3.5	32 28 0 5 54 27 000 111 000 211 111 211 000 000 111
L7	9 0 7 0 1 0 0	4 6 26 23 35 0 0 0 3.6	46 41 0 4 36 36 000 000 211 111 000 211 000 000 111
L8	9 0 6 0 2 0 0	12 9 36 24 17 0 0 0 4.0	39 24 0 5 51 30 000 000 000 111 121 222 000 121 111
L9	9 0 6 0 3 0 0	8 4 34 27 23 0 0 0 2.8	42 27 0 7 46 41 000 111 221 221 121 222 000 000 211
L10	9 0 1 7 0 5 0 0 0	0 6 23 30 28 0 0 0 3.3	61 33 0 7 29 52 000 000 000 221 211 112 211 211 211
L11	9 0 7 0 1 0 0	10 3 22 24 32 0 0 0 3.9	53 39 0 5 35 39 000 000 211 111 111 211 000 000 211
L12	9 0 7 0 1 0 0	6 6 25 24 31 0 0 0 3.6	48 37 0 5 38 36 000 000 221 111 111 211 000 000 211
L13	9 0 7 1 1 0 0	21 5 22 24 21 0 0 0 4.0	50 28 0 4 49 32 000 000 211 000 221 111 000 000 211
L14	9 0 6 1 1 0 0	29 9 20 18 16 0 0 0 3.7	45 23 0 3 59 23 000 000 000 111 221 222 121 121 211
L15	9 0 7 0 1 0 0	0 15 26 22 28 6 0 0 3.3	47 40 0 5 38 36 000 000 211 000 111 000 222 121 000 211
L16A	9 2 9 2 0 0 1 6	0 1 55 11 13 10 0 0 3.6	16 29 0 5 59 24 000 211 121 221 000 222 111 000 211
L16B	9 0 6 0 5 0 1	6 7 42 13 27 0 0 0 3.4	22 32 0 5 55 25 000 211 000 211 121 221 111 000 211
L17	9 0 7 0 1 1 2	0 1 38 25 25 3 0 0 4.4	30 35 0 5 39 36 000 000 000 211 000 212 000 211 111
L18	9 0 7 1 2 0 0	43 21 4 14 11 0 0 0 2.7	77 15 0 5 68 18 000 000 000 000 211 000 211 000 111
L19	9 0 6 1 0 1 0	16 4 38 13 22 0 0 0 3.7	25 28 0 4 50 23 000 000 000 111 221 112 000 221 111
L20	9 0 7 1 1 0 0	15 18 12 29 21 0 0 0 3.5	49 27 0 5 44 37 000 000 000 211 221 112 211 111 111
L21	9 0 6 1 0 1 0	10 4 37 20 22 0 0 0 3.7	34 28 0 6 51 29 000 000 121 111 211 221 000 000 111
L22	9 0 6 0 1 0 0	12 3 37 19 22 0 0 0 3.7	33 29 0 5 52 28 000 000 000 211 111 221 000 000 000
L23	9 1 7 0 1 0 1	0 12 28 21 26 0 0 0 3.1	41 39 0 4 46 121 600 211 000 000 111 111 000 111
L24	9 0 6 0 2 0 1	8 2 51 7 23 0 0 0 3.5	11 29 0 7 61 18 000 000 000 211 000 211 000 211 111
L25	9 0 5 0 2 0 0	6 3 58 6 18 0 0 0 3.5	8 24 0 6 67 13 000 000 000 211 000 211 000 211 111
L26	9 0 7 1 2 0 0	20 6 26 26 18 0 0 0 3.2	49 23 0 7 51 36 000 000 121 111 211 211 000 000 111
L27	9 0 7 0 2 0 0	8 6 26 27 32 0 0 0 3.2	56 37 0 7 36 44 221 000 211 211 211 211 000 211
L28	9 2 9 2 0 1	0 2 46 18 16 10 0 0 3.5	27 32 0 7 50 36 000 000 000 211 000 221 000 111 211
L29	9 0 6 1 2 0 1	40 4 19 16 17 8 0 0 2.7	45 21 0 4 63 24 000 111 000 111 211 211 000 000 211
L30	9 0 7 1 2 0 1	30 15 12 18 22 0 0 0 2.8	59 26 0 4 56 27 000 000 111 000 211 111 111 000 211
L31	9 0 5 0 2 0 1	30 12 13 12 7 0 0 0 2.3	26 11 0 5 74 16 000 000 000 111 221 111 111 000 111
L32	9 0 6 1 2 0 1	37 13 14 17 15 0 0 0 2.8	54 19 0 5 63 25 000 000 000 221 221 211 000 111
L33	9 0 7 0 2 0 0	10 10 15 24 13 0 0 0 3.3	61 39 0 4 35 44 221 211 111 121 000 111 000 000 211
L34	9 0 7 1 2 0 1	29 15 13 20 18 0 0 0 2.9	60 23 0 4 57 27 000 111 000 111 000 211 222 211 000 211
L35	9 0 6 0 2 0 0	19 15 26 6 23 0 0 0 3.4	17 29 0 4 59 13 000 000 000 211 221 112 111 000 211

1	2.3	4.5	6.7	8	9	10	11	12	13	14	15	16	17	18	19	20	21	22	425	728	031	334	637	940	243	586	48
148	4.0	7.0	2.0	0.0	10	13	7	34	28	0.0	0.0	4.0	83	35	0.4	29	84	000	221	000	211	211	000	111	000	211	
150	4.1	7.0	2.0	0.0	8	9	19	31	26	0.0	0.0	3.4	60	32	0.5	36	42	000	211	000	111	000	111	000	111	211	
152	4.2	9.2	2.0	0.0	0	3	64	8	22	1.0	0.0	3.7	6	29	0.5	66	16	000	000	211	111	000	211	111	000	211	
153	4.0	4.0	2.0	0.0	32	8	45	3	8	0.0	0.0	2.5	6	12	0.4	85	6	000	000	000	111	221	221	211	000	211	
154	4.0	5.1	2.0	0.0	36	18	33	5	9	0.0	0.0	2.3	12	12	0.3	83	7	000	000	000	111	211	211	211	000	211	
155	4.0	5.0	2.0	0.0	18	8	48	10	12	0.0	0.0	2.6	16	17	0.5	73	16	000	000	000	000	211	222	211	000	211	
156	4.0	6.0	5.0	1	14	9	36	12	22	0.0	0.0	3.7	25	28	0.4	58	22	000	000	211	111	211	221	000	000	211	
157A	4.0	5.0	2.0	0.0	18	5	51	5	17	0.0	0.0	2.6	8	21	0.6	74	15	000	000	000	111	211	222	211	000	211	
157B	4.0	5.1	2.0	0.0	34	12	36	8	7	0.0	0.0	2.0	18	11	0.4	81	12	000	000	211	000	211	221	000	000	211	
158	4.0	6.0	2.0	0.0	4	2	57	10	22	0.0	0.0	2.9	14	26	0.6	63	22	000	000	000	111	111	211	111	211	211	
159	4.0	7.0	5.0	0.0	16	2	6	18	43	0.0	0.0	2.7	72	47	0.8	24	42	211	111	111	111	111	211	000	000	211	
160	4.0	6.1	2.0	1	21	2	37	13	20	0.0	0.0	3.6	25	26	0.5	60	24	000	211	000	111	211	212	111	111	111	
161	4.0	6.0	2.0	0.0	12	8	33	16	23	0.0	0.0	4.1	31	30	0.4	54	25	000	000	211	000	211	111	111	000	111	
162	4.0	7.0	1.0	0.0	6	6	33	20	29	0.0	0.0	3.6	36	35	0.6	45	34	000	111	000	211	211	211	000	000	111	
163A	2.0	7.0	1.0	0.0	0	3	29	24	28	11	0.0	3.4	44	45	0.5	31	40	000	111	211	111	111	111	000	000	111	
163B	2.0	7.0	1.0	0.0	9	2	25	19	39	0.0	0.0	3.7	92	45	0.5	36	36	000	221	000	111	111	111	000	000	000	111
164	2.0	6.0	3.1	1	31	5	15	9	6	0.0	0.0	1.8	35	9	0.5	51	11	000	000	000	211	221	222	211	000	211	
165	2.0	7.0	1.0	1	10	1	22	24	34	0.0	0.0	4.3	91	42	0.4	33	35	000	121	232	211	211	111	000	000	211	
166	2.0	7.0	1.1	0	8	0	10	29	46	0.0	0.0	3.7	73	52	0.3	39	40	000	000	000	221	211	121	211	000	211	
167	2.0	7.0	2.0	0.0	0	1	12	36	44	0.0	0.0	3.4	74	50	0.4	13	52	000	211	000	211	000	111	000	000	211	
168	2.0	7.0	1.0	0.0	5	1	14	33	43	0.0	0.0	3.4	69	48	0.4	39	48	000	211	000	211	111	111	000	211	211	
170	4.1	6.0	2.0	1	19	8	26	26	16	0.0	0.0	3.2	49	21	0.5	52	34	000	000	221	111	211	221	211	000	211	
171	4.1	5.1	3.1	2	27	13	33	19	3	0.0	0.0	1.6	35	5	0.6	74	21	000	000	000	111	211	211	211	000	211	
173	4.2	9.2	1.0	0.0	0	4	27	23	31	6	0.0	3.5	45	42	0.7	33	49	000	000	211	000	000	211	000	000	211	
174	4.8	7.1	1.0	0.0	0	4	18	30	41	1.0	0.0	3.5	62	48	0.5	22	47	000	000	211	111	000	212	211	111	211	
175	4.8	6.1	5.0	1	23	5	33	16	17	0.0	0.0	3.2	31	22	0.4	62	23	000	111	000	111	211	221	111	000	211	
182	7.0	6.1	2.0	0.0	54	10	16	9	7	0.0	0.0	2.4	35	18	0.5	80	12	000	000	000	221	211	111	000	000	111	
183	7.0	6.1	2.0	1	32	11	29	13	10	0.0	0.0	3.3	25	15	0.5	71	16	000	211	111	111	211	211	111	000	000	111
184	7.1	4.0	5.0	1	35	9	41	6	4	0.0	0.0	1.2	12	9	0.5	85	18	000	111	000	000	211	221	111	111	211	
185	7.1	4.0	4.0	2	26	19	38	2	9	0.0	0.0	1.8	5	12	0.5	82	9	000	000	000	000	211	221	111	111	211	
186	7.1	5.1	2.0	1	35	18	37	6	4	0.0	0.0	1.6	13	7	0.4	86	8	000	000	000	111	211	221	211	111	111	
187	7.1	5.0	4.2	2	24	21	33	6	9	0.0	0.0	1.7	14	12	0.5	78	12	000	000	000	000	221	221	221	111	111	
188	7.0	6.1	2.2	0	34	19	19	13	9	0.0	0.0	2.8	39	13	0.4	73	16	000	000	000	000	211	211	211	000	211	
189	7.0	5.1	2.1	1	37	9	31	11	7	0.0	0.0	2.5	26	11	0.5	77	15	000	000	111	111	221	221	211	000	111	
190	7.0	6.1	2.1	1	30	15	29	11	9	0.0	0.0	3.3	27	14	0.4	74	15	000	000	000	111	211	221	211	000	111	
191	7.1	5.0	2.2	2	23	19	19	9	5	0.0	0.0	1.6	18	8	0.5	82	12	000	000	000	000	221	221	211	211	111	
192	7.0	6.1	2.1	2	28	17	19	18	12	0.0	0.0	3.1	47	17	0.4	65	22	000	000	000	211	221	221	211	000	211	

	1	2	3	4	5	6	7	8	9	10	11	12	13	14	15	16		
L06		1	0	0	2	0	0		0	11	00	14	12	0	0	0	3	0
L07		1	0	0	2	0	0		1	0	0	2	11	17	0	0	0	0
L08		1	0	1	1	0	0		0	3	23	22	27	10	0	0	0	2
L09		1	0	2	1	0	0		0	0	20	26	19	10	0	0	0	0
L10		1	0	2	2	0	0		0	5	56	11	13	0	0	0	0	1
L11		1	0	2	2	0	0		0	10	59	6	0	0	0	0	1	7
L12		1	0	0	1	0	0		0	0	0	5	13	0	0	0	0	0
L13		1	0	2	1	0	0		0	0	21	11	34	0	0	0	3	9
L14		1	0	2	1	0	0		0	3	21	24	29	10	0	0	3	5
L15		1	0	0	2	0	0		1	1	0	13	13	27	0	0	0	2
L16		1	0	2	2	0	0		0	1	0	11	33	0	0	0	2	6
L17		1	0	0	2	0	0		2	15	25	19	12	0	0	0	2	7
L18		1	0	0	2	0	0		1	13	02	16	10	0	0	0	3	1
L19		1	0	0	3	2	0		0	12	21	15	01	0	0	0	3	5
L20		1	0	0	2	0	0		2	3	51	6	15	0	0	0	1	6
L21		1	0	0	1	2	0		20	5	16	26	9	0	0	0	2	0
L22		1	0	1	1	3	0		31	0	10	14	0	0	0	0	1	2
L23		1	0	0	2	0	0		2	6	10	02	0	0	0	0	2	0
L24		1	0	2	2	0	0		1	0	11	33	0	0	0	2	6	
L25		1	0	2	2	0	0		2	15	25	19	12	0	0	0	2	7
L26		1	0	0	1	2	2		1	13	02	16	10	0	0	0	3	1
L27		1	0	0	2	0	0		0	12	21	15	01	0	0	0	3	5
L28		1	0	0	2	0	0		1	7	03	22	0	0	0	0	1	6
L29		1	0	0	2	0	0		2	3	51	6	15	0	0	0	1	6
L30		1	0	0	1	2	0		20	5	16	26	9	0	0	0	2	0
L31		1	0	0	1	3	0		31	0	10	14	0	0	0	0	1	2
L32		1	0	0	1	1	0		2	6	10	02	0	0	0	0	2	0
L33		1	0	0	1	3	0		35	10	25	20	13	0	0	0	2	1
L34		1	0	0	1	0	0		12	17	10	14	0	0	0	0	1	0
L35		1	0	0	1	5	0		0	1	39	24	31	0	0	0	3	1
L36		1	0	0	2	0	0		0	0	0	20	17	0	0	0	2	0
L37		1	0	0	2	0	0		0	0	0	20	17	0	0	0	2	0
L38		1	0	0	2	0	0		0	1	56	12	17	0	0	0	2	0
L39		1	0	0	2	0	0		17	3	10	22	23	0	0	0	1	3
L40		1	0	0	2	1	2		0	1	10	33	02	0	0	0	3	0
L41		1	0	0	3	0	0		7	10	14	34	24	0	0	0	3	3
L42		1	0	0	1	1	2		0	0	0	31	23	0	0	0	2	0
L43		1	0	0	1	0	0		0	0	0	35	02	0	0	0	2	0
L44		1	0	0	2	0	0		0	0	0	30	30	0	0	0	0	1
L45		1	0	0	2	0	0		0	1	20	33	2	0	0	0	3	1
L46		1	0	0	2	0	0		0	0	0	16	16	20	0	0	0	2
L47		1	0	0	2	0	0		10	2	10	23	16	0	0	0	2	0
L48		1	0	0	2	0	0		0	0	0	0	0	0	0	0	2	0
L49		1	0	0	2	0	0		0	0	0	0	0	0	0	0	2	0
L50		1	0	0	2	0	0		0	0	0	0	0	0	0	0	2	0
L51		1	0	0	2	0	0		0	0	0	0	0	0	0	0	2	0
L52		1	0	0	2	0	0		0	0	0	0	0	0	0	0	2	0
L53		1	0	0	2	0	0		0	0	0	0	0	0	0	0	2	0
L54		1	0	0	2	0	0		0	0	0	0	0	0	0	0	2	0
L55		1	0	0	2	0	0		0	0	0	0	0	0	0	0	2	0
L56		1	0	0	2	0	0		0	0	0	0	0	0	0	0	2	0
L57		1	0	0	2	0	0		0	0	0	0	0	0	0	0	2	0
L58		1	0	0	2	0	0		0	0	0	0	0	0	0	0	2	0
L59		1	0	0	2	0	0		0	0	0	0	0	0	0	0	2	0
L60		1	0	0	2	0	0		0	0	0	0	0	0	0	0	2	0
L61		1	0	0	2	0	0		0	0	0	0	0	0	0	0	2	0
L62		1	0	0	2	0	0		0	0	0	0	0	0	0	0	2	0
L63		1	0	0	2	0	0		0	0	0	0	0	0	0	0	2	0
L64		1	0	0	2	0	0		0	0	0	0	0	0	0	0	2	0
L65		1	0	0	2	0	0		0	0	0	0	0	0	0	0	2	0
L66		1	0	0	2	0	0		0	0	0	0	0	0	0	0	2	0
L67		1	0	0	2	0	0		0	0	0	0	0	0	0	0	2	0
L68		1	0	0	2	0	0		0	0	0	0	0	0	0	0	2	0
L69		1	0	0	2	0	0		0	0	0	0	0	0	0	0	2	0
L70		1	0	0	2	0	0		0	0	0	0	0	0	0	0	2	0
L71		1	0	0	2	0	0		0	0	0	0	0	0	0	0	2	0
L72		1	0	0	2	0	0		0	0	0	0	0	0	0	0	2	0
L73		1	0	0	2	0	0		0	0	0	0	0	0	0	0	2	0
L74		1	0	0	2	0	0		0	0	0	0	0	0	0	0	2	0
L75		1	0	0	2	0	0		0	0	0	0	0	0	0	0	2	0
L76		1	0	0	2	0	0		0	0	0	0	0	0	0	0	2	0
L77		1	0	0	2	0	0		0	0	0	0	0	0	0	0	2	0
L78		1	0	0	2	0	0		0	0	0	0	0	0	0	0	2	0
L79		1	0	0	2	0	0		0	0	0	0	0	0	0	0	2	0
L80		1	0	0	2	0	0		0	0	0	0	0	0	0	0	2	0
L81		1	0	0	2	0	0		0	0	0	0	0	0	0	0	2	0
L82		1	0	0	2	0	0		0	0	0	0	0	0	0	0	2	0
L83		1	0	0	2	0	0		0	0	0	0	0	0	0	0	2	0
L84		1	0	0	2	0	0		0	0	0	0	0	0	0	0	2	0
L85		1	0	0	2	0	0		0	0	0	0	0	0	0	0	2	0
L86		1	0	0	2	0	0		0	0	0	0	0	0	0	0	2	0
L87		1	0	0	2	0	0		0	0	0	0	0	0	0	0	2	0
L88		1	0	0	2	0	0		0	0	0	0	0	0	0	0	2	0
L89		1	0	0	2	0	0		0	0	0	0	0	0	0	0	2	0
L90		1	0	0	2	0	0		0	0	0	0	0	0	0	0	2	0
L91		1	0	0	2	0	0		0	0	0	0	0	0	0	0	2	0
L92		1	0	0	2	0	0		0	0	0	0	0	0	0	0	2	0
L93		1	0	0	2	0	0		0	0	0	0	0	0	0	0	2	0
L94		1	0	0	2	0	0		0	0	0	0	0	0	0	0	2	0
L95		1	0	0	2	0	0		0	0	0	0	0	0	0	0	2	0
L96		1	0	0	2	0	0		0	0	0	0	0	0	0	0	2	0
L97		1	0	0	2	0	0		0	0	0	0	0	0	0	0	2	0
L98		1	0	0	2	0	0		0	0	0	0	0	0	0	0	2	0
L99		1	0	0	2	0	0		0	0	0	0	0	0	0	0	2	0
L100		1	0	0	2	0	0		0	0	0	0	0	0	0	0	2	0

17 18 19 20 21 22-225-728-031-336-637-940-243-546-48

1234	3 1 7 0 2 0 0	0	2 32 32 29	0 0 0 3 0	49 32 0 7 34 47 000 000 000 211 211 222 000 000 211
1235	3 0 7 0 1 0 0	4	0 36 49	0 0 0 3 0	85 54 0 7 10 62 800 000 000 211 211 111 000 211 211
1236	3 1 6 0 3 0 0	16	4 30 28 14	0 0 0 2 7	47 22 0 7 50 38 000 000 000 211 211 111 000 211
1237	3 2 9 2 1 1 2	0	0 31 21 17 24	0 0 3 3	39 46 0 6 33 45 000 000 221 211 000 211 000 211 211
1238	3 0 7 0 1 0 0	1	0 9 33 51	0 0 0 3 6	78 57 0 6 10 56 000 111 000 211 211 111 000 000 211
1239	2 0 7 0 1 0 0	3	0 17 28 44	0 0 0 4 0	60 51 0 5 20 45 000 111 000 211 211 111 000 111 211
1240	2 2 9 2 1 0 0	0	1 39 16 21	17 0 0 3 6	27 44 0 6 40 38 000 000 211 211 000 211 000 111 211
1241	2 0 7 0 1 0 0	0	1 25 20 46	3 0 0 3 6	43 55 0 6 25 44 000 000 211 111 111 211 000 111 211
1242	2 0 7 0 1 0 0	0	1 25 27 18	21 0 0 4 2	50 47 0 5 26 44 000 211 000 211 111 211 000 000 211
1243	2 0 7 0 1 0 0	8	1 23 21 41	0 0 0 3 6	46 47 0 4 32 35 000 111 000 211 211 111 000 211 111
1244	2 0 6 0 1 0 0	0	3 47 14 19	10 0 0 3 2	22 35 0 6 51 30 000 211 000 211 000 211 000 000 111
1245	2 0 7 0 1 0 0	0	1 24 19 32	17 0 0 4 0	43 55 0 4 25 38 000 000 221 211 111 211 000 000 111
1246	2 0 7 1 1 0 0	13	2 27 20 32	0 0 0 3 6	41 38 0 6 42 34 000 111 000 211 211 211 000 000 211
1247	2 0 7 0 1 0 0	0	1 24 23 28	17 0 0 3 7	48 52 0 5 25 44 000 000 221 211 211 211 000 000 211
1248	2 2 9 2 1 0 0	0	1 27 22 29	13 0 0 3 7	44 48 0 5 29 42 000 000 212 211 211 111 000 211 211
1249	5 0 6 0 2 1 0	2	2 45 18 29	0 0 0 3 1	28 34 0 5 48 31 000 000 211 000 211 211 000 000 211
1250	5 2 9 2 1 0 0	0	5 23 18 33	12 0 0 3 9	42 51 0 6 31 45 000 000 211 111 000 211 000 111 211
1251	5 2 9 2 2 0 0	0	1 77 5 13	0 0 0 2 4	5 18 0 6 78 12 000 000 111 111 211 211 000 000 111
1252	5 0 7 1 2 1 0	26	7 14 31 17	0 0 0 3 4	67 22 0 6 46 40 000 111 000 211 211 211 111 111 211
1253	5 0 7 0 1 0 0	1	2 33 22 34	0 0 0 4 0	39 41 0 5 36 35 000 211 000 211 211 211 111 000 111
1254	5 0 7 0 2 0 0	18	6 4 29 36	0 0 0 3 9	46 43 0 5 28 47 000 000 211 211 111 111 111 211
1255	5 0 7 0 1 0 0	5	1 32 20 36	0 0 0 3 8	37 42 0 6 58 41 000 000 211 111 211 111 000 211 211
1256	5 0 6 0 2 0 0	17	8 28 21 20	0 0 0 3 7	42 26 0 5 53 30 000 000 211 211 211 000 000 211
1257	5 0 7 1 1 1 0	19	12 14 21 29	0 0 0 3 0	59 35 0 7 44 37 800 111 221 111 211 211 000 111
1258	5 0 6 0 2 0 0	10	7 40 16 19	0 0 0 3 7	28 25 0 5 56 23 000 111 000 211 211 211 000 000 111
1259	5 0 6 0 1 0 0	4	3 40 23 21	0 0 0 3 9	35 28 0 5 48 33 000 000 211 111 211 211 000 000 111
1260	5 0 6 0 2 0 1	4	6 35 21 22	0 0 0 3 5	36 34 0 6 45 35 000 000 222 211 211 221 111 000 111
1261	5 0 7 0 1 1 2	0	3 27 26 19	16 0 0 4 3	48 43 0 6 30 49 000 211 000 211 111 111 000 111 111
1262	5 1 5 0 2 0 0	20	7 46 14 11	0 0 0 1 9	22 14 0 6 72 20 000 000 211 211 211 111 211 111
1263	5 1 5 0 4 2 0	14	16 43 10 13	0 0 0 1 8	18 17 0 6 73 17 000 000 000 111 211 211 211 111
1264	5 0 5 0 2 0 0	20	11 43 14 6	0 0 0 1 6	24 9 0 5 73 17 000 000 000 211 221 211 211 000 111
1265	5 0 7 0 1 0 0	19	1 17 18 33	0 0 0 5 5	50 44 0 5 36 29 000 000 000 211 211 211 111 111 000
1266	5 0 7 1 4 2 2	18	2 27 25 22	0 0 0 3 0	47 27 0 6 48 37 000 000 000 211 211 211 000 211 211
1267	5 0 5 0 1 2 2	3	1 67 8 13	0 0 0 4 1	10 21 0 4 71 12 000 000 000 211 221 211 000 111 111
1268	5 0 6 0 2 0 0	19	8 28 16 18	0 0 0 4 7	39 27 0 5 54 28 000 000 000 211 221 211 000 000 111
1269	5 0 7 0 1 0 0	6	1 22 19 43	0 0 0 4 7	46 51 0 4 29 35 000 111 222 211 211 211 000 111 211
1270	5 1 5 0 4 2 2	20	7 44 8 12	0 0 0 2 0	15 15 0 7 71 15 000 000 000 211 211 211 000 000 111

	1	2	3	4	5	6	7	8	9	10	11	12	13	14	15	16	17	18	19	20	21	22	23	24	25	26	27	28	29	30	31	32	33	34	35	36	37	38	39	40	41	42	43	44	45	46	47	48	49	50	51	52	53	54	55	56	57	58	59	60	61	62	63	64	65	66	67	68	69	70	71	72	73	74	75	76	77	78	79	80	81	82	83	84	85	86	87	88	89	90	91	92	93	94	95	96	97	98	99	100																																																																																																																																																																																																																																																																																																																																																																																																																																																																																																																																																																																																																																																																																																																																																																																																																																																																																																																																																																																																																																																																																																																																																																															
00-34	5	1	5	0	2	0	0	18	5	51	13	10	0	0	0	1.9	20	13	0.7	74	19	000	000	000	211	211	221	211	211	111	111																																																																																																																																																																																																																																																																																																																																																																																																																																																																																																																																																																																																																																																																																																																																																																																																																																																																																																																																																																																																																																																																																																																																																																																																																																																				

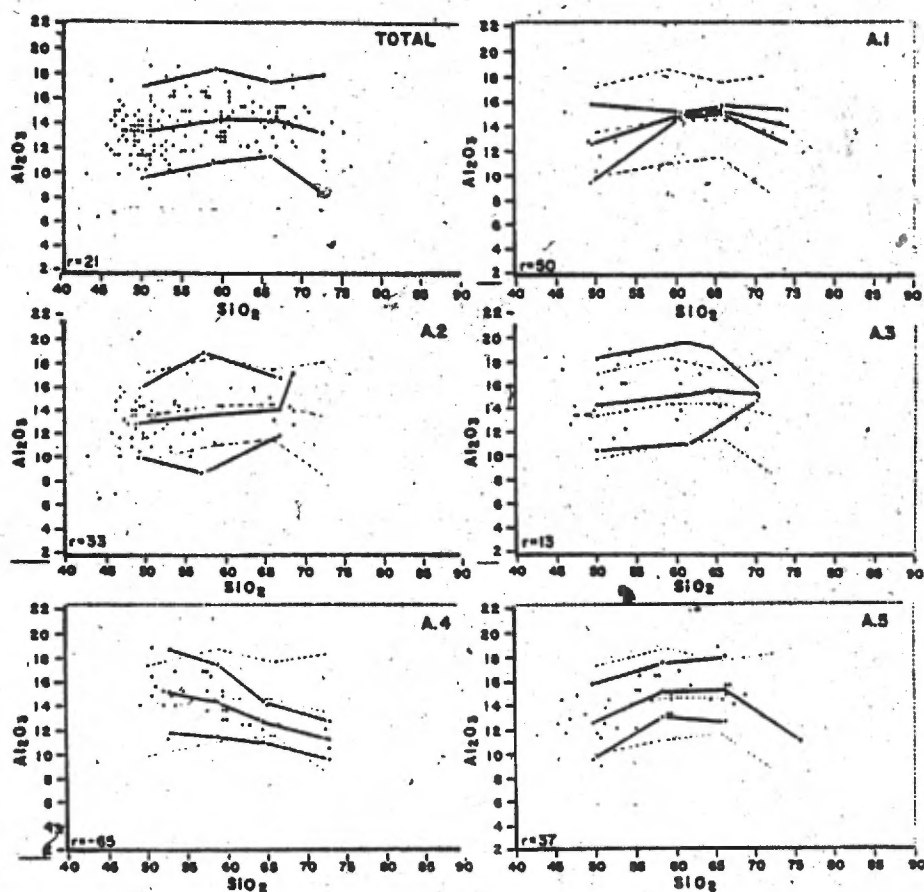
Appendix D.

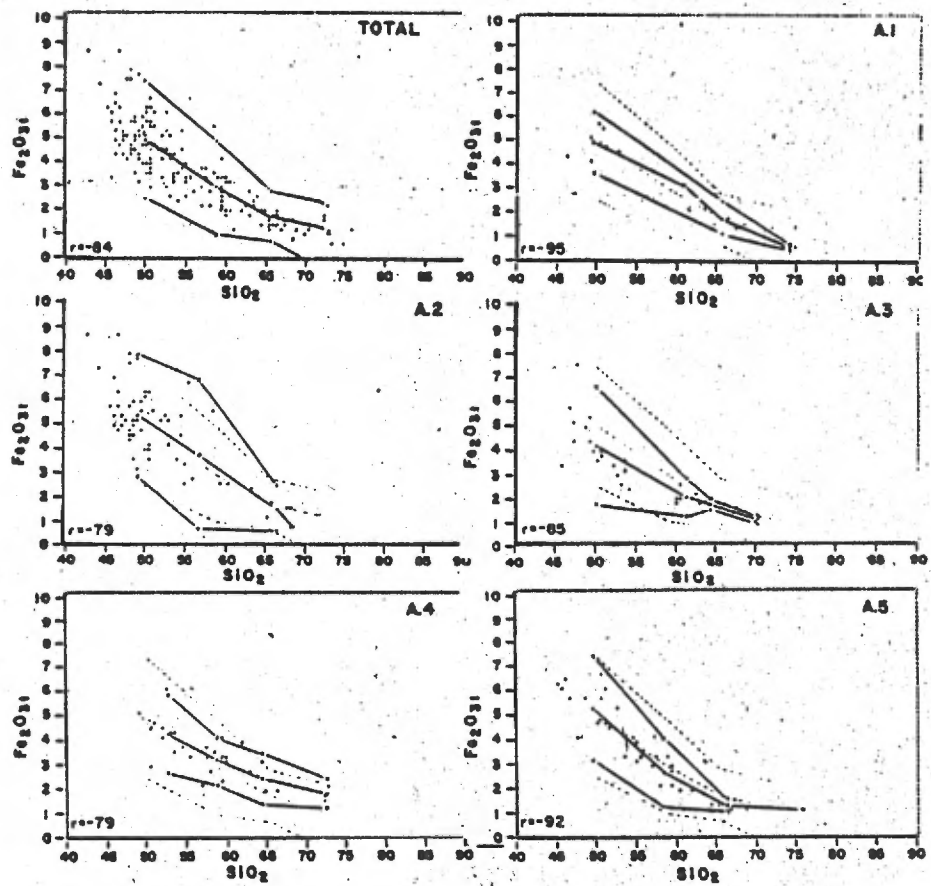
HARKER VARIATION DIAGRAMS - BACHELOR LAKE GEOCHEMISTRY

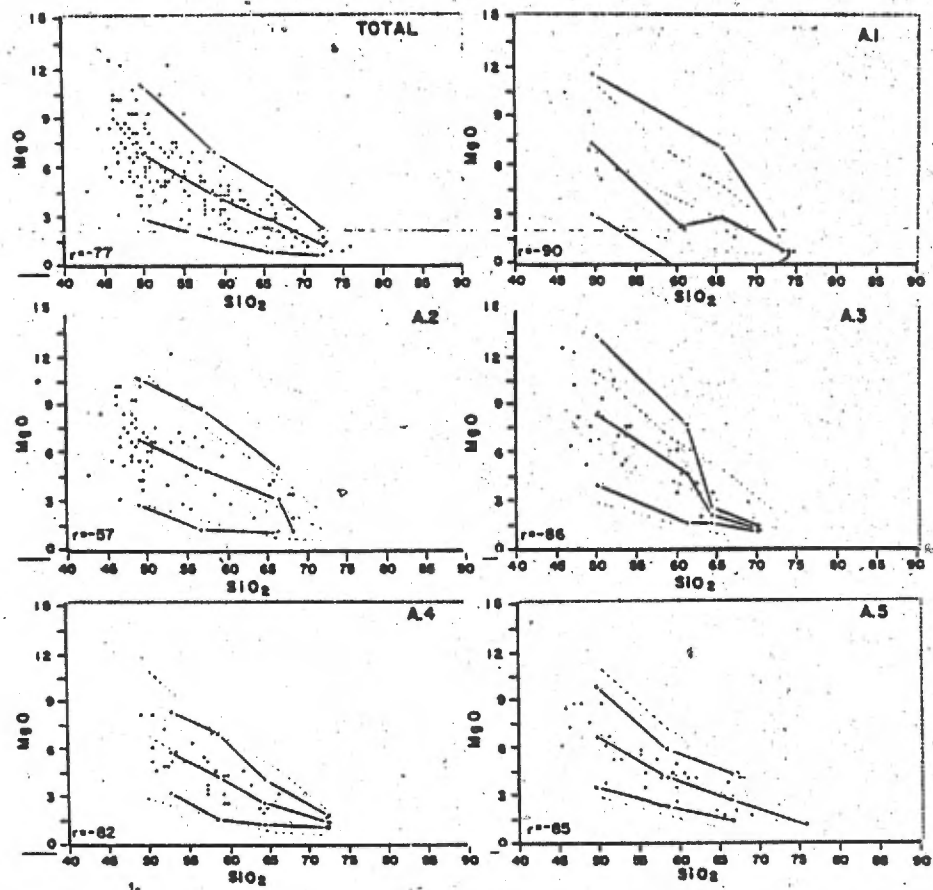
Harker-type variation diagrams have been plotted for each element and selected element ratios of all fresh rocks. Values are in weight percent oxide for major elements and in PPM for trace elements.

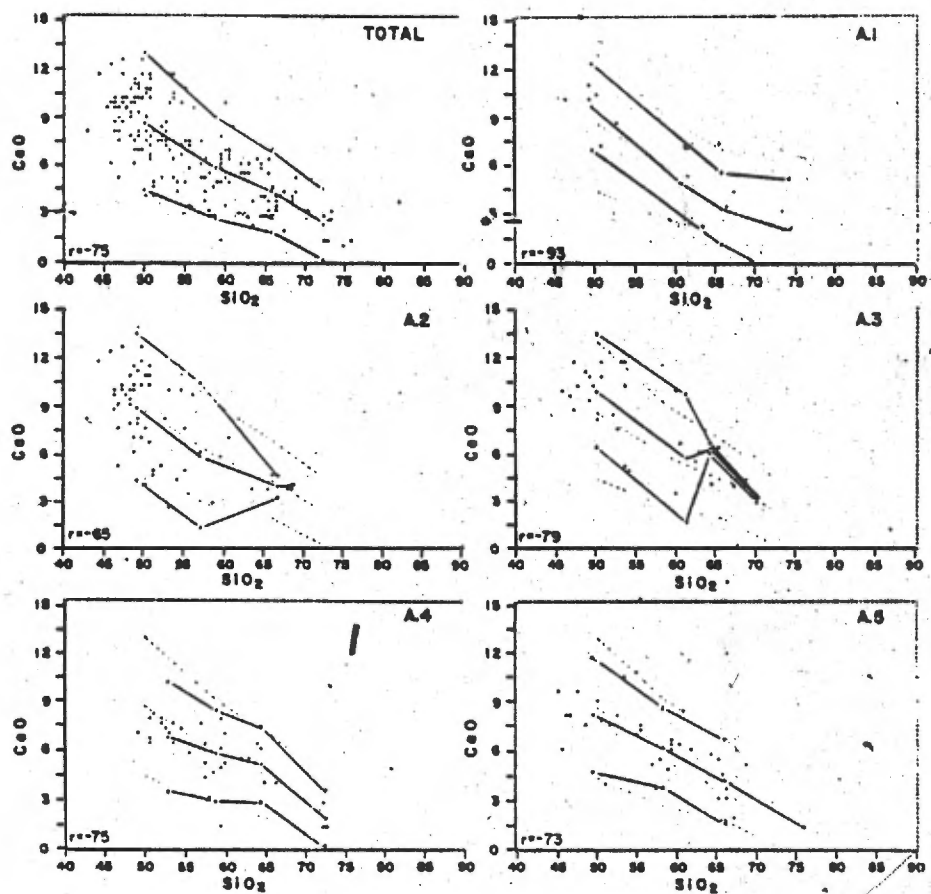
The first plot (ie. "Total") for each element or ratio contains data points for all fresh rocks in the Bachelor Lake Region. Three lines are located on this plot, joining the mean, plus, and minus 2 standard deviation locations for basalt, andesite, dacite, and rhyolite rock types. These lines are transposed to the corresponding plots of each geographic area (ie. A.1 to A.5) as dashed lines, for comparison with each new set of mean and 2 standard deviation lines.

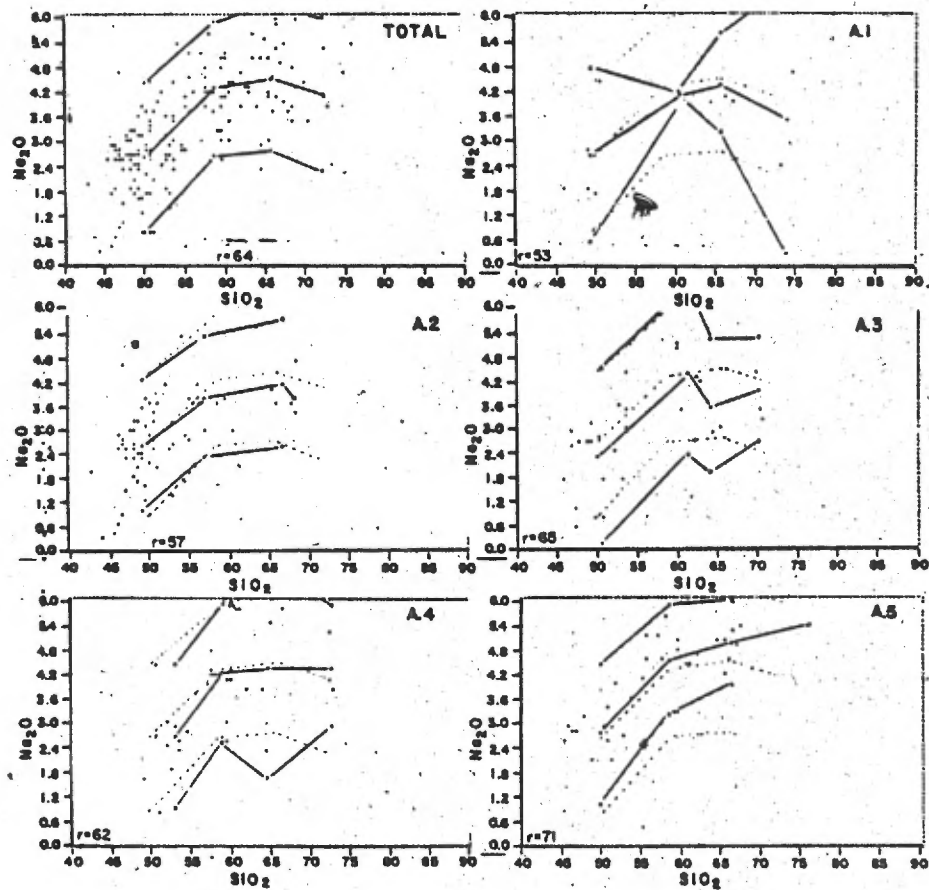
The correlation coefficient (r) is listed on each plot, to give an indication of the degree of linearity of the data.

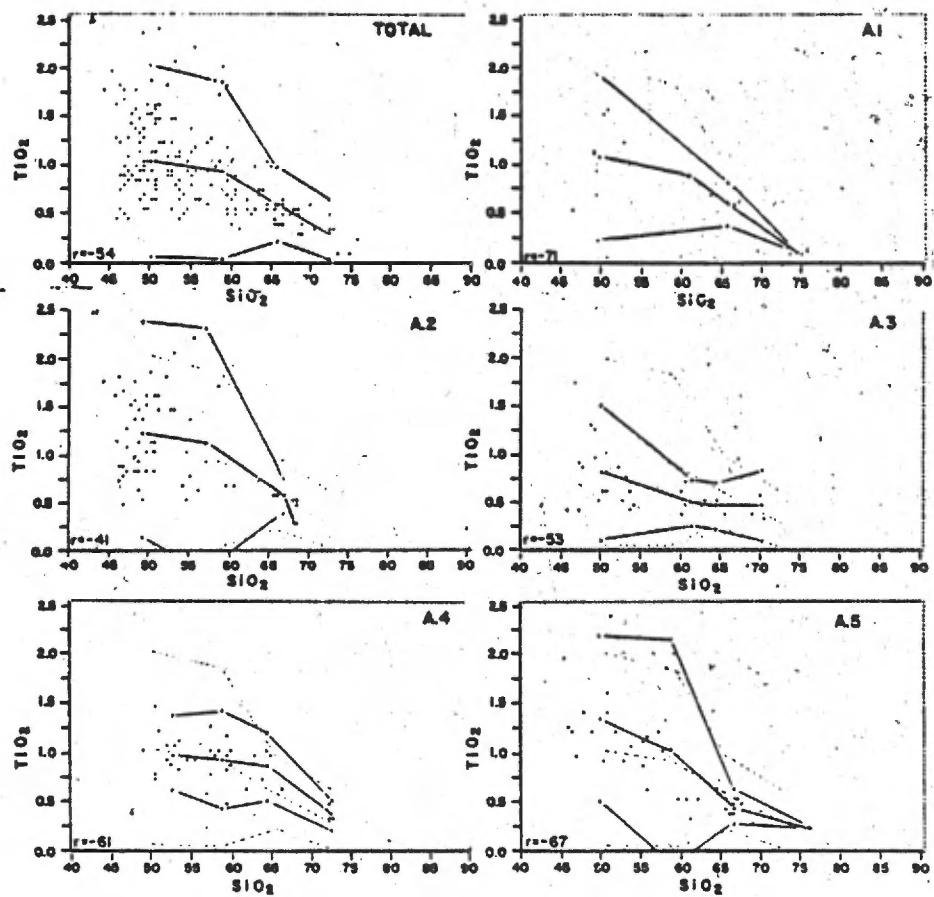


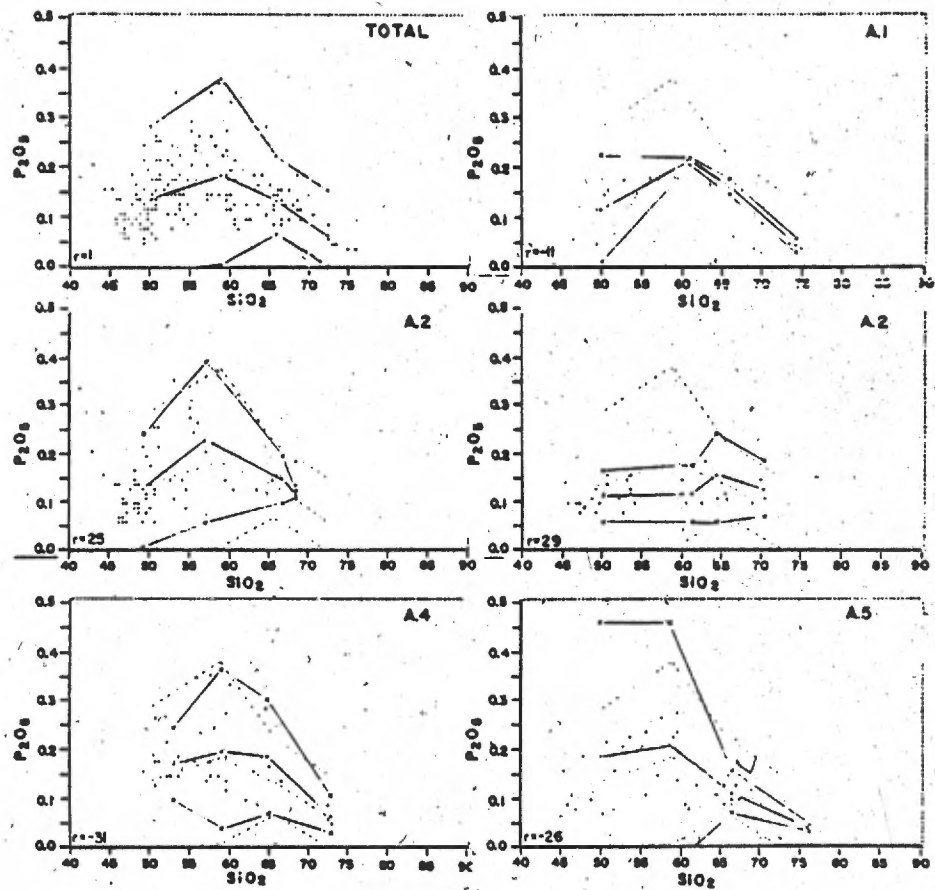


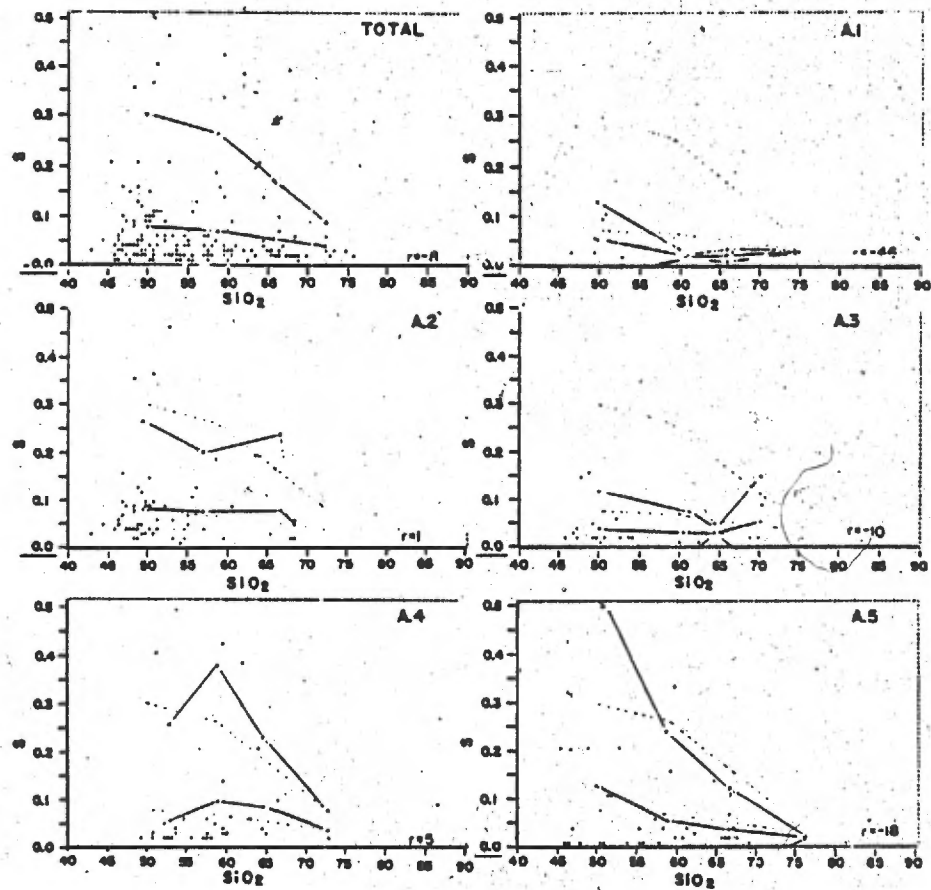


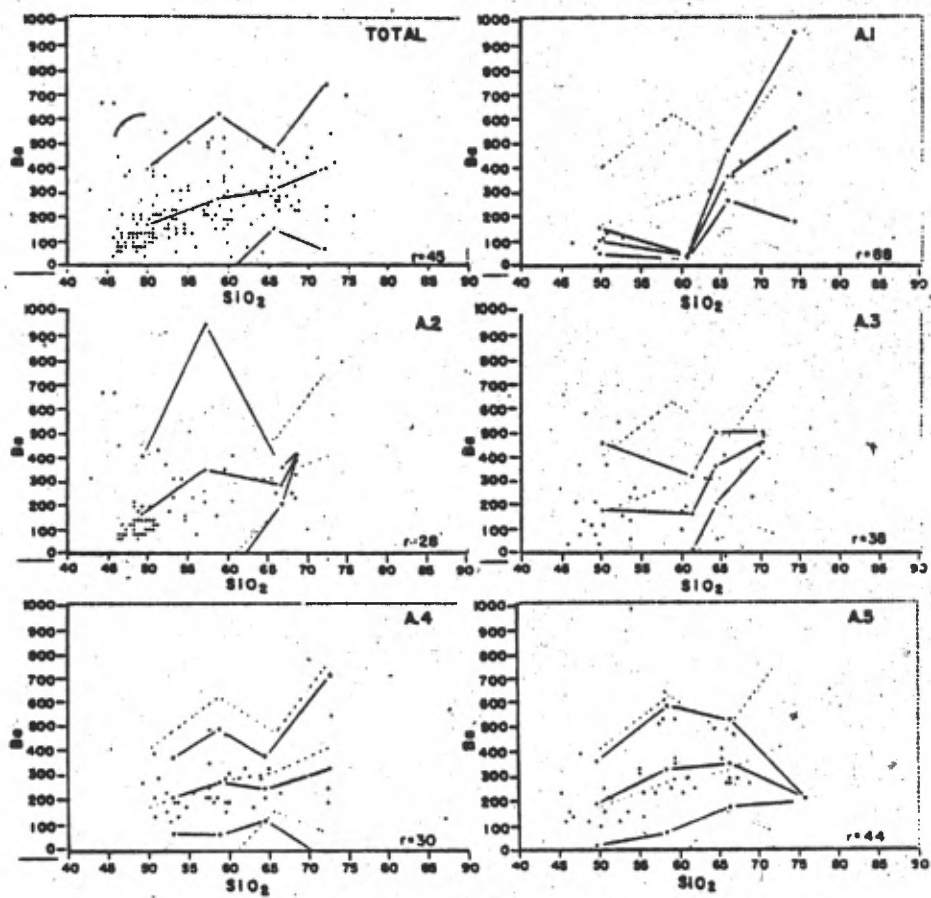


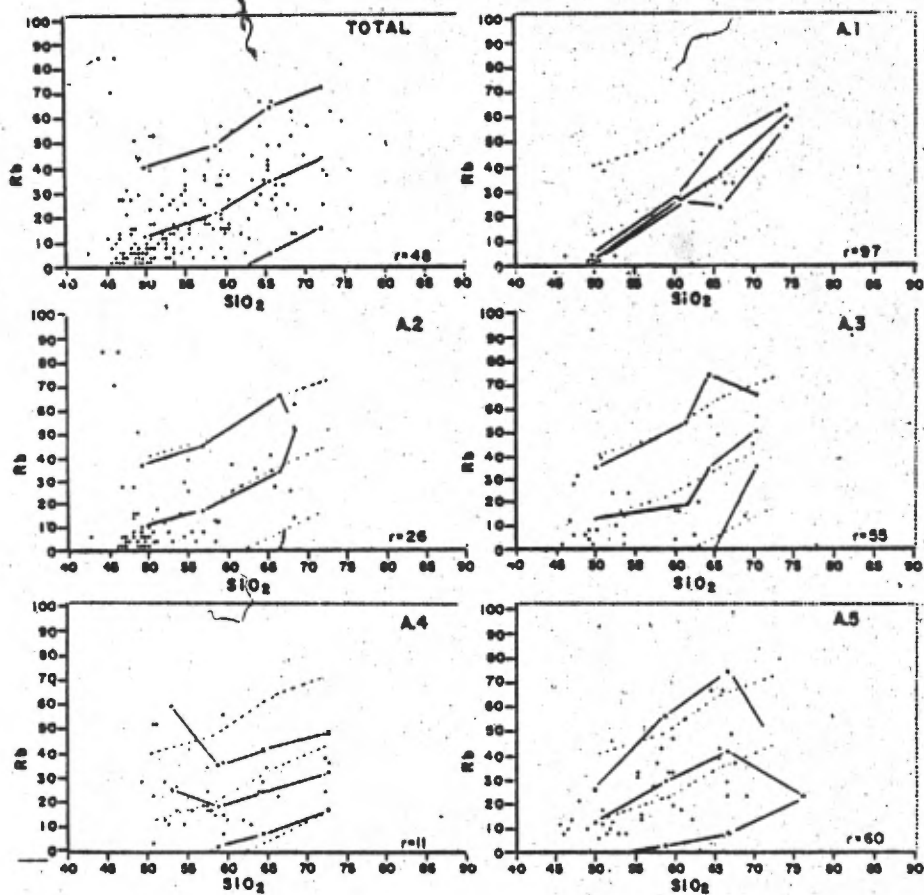


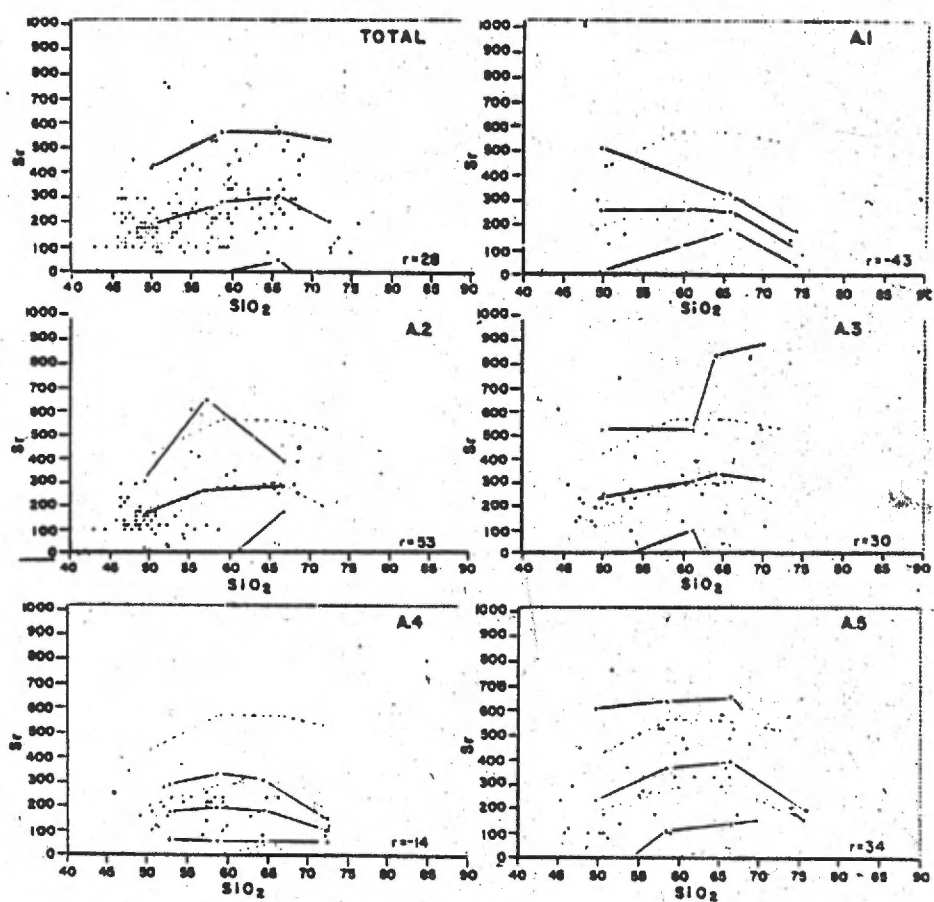


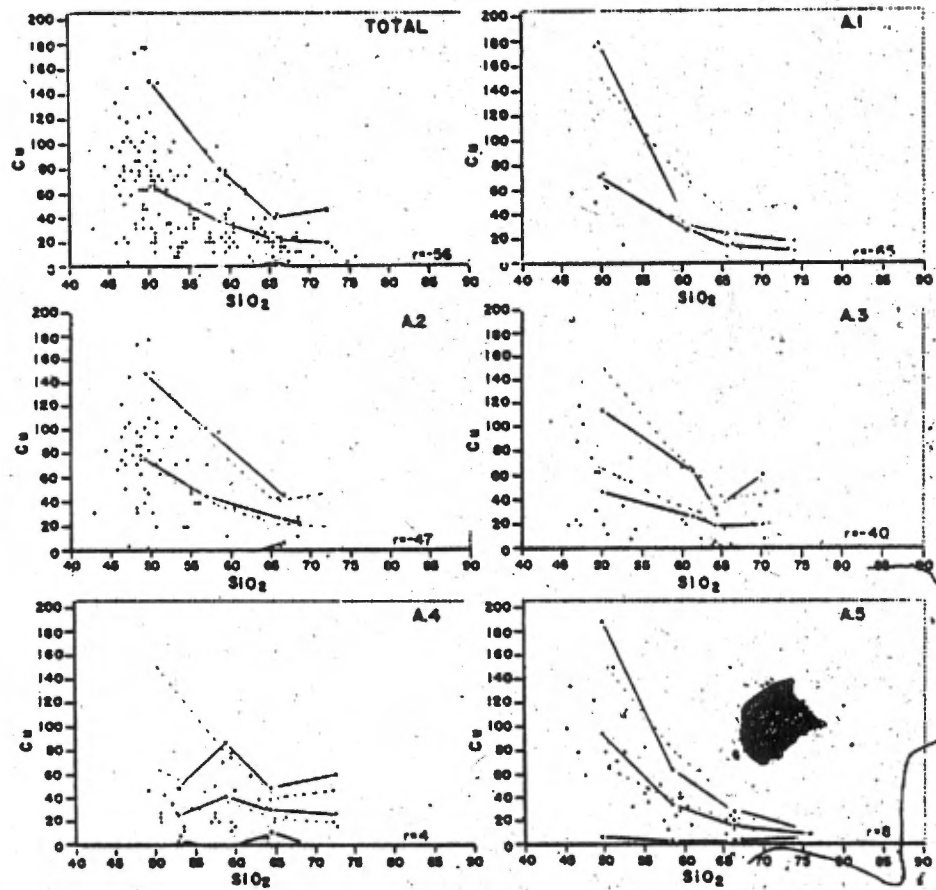


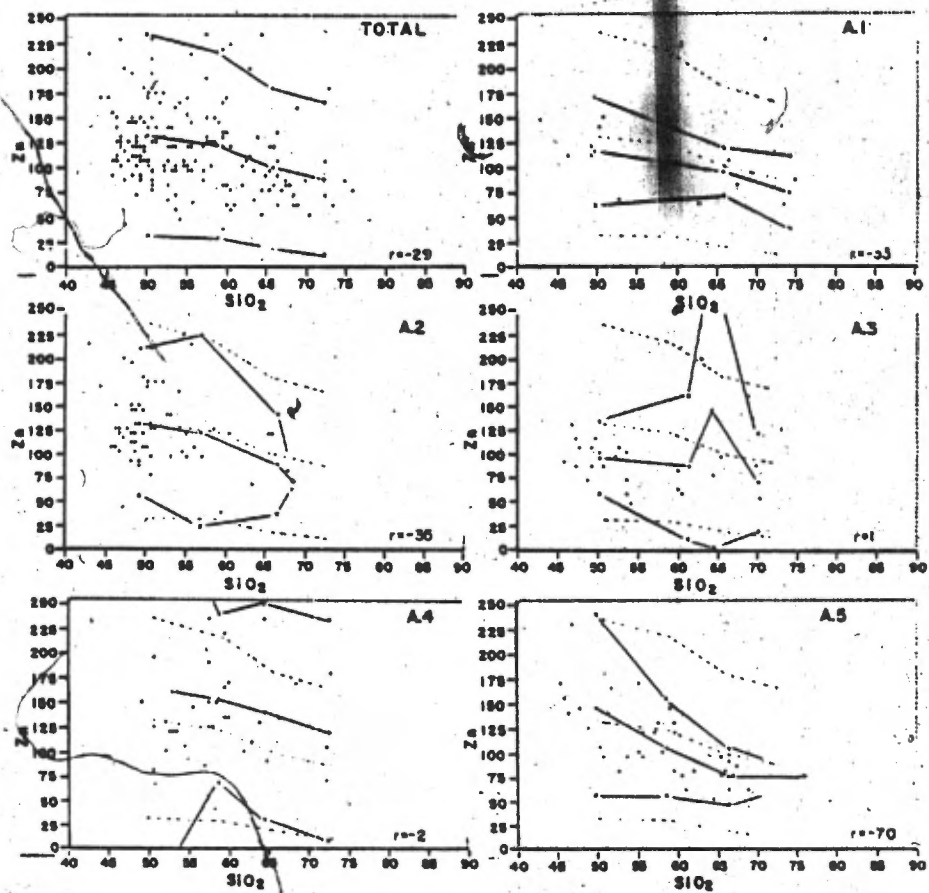


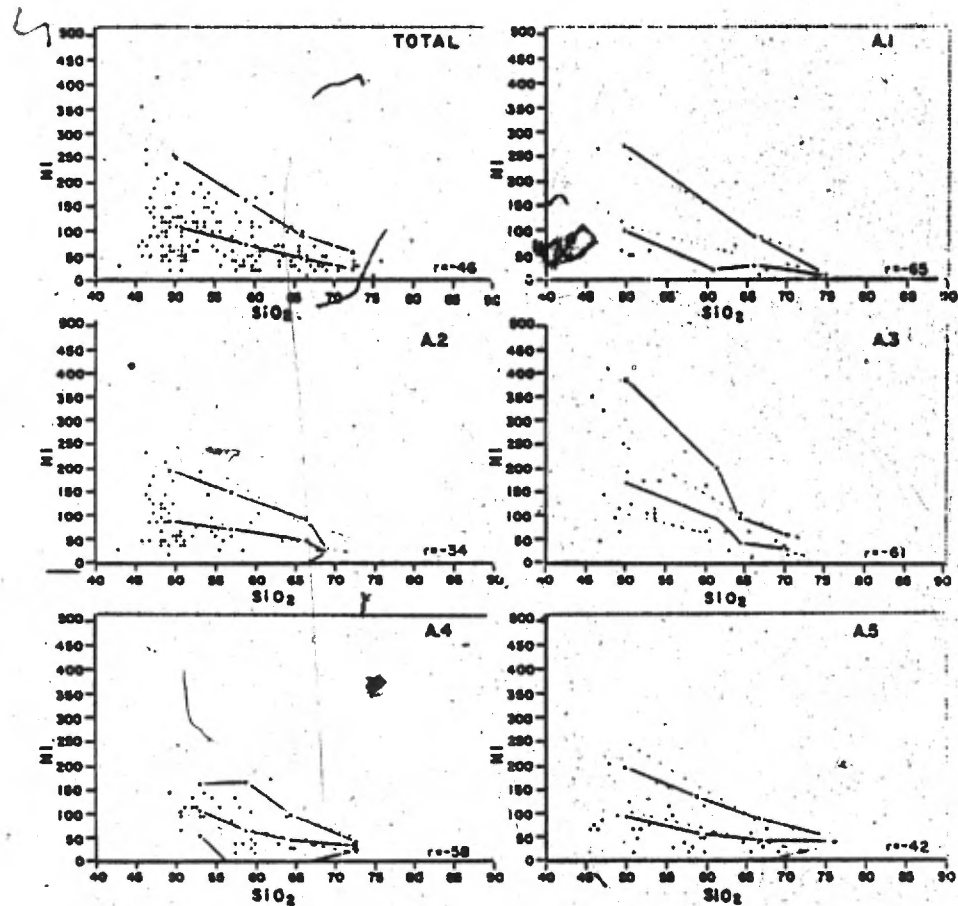


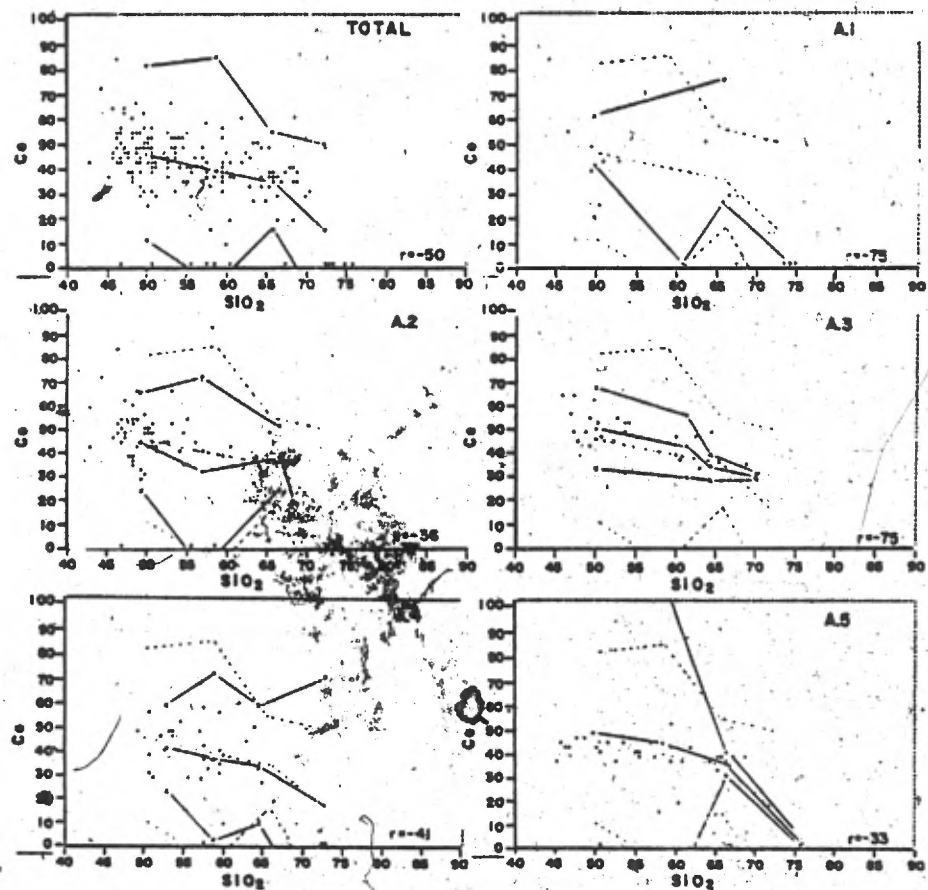


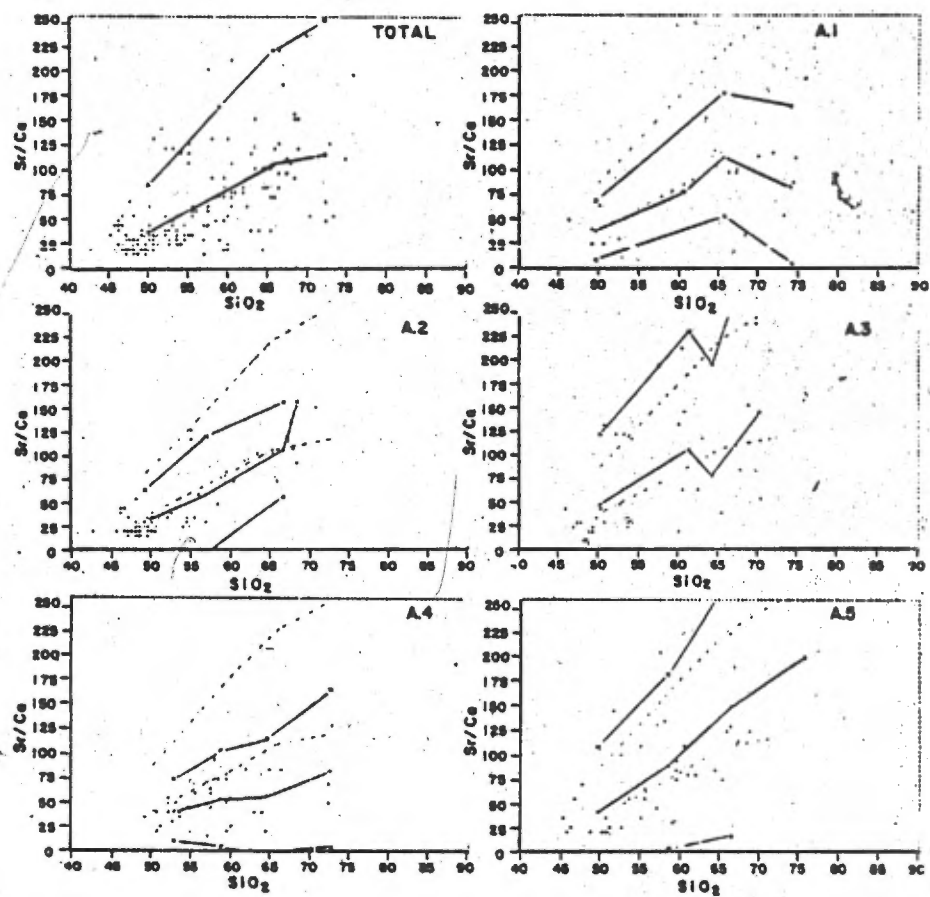


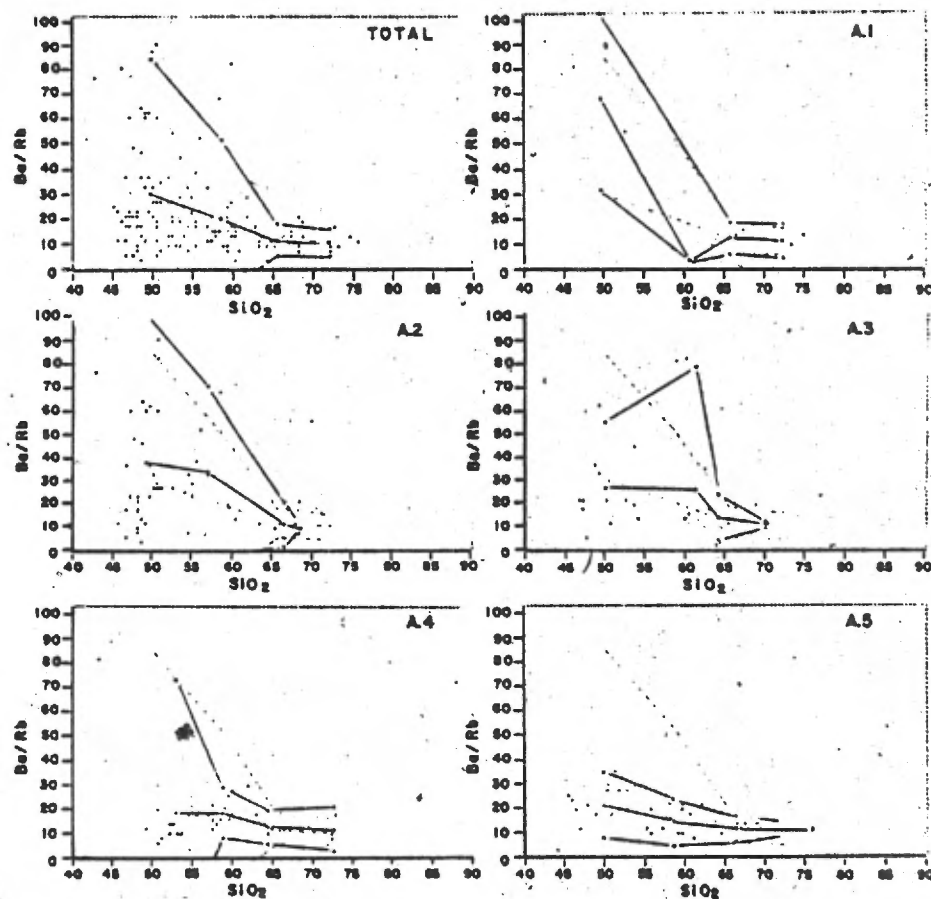


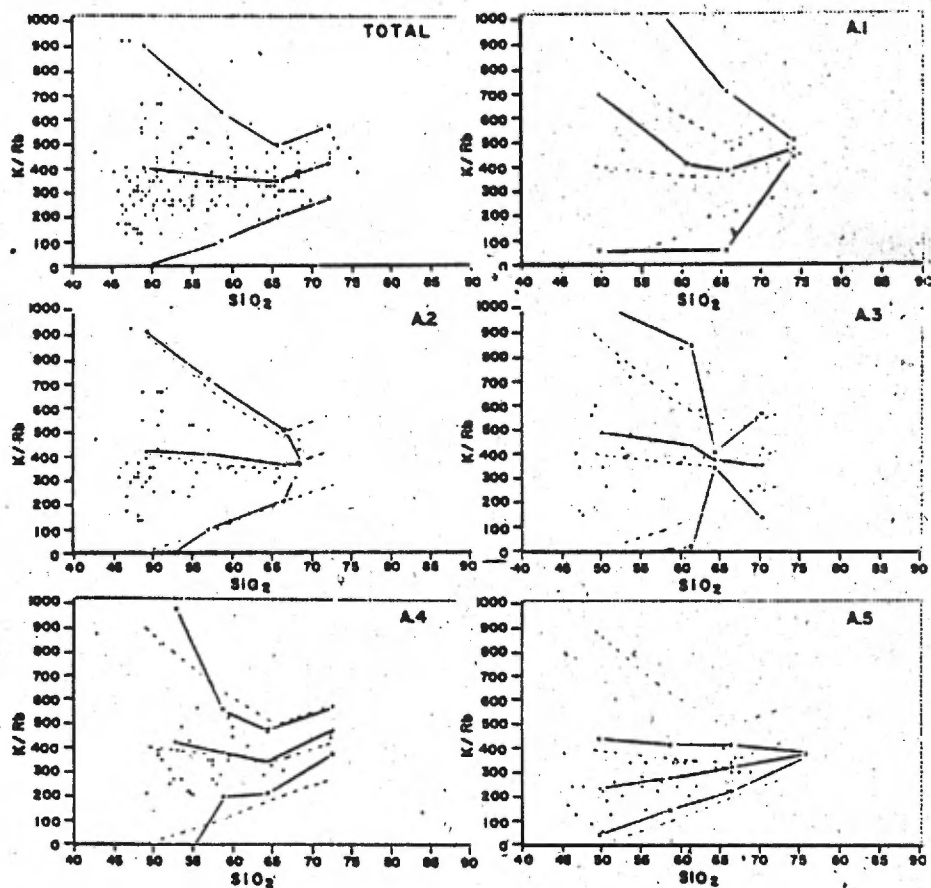


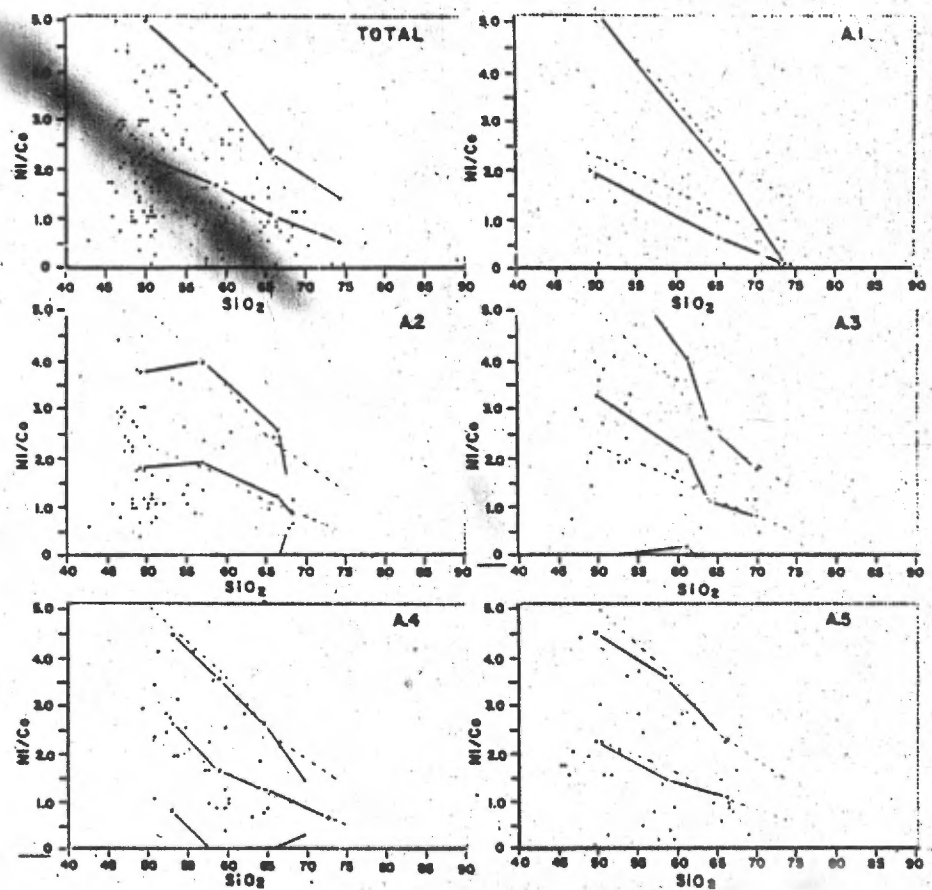












Appendix E
GEOCHEMICAL DATA FOR THE BACHELOR LAKE AREA

SPEC. NO.	SiO2	AL2O3	Fe2O3	FeO	MgO	CaO	Na2O	K2O	TiO2	MnO	P2O5	S	BA	BB	SR	CO	SB	CO	BI	K/BBB1/BBK/BBB/BBK/BAVI/CO					
L1	62.10	12.38	3.71	5.26	4.53	5.38	3.85	0.57	0.61	0.20	0.09	0.38	328	12	301	55	102	60	165	394	27	15	0.039	14	2.8
L2	51.85	15.07	3.92	7.68	7.11	7.54	2.43	0.36	1.04	0.20	0.21	0.01	142	12	266	32	100	45	106	249	12	11	0.045	21	2.4
L3	57.92	16.32	2.55	5.00	6.97	3.15	4.25	0.45	0.97	0.19	0.24	0.01	180	16	198	14	127	31	109	233	11	18	0.081	20	3.5
L4	54.41	15.35	3.70	7.35	4.97	7.29	2.71	0.50	0.91	0.29	0.17	0.05	153	10	200	27	106	51	129	415	15	20	0.050	27	2.5
L5	47.18	14.00	5.09	10.05	8.21	6.83	1.53	0.67	1.01	0.25	0.15	0.01	250	27	140	43	150	47	138	204	9	39	0.193	22	2.9
L6	60.10	13.48	3.12	6.04	4.11	4.93	4.03	0.63	0.84	0.18	0.19	0.02	301	12	177	45	136	38	34	435	25	29	0.068	17	0.9
L7	52.24	14.14	4.42	8.70	4.74	7.76	2.95	0.98	0.89	0.37	0.14	0.04	220	28	183	31	130	45	128	290	8	44	0.153	36	2.6
L8	57.32	16.66	3.16	6.20	3.37	4.97	4.16	0.58	1.23	0.30	0.14	0.01	234	18	204	47	125	58	127	267	13	23	0.084	20	2.2
L9	57.20	16.74	1.92	3.79	5.40	7.63	3.95	0.69	0.55	0.16	0.13	0.01	206	17	58	17	85	47	76	336	15	94	0.293	21	1.6
L10	50.68	14.93	2.71	5.32	8.02	7.85	2.64	0.98	0.71	0.13	0.17	0.01	387	22	88	14	80	56	57	369	18	92	0.250	21	1.0
L11	53.74	13.86	4.11	8.18	5.60	7.38	2.51	0.49	1.11	0.20	0.18	0.03	120	16	167	12	118	47	90	254	3	24	0.095	33	1.9
L12	53.14	14.65	4.11	8.09	5.18	6.51	2.92	1.03	1.04	0.19	0.17	0.01	170	23	218	5	120	48	93	371	7	39	0.105	50	1.9
L13	59.48	13.58	3.25	6.24	2.50	7.81	2.56	0.89	1.17	0.20	0.18	0.02	188	14	79	15	221	56	15	527	13	91	0.177	39	0.3
L14	64.27	11.82	2.91	5.78	1.82	6.03	2.34	1.53	0.99	0.19	0.28	0.03	198	28	68	35	234	31	21	453	7	186	0.411	64	3.7
L15	50.74	14.83	4.32	8.53	6.00	6.65	2.69	2.39	0.74	0.26	0.12	0.02	208	52	80	22	197	24	98	381	8	248	0.650	95	3.4
L16A	53.91	15.87	3.29	6.40	4.11	5.53	7.05	0.17	0.95	0.22	0.21	0.04	110	3	138	30	120	23	44	470	37	10	0.021	12	1.9
L16B	57.63	13.59	3.18	6.22	3.73	6.28	4.80	1.09	0.76	0.21	0.14	0.05	485	24	171	49	235	41	46	377	20	52	0.140	18	1.4
L17	50.56	16.25	4.34	8.50	5.00	6.41	4.41	0.16	1.43	0.24	0.26	0.02	111	1	152	19	124	37	86	1328	111	8	0.006	11	2.3
L18	70.11	12.69	1.81	3.57	2.35	2.84	0.45	3.41	0.44	0.58	0.08	0.06	268	60	66	18	220	12	25	471	4	429	0.909	105	2.0
L20	0.0	0.0	0.0	0.0	0.0	0.0	0.0	0.0	0.0	0.0	0.0	0.0	238	25	382	20	171	41	107	0	0	0.065	0	2.0	
L24	60.24	12.74	3.02	5.92	2.44	6.81	4.37	0.68	1.02	0.20	0.33	0.02	183	12	100	11	172	7	7	470	15	56	0.120	30	1.0
L27	56.71	15.67	3.09	6.00	4.09	6.75	1.39	2.90	0.89	0.24	0.13	0.04	258	90	111	27	211	48	45	267	3	216	0.411	53	0.4
L28	57.38	15.25	3.26	6.40	5.08	4.1	4.27	0.65	1.00	0.21	0.17	0.02	200	16	118	25	188	36	31	337	13	45	0.135	24	0.4
L29	58.28	14.43	3.33	6.60	4.61	4.34	4.26	0.47	0.99	0.22	0.14	0.04	200	14	225	67	152	35	28	278	14	17	0.062	19	0.8
L30	52.41	11.09	6.05	11.83	4.73	7.10	1.77	0.28	0.85	0.61	0.14	0.01	109	9	139	24	120	48	107	258	12	16	0.096	21	2.2
L35	52.46	14.87	2.29	4.50	9.39	7.93	3.23	1.92	0.60	0.15	0.17	0.09	418	33	477	44	114	47	241	482	13	33	0.049	34	5.1
L36A	54.79	15.02	2.78	5.48	6.39	1.69	5.88	0.34	0.85	0.14	0.02	0.16	78	5	79	17	90	27	30	564	14	35	0.063	43	1.1
L36B	59.10	16.51	2.84	5.58	4.26	1.41	6.79	0.46	0.84	0.09	0.24	0.08	60	6	61	14	89	41	33	634	10	62	0.098	63	0.8
L37	60.97	15.13	2.14	4.08	4.62	6.17	2.96	0.94	0.77	0.11	0.14	0.01	220	18	181	35	103	44	86	451	12	44	0.099	36	1.1
L38	54.40	15.33	2.89	5.68	9.27	5.54	2.32	1.02	0.75	0.13	0.13	0.01	149	16	179	27	112	43	35	529	9	47	0.089	54	0.6
L39	52.77	16.38	2.70	5.20	5.91	7.62	5.87	0.26	0.83	0.19	0.11	0.01	131	5	160	43	87	35	90	431	26	13	0.031	14	2.4
L40	51.12	15.62	3.48	6.86	2.94	10.89	5.15	0.63	0.92	0.21	0.17	0.02	150	20	200	140	270	975	394	261	8	26	0.100	34	0.4
L41	63.77	9.46	1.79	3.43	1.96	7.58	2.15	0.63	0.41	0.36	0.10	0.02	199	16	85	7	108	400	21	324	12	63	0.188	26	0.0
L42A	65.04	11.21	2.31	4.50	1.45	8.46	1.34	2.46	0.42	0.31	0.10	0.02	213	51	44	29	146	31	27	400	4	443	1.109	95	0.9
L42B	66.68	13.76	1.57	3.04	2.04	2.65	3.79	1.99	0.56	0.26	0.17	0.31	175	36	50	29	6210	18	14	458	5	239	0.720	94	0.4
L43	64.58	11.23	1.89	3.71	2.00	6.14	1.61	2.12	0.47	0.25	0.12	0.04	120	57	51	31	169	21	29	308	2	345	1.114	144	1.4

SPIC.NO.	STG2	AL203	PR203	FLO	NGO	CAO	BA20	K20	TIG2	RPO	P205	S	BA	BB	SR	CU	2R	CO	NI	K/BBBA/BAK/SBEB/SBR/BAVI/CO					
L44	55.55	13.92	2.74	5.32	10.01	5.25	1.77	1.64	0.74	0.29	0.12	0.01	210	23	270	0	152	40	44	591	9	50	0.085	64	1.1
L45	64.67	12.32	2.44	4.70	1.69	7.38	1.48	2.53	0.47	0.24	0.11	0.01	148	66	52	25	142	0	27	318	2	403	1.265	141	0.0
L47	54.39	15.32	3.91	7.64	3.83	1.29	3.04	2.42	0.80	0.21	0.13	0.03	271	54	70	6	426	34	42	358	5	286	0.800	74	1.2
L48	53.62	15.74	4.70	9.22	4.51	8.00	0.75	2.06	1.22	0.34	0.17	0.40	280	51	108	34	288	27	113	335	5	158	0.472	61	4.1
L50	53.47	16.93	3.49	6.96	5.81	6.32	2.23	1.50	0.82	0.15	0.14	0.02	172	26	160	6	158	45	141	478	7	77	0.163	72	3.1
L52	54.17	14.11	2.88	5.60	3.44	4.41	7.38	0.43	1.01	0.15	0.20	0.05	189	20	181	18	121	30	1	178	9	19	0.110	18	0.0
L53	72.63	11.10	1.69	3.30	1.43	1.27	5.27	1.26	0.43	0.13	0.08	0.05	100	23	60	43	71	48	31	454	8	174	0.383	58	0.6
L54	71.23	10.51	1.97	3.82	1.20	1.22	3.83	2.28	0.28	0.16	0.04	0.01	546	36	108	12	182	0	21	525	15	175	0.333	34	0.0
L55	65.24	14.01	1.75	3.40	2.07	3.80	5.52	1.30	0.95	0.13	0.16	0.02	322	34	223	15	88	26	23	317	9	48	0.152	33	0.0
L56	57.33	12.75	3.19	6.39	3.01	5.96	4.11	1.44	0.97	0.22	0.27	0.42	451	36	196	71	164	30	24	332	13	60	0.183	24	0.0
L57A	66.38	12.22	1.74	3.40	3.01	3.82	5.89	0.80	0.60	0.12	0.13	0.09	220	22	222	18	134	18	37	301	10	29	0.099	38	2.1
L57B	72.33	11.98	1.38	2.60	1.04	2.73	4.14	1.97	0.30	0.06	0.05	0.02	235	38	86	14	104	0	22	430	6	190	0.442	69	0.0
L58	59.73	14.40	2.30	4.40	4.31	4.72	6.61	0.37	0.47	0.12	0.11	0.13	140	6	229	74	137	39	99	511	23	13	0.026	21	2.5
L59	52.53	18.99	2.63	5.16	13.72	3.50	0.74	0.28	0.35	0.05	0.02	0.02	69	5	542	11	58	53	61	444	14	4	0.009	33	1.2
L60	62.99	12.31	2.61	5.03	3.57	5.32	4.30	0.40	0.93	0.19	0.15	0.05	155	10	142	37	110	44	25	332	16	28	0.070	21	0.6
L61	57.74	13.47	3.52	6.91	2.90	6.16	3.84	1.30	1.24	0.22	0.35	0.81	340	33	242	20	149	0	9	327	10	44	0.136	31	0.0
L62	55.35	14.40	3.27	6.41	6.24	5.75	3.78	1.01	0.91	0.22	0.17	0.01	223	15	227	27	143	27	110	558	15	36	0.066	37	4.1
L63A	48.53	14.17	5.04	9.95	7.43	6.82	3.26	0.43	1.09	0.22	0.09	0.01	155	14	85	85	143	54	83	254	11	41	0.164	23	1.5
L63B	54.49	11.82	4.43	8.61	6.65	6.67	2.85	0.25	0.99	0.22	0.08	0.03	123	4	108	71	99	47	58	518	31	19	0.037	16	1.2
L64	54.61	10.06	1.32	2.59	1.39	1.89	1.67	0.90	0.19	0.16	0.03	0.01	217	22	201	18	137	22	20	339	10	37	0.109	35	0.9
L65	52.44	12.85	5.16	10.88	3.98	8.17	2.52	0.17	1.43	0.26	0.14	0.46	150	6	200	93	142	43	68	235	25	7	0.030	9	1.5
L66	47.67	12.14	5.89	11.51	3.50	11.84	1.17	0.07	1.02	0.47	0.10	0.02	70	2	133	42	121	49	117	290	35	4	0.015	8	2.4
L67	46.77	15.47	5.17	10.64	5.03	12.61	1.42	0.11	0.81	0.28	0.07	0.08	60	1	98	103	114	67	179	913	60	10	0.011	15	2.9
L68	47.65	14.30	4.64	9.12	4.70	12.46	1.56	0.12	0.80	0.32	0.07	0.02	64	3	108	106	105	54	170	332	21	9	0.030	15	3.0
L70	60.55	15.95	2.46	4.63	2.75	6.04	2.96	1.35	0.64	0.15	0.12	0.06	402	35	334	32	121	41	104	320	11	33	0.105	27	2.5
L71	64.49	17.29	0.66	1.23	1.00	3.95	3.89	2.19	0.26	0.04	0.11	0.05	404	51	437	19	68	18	15	354	8	41	0.116	45	0.8
L73	50.09	14.90	2.48	5.23	6.30	12.97	3.60	0.69	0.85	0.19	0.58	0.01	618	28	980	25	117	48	307	286	31	5	0.020	9	6.4
L74	44.50	14.95	4.73	9.22	6.34	9.86	2.02	0.69	0.81	0.28	0.08	0.03	120	50	150	61	120	54	205	114	2	38	0.333	47	3.8
L75	63.72	12.44	2.50	4.41	1.98	6.21	3.86	0.82	0.68	0.18	0.18	0.20	282	24	166	27	131	49	86	283	12	41	0.145	24	1.8
L72	73.49	8.25	1.61	3.03	1.45	1.87	1.65	1.68	0.27	0.12	0.0	0.08	289	65	48	19	126	0	20	214	4	290	1.354	48	0.0
L83	69.46	12.03	2.28	4.42	2.13	2.72	3.33	1.79	0.71	0.18	0.17	0.13	345	47	111	8	194	0	25	316	7	133	0.432	43	0.0
L34	74.26	11.66	0.84	1.60	1.03	2.56	4.75	1.55	0.35	0.06	0.08	0.02	196	21	77	12	57	23	16	612	9	167	0.272	65	0.7
L85	70.34	11.30	1.21	2.38	1.19	4.74	4.37	3.08	0.45	0.08	0.10	0.29	254	50	131	63	76	38	17	511	5	195	0.382	100	0.5
L86	73.52	12.52	1.04	2.17	0.90	1.34	4.34	2.37	0.48	0.04	0.10	0.15	291	40	59	37	48	16	18	491	7	333	0.678	67	1.1
L87	64.44	12.33	1.17	2.38	1.11	4.90	3.89	3.50	0.47	0.04	0.11	0.21	325	65	92	20	76	8	23	447	5	315	0.707	89	0.0
L88	69.44	12.46	1.99	3.82	1.83	2.68	2.22	3.23	0.39	0.15	0.04	0.07	520	85	133	44	148	0	32	315	6	201	0.639	51	0.0

	SPEC. NO.	SI02	AL2O3	FE2O3	FeO	H2O	CaO	Na2O	K2O	TiO2	MnO	P2O5	S	BA	BB	SR	CU	ZN	CO	BI	K	BRRA	BOR	SI00	SRK	BAPI	CU
L89	71.75	11.56	1.72	3.23	1.57	2.88	3.57	1.44	0.48	0.11	0.12	0.43	440	33	110	28	128	0	23	362	13	108	0.300	27	0.0		
L90	69.08	12.41	2.36	4.41	1.97	2.31	3.41	2.43	0.73	0.15	0.07	0.27	335	63	90	35	179	41	30	320	5	224	0.700	40	0.7		
L91	68.05	14.35	1.06	2.12	1.14	2.47	4.59	3.22	0.65	0.09	0.18	0.11	262	53	142	15	91	0	27	504	5	188	0.373	152	0.0		
L92	65.64	13.38	2.40	4.61	1.88	4.31	2.24	2.05	0.57	0.19	0.11	0.08	344	71	77	14	104	0	37	333	5	307	0.922	68	0.0		
L93	69.09	10.81	1.41	2.66	1.37	6.06	4.05	2.09	0.45	0.14	0.11	0.13	325	41	147	16	100	27	25	421	8	117	0.279	53	0.9		
L94	50.55	14.86	2.44	4.77	5.83	11.98	3.86	2.82	0.49	0.23	0.15	0.02	542	103	278	14	167	65	57	227	5	84	0.371	43	0.9		
L95	74.47	8.39	1.43	2.73	1.23	2.64	0.98	5.10	0.30	0.08	0.07	1.30	434	83	94	60	178	9	21	510	5	450	0.883	97	0.9		
L96	65.41	11.99	2.32	4.60	2.27	5.61	4.29	0.70	0.51	0.18	0.10	0.05	319	22	146	17	184	34	32	264	15	39	0.151	14	0.9		
L97	63.13	12.46	2.33	4.60	3.12	3.88	4.51	2.69	0.66	0.17	0.13	0.04	469	56	222	13	172	25	29	398	8	100	0.252	47	1.2		
L98	64.28	12.17	2.47	4.93	3.01	4.10	3.05	2.82	0.72	0.17	0.14	0.03	883	65	138	24	155	40	35	360	14	169	0.471	26	0.9		
L99	55.08	17.33	2.13	6.01	3.13	5.97	2.54	3.55	1.02	0.17	0.18	0.02	1008	80	121	11	145	5	49	368	13	243	0.661	29	9.4		
L100	69.98	14.93	2.45	4.68	3.08	3.58	6.79	0.64	0.70	0.13	0.14	0.02	84	21	106	23	122	0	27	252	4	50	0.198	63	0.0		
L101	57.93	15.97	2.62	5.03	3.94	5.05	3.60	2.62	0.96	0.14	0.16	0.01	274	63	174	10	122	43	62	345	4	124	0.362	79	1.4		
L102	56.78	15.98	2.87	5.58	4.19	5.84	2.64	2.64	1.03	0.17	0.18	0.01	268	61	170	24	126	17	65	362	4	129	0.358	82	3.4		
L103	51.66	16.79	2.69	5.36	3.49	11.56	4.02	1.14	1.01	0.22	0.21	0.02	230	37	215	27	144	17	92	255	6	44	0.172	41	5.4		
L106	47.65	12.83	3.42	6.62	5.73	11.86	4.43	3.60	0.90	0.30	0.13	0.25	208	123	330	45	176	51	99	242	2	90	0.372	143	1.9		
L104	53.75	14.48	2.82	5.42	4.38	8.17	4.50	2.64	0.97	0.17	0.19	0.08	160	100	285	23	108	34	77	219	2	76	0.350	136	2.3		
L107	59.04	11.70	2.48	4.88	3.41	8.32	2.24	4.53	0.74	0.17	0.12	1.04	440	129	178	33	131	26	33	291	3	211	0.724	45	1.3		
L108	69.82	15.76	0.42	8.79	0.74	1.52	4.25	3.70	0.12	0.01	0.06	0.03	1632	46	792	12	72	0	0	667	35	38	0.059	14	0.0		
L108B	73.48	13.14	0.34	0.78	0.51	1.09	5.14	4.58	0.02	0.0	0.03	0.09	282	70	160	4	37	14	0	543	4	237	0.248	134	0.0		
L109	93.02	0.48	0.91	1.68	0.89	2.61	0.67	0.16	0.0	0.0	0.06	0.01	582	0	294	531	936	32	12	0	0	5	0.0	2	0.4		
L111	45.78	0.63	0.73	1.40	9.50	0.74	0.26	0.39	0.0	0.0	0.04	0.71	612	6	33	999	62	44	0	539	102	98	0.182	5	0.0		
L112	70.72	11.45	1.05	2.00	1.18	3.13	3.32	5.03	0.36	0.08	0.11	0.97	381	75	140	15	80	62	9	554	5	298	0.535	109	0.2		
L113	74.51	10.50	1.18	2.27	1.31	2.42	4.60	1.22	0.41	0.10	0.11	0.07	335	30	88	30	96	62	11	337	11	115	0.341	30	0.2		
L114	75.88	7.37	1.81	3.44	1.01	2.29	1.37	4.84	0.28	0.03	0.07	3.32	218	56	79	5	68	20	13	717	4	508	0.709	144	0.7		
L115	57.10	13.74	2.84	5.59	2.57	6.07	5.68	2.83	0.88	0.24	0.17	0.48	363	77	152	78	118	11	17	305	5	154	0.507	64	1.5		
L116	54.19	13.70	1.05	5.55	3.88	7.09	4.87	3.37	1.10	0.17	0.16	1.24	281	187	198	139	109	26	13	261	3	141	0.540	99	0.5		
B1	44.23	4.93	4.83	13.28	9.72	9.80	0.55	0.71	1.78	0.48	0.13	0.05	435	83	188	120	152	84	1270	71	5	31	0.441	13	15.1		
B2	53.04	10.21	4.94	9.80	12.22	2.28	1.38	0.41	2.87	0.07	0.35	0.05	217	12	140	100	93	65	540	283	18	24	0.085	15	6.3		
B3	62.81	5.15	1.92	7.62	3.22	12.05	0.48	0.63	1.57	0.31	0.17	0.12	502	27	220	122	96	95	565	193	19	23	0.123	10	5.9		
B4	44.17	6.38	7.28	14.40	8.31	11.65	0.30	1.81	1.73	0.43	0.15	0.04	658	84	85	81	170	71	1010	178	0	176	0.988	22	14.2		
B5	50.03	12.91	5.17	10.15	4.60	10.66	1.99	0.33	1.20	0.23	0.08	0.02	142	8	88	142	146	52	16	342	18	31	0.090	19	0.3		
B6	49.95	13.72	6.16	12.10	5.89	3.99	3.72	0.16	1.08	0.13	0.08	0.14	126	4	78	122	173	50	45	332	32	17	0.051	10	0.9		
B7	58.43	6.57	4.14	9.34	10.66	2.68	1.15	0.46	1.31	0.0	0.16	0.18	163	2	239	62	54	68	1050	1909	82	15	0.008	23	15.4		
B8	59.57	14.90	1.42	6.74	6.05	11.48	3.44	0.14	0.80	0.21	0.05	0.02	90	1	160	91	125	48	75	1142	90	7	0.006	12	1.6		
B9	48.75	16.25	1.86	7.68	5.56	11.45	3.27	0.16	0.84	0.22	0.0	0.01	83	5	159	48	73	44	103	265	17	8	0.031	16	2.3		

SPEC. NO.	SI02	AL2O3	FE2O3	PEG	H2O	CAO	HA2O	K2O	TIO2	H2O	P2O5	S	BA	BB	SB	CB	EB	CO	BT	E/SBBB/BBK/SBBB/SBK/SBNT/CO					
B10	43.06	16.98	3.61	7.11	5.28	11.76	3.21	0.19	0.85	0.21	0.0	0.01	89	9	297	87	110	0	100	175	10	5	0.030	17	0.0
B11	50.05	16.69	3.46	7.58	6.24	11.29	2.70	0.28	0.82	0.20	0.0	0.01	162	10	356	51	114	49	124	232	16	6	0.028	14	2.5
B12	52.80	17.42	2.60	5.16	2.50	11.78	4.62	0.39	1.04	0.22	0.10	0.02	170	21	525	31	90	58	105	154	8	6	0.040	19	1.4
B17	65.42	15.01	1.09	3.03	3.90	3.72	4.10	1.31	0.57	0.09	0.14	0.02	280	39	268	25	122	47	43	278	7	40	0.146	38	0.9
B24	68.11	14.26	1.31	2.56	3.28	3.59	3.76	0.88	0.52	0.08	0.12	0.01	230	24	272	18	82	39	20	304	10	26	0.088	31	0.5
B28	54.41	11.48	5.17	10.13	2.56	9.78	1.73	0.73	0.49	0.40	0.12	0.01	139	28	218	16	226	34	88	216	5	27	0.128	43	2.6
B2C	46.66	10.17	8.53	16.60	3.07	8.86	0.86	0.68	0.45	0.69	0.10	0.15	90	25	92	48	124	0	80	225	4	61	0.271	62	0.0
B3	48.74	13.52	3.50	6.60	10.92	11.38	1.74	0.08	0.61	0.20	0.07	0.03	45	1	90	92	111	65	109	644	45	7	0.011	14	1.7
B4	48.16	13.46	4.16	8.20	9.32	10.89	1.79	0.13	0.80	0.23	0.08	0.01	60	3	91	32	108	33	88	359	20	11	0.032	17	2.7
B5	48.03	13.64	7.79	11.69	5.29	7.78	3.34	0.40	1.75	0.28	0.16	0.07	193	25	287	66	193	36	32	132	8	11	0.087	17	0.9
B6	50.19	11.71	5.37	11.60	5.38	7.42	2.14	0.20	1.85	0.30	0.17	0.03	181	7	166	69	171	42	38	237	26	10	0.042	9	0.9
B7	52.05	12.23	5.10	9.66	5.91	5.03	4.17	0.46	1.82	0.22	0.16	0.08	360	10	99	59	176	44	45	381	36	38	0.101	10	1.0
B8	48.67	12.60	5.71	11.38	8.08	5.94	2.43	0.13	1.46	0.21	0.13	0.12	125	2	99	70	132	42	37	539	63	10	0.020	8	0.9
B9A	49.64	11.52	5.36	10.40	4.16	10.17	3.21	0.07	1.60	0.28	0.11	0.08	122	2	155	80	146	30	51	290	61	3	0.012	4	1.7
B9C	45.43	12.02	5.67	11.20	5.35	12.37	0.35	2.61	1.62	0.45	0.13	0.03	662	70	124	63	107	45	44	309	9	174	0.565	32	1.0
B10A	66.42	12.64	1.45	2.60	3.28	3.57	4.76	0.67	0.48	0.09	0.13	0.04	229	12	380	22	72	40	43	463	19	14	0.032	24	1.1
B19B	67.07	13.19	0.90	1.73	1.67	5.13	4.70	1.40	0.35	0.05	0.11	0.63	288	21	310	16	274	31	33	553	14	37	0.067	40	1.1
B11	48.16	19.98	7.36	11.85	5.73	9.32	2.63	0.20	1.54	0.27	0.14	0.08	181	12	151	95	152	38	41	138	15	10	0.079	9	1.0
B12	55.92	11.95	2.63	5.13	6.85	9.75	4.19	0.09	0.58	0.18	0.26	0.12	52	1	390	37	104	44	37	747	52	1	0.026	14	0.8
B13	50.62	14.08	4.08	7.98	4.41	10.26	2.52	0.08	1.10	0.22	0.12	0.36	81	1	147	102	94	41	46	664	81	4	0.007	8	1.1
B14	49.96	13.71	3.89	7.63	7.05	10.83	2.87	0.08	1.08	0.22	0.13	0.08	89	0	127	27	103	47	51	0	8	5	0.0	7	1.0
B15	48.98	10.57	7.62	12.35	4.31	7.78	2.46	0.14	2.36	0.26	0.24	0.11	181	3	115	34	152	28	8	387	60	10	0.026	6	0.3
B16	58.25	11.26	5.32	10.42	3.28	2.71	3.74	0.08	1.72	0.21	0.37	0.18	133	2	84	95	125	0	22	332	67	7	0.024	4	0.0
B17	58.38	15.79	2.55	4.59	5.20	4.59	2.75	2.60	0.77	0.17	0.17	0.15	510	76	351	54	111	40	190	283	7	61	0.217	41	4.8
B18	46.97	13.27	4.90	9.61	8.54	10.05	2.25	0.10	1.07	0.23	0.05	0.03	62	3	102	0	41	45	96	276	21	8	0.029	13	2.1
B20	50.29	11.53	5.43	10.44	5.20	7.27	4.49	0.15	1.54	0.22	0.15	0.10	124	0	93	60	148	41	42	0	0	13	0.0	18	0.0
B22	49.88	10.45	5.68	11.11	5.85	10.39	1.68	0.07	1.51	0.25	0.14	0.09	103	0	427	73	130	23	41	0	0	1	0.0	6	1.8
B23	45.96	15.28	4.22	8.26	10.65	10.19	1.00	0.11	0.51	0.22	0.05	0.02	80	1	322	55	111	53	263	913	80	2	0.003	11	5.0
B24	44.87	12.92	4.10	7.46	9.19	11.31	2.72	0.09	0.63	0.23	0.04	0.05	54	0	163	49	110	48	188	0	0	5	0.0	14	2.3
B25	60.70	15.00	3.00	5.87	2.22	4.67	4.16	1.23	0.84	0.16	0.21	0.01	27	25	248	24	225	0	7	408	1	41	0.101	378	0.0
B26	49.02	13.00	4.98	9.75	7.03	10.31	1.40	0.06	0.91	0.22	0.11	0.02	69	0	276	174	118	37	48	0	0	2	0.0	7	1.3
B27	67.52	15.41	1.21	2.37	1.54	4.17	3.97	1.85	0.44	0.07	0.15	0.01	412	32	280	7	80	0	8	479	13	54	0.114	37	0.0
B28A	57.86	2.99	2.91	5.72	18.67	7.41	0.57	0.11	0.51	0.14	0.03	0.01	31	1	37	5	58	60	380	913	31	24	0.027	29	6.3
B28B	59.43	2.97	2.61	6.86	18.70	5.11	0.41	0.11	0.52	0.10	0.03	0.01	22	2	40	6	42	70	363	456	11	22	0.050	41	5.2
B29A	52.47	12.77	4.32	8.45	5.76	4.74	3.09	0.11	1.21	0.17	0.17	0.01	108	2	146	12	66	41	52	456	54	6	0.014	8	1.3
B29B	47.97	14.0	1.83	1.62	1.67	1.58	1.33	0.44	0.22	0.04	0.26	0.01	102	1	47	0	9	40	32	3652	102	41	0.012	35	0.8

SPEC. NO.	SI02	AL203	FE203	FLO	HGO	CAO	HA2O	K2O	TIO2	HNO	P2O5	S	BA	BB	SR	CU	SB	CO	NI	E/BBBA/BBK/SPRR/SRR/BAWI/CO					
B010	58.02	3.93	2.52	7.06	17.24	9.43	0.76	0.12	0.64	0.16	0.03	0.01	42	2	50	10	60	60	329	498	21	19	0.040	23	5.5
B031	56.03	3.56	3.56	7.98	15.77	8.13	0.71	0.13	0.71	0.17	0.03	0.03	53	0	69	201	70	55	327	0	0	13	0.0	17	5.9
B032	63.34	10.05	1.10	8.02	1.35	4.37	4.60	0.16	1.04	0.19	0.36	0.02	107	3	105	6	94	0	32	442	36	12	0.029	12	0.0
B033	58.23	12.92	3.10	4.06	7.96	6.15	0.59	1.23	0.85	0.16	0.14	0.01	198	53	220	10	118	47	101	192	4	46	0.241	51	2.2
B034	63.31	15.09	1.91	3.74	-5.30	1.97	5.10	0.94	0.67	0.11	0.16	0.01	308	43	209	14	97	49	55	181	7	37	0.204	25	1.1
G1	59.63	14.48	2.31	4.52	5.77	5.60	3.89	0.77	0.64	0.10	0.14	0.01	349	19	326	6	36	38	83	336	18	19	0.058	18	2.2
G2	53.07	4.67	1.95	7.50	14.71	10.35	1.50	0.15	0.70	0.21	0.02	0.01	83	3	95	78	92	54	271	415	28	13	0.032	15	5.0
G3	55.39	9.92	6.59	12.90	2.37	3.15	3.68	0.23	2.21	0.25	0.24	0.10	220	6	70	36	214	0	22	318	37	27	0.046	4	0.0
G4	48.10	11.44	5.62	11.02	6.54	9.00	3.24	0.18	1.35	0.22	0.13	0.35	110	5	111	171	146	53	57	298	22	13	0.045	13	1.1
G5	49.17	13.44	4.34	8.51	8.31	10.75	2.28	0.20	0.93	0.19	0.08	0.03	85	14	144	29	89	59	123	118	6	11	0.097	19	2.1
G6	48.24	13.82	4.51	8.63	7.75	10.32	2.55	0.23	0.94	0.21	0.09	0.07	91	6	155	82	121	51	113	318	15	12	0.039	20	2.2
G7	50.67	13.33	3.76	7.34	6.63	10.48	3.23	0.31	1.00	0.18	0.11	0.02	125	5	160	17	74	51	61	514	25	16	0.031	20	1.2
G9	46.69	11.61	4.27	12.28	6.18	9.09	2.61	0.13	1.63	0.22	0.09	0.09	109	3	126	69	118	49	36	359	36	8	0.024	9	0.7
G10	66.16	13.37	1.58	3.07	4.06	4.49	3.68	0.94	0.57	0.09	0.15	0.16	247	26	230	39	121	36	86	306	10	34	0.113	32	2.4
G11	51.22	10.68	3.97	7.76	6.69	9.87	2.69	0.27	1.47	0.20	0.10	0.01	294	2	290	69	138	52	189	1120	147	7	0.007	7	1.6
G12	47.69	12.72	5.09	9.95	7.18	9.52	2.97	0.07	1.48	0.24	0.12	0.03	93	2	88	77	126	37	83	290	47	6	0.023	6	2.3
G13	46.90	13.06	5.13	10.66	7.57	10.20	2.52	0.07	1.23	0.24	0.09	0.03	84	0	220	145	201	48	115	0	0	3	0.0	7	2.4
G14	48.62	12.91	4.42	8.68	9.38	10.07	1.73	0.06	0.90	0.22	0.07	0.04	50	0	185	74	100	54	142	0	0	3	0.0	10	2.6
G15	66.58	15.40	1.67	3.24	1.73	3.34	4.12	1.72	0.55	0.11	0.15	0.02	368	31	221	11	163	28	1	460	12	64	0.140	36	3.0
G16	75.02	13.52	0.45	0.83	0.62	0.78	4.68	3.14	0.07	0.03	0.03	0.02	780	58	61	0	85	0	0	449	12	427	0.951	37	0.0
G17	73.72	14.50	0.43	0.84	0.63	2.97	2.36	3.49	0.07	0.05	0.04	0.02	420	61	110	9	59	0	0	474	7	263	0.555	64	0.0
G19	68.46	14.90	0.68	2.81	1.79	3.58	3.45	3.08	0.44	0.07	0.12	0.01	316	61	232	8	61	34	19	419	5	110	0.241	80	0.6
G20	62.93	13.95	1.72	3.33	3.18	7.73	2.12	2.30	0.61	0.13	0.18	0.09	589	65	535	30	84	43	55	293	9	35	0.122	32	1.3
G21	42.72	9.87	8.56	16.75	4.60	8.03	1.87	0.22	3.70	0.25	0.20	0.02	301	4	84	26	215	41	19	456	75	23	0.048	6	0.8
G22	59.08	11.49	5.22	8.24	2.15	4.71	4.42	0.11	1.40	0.21	0.47	0.12	132	3	117	21	106	0	23	304	44	7	0.026	6	0.0
G23	48.81	15.10	3.01	5.91	10.35	11.21	2.27	0.20	0.49	0.19	0.05	0.02	58	6	144	100	89	32	96	276	10	11	0.042	28	3.0
G24	51.01	12.13	5.50	10.79	6.65	4.91	3.78	0.07	1.61	0.21	0.21	0.03	107	1	100	59	174	41	41	581	107	5	0.010	5	1.0
G25	51.14	12.09	5.40	10.54	7.65	4.65	2.10	1.27	1.47	0.24	0.25	0.05	411	16	92	72	127	40	29	658	26	114	0.174	25	0.7
G26	50.74	10.95	6.17	12.11	5.07	6.73	2.78	1.10	1.59	0.31	0.25	0.09	120	2	64	67	208	44	27	415	60	12	0.031	6	0.6
G27	54.75	13.18	3.16	6.21	9.43	4.84	2.73	1.53	0.77	0.16	0.27	0.06	498	24	426	45	97	34	48	529	21	29	0.056	25	1.4
G28	48.81	14.60	4.99	9.74	5.49	8.00	3.65	0.16	1.36	0.22	0.21	0.04	121	0	111	48	86	44	24	0	0	12	0.0	11	0.6
G29	49.54	11.43	5.56	10.79	7.27	6.91	3.08	0.08	1.48	0.25	0.19	0.09	110	0	140	174	180	47	53	0	0	5	0.0	6	1.1
G30	44.50	16.09	5.45	11.05	6.96	4.98	4.71	0.06	0.86	0.23	0.06	0.06	62	0	80	101	118	43	132	0	0	6	0.0	8	3.0
G31	46.23	14.61	5.12	8.63	10.25	8.59	2.58	0.06	0.70	0.22	0.05	0.04	43	0	219	72	104	52	231	0	0	2	0.0	12	4.4
G32	46.45	15.21	4.65	9.11	10.26	7.49	2.79	0.06	0.74	0.21	0.05	0.06	47	3	209	81	101	54	156	166	16	2	0.014	10	2.0
G33	46.19	13.73	4.79	9.34	8.92	9.71	2.93	0.06	0.87	0.23	0.06	0.04	68	0	284	92	124	48	139	0	0	2	0.0	7	2.9

SPEC. NO.	ST02	AL2O3	FE2O3	FIO	HGO	CAO	FA2O	K2O	TIO2	HNO	P2O5	S	BA	BB	SB	CU	ZN	CO	NI	K/BBBA/BBK/SBBB/SBK/BBBI/CO					
G34	63.30	15.96	2.13	4.16	1.69	3.47	5.62	1.29	0.71	0.11	0.12	0.19	309	33	251	23	66	26	35	324	9	42	0.131	34	1.4
G36	58.92	17.13	2.30	4.58	4.63	7.07	3.89	1.21	1.35	0.20	0.29	0.04	1039	38	604	49	121	53	51	264	27	16	0.063	9	1.0
DU1A	59.38	16.40	1.49	2.94	2.79	8.32	9.44	0.65	0.42	0.09	0.09	0.04	103	20	100	179	45	32	20	269	5	53	0.200	52	0.6
DU1B	49.29	11.10	3.65	7.14	7.01	12.53	2.95	2.27	0.85	0.25	0.08	0.02	391	63	362	32	135	51	45	299	6	52	0.174	48	0.8
L72	53.19	13.25	4.03	7.9	5.50	4.86	2.07	4.14	1.91	0.17	0.21	0.46	762	134	205	285	125	54	69	256	6	167	0.654	45	1.3
D01	76.00	11.00	0.95	1.87	1.05	1.29	5.43	1.00	0.19	0.06	0.03	0.01	190	22	178	3	73	0	32	377	9	46	0.124	43	0.0
D76	56.27	16.32	2.25	4.41	2.22	7.65	5.88	0.80	1.73	0.21	0.54	0.33	244	18	480	10	146	0	9	368	14	13	0.038	27	0.0
D05	50.29	8.91	6.57	12.87	3.66	7.72	3.40	0.84	1.42	0.46	0.62	0.82	237	16	167	84	232	0	11	435	15	41	0.096	29	0.0
D06	50.08	16.51	2.03	4.00	2.16	5.50	5.65	1.86	1.83	0.15	0.56	0.03	525	42	510	6	101	14	18	367	13	30	0.002	29	1.3
D07	59.28	13.18	2.67	5.23	2.42	6.50	4.83	1.33	1.82	0.14	0.27	0.33	529	32	420	40	132	52	41	345	17	26	0.076	20	0.4
D08	44.87	12.50	6.21	12.22	6.03	9.68	2.58	0.46	1.96	0.25	0.15	0.20	226	10	213	96	172	35	61	381	23	17	0.047	16	1.7
D09	44.69	14.98	5.20	10.20	6.67	9.84	3.11	0.65	1.43	0.22	0.16	0.11	249	15	255	39	142	35	107	359	17	21	0.059	21	3.1
DU10	54.31	16.56	2.74	5.36	2.67	4.08	7.12	0.90	1.65	0.16	0.52	0.06	471	16	740	18	139	26	6	466	29	10	0.022	15	0.2
DU11	58.29	23.44	1.17	2.30	1.35	1.52	7.94	3.10	0.61	0.08	0.22	0.0	1142	35	390	0	78	0	0	735	33	65	0.090	22	0.0
D112	57.24	14.56	2.04	5.42	5.06	5.03	5.17	0.69	1.20	0.14	0.14	0.05	224	25	153	46	118	43	30	229	9	37	0.166	25	0.7
L21	49.11	12.62	5.04	9.88	3.63	10.63	4.36	1.39	1.11	0.11	0.09	0.04	151	52	138	167	110	20	44	221	3	83	0.377	74	2.2
L72	47.56	13.48	7.40	6.35	8.04	10.29	2.62	0.52	0.87	0.22	0.08	0.14	120	30	192	101	106	44	409	143	4	22	0.154	35	9.3
L73	60.19	13.11	1.86	3.65	3.45	9.86	5.01	0.10	0.59	0.14	0.14	0.06	82	1	120	64	62	38	63	430	82	6	0.008	10	1.7
L75	55.98	12.84	1.76	3.46	7.58	9.78	5.44	0.11	0.43	0.16	0.16	0.0	0	0	0	0	0	0	0	0	0	0	0	0	0.0
L76	64.25	15.52	1.80	3.53	3.22	3.95	2.85	2.54	0.49	0.13	0.10	0.04	41	55	277	25	76	48	100	383	1	76	0.199	514	2.1
L77	62.38	16.07	1.40	2.74	3.85	4.09	4.90	2.20	0.50	0.10	0.17	0.08	1255	43	774	19	72	36	61	424	29	23	0.054	14	1.7
L78	51.93	11.42	3.11	6.10	10.46	8.41	2.45	1.99	0.85	0.17	0.10	0.05	530	21	730	57	94	43	174	786	25	22	0.029	31	4.1
L19	69.05	12.35	1.04	2.09	2.61	4.31	5.97	0.35	0.33	0.12	0.09	0.01	219	12	455	17	160	33	37	242	18	6	0.026	13	1.1
L710	61.13	17.05	1.63	3.21	1.75	6.10	4.20	0.82	0.50	0.14	0.18	0.02	291	18	509	20	198	31	16	378	16	13	0.035	23	0.5
L711	70.18	15.61	0.82	1.62	1.12	3.04	4.44	1.42	0.57	0.04	0.14	0.01	439	44	510	31	86	28	32	267	10	23	0.086	26	1.1
L712	53.27	12.39	3.10	6.09	7.38	10.06	2.99	1.05	0.71	0.21	0.15	0.01	218	12	188	51	56	47	113	726	18	46	0.064	39	2.4
L713	45.46	17.65	3.22	6.29	12.70	9.92	1.68	0.06	0.39	0.18	0.09	0.01	17	0	283	14	92	63	353	0	0	2	0.0	29	5.6
L714A	65.63	14.52	1.45	2.84	2.09	6.36	2.96	2.02	0.33	0.12	0.11	0.02	400	47	152	10	94	35	56	356	9	110	0.309	41	1.6
L714B	70.38	15.24	0.94	1.93	0.76	2.90	3.49	2.80	0.30	0.07	0.10	0.00	470	55	102	2	49	29	11	422	9	227	0.539	49	0.4
L715	53.43	16.22	3.49	6.82	7.05	5.12	4.46	0.17	0.58	0.17	0.12	0.01	128	3	77	4	100	30	92	470	43	18	0.039	11	3.1
L716A	54.14	18.64	2.27	4.45	7.41	4.88	5.15	0.59	0.45	0.11	0.09	0.01	258	21	394	10	47	51	169	233	12	12	0.053	18	3.3
L716B	56.28	15.76	2.04	4.61	5.20	6.91	6.84	0.20	0.48	0.12	0.11	0.0	0	0	0	0	0	0	0	0	0	0	0	0	0.0
L717	60.30	14.14	2.43	4.77	4.75	6.59	3.47	0.44	0.70	0.11	0.17	0.0	0	0	0	0	0	0	0	0	0	0	0	0	0.0
L718	50.50	14.47	3.82	5.44	9.35	10.88	1.65	0.15	0.79	0.19	0.15	0.0	0	0	0	0	0	0	0	0	0	0	0	0	0.0
L720	53.22	16.58	2.44	4.47	5.10	11.74	1.64	1.66	0.76	0.14	0.14	0.0	0	0	0	0	0	0	0	0	0	0	0	0	0.0
L721	53.30	14.06	3.00	5.88	5.54	11.84	3.53	0.07	0.40	0.16	0.11	0.01	38	0	268	78	68	52	97	0	0	2	0.0	15	1.9

SPEC. NO.	SI02	AL2O3	FE2O3	PI0	NG0	CA0	HA20	K20	TI02	HNO	P2O5	S	BA	BB	SB	CU	ED	CO	BI	K/BBBA/BRE/SRBB/SRE/BAVI/CO					
L722	47.09	14.37	4.13	5.05	12.17	11.68	0.46	1.04	0.40	0.17	0.09	0.01	369	25	220	14	87	63	322	345	15	39	0.114	23	5.1
L723	50.35	15.94	3.60	5.50	8.04	11.74	0.79	1.17	0.59	0.18	0.13	0.01	359	37	206	7	84	46	123	262	10	47	0.180	27	2.7
L724	50.06	17.33	3.37	6.60	6.35	8.20	2.76	0.21	0.61	0.16	0.11	0.0	102	5	232	14	99	51	186	348	20	7	0.022	17	3.6
L725	60.07	17.74	1.57	3.37	6.01	3.41	5.12	0.61	0.34	0.09	0.11	0.0	161	14	320	19	82	45	160	361	12	15	0.044	31	3.4
L726	62.17	15.54	1.94	3.82	4.01	5.31	4.38	0.21	0.45	0.13	0.09	0.0	66	3	230	5	103	45	61	581	33	7	0.013	24	1.4
L727	46.29	17.37	3.71	9.35	3.20	9.65	4.09	1.08	2.62	0.19	0.39	0.14	550	30	246	34	142	23	32	298	18	36	0.122	16	1.4
L729	48.81	13.67	4.22	8.28	7.54	10.90	2.59	0.13	0.96	0.21	0.07	0.04	61	1	170	29	104	54	113	1079	61	6	0.006	17	2.1
L729	46.63	12.62	5.59	10.94	6.37	9.74	2.58	0.47	1.73	0.23	0.09	0.02	199	10	127	20	132	56	41	390	20	30	0.079	19	0.7
L731	48.99	11.71	5.18	10.13	6.48	9.29	3.14	0.43	1.27	0.21	0.12	0.01	194	6	93	61	86	42	57	594	32	38	0.065	18	1.4
L732	48.64	13.78	4.85	9.50	5.09	11.12	2.69	0.20	1.32	0.17	0.10	0.15	105	3	124	71	72	47	87	553	35	13	0.024	15	1.4
L733	52.09	19.90	1.76	3.47	4.78	10.53	3.56	2.15	0.35	0.14	0.07	0.0	340	50	270	4	65	45	104	356	7	66	0.185	52	2.3
L734	52.43	18.00	2.87	5.60	6.95	7.42	3.66	0.36	0.51	0.17	0.07	0.01	141	7	229	31	106	53	102	426	20	13	0.031	21	1.9
L735	49.46	13.87	1.74	7.32	11.13	10.16	0.67	0.06	0.50	0.21	0.09	0.01	23	8	218	59	117	61	245	0	0	2	0.0	22	4.0
L736	60.37	14.58	1.81	3.56	4.52	6.73	3.49	0.64	0.45	0.09	0.09	0.02	183	14	280	17	54	35	43	379	13	18	0.050	29	1.2
L737	47.44	14.01	4.44	8.70	9.16	8.23	3.96	0.06	0.71	0.24	0.05	0.01	51	0	60	86	97	50	143	0	0	8	0.0	8	2.9
L738	47.23	13.42	5.04	9.88	10.21	8.84	0.99	0.06	0.90	0.24	0.07	0.03	61	3	149	116	113	47	142	166	20	3	0.020	9	3.0
B51	48.51	13.20	5.56	10.89	7.54	7.59	1.99	0.07	1.19	0.26	0.09	0.20	102	7	80	121	127	46	87	83	15	7	0.008	5	1.9
B52	50.15	13.17	4.08	7.99	7.67	8.17	4.59	0.09	0.90	0.22	0.06	0.03	82	4	82	89	94	43	117	186	21	9	0.044	9	2.7
B53	49.95	11.64	4.55	8.90	8.68	9.05	2.83	0.08	0.89	0.24	0.06	0.0	76	3	88	74	105	41	121	221	25	7	0.034	8	3.0
B54	45.32	14.49	6.02	11.60	8.51	6.05	2.90	0.10	1.27	0.29	0.08	0.0	108	5	72	131	157	43	71	166	22	11	0.069	7	1.7
B55	52.51	11.88	5.12	10.05	4.96	8.24	2.67	0.12	0.92	0.43	0.20	0.20	92	5	115	77	82	35	70	199	18	8	0.044	10	2.0
B56	53.90	14.58	1.48	6.82	7.33	4.34	5.45	0.56	0.67	0.14	0.14	0.0	305	13	58	16	164	40	139	357	23	80	0.224	15	3.5
B57	46.20	11.49	4.48	12.70	7.27	7.96	2.73	0.23	1.18	0.27	0.10	0.0	134	8	105	213	138	42	62	238	17	14	0.008	14	1.5
B58	57.03	12.47	3.68	7.20	6.24	5.88	3.06	0.36	0.91	0.26	0.20	0.03	191	6	108	67	96	39	49	498	32	27	0.056	15	1.3
B59	46.60	12.81	5.56	10.90	8.66	8.06	2.72	0.17	0.97	0.22	0.07	0.03	110	12	289	77	231	42	83	117	9	4	0.042	12	2.0
B510	47.75	13.79	4.70	9.23	5.72	14.40	3.48	0.09	0.96	0.25	0.06	0.03	90	3	92	120	120	46	132	249	30	8	0.033	8	2.9
B511	55.26	15.29	3.14	6.17	4.17	7.49	5.15	0.24	0.59	0.18	0.10	0.0	118	14	317	42	93	38	93	142	8	6	0.044	16	2.4
B512	48.18	12.49	4.06	7.97	7.49	11.50	3.26	0.84	1.11	0.24	0.16	0.03	368	37	320	79	138	42	149	250	14	21	0.084	18	3.5
B513	62.02	16.42	1.63	3.19	2.63	2.74	8.96	0.08	0.61	0.08	0.10	0.0	68	2	310	3	90	38	30	332	34	2	0.007	9	0.8
B514	61.17	15.07	2.20	4.46	3.57	7.77	1.63	1.19	0.77	0.13	0.12	0.03	278	42	342	58	114	40	46	235	6	28	0.123	26	1.2
B515	51.34	14.46	4.34	9.05	4.99	7.47	3.97	0.26	1.18	0.21	0.15	0.10	282	8	752	67	164	43	63	269	25	2	0.001	10	1.5
B516	54.48	12.10	3.83	7.52	5.46	10.84	0.42	0.98	1.11	0.19	0.20	0.03	311	30	239	81	170	39	145	271	10	34	0.124	26	3.7
B517	53.74	13.41	3.15	6.18	5.40	10.51	3.66	0.21	1.09	0.16	0.22	0.0	140	5	357	26	96	44	156	348	24	4	0.014	12	3.4
B518	59.51	14.34	2.87	5.62	3.37	6.28	3.24	1.26	0.97	0.17	0.23	0.01	353	45	323	22	120	36	5	232	8	32	0.139	29	0.1
B519	59.53	12.06	2.03	5.94	6.26	6.94	1.59	1.89	0.90	0.16	0.15	0.03	480	47	390	63	187	40	149	333	10	40	0.121	32	3.7
B520	57.52	16.47	3.20	4.27	3.84	3.59	4.61	1.11	1.00	0.17	0.26	0.0	502	35	519	17	132	37	6	243	14	17	0.068	18	0.1

SPEC. NO. ST02 AL203 FE203 FLO HGO CAG NA2O K2O TIO2 HNO P2O5 S BA BB BR CB EN CO SI K/BBBA/BBK/BBB/BBK/BAVI/CO

PS21	55.28	16.31	3.14	6.15	3.39	7.14	4.59	0.48	1.13	0.15	0.23	0.0	219	12	250	32	119	39	17	332	18	15	0.048	14	0.4
BS22	55.09	15.11	2.96	5.82	5.66	6.84	4.09	0.90	0.85	0.17	0.20	0.0	295	32	502	38	100	40	113	233	9	14	0.064	25	2.8
BS23	47.47	14.96	3.92	7.69	8.60	9.52	3.09	0.55	1.40	0.20	0.18	0.0	376	19	432	57	145	46	204	240	20	10	0.004	12	4.4
BS24	66.67	14.89	1.24	2.49	2.63	3.72	5.32	1.09	0.43	0.0	0.09	0.06	281	27	320	6	60	35	28	335	10	27	0.002	32	0.8
BS25	64.67	14.51	1.21	2.38	1.84	5.62	4.99	2.60	0.56	0.0	0.10	0.13	488	66	323	17	50	35	30	327	7	64	0.204	44	0.9
BS26	65.37	18.63	1.22	2.37	1.53	2.92	5.00	1.77	0.39	0.0	0.08	0.01	360	37	570	3	94	31	14	397	10	25	0.065	40	0.5
BS27	51.11	12.26	1.94	11.67	6.48	3.91	2.02	0.09	2.42	0.81	0.18	0.10	197	6	58	146	148	184	84	124	33	12	0.104	3	0.2
BS28	60.04	14.68	2.21	4.31	4.19	7.64	3.14	0.40	0.55	0.65	0.20	0.01	88	8	138	12	34	73	61	415	11	24	0.058	37	0.8
BS29	59.16	15.70	2.86	5.44	1.81	3.21	7.79	0.14	1.26	0.32	0.32	0.0	240	4	236	42	188	86	60	290	60	4	0.017	4	0.7
BS31	58.97	13.20	1.18	6.23	4.06	4.95	3.19	1.28	2.02	0.38	0.22	0.15	242	32	87	18	144	148	40	332	8	122	0.218	43	0.3
BS32A	57.47	11.21	5.56	10.90	5.91	7.67	2.50	0.21	1.62	0.58	0.21	0.0	145	10	79	65	95	39	58	174	15	22	0.127	12	1.5
BS33	67.51	13.06	1.39	2.70	3.99	1.88	5.38	1.27	0.45	0.0	0.09	0.01	279	35	151	0	83	37	58	301	12	69	0.232	37	1.6
BS34	66.73	15.48	1.30	2.23	2.74	3.11	5.96	0.78	0.34	0.0	0.08	0.01	262	21	485	16	98	36	33	308	12	33	0.043	24	0.9
BS35	68.85	14.65	0.96	1.88	1.63	5.20	4.37	0.80	0.27	0.0	0.11	0.0	265	22	452	7	61	38	9	301	12	14	0.049	25	0.2
BS37	66.87	15.57	1.01	1.98	1.94	3.95	4.91	2.01	0.52	0.0	0.12	0.03	455	47	528	13	74	33	23	355	10	31	0.049	36	0.7
BS38	65.52	15.05	1.17	2.30	2.57	5.53	4.23	1.58	0.49	0.0	0.12	0.01	401	41	271	14	77	37	50	319	10	40	0.151	32	1.4
BS39	61.82	15.43	1.82	3.56	3.83	5.95	4.68	0.34	0.51	0.17	0.12	0.02	239	12	325	59	79	41	105	235	20	8	0.037	11	2.6
BS40	59.72	14.73	2.03	3.97	4.83	6.15	4.99	0.73	0.52	0.15	0.13	0.01	344	18	360	36	81	42	110	336	19	16	0.050	17	2.4
BS41A	65.93	14.37	1.17	2.29	3.55	4.36	4.52	1.75	0.37	0.0	0.14	0.01	260	66	368	19	80	38	82	220	4	39	0.179	55	2.2
BS41B	61.12	15.26	1.07	2.09	4.02	8.49	4.49	1.36	0.31	0.13	0.07	0.83	271	54	445	12	68	35	47	209	5	25	0.121	61	1.3
BS41	60.57	16.74	1.74	3.48	4.86	6.18	4.45	0.60	0.48	0.09	0.08	0.01	221	15	472	27	76	17	47	332	35	18	0.032	22	2.8
BS42	57.43	18.05	1.93	3.76	5.97	5.54	2.72	2.27	0.56	0.01	0.11	0.0	520	47	338	14	135	39	129	400	11	55	0.139	36	3.3
BS4290	62.95	15.42	1.44	2.83	3.61	6.44	3.44	1.59	0.48	0.07	0.08	0.0	305	34	232	10	100	39	102	384	9	56	0.146	43	2.6
BS465	58.46	16.19	2.50	4.88	7.58	3.57	2.66	1.35	0.47	0.22	0.09	0.8	370	32	205	65	207	41	142	350	12	54	0.156	30	3.5
BS415	60.84	15.67	1.79	3.50	4.18	4.17	4.18	1.08	0.48	0.14	0.10	0.06	268	28	192	17	88	39	130	320	10	46	0.145	33	3.3
BS417	62.54	17.12	1.70	3.33	3.38	3.70	2.33	3.44	0.57	0.66	0.12	0.07	622	83	136	21	618	36	59	344	7	209	0.610	45	1.6
BS415	57.90	16.61	2.56	5.63	6.57	3.87	1.10	2.82	0.60	0.76	0.11	0.0	680	66	84	43	720	39	135	354	10	278	0.786	34	3.4
BS417	55.12	18.44	2.91	5.70	9.19	1.65	0.71	2.73	0.61	0.65	0.12	0.8	290	59	67	73	732	39	153	384	5	338	0.880	78	3.9
BS465	62.43	19.02	1.86	3.65	4.18	1.96	3.32	1.91	0.52	0.0	0.12	0.0	375	43	250	12	234	39	62	368	9	63	0.171	42	1.6
BS417C	59.20	19.31	1.57	3.07	3.60	6.92	3.86	1.44	0.55	0.05	0.11	0.01	360	36	382	30	93	38	82	332	10	39	0.119	33	2.2
BS4230	59.12	16.47	1.63	3.18	3.71	7.18	3.70	0.98	0.56	0.08	0.10	0.0	300	24	302	21	184	38	72	338	13	26	0.079	27	1.9
BS405	60.85	16.92	1.65	3.23	4.94	4.03	1.82	2.35	0.55	0.26	0.10	0.0	449	52	171	14	105	34	104	375	9	114	0.304	43	3.8
BS417	61.13	16.38	1.85	3.64	6.18	2.78	2.95	0.84	0.47	0.03	0.13	0.0	251	18	158	0	124	39	102	387	14	44	0.113	27	2.6
BS415	65.10	15.70	1.87	2.09	2.28	5.70	3.82	1.45	0.29	0.09	0.07	0.04	321	32	192	29	216	35	29	376	10	62	0.167	37	0.8
BS417	67.51	15.56	1.08	2.11	2.80	3.46	5.03	0.89	0.28	0.0	0.08	0.0	216	21	190	3	118	36	24	351	10	38	0.111	34	0.7
BS465	54.60	21.12	1.89	3.69	5.19	5.47	4.21	1.53	0.68	0.21	0.13	0.0	387	35	306	38	138	38	136	362	11	41	0.114	32	3.6

SPEC. NO.	SI02	AL2O3	FE2O3	FeO	K2O	CaO	Na2O	K2O	TiO2	MgO	P2O5	S	BA	BB	BE	CB	EN	CO	BT	K/BBBA/BBB/BBB/BBB/BBB/CO					
05-535	61.41	16.16	1.60	3.30	5.45	5.01	3.32	0.85	0.48	0.10	0.12	0.03	320	21	245	5	124	38	97	336	15	28	0.046	22	2.0
05-540	44.01	27.92	3.69	7.22	8.83	1.83	2.65	2.73	0.84	0.09	0.14	0.02	622	66	320	38	505	48	227	343	9	70	0.204	36	4.7
06-40	62.78	17.96	1.48	2.92	4.47	3.04	0.82	4.06	0.54	0.50	0.73	2.64	674	99	74	0	66	38	105	340	7	455	1.337	50	2.8
06-140	63.18	15.48	2.01	3.93	7.02	2.18	2.04	1.30	0.42	0.24	0.09	0.30	470	25	97	9	988	39	123	431	19	111	0.254	22	3.2
06-240	57.92	20.04	1.87	3.88	5.69	3.95	1.93	2.60	0.54	0.25	0.09	0.03	502	52	160	24	572	36	99	415	10	134	0.325	42	2.8
06-340	69.85	15.76	2.44	4.77	8.33	2.38	1.86	1.63	0.46	0.22	0.09	0.35	584	38	92	28	900	43	287	802	17	148	0.349	23	6.7
06-440	62.43	18.01	1.56	3.64	2.78	5.47	1.14	3.59	0.45	0.16	0.08	1.92	812	76	171	22	150	39	121	392	11	174	0.444	36	3.1
06-540	62.93	17.29	1.45	2.86	3.87	4.58	4.38	0.41	0.41	0.15	0.10	0.30	280	14	291	7	375	37	78	341	20	17	0.048	18	2.1
07-165	61.02	18.75	2.26	4.42	8.75	2.31	3.35	0.14	0.47	0.26	0.19	1.25	60	4	41	317	1134	37	120	290	15	14	0.049	19	5.2
10-40	62.72	13.82	1.66	3.25	5.69	5.54	4.00	0.56	0.42	0.20	0.10	0.01	388	13	141	26	118	42	191	357	30	32	0.092	11	4.5
10-215	60.85	18.78	1.65	3.24	2.45	6.45	3.74	1.04	0.44	0.17	0.10	0.02	310	22	212	20	361	36	89	392	14	48	0.164	27	2.5
10-315	59.63	17.26	1.84	3.60	3.91	7.15	3.39	0.93	0.46	0.24	0.11	0.20	398	22	192	24	349	36	66	350	18	48	0.115	19	2.4
10-390	63.59	14.83	1.48	2.96	2.64	6.50	2.28	1.94	0.53	0.21	0.09	0.03	760	39	220	123	411	37	37	417	19	73	0.177	21	1.0
23-90	65.78	14.78	1.15	2.25	2.20	3.93	3.00	1.52	0.37	0.13	0.08	1.50	378	34	339	14	332	38	72	371	11	37	0.100	33	1.9
23-190	61.82	17.46	1.35	2.65	3.00	7.49	2.28	1.92	0.45	0.21	0.09	1.15	398	44	271	30	166	37	86	342	9	58	0.162	40	2.3
23-252	54.74	7.82	9.04	17.78	1.54	6.14	0.55	1.03	0.08	0.11	0.09	9.99	200	15	28	999	281	37	40	570	13	305	0.536	42	1.1
23-257	71.20	10.99	3.81	7.44	0.98	1.38	0.67	2.37	0.20	0.03	0.08	6.21	292	38	41	999	102	87	36	517	8	479	0.327	67	2.4
23-290	56.04	18.28	2.03	3.97	3.45	10.34	1.67	2.10	0.48	0.27	0.09	1.75	438	50	250	55	212	43	129	348	9	69	0.200	40	3.0
23-490	59.66	20.24	2.93	5.74	3.69	1.22	1.60	3.25	0.65	0.13	0.11	4.29	601	72	136	42	139	47	113	374	8	194	0.529	44	2.4
23-645	56.44	6.79	8.74	17.14	5.50	1.22	0.23	0.32	0.17	0.11	0.17	9.99	68	8	8	999	68	0	49	332	9	332	1.000	39	0.0
23-690	58.21	15.45	2.09	4.09	7.44	7.27	1.63	0.71	0.53	0.29	0.18	0.14	200	24	269	44	239	43	154	245	8	21	0.084	29	3.6
23-790	46.28	24.48	4.68	9.18	7.74	1.61	0.33	3.14	0.61	0.15	0.33	0.35	446	81	98	34	314	48	123	321	6	245	0.827	58	2.6
27-190	60.87	21.71	1.69	3.31	2.36	4.62	1.20	3.74	0.45	0.14	0.09	1.50	578	84	149	14	102	35	48	371	7	209	0.544	56	1.4
27-490	61.17	15.90	2.55	4.98	6.22	2.60	3.04	0.79	0.47	0.24	0.20	1.15	170	22	81	25	82	41	130	298	8	80	0.272	38	3.2
27-690	60.46	15.10	1.91	3.74	6.54	6.12	2.26	0.75	0.42	0.22	0.09	0.01	223	21	169	15	162	40	135	296	11	36	0.124	27	3.4
27-840	62.51	19.97	1.11	2.17	3.45	4.03	0.35	0.91	0.47	0.17	0.10	0.05	281	23	300	3	124	32	57	328	12	22	0.064	26	1.6
27-1015	57.33	14.66	3.43	6.72	6.97	3.13	1.97	0.32	0.45	0.29	0.27	1.95	155	17	103	43	224	36	93	253	9	41	0.165	27	2.6
27-1107	58.95	8.54	6.91	13.51	7.27	1.24	0.10	0.11	0.07	0.20	0.08	5.12	22	3	2	999	201	0	84	304	7	454	1.500	41	0.0
27-1140	53.16	12.79	2.71	5.31	10.42	10.35	1.60	0.11	0.43	0.39	0.10	0.01	39	3	110	34	194	58	309	304	13	8	0.027	23	6.4
27-1190	54.41	13.92	2.49	4.90	9.45	5.02	2.49	0.19	0.43	0.19	0.11	0.15	102	7	95	44	224	48	248	225	15	16	0.074	15	5.2

REFERENCES

Abbey S., (1977) Studies in "Standard Samples" for Use in the General Analysis of Silicate Rocks and Minerals, Part 5 GSC Paper 77-34.

----- (1974) Studies in "Standard Samples" of Silicate Rocks and Minerals, Part 4 GSC Paper 74-41

Adams J.H., (1971) Geochemistry of the Rocks Enclosing the Lingwick Copper-Lead-Zinc Mineralization Unpub. Thesis, Carleton Univ. Ottawa.

Allard G., (1972) Introduction XXIV IGC Guidebook, Field Excursions A41-C41.

Allman M. & Lawrence D., (1972) Geological Laboratory Techniques (Ch.7) London-Blandford Press.

Anderson C.A., (1969) Massive Sulphide Deposits and Volcanism Econ. Geol., V64, p.129-146.

Anhaeusser C.R., (1976) The Nature and Distribution of Archean Gold Mineralization in South Africa Min.Sci.Eng., V8, p.46-84.

-----, (1974) Precambrian Tectonic Environments Ann. Rev. Earth & Plan. Sci Lett., V3, p. 31-53.

-----, (1971) Cyclic Volcanicity and Sedimentation in the Evolutionary Development of Archean Greenstone Belts of Shield Areas In: GSAust. Sp.Pub.3 (Glover, ed.), p.57-70.

Ardnt N., (1976) Ultramafic Rocks of Munro Township: Economic and Tectonic Implications GAC Sp. Paper No.14, p.617-657.

----- (1975) Ultramafic flows of Munro Township Plate Tectonics and Ore Deposits (Strong, ed.) Sp.Pub GAC

-----, Naldrett A.J. & Pyke D.R., (1977) Komatiitic and Iron-rich Tholeiitic Lavas of Munro Township, Northeast Ontario J.Pet. V18, p.319-369.

Armbrust G.A., Oyarzum M.J. & Arias F.J., (1971) Rubidium as a Guide to Org at El Teniente (Braden), Chile Econ.Geol., V66, p.977.

Ayres L.D., (1977) Importance of Stratigraphy in Early Precambrian Volcanic Terrains in: Volcanic Regimes in Canada (Baragar, Coleman, Hall ed.), GAC Sp.Pap.16.

Bald R.C., (1977) Pre-volcanism, Archean Sialic Crust, Gundy-Tannis Lake Area, Northwestern Ontario. in: Center for Prec. Studies, U. of Man., Ann. Rept., p.98-105.

Baragar W.R.A., (1977) Volcanism of the Stable Crust GAC Sp.Pap. 6, p.377-405.

-----, (1972) Some Physical & Chemical Aspects of Precambrian Volcanic Belts of the Canadian Shield Earth Physics Branch Pub., V42, p.129/140.

----- & Goodwin A.M., (1968) Andesites and Archean Volcanism of the Canadian Shield in: The Andesite Conference, Internat. U. Mantle Comm.

-----, & McGlynn (1977) On the Basement of Canadian Greenstone Belts: Discussion Geosci.Can., V5, p.13-15.

Barnes H.L. & Czamanske G.K., (1967) Solubility and Transport of Ore Minerals Ch.8 in Barnes H.L. (ed.) Geochemistry of Hydrothermal Ore Deposits p.334-381.

Bartram G.D. & McCall G.J.H., (1971) Wallrock Alteration Associated with Auriferous Lodes in the Golden Mile, Kalgoorlie In: GSAust. Sp.Pap.3 (Glover, ed.), p.191-200.

Becke F., (1903) Die Eruptivgebiete der bohmischen Mittelgebirge und der amerikanischen Andes. Tschermak's mineral. u petroq. Mitt. XXII.

Bernstein F., (1962) Application of X-ray Fluorescence Analysis to Process Control Advances in X-ray Analysis, V5, p.486-499.

Best M.G., (1969) Differentiation of Calc-Alkaline Magmas In: Proc. Andesite Conf. (McBirney, ed.), Oregon Dept.Geol.Min.Ind. Bull., V65, p.65-73.

Bickle M.S., Martin A., & Nisbet E. (1975) Basaltic and Peridotitic Komatiites and Stromatolites Above A Basal Unconformity in the Belingue Greenstone Belt, Rhodesia Earth & Plan.Sci.Lett., V27, p.155-162.

Blake D.A.W., (1953) Waswanipi Lake Area (East Half) Quebec Dept. of Mines, GR59.

-----, (1949) Waswanipi Lake Area (East Half), Abitibi East County Quebec Dept. of Mines, P.R.233.

Boyle R.W., (1959) The Geochemistry, Origin and Role of Carbon Dioxide, Water, Sulphur and Boron in the Yellowknife Gold Deposits, NWT. Econ. Geol., V54, p.1506-1524.

Brooks C. & Hart S.R., (1974) On the Significance of Komatiite Geology, V2, p.107-110.

-----, (1972) An extrusive Basaltic Komatiite from a Canadian Metavolcanic Belt CJES, v9, p.1250-1253.

Carmichael I., Turner F.J. & Verhoogen J., (1974) Igneous Petrology McGraw-Hill Book Co.

Cawthorn R.G. & O'Hara M.J., (1976) Amphibole Fractionation in Calc-Alkaline Magma Genesis Am.J.Sci., V276, p.309-329.

Champion K.P., Hurst H.J. & Whitten R.N., (1968) Tables of Mass Absorption Coefficients for Use in X-ray Spectro-Chemical Analysis Aust. Atom. En. Comm. AAEC/TM454.

Church B.N., (1975) Quantitative Classification and Chemical Comparison of Common Volcanic Rocks GSA Bull., V86, p.257-263.

Claissie F. & Sampson C., (1962) Heterogeneity Effects in X-ray Analysis Advances in X-ray Analysis, V5, p.335-354.

Claveau J., (1948) Waswanipi Lake Area (West Half), Abitibi East County Quebec Dept. of Mines, P.R.217.

Condie K.C., (1976) Trace-element Geochemistry of Archean Greenstone Belts Earth-Sci Rev., V12, p.393-417.

Cooley W.W. & Lohnes P.R., (1971) Multivariate Data Analysis John Wiley & Sons

Correns C.W., (1969) Introduction to Mineralogy Springer-Verlag, 485pp.

Cross W., Iddings J.P., Pirsson L.V. & Washington H.S., (1902) A Quantitative Chemico-Mineralogical Classification and Nomenclature of Igneous Rocks J.of Geol., V10, p.555-690.

(1903) Quantitative Classification of Igneous Rocks, Based on Chemical and Mineralogical Characteristics with a Systematic Nomenclature Whitman Cross, Chicago.

- (1912) Modification of the Quantitative System of Classification of Igneous Rocks J.of Geol., V20, p.550-561.
- Czamanske G.K., Hower, J. & Millard R.C., (1966) Non-Proportional, Non-Linear Results from X-ray Emission Techniques, Involving Moderate Dilution Rock Fusion Geoch.Cosmoch.Acta. V3, p.745-756.
- Daly R., (1933) Igneous Rocks and the Depths of the Earth McGraw-Hill
- Davenport P.H. (1972) The Application of Geochemistry to Base Metal Exploration in the Birch-Uchi Lakes Volcano-Sedimentary Belt, NW Ontario PhD Thesis, Queens University, Kingston.
- Davis J.C., (1973) Statistics and Data Analysis in Geology John Wiley & Sons.
- (1964) ASTM Standards, Part 30, p.503-511 ASTM-E177-61T.
- DeJongh W.K., (1975) Table of Influence Coefficients Unpub. Rept. for Philip's Application Laboratory, Eindhoven, Holland.
- Descarreaux J., (1973) A Petrochemical Study of the Abitibi Volcanic Belt and Its Bearing on the Occurrence of Massive Sulphide Ores CIMM Bull. V66, p.61-69.
- , (1976) Map and Geochemical Data - Bachelor Lake Area Unpublished Company Report.
- Dixon W. & Massey F., (1969) Introduction to Statistical Analysis McGraw-Hill Book Co.
- Donovan P.R. & James C.H., (1967) Geochemical Dispersion in Glaciated Overburden Over the Tynagh (Northgate) Base Metal Deposit, W-Central Eire GSC Pap. 66-54, p.89-110.
- Doucet R., (1973) Rapport Final - Projet 10-806 Le Tac, Comte Abitibi-Est Soquem Lté, Internal Company Report.
- Dreimanis A., (1960) Geochemical Prospecting for Cu, Pb and Zn in Glaciated Areas, Eastern Canada XXI IGC, Part II, Norway, p.6-19.
- Dresser J.A. & Denis T.C., (1944) Waswanipi-Chibougamau Area in: Geology of Quebec, VII, Quebec Dept. of Mines, G.R.20.

- Dugas J., (1975) Geology of the East Half of Lesueur Township Min. des Rich. Nat., RP612.
- , (1950) Southwest Part of Lesueur Township Quebec Dept. of Mines, PR243.
- Dumont G.H., (1959) Report on Waswanipi Lake Property Unpub. Chesbar Chibougamau Resources Inc. company report.
- Duquette G., (1972) Chibougamau-Chapais Greenstone Belt Ch.5 in XXIV IGC Guidebook, Field Excursions A41-C41.
- , (1968) Geology & Principal Mineral Deposits, Chibougamau District MRNQ, Map 1686 and Geologic Report No.ES8.
- Eade K.E. & Fahrig W.F., (1971) Geochemical Evolutionary Trends of Continental Plate - A Preliminary Study of the Canadian Shield Bull. Can. Geol. Survey, V179, 51pp.
- Eckstrand E.O., (1972) Ultramafic Flows & Nickel Sulphide Deposits in the Abitibi Orogenic Belt GSC Paper 72-1A (Report of Activities), p.75-81.
- Eggler D.H., (1974) Application of a Portion of the System $\text{CaAl}_2\text{Si}_2\text{O}_8\text{-MgO-FeO-O}_2\text{-H}_2\text{O-CO}_2$ to the Genesis of the Calc-alkaline Suite. Am.Jour.Sci., V274, p.297-318.
- Eskola P. (1939) Die Entstehung der Gesteine In: Barth, Correns & Eskola (ed), Springer-Verlag.
- Eugster H.P. & Chou I.M., (1973) The Depositional Environments of Precambrian Banded Iron Formation Econ.Geol. V68, p.1144-1168.
- Ferguson S.A., (1966) The Relationship of Mineralization to Stratigraphy in the Porcupine and Red Lake Areas, Ontario. GAC Sp.Pap. 3, p.99-120.
- Franklin J.M., Kasarda J. & Poulsen K.H., (1975) Petrology & Chemistry of the Alteration Zone of the Mattabi Massive Sulphide Deposit Econ.Geol., V70, p.63-79.
- Frey F.A. (1974) Atlantic Oceanic Floor: Geochemistry and Petrology of Basalts From Legs 2 & 3 of the Deep Sea Drilling Project J.Geoph.Res., V79, p.5507-5527.
- Fryer B.J., Kerrich R., Hutchinson, R.W. & Pierce J., (1979) Archean Precious Metal Hydrothermal Systems, Dome Mine, Abitibi Greenstone Belt CJES, V16, p.421-439.
- Fyfe W.S. & Henley R.W. (1973) Some Thoughts on Chemical Transport and Processes with Particular Reference to Gold Min.Sci.Eng., V15, p.293-303.

- Gannicott R.A., Armbrust G.A., Agterberg F.P., (1979) Use of Trend Surface Analysis to Delimit Hydrothermal Alteration Patterns. CIMM Bull., V72, p.82-89.
- Garrett R.G., (1971) The Dispersion of Copper and Zinc in Glacial Overburden at the Louvem Deposit, Val d'Or, Quebec in: Geochemical Exploration, CIMM, Sp.Vol.11.
- Gelinas L. & Brooks C., (1974) Archean Quench-Texture Tholeiites CJES, V11, p.324-340.
- , Perrault G., Carigan J., Trudel P., & Grasso F., (1977) Chemo-Stratigraphic Divisions Within the Abitibi Volcanic Belt, Rouyn-Noranda District, Quebec in: GAC Sp.Pap.16, p.265-295.
- Gilmour P., (1965) Origin of the Massive Sulphide Mineralization in the Noranda District, NW Quebec GAC Proc., V16, p.63-81.
- Gobeil A., (1980) Etude Lithogeochemique des roches volcaniques dans la region de la Mine Lemoine, district de Chibougamau, Quebec CIM Bull., May 1980, p.86-95.
- Goodwin A.M., (1977) Archean Volcanism in the Superior Province, Canadian Shield in: Volcanic Regimes in Canada (Baragar, Coleman, Hall ed.), GAC Sp.Pap.16.
- , (1973) Archean Iron-Formations and Tectonic Basins of the Canadian Shield Econ.Geol., V68, p.915-933.
- (1971) Metallogenic Patterns and Evolution of the Canadian Shield Symposium on Archean Rocks, G.S.Aust. Sp.Pub No.3, p.157-174.
- , et al, (1972) The Superior Province in: Variations in Tectonic Styles (Price & Douglas ed.) GAC Sp.Paper No.11.
- , & Ridler R.H., (1970) The Abitibi Orogenic Belt in: Symposium on Basins and Geosynclines (Baer ed.) GSC Paper 70-40.
- Gorman B.E., Pearce T.H. & Birkett T.C., (1978) On the Structure of Archean Greenstone Belts Prec. Res. V6, p.23-41.
- Govett G.J.S & Goodfellow W.D., (1975) Development of Rock Geochemical Techniques for Detecting Buried Sulphide Deposits Econ.Geol., V70, p.246(abs).
- Graham R.B., (1957) Southwest Part of Lesueur Township Quebec Dept. of Mines, GR.72.

Green D.H., (1975) Genesis of Archean Peridotitic Magmas and Constraints on Archean Geothermal Gradients and Tectonics. Geology, V3, p.15-18.

-----, (1972) Archean Greenstone Belts may include Terrestrial Equivalents of Lunar Maria. E & Plan. Sci. Lett., V15, p.263.

----- & Ringwood A.E., (1967) The Genesis of Basaltic Magmas Cont.Min.Pet., V15, p.103-190.

Green T.H., (1972) Crystallization of Calc-Alkaline Andesite under Controlled High-Pressure Hydrous Conditions Cont.Min.Pet., V34, p.150-166.

----- & Ringwood A.E., (1967) Crystallization of Basalt & Andesite Under High Pressure Hydrous Conditions E. & Plan.Sci.Lett. V3, p.481-489.

-----, (1966) Origin of the Calc-Alkaline Igneous Rock Suite E. & Plan.Sci. Lett., V1, p.307-316.

Grenier P.E., (1967) Annotated Bib: Metallic Mineralization in Noranda, Mattagami, Val d'Or & Chibougamau Ministere des Richesses Naturelles, Sp.Pub No.2.

Hallberg J.A., (1976) The Archean Marda Igneous Complex, W. Australia Prec.Res., V3, p.111-136.

----- & Williams D.A.C., (1972) Archean Mafic and Ultramafic Rock Associations in the Eastern Goldfields Region, W. Australia Earth & Plan.Sci.Letters, V15, p.191-200.

Harker A., (1909) The Natural History of Igneous Rocks MacMillan

Hawkes H.E., (1970) Bibliography on Geochemical Prospecting 3rd Int.Geochem.Expl.Symp., Toronto, 45pp.

Hawkesworth C.J. & O'Nions R.K., (1977) The Petrogenesis of some Archean Volcanic Rocks from Southern Africa J.Pet., V18, p.487-520.

Heinrich K.F., (1966) X-ray Absorption Uncertainty in: The Electron Microprobe (McKinely Ed.), John Wiley.

Hodgson C.J. & Lydon J.W. (1977) Geologic Setting of Volcanogenic Massive Sulphide Deposits and Active Hydrothermal Systems CIMM Bull., V

Holmes A., (1921) Petrographic Methods and Calculations London.

Huang W.T., (1962) Petrology McGraw-Hill Book Co.

Hutchinson R.W., (1976) Lode Gold Deposits: The Case for Volcanogenic Derivation In: Proc. Vol. Pac. NW. Minerals Conf., Oregon Dept Geol. Min. Ind. Bull., p.64-105.

-----, (1973) Volcanogenic Sulphide Deposits and their Metallogenic Significance Econ. Geol., V68, p.1223-1246.

-----, (1971) Mineral Potential of Greenstone Belts in NW Ontario Paper presented at: Ann. Conf. of Inst. on Lake Superior Geology, Thunder Bay, Ontario, May, 1970.

-----, (1965) Genesis of Canadian Massive Sulphide Deposits, Reconsidered by Comparison to Cyprus Deposits CIMM Bull., V58, p.972-986.

-----, & Hodder R.W., (1972) Possible Tectonic and Metallogenic Relationships between Porphyry Copper and Massive Sulphide Deposits CIMM Bull., V65, p.34-40.

-----, Ridler R.H. & Suffel G.G., (1971) Metallogenic Relationships in the Abitibi Belt, Canada Trans. Can. Inst. Min., V74, p.106-115.

Imreh L., (1976) Nouvelle Lithostratigraphie a l'Ouest de Val d'Or MDRN, DP-349, 361pp.

Irvine T.N. & Baragar W.R.A., (1971) A Guide to the Classification of Common Volcanic Rocks CJES, V8, p.523-548.

Jenkins R. & DeVries J., (1973) Practical X-ray Spectrometry Philips Technical Library, Springer-Verlag.

Jensen L.S., (1978) Archean Komatiitic, Tholeiitic, Calc-Alkaline and Alkalic Volcanic Sequences in the Kirkland Lake Area GSA-GAC Field Guide, Toronto.

Jensen L.S., (1976) A New Cation Plot for Classifying Subalkaline Volcanic Rocks ODM Misc.Pap. 66, 22pp.

Johannsen A., (1939) A Descriptive Petrography of the Igneous Rocks University of Chicago Press (VI-V4).

Jolly W.T., (1977) Relations Between Archean Lavas and Intrusive Bodies of the Abitibi Greenstone Belt, Ontario-Quebec in: GAC Sp.Pap. 16, p.311-330.

-----, (1976) Metamorphic History of the Abitibi Belt in: Report of Activities, GSC Paper 77-1A, p.191-196.

- (1975) Subdivision of the Archean Lavas of the Abitibi Area, Canada, From Fe-Mg-Ni-Cr Relations Earth & Plan. Sci. Letters, V27, p.200-210.
- (1974) Regional Metamorphic Zonation as an Aid in Study of Archean Terrains, Abitibi Region, Ontario Can. Min., V12, p.499-508.
- Joreskog K.G., Klovan J.E. & Reymont R.A., (1976) Geologic Factor Analysis Elsevier.
- Kalliokoski J., (1968) Structural Features and Some Metallogenic Patterns in the Southern Part of the Superior Province, Canada CJES, V5, p.1199-1208.
- Kim J., (1975) Factor Analysis in: SPSS, 2nd ed., McGraw-Hill Book Co.
- Kinkle A.R., (1966) Massive Pyritic Deposits Related to Volcanism and Possible Methods of Replacement Econ. Geol., V61, p.673-694.
- Klecka W., (1975) Discriminant Analysis in: SPSS, 2nd ed., McGraw-Hill Book Co.
- Krauskopf K.B. (1967) Source Rocks for Metal-Bearing Fluids Ch.1 in: Geochemistry of Hydrothermal Ore Deposits (Barnes, ed.).
- Kroner A., (1976) Proterozoic Crustal Evolution in parts of Southern Africa and Evidence for Extensive Sialic Crust since the end of the Archean Phil. Trans. R. Soc. London, VA280, p.541-554.
- Kuno H., (1968) Origin of Andesite and its Bearing on Island Arc Structure Bull. Volcanol., V32, p.141-176.
- Kushiro I. & Yoder H.S., (1969) Melting of Forsterite & Enstatite at High Pressures Under Hydrous Conditions. Carn. Inst. Yearbook, V67, p.153-158.
- Larsen E.S., (1938) Some New Variation Diagrams J. of Geology, V43.
- Larson L. & Webber G.R., (1977) Chemical and Petrographic Variations in Rhyolite Zones in the Noranda Area, Quebec. CFM Bull., V , p.80-93.
- Latullipe M., (1976) Val d'Or - Malartic Geological Excursion MdRN, DP-367.
- (1972) The Val d'Or - Malartic Area Ch.3 in 24th IGC Field Excursion A41-C41 Guidebook.

- Leake B.E., (1970) The Chemical Analysis of Rock Powders by Automatic X-ray Fluorescence Chem.Geol., V5, p.7-86.
- Longley W.W., (1951) Bachelor Lake Area Quebec Dept. of Mines, GR47.
- MacDonald G.A., (1968) Composition and Origin of Hawaiian Lavas GSA Mem.116, p.477-522.
- MacGregor A.M., (1951) Some Milestones in the Precambrian of Southern Rhodesia Proc. Geol. Soc. South Africa, V54, p.27-31.
- MacIntosh J.A., (1967) Southeast Quarter of Nelligan Township Quebec Dept. of Nat. Res., PR568.
- MacKenzie G.S., (1934) Pusticamica Lake Area, Abitibi Territory Quebec Bureau of Mines, Ann.Rept., Pt.C.
- McCall G.J., (1971) Some Ultrabasic and Basic Igneous Rock Occurrences in the Archean of Western Australia Geol. Soc. Aust., Sp.Pub. 3, p.429-442.
- Mennard G.W., (1973) The Syngenetic Massive Sulphide Deposits Preprint 73-5-53, Chicago Meeting AIME, Feb. 1973.
- Meyer C. & Hemley J.J., (1967) Wall Rock Alteration In: Geochemistry of Hydrothermal Ore Deposits (Barnes, ed.).
- Miyashiro A., (1968) Metamorphism of Mafic Rocks in: Basalts, V2 (Hess & Poldervaart ed.), p.799-834, Interscience Series, John Wiley & Sons.
- Moorehouse W.W., (1970) A Comparative Atlas of the Textures in Archean and Younger Volcanic Rocks GAC Sp.Pap.8 (C. Fawcett ed.).
- (1959) The Study of Rocks in Thin Section Geoscience Series, Harper Bros., N.Y., 575pp.
- Mueller R. & Saxena S., (1977) Chemical Petrology Springer Verlag, N.Y., 394pp.
- Naldrett A.J., (1973) Nickel Sulphide Deposits - Classification and Genesis Trans. CIMM, V76, p.183-201.
- , (1970) Ultramafic and Related Rocks of the Abitibi Orogen GSC Pap. 70-40, p.24-29.
- & Ardnnt N.T., (1976) Volcanogenic Nickel Deposits with some Guides for Exploration Soc.Min.Eng. AIME (Trans.), V260, p.13-15.

- , & Gasparri K. (1971) Archean Nickel Sulphide Deposits in Canada, their Classification, Geologic Setting, and Genesis. Geol. Soc. Aust., Sp.Pub. 3, p.201-226.
- & Goodwin A.M., (1977) Volcanic Rocks of the Blake River Group, Abitibi Greenstone Belt, Ontario, and their Sulfur Content CJES, V14, p.539-550.
- & Turner A.R., (1977) The Geology and Petrogenesis of a Greenstone Belt and Related Nickel Sulphide Mineralization at Yakabindie, W. Australia Prec.Res., V5, p.43-103
- & Cabri L.J., (1976) Ultramafic and Related Mafic Rocks: Their Classification and Genesis with Special Reference to the Concentration of Nickel Sulphides and Platinum-Group Elements Econ.Geol., V71, p.1131-1158.
- Nesbitt R.W., (1971) Skeletal Crystal Forms in the Ultramafic Rocks of the Yilgarn Block, W. Australia Geol.Soc.Aust., Sp.Pub.No.3, p.331-350.
- , & Sun S., (1976) Geochemistry of Archean Spinifex-Textured Peridotites and Magnesian and Low-Magnesian Tholeiites E. & Plan. Sci. Lett., V433-453.
- Nie N., Hull C., Jenkins J., Steinbrenner K., & Bent D., (1975) SPSS - Statistical Package for the Social Sciences McGraw-Hill Book Co.
- Niggli P., (1931) Die quantitative mineralogische Klassifikation der Eruptivgesteine Schweiz. mineral. petrol. Mitt., VII.
- Nisbet E.G., Bickle J. & Martin A., (1977) The Mafic and Ultramafic Lavas of the Belingwe Greenstone Belt, Rhodesia J.Pet., V18, p.521-566.
- Noble D.C., (1968) Systematic Variation in Major Elements in Commendite and Pantellerite Glasses Earth Plan. Sci. Letters, V4, p.167-172.
- Nockolds S.R., (1954) Average Chemical Composition of Some Igneous Rocks Bull GSA, V65, p.1007-1032.
- & Allen R., (1953, 1954, 1956) The Geochemistry of Some Igneous Rock Series Geoch.Cosmoch.Acta, V4, p.105-142; V5, p.245-285, V9, p.34-77.

- Norish K. & Chappell B.W., (1967) X-ray Fluorescence Spectrography in: Physical Methods in Determinative Mineralogy (Zussman ed.) - Academic Press, London, p. 161-214.
- Olade M.A. & Fletcher R.K., (1975) Primary Dispersion of Rubidium and Strontium Around Porphyry Copper Deposits, Highland Valley, B.C. Econ.Geol., V70, p.15-21.
- Osborn E.F., (1962) Reaction Series for Subalkaline Igneous Rocks based on Different Oxygen Pressure Conditions Am. Min., V47, p.211.
- Ostle B., (1969) Statistics in Research Iowa State University Press.
- Oyarzum M.J., (1974) Rubidium & Strontium as a Guide to Mineralization Emplaced in some Chilean Andesitic Rocks Paper: 5th Int.Geoch.Expl.Symp., Vancouver.
- Peacock R., (1931) Classification of Igneous Rock Series J. of Geol. V39, p.54-67.
- Pearce T.H., (1974) Quench Plagioclase from Some Archean Basalts CJES, V11, p.715-719.
- & Birkett T.C., (1974) Archean Metavolcanics from Thackeray Township, Ontario Can.Min., V12, p.509-519.
- & Donaldson J.A., (1974) Proterozoic Quench-Texture Basalts from the Labrador Geosyncline CJES, V11, p.1611-1615.
- , Gorman B.E., & Birkett T.C., (1975) The TiO₂-K₂O-P₂O₅ Diagram: A Method of Discriminating Between Oceanic and Non-Oceanic Basalts Earth & Plan.Sci.Lett., V24, p.419-426.
- Pollock J.P., Schillinger A.W. & Bur T., (1960) A Geochemical Anomaly Associated with a Glacially Transported Boulder Train, Mt.Bohemia, Keeweenaw Co., Michigan XXI IGC, Norway, p.20-27.
- Pyke D.R., (1975) On the Relationship of Gold Mineralization and Ultramafic Rocks in the Timmins Area ODM Misc.Pap. 62, 23p.
- Ramberg H., (1973) Model Studies of Gravity Controlled Tectonics by the Centrifuge Technique in: deJong & Scholten (ed.), Gravity & Tectonics, J.Wiley NY, p.49-66.

- , (1971) Model Studies in Relation to Intrusion of Plutonic Bodies In: Newall & Rast (ed.); Mechanism of Igneous Intrusion Geol. Jour., Sp.Issue 2, p.261-286.
- Rammel R.J., (1967) Understanding Factor Analysis N.Y.
- Ridler R.H., (1975) The Gold Metallogeny of Archean Exhalites Econ.Geol., V70, p.250(abs).
- Ringwood A.E. (1975) Composition and Petrology of the Earth's Mantle Pt.1 Crust and Upper Mantle McGraw-Hill Internat. Series, p.11-318.
- Rinsait J.M., (1974) Mineral Assemblages and Low Grade Metamorphic-Metasomatic Alterations in an Archean Greenstone Belt, Malartic, Quebec Can.Min., V12, p.520-526.
- Roberts R.G., (1975) The Geological Setting of the Mataqami Lake Mine, Que. Econ. Geol., V70, p.115-129.
- Rosenbusch H., (1906) Mikroskopische Psysiographie Germany.
- Rozeboom W., (1966) Foundations of the Theory of Prediction Dorsey Press.
- Sakrison H.C., (1966) Chemical Studies of the Host Rocks of the Lake Dufault Mines, Quebec PhD Thesis, McGill U., Montreal.
- Salmon M.C., (1964) A Highly Simplified Multielement Calibration System for Semiquantitative X-ray Spectrographic Analysis in: Advances in X-ray Analysis, V7, Plenum Press.
- Sangster D.F., (1980) Quantitative Characteristics of Volcanogenic Massive Sulphide Deposits CIM Bull, V , p.74-81.
- , (1972) GSC Paper 72-
- Sawkins F.J., (1972) Sulfide Ore Deposits in Relation to Plate Tectonics J of Geol., V80, p.377-397.
- Shalgosky H.I., (1960) Fluorescent X-ray Spectroscopy Ch.5 in: Methods in Geochemistry (Smales & Wager ed.) p.111-147, Interscience Pub.
- Shand S.J. (1927) The Eruptive Rocks John Wiley.
- Sharpe J.I. (1968) Geology and Sulphide Deposits of the Mataqami Area, Abitibi-East QdNR, Geol.Rept. 137, 122pp.

Shaw G., (1939) Opawica and Lewis Lakes Area GSC Prel. Paper 39-2.

Skinner B.J. & Barton P.B., (1973) Genesis of Mineral Deposits Ann. Rev. Earth & Plan. Sciences, p.183-211.

Smith J.V. (1956) The Powder Patterns and Lattice Parameters of Plagioclase Feldspars: I. The Soda-rich Plagioclases Min.Mag., V31, p.47-68.

----- & Yoder H.S. (1956) Variations in X-ray Powder Diffraction Patterns of Plagioclase Feldspars Am.Min., V41, p.632-647.

Sorby H.C., (1856) On Slaty Cleavage as Exhibited in the Devonian Limestones of Devonshire Phil.Mag., VI1, p.20-37.

Spence C.D. & deRosen-Spence A.F., (1975) The Place of Sulphide Mineralization in the Volcanic Sequence at Noranda, Quebec. Econ.Geol., V70, p.90-101.

Spitz G., (1973) Etude Petrographique et Petrochemique Des Roches Volcaniques Autour du Gisement de Louvem MSc Thesis, Ecole Polytechnique, Montreal.

Sproule J.C., (1940) Puskitamika Lake Area, Abitibi Territory GSC Map 570A.

Stockwell C.H. (1964) 4th Report on Structural Provinces, Orogenesis And Time Classification of Rocks of the Canadian Precambrian Shield GSC Pap. 64-17, Pt.II, P.1-24.

Streck A., (1969) Kaledonische Metamorphose NE-Gronland, Habilitationsschrift, Basel.

Streckeisen A.L., (1976) To Each Plutonic Rock Its Proper Name Earth Science Reviews, VI2, p.1-33.

----- (1973) Plutonic Rocks Geotimes, Oct., p.26.

San S. & Nesbitt R.W., (1978) Petrogenesis of Archean Ultrabasic and Basic Volcanics, Evidence Cont.Min.Pet., V65, p.301-325.

Tatsuoka M.M., (1971) Multivariate Analysis John Wiley & Sons.

Tilley C.E., (1950) Some Aspects of Magmatic Evolution Quart. J. Geol. Soc. London, VI06, p.37-61.

Turner F.J., (1968) Metamorphic Petrology McGraw-Hill Book Co.

-----, & Verhoogen J., (1960) Igneous and Metamorphic Petrology McGraw-Hill Book Co.

Van de Walle M., (1970) Geology of the Northwest Quarter of Lesueur Township Quebec Dept. of Nat. Res., PR599.

Victoreen J.A., (1949) The Calculation of X-ray Mass Absorption Coefficients J.Appl.Phys., V20, p.1141.

Viljeon M.J. & Viljoen R.P., (1969) Evidence of the Existence of a Mobile Extrusive Peridotitic Magma from the Komati Formation of the Onverwacht Group Geol.Soc.S.Afr., Sp.Pub.No.2, p.87-112.

Viswaathan S., (1974) Basaltic Komatiite Occurrences in the Kolar Gold Field of India Geol. Mag., VIII, p.353-354.

Volborth A., (1969) Preparation and Decomposition of Samples Ch.2 in: Elemental Analysis in Geochemistry, p.5-41, Elsevier.

Wager L.R. & Deer W.A., (1939) Geologic Investigations in Eastern Greenland, Part III Medd. Gronland, V5, p.1-352.

Wanerd R. & Uken E., (1971) X-ray Techniques Ch.9 in: Modern Methods of Geochemical Analysis, p.245-270.

Wenk C. & Keller F. (1969) Schweiz. Mineral. Petrog. Mitt. V49, p.157-198.

Williams D.A.C., (1972) Archean Ultramafic, Mafic, and Associated Rocks, Mt. Monger, W. Australia J.Geol.Soc.Aust., VI9, Pt.2, p.163-188.

Williams H., Turner F.J., & Gibling C.M., (1954) Petrography W.H. Freeman & Co.

Wilson H.B.D. & Morrice M.G., (1977) The Volcanic Sequence in Archean Shields in: Volcanic Regimes in Canada (Baragar, Coleman, Hall, ed.), p.355-376.

-----, Ziehlke D.V., & Beakhouse G.P., (1976) Development of Greenstone-Granite Terrains in the Archean Shield Center for Precambrian Studies, Univ. of Man., Ann.Rept., p.2-21.

Windley B.F., (1973) Crustal Development in the Precambrian Phil. Trans. R. Soc. Lond., VA273, p.321-341.

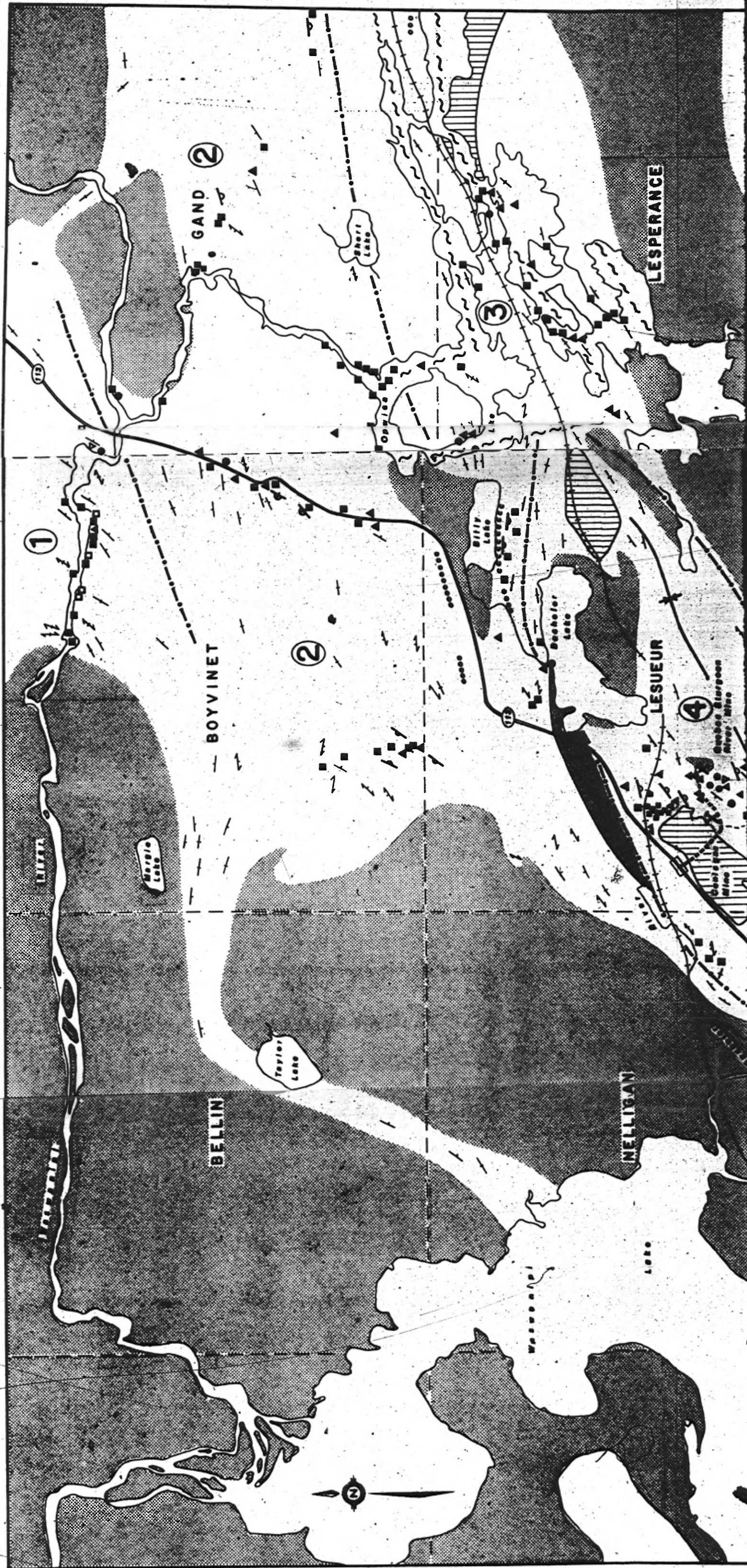
-----, & Bridgewater D., (1971) The Evolution of Archean Low and High Grade Terrains Geol. Soc. Aust., Sp.Pub.3, p. 33-46.

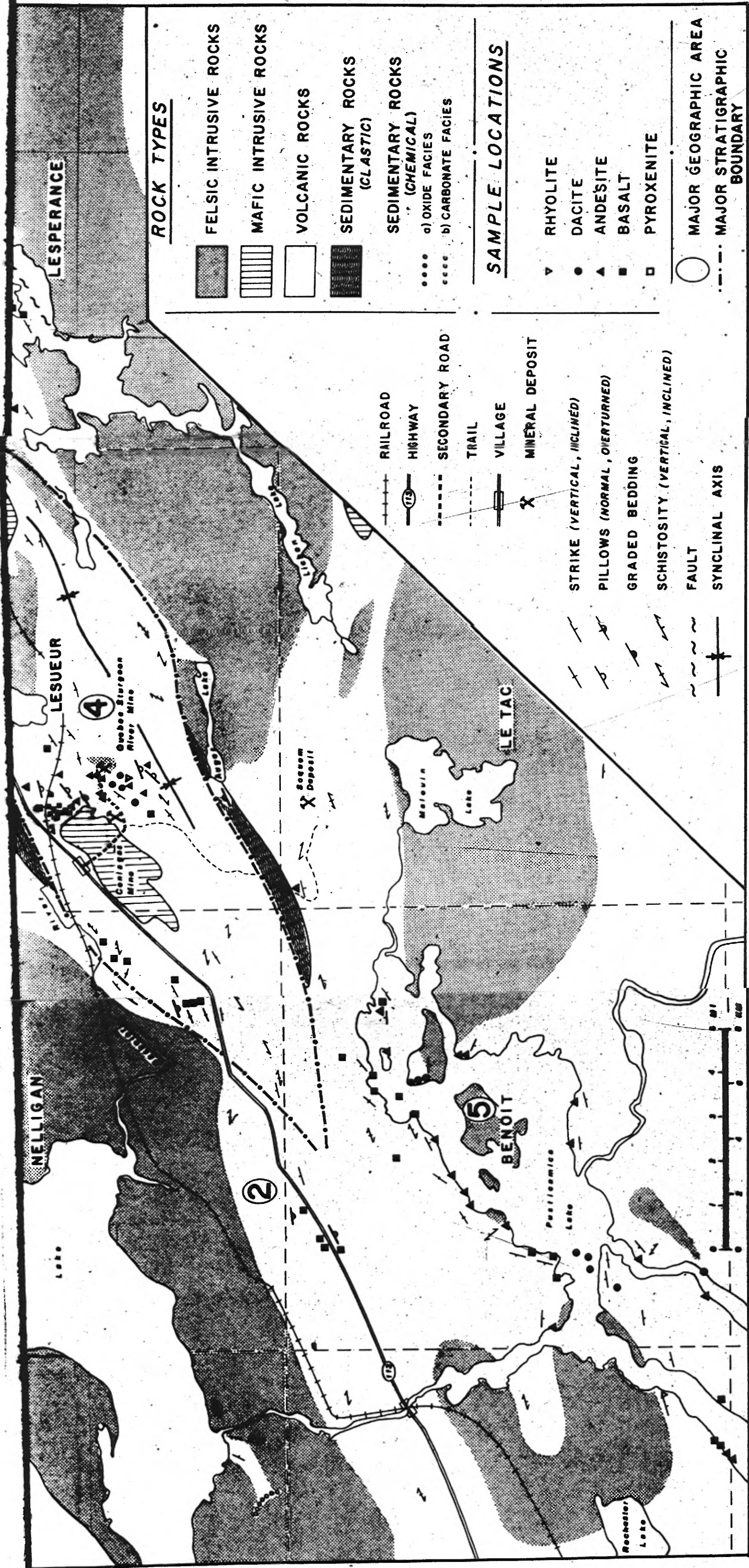
Winkler H.G. (1976) Petrogenesis of Metamorphic Rocks (4th ed.) Springer-Verlag 333pp.

Wyllie P.J., (1971) The Dynamic Earth. John Wiley & Sons.

Yoder H.S. & Tilley C.E., (1962) Origin of Basaltic Magmas: An Experimental Study of Natural and Synthetic Rock Systems J.Pet., V3, p.342-532.

Zirkel F., (1893) Lehrbuch der Petrographie VI, p.834.





ROCK TYPES

- FELSIC INTRUSIVE ROCKS
- MAFIC INTRUSIVE ROCKS
- VOLCANIC ROCKS
- SEDIMENTARY ROCKS (CLASTIC)
- SEDIMENTARY ROCKS (CHEMICAL)
 - a) OXIDE FACIES
 - b) CARBONATE FACIES

SAMPLE LOCATIONS

- RHYOLITE
- DACITE
- ANDESITE
- BASALT
- PYROXENITE

- MAJOR GEOGRAPHIC AREA
- MAJOR STRATIGRAPHIC BOUNDARY

- RAILROAD
- HIGHWAY
- SECONDARY ROAD
- TRAIL
- VILLAGE
- MINERAL DEPOSIT
- STRIKE (VERTICAL, INCLINED)
- PILLOWS (NORMAL, OVERTURNED)
- GRADED BEDDING
- SCHISTOSITY (VERTICAL, INCLINED)
- FAULT
- SYNCLINAL AXIS